

A novel protocol for the quantification of temporal and postural gait parameters of rats and humans

June Kazira Madete, B.Eng (Hons)



PhD Thesis
November 2011

Institute of Medical Engineering and Medical Physics
School of Engineering
Cardiff University

ABSTRACT

Animal models have been used for many years to generalise the human condition of various neurological diseases. It is important that the behavioural attributes from the animal model directly correlate with those found in the human pathology. Motion analysis (MA) techniques provide a platform for direct correlation analysis between the two species, which is an important step for translational medicine.

A novel three dimensional (3D) MA protocol was developed to investigate temporal and postural gait variables in both rats and humans. Gait studies involving rats are mainly based on movement scores or descriptive approaches to discerning differences in behaviour or function. Therefore, a protocol utilising a quantitative 3DMA technique during gait was developed. Data was acquired to describe function and behavioural attributes in animal models of Parkinson's disease (PD) and stroke in terms of temporal gait and postural adjustments and on a healthy cohort of humans.

The study explored the practicality of the developed protocol to investigate the effects of unilateral dopamine depletion on rat locomotion while walking on beams of varying widths (wide, narrow and graduated). Temporal and postural gait parameters of ten male Lister Hooded rats (five controls (CNL) and five hemi-parkinsonian (PNL)) were observed using passive markers placed in locations that were representative of their four limbs and their body axis. Significant differences ($p < 0.05$) were found between the PNL and CNL rats for speed along the wide beam and stride lengths for the left (impaired) fore-limb; on the narrow beam and the wide beam and for the left (impaired) hind limb on the graduated beam. The PD rats moved on the wide beam with a significantly greater *roll* range of motion (ROM) coupled with a positively biased *roll* kinematic waveform during one gait cycle. Whilst walking on the narrow beam, they displayed an increased use of the ledge and placed their tail towards the right. The results demonstrate that marker-based MA can provide an effective and simple approach to quantifying temporal gait parameters for rat models of PD. They also reveal how the width of the path affects the locomotion in both experimental cohorts.

The novel protocol was applied to investigate the effects of Middle Cerebral Artery Occlusion (MCAO) and graft on rat locomotion while walking on a wide beam. The data collection was carried out before and after surgery to investigate temporal and postural gait parameters of 50 male Wistar rats. Significant differences ($p < 0.05$) were found between the control and MCAO rats for *roll* ROM coupled with a positively biased *roll* kinematic waveform during one gait cycle. Using the data collected, a classification tool based around the Dempster-Shafer theory enabled the objective classification of the rat cohorts into a MCAO group, a control group and a graft group. The *roll* ROM and swing time data were transformed into a set of belief values that the animals had graft, lesion or normal gait. The belief values were then represented on a simplex plot, which enables the final classification of a rat, and the level of benefit achieved by lesion or graft surgery to be visualised. The tool was able to classify rats with an accuracy of between 81% and 94.84% accuracy. The tool also indicated that swing time and *roll* were the most influential variables in distinguishing differences in gait after MCAO lesion and graft. Further work is required on the graft data as some inconsistencies were found, but the classification allowed better comparisons between groups than just using ANOVA alone by taking this level of uncertainty and producing a clear comparison between the cohorts.

Initial studies have demonstrated a practical and visual approach that can discriminate between gait function in the rat model. Therefore to achieve the aim of the thesis, a cohort of healthy humans were tested to replicate the data collection and processing protocols developed for animal MA. The marker based protocol was carried out to investigate temporal and postural gait parameters of 10 healthy human subjects (five male: five female). The data collected compared well with published data for normal human gait therefore validating the human based protocol. The results identified variables that were easily correlated with rat data. Similarities in body orientation patterns were recorded and discussed.

In conclusion, a novel protocol was developed that allowed a simple, non-invasive, practical, and sensitive approach to over ground gait data acquisition for the rat models and a healthy human cohort. Further work that would involve patients with neurological disease will enable the full validation of the protocol. This in turn would provide answers to the argument: 'Is the use of animal models of the disease effective approach for clinical research?'

DECLARATION

This work has not previously been accepted in substance for any degree and is not being concurrently submitted in candidature for any degree.

Signed.....(June Madete)

Date.....

STATEMENT 1

This thesis is being submitted in partial fulfilment of the requirements for the degree of PhD

Signed.....(June Madete)

Date.....

STATEMENT 2

This thesis is the result of my own investigation, except where otherwise stated. Other sources are acknowledged by explicit references.

Signed..... (June Madete)

Date.....

STATEMENT 3

I hereby give consent for my thesis, if, accepted, to be available for photocopying and for inter-library loan, and for the title and summary to be made available to outside organisations.

Signed..... (June Madete)

Date.....

STATEMENT 3

I hereby give consent for my thesis, if, accepted, to be available for photocopying and for inter-library loan, after expiry of a bar on access previously approved by the graduate development committee.

Signed.....(June Madete)

Date.....

ACKNOWLEDGEMENTS

First and foremost I would like to thank my sponsors (The Aga Khan Foundation) without whose help I would not have had the resources to carry out this research. I would also like to express my appreciation to my supervisor Dr. Cathy Holt for all her input, ongoing encouragement and tremendous patience over the last few years. The research stemmed from her vision years ago and together we have taken a major step into interdisciplinary motion analysis and across species. I have learnt valuable personal and professional lessons and skills from her and I really appreciate her constant belief in me and my work.

Secondly, I would like to thank everyone in the Brain Repair group at Cardiff University for their enthusiasm and help in this pilot project, for providing their time and resources towards all the animal work carried out. I am very thankful for their input into the results and published work that has formed a big chunk of this thesis. I would like to mention Prof. Steve Dunnett, Dr. Alex Klein, Dr. Becky Trueman and Anna Fuller from the group for their active advice, support and guidance that was extremely helpful in achieving the outlined aim of the research. Am mostly thankful for how they selflessly shared their time to give a bio-scientist perspective on my results and bearing with me through many hours of data collection and constant questions about the brain.

Thirdly, I am hugely grateful to all my colleagues and friends who took part in the human motion analysis trial without them my thesis would be incomplete. Finally, to my family in Kenya for keeping me grounded, reminding me that I am never alone and believing in me no matter what. A special thanks to my Mack family, who have been with me when I needed a laugh, a cry or even a hug. They provided much needed support, encouragement, thoughtfulness and patients without which I could not have completed this thesis. I cannot finish without giving a special mention to my daughter Neema, you are my inspiration and I love you.

TABLE OF CONTENTS

ABSTRACT	I
DECLARATION	I
ACKNOWLEDGEMENTS	IV
ABBREVIATIONS	IX
NOTATION	XI
LIST OF FIGURES	XII
LIST OF TABLES	XVIII
1. INTRODUCTION AND LITERATURE REVIEW	1-1
1.1. Introduction	1-1
1.2. Background	1-3
1.2.1. Brain storming.....	1-3
1.2.2. Rat models	1-11
1.2.3. The Gait Cycle	1-11
1.2.4. Postural control during gait	1-13
1.2.5. Brain function during gait	1-14
1.2.6. Parkinson’s disease	1-15
1.2.7. Stroke	1-17
1.3. Literature Review	1-20
1.3.1. Human based motion analysis.....	1-20
1.3.2. 3D Marker Based Human Motion Analysis.....	1-23
1.3.3. Non -marker based rat motion analysis	1-26
1.3.4. Marker based rat motion analysis	1-29
1.4. Aim and Objectives	1-32

1.5. Thesis Summary	1-33
2. PROTOCOL DEVELOPMENT	2-1
2.1. Introduction	2-1
2.2. Data Collection.....	2-4
2.2.1. Qualisys motion analysis system	2-4
2.2.2. Calibration.....	2-4
2.2.3. Protocols	2-6
2.3. Data Processing.....	2-22
2.3.1. Temporal Gait parameters.....	2-24
2.3.2. Postural Parameters	2-29
2.3.3. Limb and paw placements analysis.....	2-36
2.3.4. Statistical and Error Analysis.....	2-37
2.3.5. Classification using Dempster-Shafer theory (DST)	2-38
2.4. Comparing Human and rat protocol.....	2-47
2.4.1. Cameras and calibration	2-47
2.1. Data processing.....	2-49
2.2. Outputs.....	2-49
2.2.1. Temporal parameters	2-49
2.2.2. Postural parameters	2-51
3. QUANTIFYING LOCOMOTION OF PARKINSON'S DISEASE RATS	3-1
3.1. Introduction	3-1
3.2. Methods	3-2
3.3. Data Processing.....	3-4
3.4. Results	3-6

3.4.1.	Temporal Gait Parameters.....	3-6
3.4.2.	Postural gait Parameters	3-14
3.5.	Discussion	3-21
4.	QUANTIFYING LOCOMOTION OF STROKE RATS	4-1
4.1.	Introduction	4-1
4.2.	Methods	4-3
4.2.1.	Data collection	4-3
4.2.2.	Data processing.....	4-7
4.2.3.	Statistical and error analysis	4-8
4.3.	Results	4-10
4.3.1.	Temporal Gait Parameters.....	4-10
4.3.2.	Postural parameters (ROM).....	4-14
4.3.3.	Postural parameters (ROM).....	4-15
4.3.4.	Kinematic waveforms and classification simplex plots	4-16
4.4.	Discussion	4-30
4.4.1.	Temporal and postural gait parameters.....	4-31
4.4.2.	Classification	4-33
5.	QUANTIFYING LOCOMOTION OF HEALTHY HUMANS.....	5-1
5.1.	Introduction	5-1
5.2.	Methods	5-3
5.2.1.	Data collection	5-3
5.2.2.	Data processing.....	5-3
5.2.3.	Statistical and error analysis	5-5
5.3.	Results	5-6

5.3.1. Comparisons between the three Walkways5-6

5.3.2. Comparisons between the male and female cohorts 5-11

5.4. Discussion 5-18

6. DISCUSSION..... 6-1

7. CONCLUSIONS AND FURTHER WORK 7-1

7.1. Conclusions 7-1

7.2. Further work 7-6

8. REFERENCES..... 8-1

A. APPENDICES A-1

ABBREVIATIONS

2D	Two Dimensional
3D	Three Dimensional
3DMA	Three Dimensional Marker Based Motion Analysis
6DOF	Six Degrees of Freedom
6OHDA	Six-Hydroxydopamine
ANOVA	Analysis of Variance
BOE	Body of Evidence
BOEc	Combined Body of Evidence
BRG	Brain Repair Group
C7	Seventh Cervical Vertebrae
CA	Carotid Artery
CN	Stroke Control
CNL	Parkinson's Control
CSV	Comma Delimited
DS	Dempster-Shafer
DST	Dempster-Shafer Theory
ECA	External Carotid Artery
GR	Graduated
GRa	Graft
GRF	Ground Reaction Force
GRS	Global Reference System
GRw	Graduated Walkway
HD	Huntington's Disease
ICA	Internal Carotid Artery
L1	First Lumbar Spine
LE	Lesion

LFL	Left Front Limb
LRS	Local Reference System
MA	Motion Analysis
MA1	Motion Analysis 1
MA2	Motion Analysis 2
MAL	Motional Analysis Laboratory
MCA	Middle Cerebral Artery
MCAO	Middle Cerebral Artery Occlusion
NR	Narrow
NRW	Narrow Walkway
PE	Pelvis
PNL	Partial Nigral-Straiatal Lesion
POST_CN	Post Surgery Controls
POST_GRA	Post Surgery Grafts
POST_LE	Post Surgery Lesion
PRE_CN	Pre Surgery Controls
PRE_GRA	Pre Surgery Graft
PRE_LE	Pre Surgery Lesion
QTM	Qualisys Track Manager
RBL	Right Back Limb
RFL	Right Front Limb
ROM	Range Of Motion
SD	Standard Deviation
SME	Standard Mean Error
WDW	Wide Walkway

NOTATION

Dx	Change in x
Dy	Change in y
$\max dx$	Maximum change in x
$\max dy$	Maximum change in y
$\min dx$	Minimum change in x
$\min dy$	Minimum change in y
$cf(v)$	Confidence Factor
A	DS Control Parameter
B	DS Control Parameter
θ	DS Control Parameter
k	DS Control Parameter
θ	DS Control Parameter
{POST_CN}	Hypothesis Rat Has Normal
{POST_LE}	Hypothesis Rat Has MCAO Gait
{POST_GRa}	Hypothesis Rat Has Graft Gait
{PRE_CN}	Hypothesis Rat Has Gait That Is Normal
{PRE_LE}	Hypothesis Rat Has Gait That Is Normal
{PRE_GRa}	Hypothesis Rat Has Gait That Is Normal
$M(.)$	Probability Mass Function
θ_L	Lower Uncertainty Limit
θ_U	Upper Uncertainty Limit
$\lambda_1, \lambda_2 \text{ and } \lambda_3$	Belief Values on The Simplex Plot

LIST OF FIGURES

FIGURE 1-1: STAIRCASE PAW REACHING APPARATUS FROM THE CARDIFF BRAIN REPAIR GROUP	1-5
FIGURE 1-2 :INITIAL DESIGN TO MIMIC THE STAIRCASE APPARATUS TO BE USED TEST HUMAN REACHING (A) RAT APPARATUS (B) INTERPRETED HUMAN APPARATUS.....	1-6
FIGURE 1-3: HUMAN REACHING EXPERIMENT DESIGN CARRIED OUT WHILE THE SUBJECT WAS STANDING....	1-7
FIGURE 1-4: BEAM AND ROTAROD APPARATUS	1-8
FIGURE 1-5: ONE HUMAN GAIT CYCLE	1-12
FIGURE 1-6: THE CROSS SECTION OF A BRAIN; THE CORTEX, THE BRAIN STEM AND THE SPINAL CORD ARE THE THREE MAIN LEVELS OF CONTROL WITHIN THE CENTRAL NERVOUS SYSTEM (ADAPTED FROM DUBUC, 2002)	1-14
FIGURE 1-7: EXAMPLE OF PAW PRINT ANALYSIS FROM METZ ET AL 2005	1-27
FIGURE 1-8: CATWALK OUTPUT EXAMPLE FROM HAMERS ET AL IN 2006, THE COLOURS ARE NORMALLY ASSIGNED BY THE PROGRAM, GREEN= RIGHT, RED= LEFT, LIGHT = FORE AND DARK = HIND.	1-28
FIGURE 1-9: SUCCESSFUL MARKER PLACEMENT ON RATS IN A STUDY BY GARNIER ET AL 2008.....	1-30
FIGURE 1-10 : EXPERIMENTAL SET UP FOR (COUTO ET AL., 2008B); THREE HIGH SPEED CAMERAS WERE POSITIONED AROUND THE HINDLIMB TO MINIMIZE MARKER OCCLUSION AND MAXIMISE RESOLUTION. REFLECTIVE MARKERS PLACED ON THE LEFT HINDLIMB OF THE RAT ARE SHOWN.	1-31
FIGURE 2-1: CALIBRATION KIT A) 'L' SHAPED FRAME AND B) 'T' SHAPED WAND	2-5
FIGURE 2-2: CALIBRATION RESULTS	2-5
FIGURE 2-3: ELEVATED BEAM (GRADUATED)	2-7
FIGURE 2-4: THE PLAN VIEW OF THE GR BEAM SHOWING THE NARROWING OF THE BEAM TOWARDS THE RESTING BOX AND THE THREE ZONES USED TO CALCULATE ZONAL SPEED.....	2-8
FIGURE 2-5: ARIAL VIEW OF THE THREE DIFFERENT BEAMS A) WD BEAM, B) NR BEAM AND C) GR BEAM.....	2-9
FIGURE 2-6: CAMERA MAP AND CALIBRATION FRAME POSITION	2-10
FIGURE 2-7: A) RAT MARKER POSITIONS B) USE OF CABLE TIES TO FASTEN MARKERS ON LIMBS.....	2-13
FIGURE 2-8: GRADUATED WALKWAY SHOWING DIMENSIONS.....	2-15
FIGURE 2-9: CARDIFF UNIVERSITY MOTION ANALYSIS LABORATORY WITH A 12 CAMERA SET UP.	2-16

FIGURE 2--10: CAMERA SET UP INCLUDING THE HEIGHT AND THE DISTANCE FROM ORIGIN OF EACH CAMERA AND POSITION OF THE CALIBRATION FRAME DURING EXTENDED CALIBRATION.....	2-17
FIGURE 2-11 : EXTENDED CALIBRATION	2-18
FIGURE 2-12: HUMAN SUBJECTS MAKER PLACEMENTS (THE DASHED LINES INDICATING POSTERIOR MARKERS)	2-20
FIGURE 2-13: HEALTHY HUMAN WALKING OUTPUT FROM QTM SHOWING FIVE GAIT CYCLES OF THE LEFT LIMB	2-21
FIGURE 2-14: PROCESSING DATA FROM THE RAT WAKING TRIAL. THE METHOD WAS ALSO APPLIED TO THE HUMAN WALKING TRIAL SINCE SIMILAR PROTOCOL WAS USED, SIMILAR OUTPUT WERE ACHIEVED...	2-23
FIGURE 2-15: EXCEL OUTPUT FOR THREE GAIT CYCLES FROM EXPORTED DATA	2-25
FIGURE 2-16: EXAMPLE OF ONE GAIT CYCLE WITH ANNOTATIONS USED TO CALCULATE STANCE TIME.....	2-26
FIGURE 2-17: EXAMPLE OF ONE GAIT CYCLE WITH ANNOTATIONS USED TO CALCULATE SWING TIME	2-27
FIGURE 2-18: EXAMPLE OF ONE GAIT CYCLE WITH ANNOTATIONS USED TO CALCULATE STRIDE LEGTH.....	2-28
FIGURE 2-19: DEFINING A RIGID BODY FOR 6DOF CALCULTIONS OF THE <i>ROLL</i> , <i>PITCH</i> AND <i>YAW</i>	2-29
FIGURE 2-20: ORIGINAL POSITION OF 6DOF IN THE GRS	2-31
FIGURE 2-21: ROTATION AROUND THE X-AXIS.....	2-31
FIGURE 2-22: ROTATION AROUND THE Y- AXIS.....	2-32
FIGURE 2-23: ROTATION AROUND THE Z- AXIS.....	2-32
FIGURE 2-24: NEW 6DOF POSITION IN THE GRS.	2-33
FIGURE 2-25: ILLUSTRATIONS OF <i>ROLL</i> <i>PITCH</i> AND <i>YAW</i>	2-36
FIGURE 2-26: PAW POSITION ALONG THE BEAM WAS SCORED AS EITHER, A) ON THE BEAM OR B) ON THE LEDGE. B) ALSO REVEALS A TAIL POSITIONED ON THE RIGHT.	2-37
FIGURE 2-27: THE CLASSIFICATION METHOD SHOWING THE INTERACTION OF ITS THREE MAIN STAGES.(A) CONVERSION OF INPUT VARIABLE, V , INTO CONFIDENCE FACTOR $CF(V)$ USING THE SIGMOID FUNCTION. θ IS THE VALUE OF V FOR WHICH $CF(V) = 0.5$. (B) CONVERSION OF CONFIDENCE FACTOR INTO BODY OF EVIDENCE (BOE) (C) CONVERSION OF THE BOE INTO ITS SIMPLEX COORDINATE, DENOTED BY THE POINT P (ADAPTED FROM BEYNON ET AL., 2002). THE SIMPLEX PLOT IS DIVIDED INTO FOUR REGIONS: 1 DENOTES THE DOMINANT POST_CN CLASSIFICATION REGION; 2 DENOTE THE DOMINANT POST_LE CLASSIFICATION REGION; 3 DENOTE THE NON-DOMINANT POST_CN CLASSIFICATION REGION AND 4 DENOTES THE NON-DOMINANT POST_LE CLASSIFICATION REGIONS. THE DOTTED VERTICAL LINE IS THE DECISION BOUNDARY.	2-40

FIGURE 2-28: INFLUENCE OF K ON CONFIDENCE FACTOR (A) POSITIVE ASSOCIATION (K = 0.25) (B) NEGATIVE ASSOCIATION (K = -0.25) (C) SMALL ABSOLUTE VALUE OF K (K = 0.2) (D) LARGE ABSOLUTE VALUE OF K (K= 2) (ADAPTED FROM JONE 2004)	2-42
FIGURE 2-29: OUTPUT DATA FROM QTM FOR THE RATS WALKING TRIAL SHOWING FIVE GAIT CYCLES.....	2-50
FIGURE 2-30: OUTPUT DATA FROM QTM FOR THE HUMAN WALKING TRIAL SHOWING FIVE GAIT CYCLES....	2-50
FIGURE 2-31: A) RAT GAIT TRAJECTORIES FOR ALL FOUR LIMBS AND B) HUMAN GAIT TRAJECTORIES FOR ALL FOUR LIMBS	2-51
FIGURE 2-32: THE <i>ROLL</i> OF THE BODY FROM LEFT TO RIGHT DURING ONE GAIT CYCLE WHICH INVOLVES ROTATIONS TOWARDS THE SIDE OF LIMB WEIGHT BEARING DURING GAIT FOR BOTH SPECIES.	2-52
FIGURE 2-33: <i>PITCH</i> ROTATION REPRESENTATIVE OF THE VERTICAL AXIAL DISPLACEMENTS WITH THE HUMAN UPPER BODY ROTATIONS MATCHING THE PATTERN OF THE ANIMAL MOTION OF A DOUBLE SINUSOIDAL PATH.....	2-53
FIGURE 2-34: <i>YAW</i> LATERAL DISPLACEMENT TOWARDS THE SIDE OF THE SUPPORTING LIMB IS ILLUSTRATE IN THE UPPER BODY WAVEFORMS AND THE ANIMAL WAVEFORMS. DISPLACEMENTS OCCUR DURING SINGLE STANCE AS THE LIMB SUPPORT SHIFTS FROM THE LEFT TO RIGHT LIMBS. MAXIMUM DISPLACEMENT IS AT AROUND 50% GAIT CYCLE DURING DOUBLE LIMB WITH	2-54
FIGURE 3-1 : TEMPORAL PARAMETERS THAT WERE FOUND TO BE SIGNIFICANTLY DIFFERENT BETWEEN THE PNL AND CNL COHORTS WHILE WALKING ALONG THE WD BEAM. THE RESULTS ARE EXPRESSED AS BAR CHARTS OF THE MEAN OF EACH COHORT WITH STANDARD MEAN ERROR	3-9
FIGURE 3-2 : TEMPORAL PARAMETERS THAT WERE FOUND TO BE SIGNIFICANTLY DIFFERENT BETWEEN THE PNL AND CNL COHORTS WHILE WALKING ALONG THE NR BEAM. THE RESULTS ARE EXPRESSED AS BAR CHARTS OF THE MEAN OF EACH COHORT WITH STANDARD MEAN ERROR BARS	3-10
FIGURE 3-3 : TEMPORAL PARAMETERS THAT WERE FOUND TO BE SIGNIFICANTLY DIFFERENT BETWEEN THE PNL AND CNL COHORTS WHILE WALKING ALONG THE GR BEAM. THE RESULTS ARE EXPRESSED AS BAR CHARTS OF THE MEAN OF EACH COHORT WITH STANDARD MEAN ERROR BARS	3-11
FIGURE 3-4: KINEMATIC WAVEFORMS FOR THE AVERAGE WALKING PERFORMANCE AND ITS SD FOR ONE GAIT CYCLE ON THE WD BEAM. THE BOLD BLACK LINES REPRESENT THE AVERAGE PERFORMANCES OF THE PNL COHORT (THE SD IS PLOTTED IN THIN BLACK LINES); THE DOTTED LINES REPRESENT THE AVERAGE PERFORMANCE OF THE CNL COHORT (THE SD IS PLOTTED IN GREY).....	3-16
FIGURE 3-5: KINEMATIC WAVEFORMS FOR THE AVERAGE WALKING PERFORMANCE AND SD FOR ONE GAIT CYCLE ON THE NR BEAM. THE BOLD BLACK LINES REPRESENT THE AVERAGE PERFORMANCES OF THE PNL COHORT (THE SD IS PLOTTED IN THIN BLACK LINES); THE DOTTED LINES REPRESENT THE AVERAGE PERFORMANCE OF THE CNL COHORT (THE SD IS PLOTTED IN GREY).....	3-17
FIGURE 3-6: KINEMATIC WAVEFORMS FOR THE AVERAGE WALKING PERFORMANCE AND ITS SD FOR ONE GAIT CYCLE ON THE GR BEAM A) ZONE 1, B) ZONE 2 AND C) ZONE 3. THE BOLD BLACK LINES REPRESENT THE AVERAGE PERFORMANCES OF THE PNL COHORT (THE SD IS PLOTTED IN THIN BLACK LINES); THE DOTTED LINES REPRESENT THE AVERAGE PERFORMANCE OF THE CNL COHORT (THE SD IS PLOTTED IN GREY) .	3-18
FIGURE 4-1: EXPERIMENTAL DESIGN AND TIMELINE OF THE STROKE MA STUDY	4-4

FIGURE 4-2: POST ANALYSIS DIVISION OF THE THREE COHORTS	4-7
FIGURE 4-3: KINEMATIC WAVEFORMS FOR THE AVERAGE WALKING PERFORMANCE AND ITS SD FOR ONE GAIT CYCLE ON THE BEAM. THE BOLD BLACK LINES REPRESENT THE AVERAGE PERFORMANCES OF THE PRE_CN COHORT (THE SD IS PLOTTED IN THIN BLACK LINES); THE DOTTED LINES REPRESENT THE AVERAGE PERFORMANCE OF THE POST_CN COHORT (THE SD IS PLOTTED IN GREY).....	4-17
FIGURE 4-4 SIMPLEX CO-ORDINATE REPRESENTATIONS OF THE BOEC FOR THE PRE_CN CLASSIFIED WITH THE POST_CN COHORTS.....	4-18
FIGURE 4-5: KINEMATIC WAVEFORMS FOR THE AVERAGE WALKING PERFORMANCE AND ITS SD FOR ONE GAIT CYCLE ON THE WD BEAM. THE BOLD BLACK LINES REPRESENT THE AVERAGE PERFORMANCES OF THE PRE_LE COHORT (THE SD IS PLOTTED IN THIN BLACK LINES); THE DOTTED LINES REPRESENT THE AVERAGE PERFORMANCE OF THE POST_LE COHORT (THE SD IS PLOTTED IN GREY).....	4-19
FIGURE 4-6 SIMPLEX CO-ORDINATE REPRESENTATIONS OF THE BOEC FOR THE PRE_LE CLASSIFIED WITH THE POST_LE COHORTS.....	4-20
FIGURE 4-7 : KINEMATIC WAVEFORMS FOR THE AVERAGE WALKING PERFORMANCE AND ITS SD FOR ONE GAIT CYCLE ON THE WD BEAM. THE BOLD BLACK LINES REPRESENT THE AVERAGE PERFORMANCES OF THE PRE_GRA COHORT (THE SD IS PLOTTED IN THIN BLACK LINES); THE DOTTED LINES REPRESENT THE AVERAGE PERFORMANCE OF THE POST_GRA COHORT (THE SD IS PLOTTED IN GREY).	4-21
FIGURE 4-8 SIMPLEX CO-ORDINATE REPRESENTATIONS OF THE BOEC FOR THE PRE_GRA CLASSIFIED WITH THE POST_GRA COHORTS	4-22
FIGURE 4-9 : KINEMATIC WAVEFORMS FOR THE AVERAGE WALKING PERFORMANCE AND SD FOR ONE GAIT CYCLE ON THE WD BEAM. THE BOLD BLACK LINES REPRESENT THE AVERAGE PERFORMANCES OF THE POST_LE COHORT (THE SD IS PLOTTED IN THIN BLACK LINES); THE DOTTED LINES REPRESENT THE AVERAGE PERFORMANCE OF THE POST_CN COHORT (THE SD IS PLOTTED IN GREY).....	4-23
FIGURE 4-10: SIMPLEX CO-ORDINATE REPRESENTATIONS OF THE BOEC FOR THE POST_CN CLASSIFIED WITH THE POST_LE COHORTS.....	4-24
FIGURE 4-11 : KINEMATIC WAVEFORMS FOR THE AVERAGE WALKING PERFORMANCE AND ITS SD FOR ONE GAIT CYCLE ON THE WD BEAM. THE BOLD BLACK LINES REPRESENT THE AVERAGE PERFORMANCES OF THE POST_GRA COHORT (THE SD IS PLOTTED IN THIN BLACK LINES); THE DOTTED LINES REPRESENT THE AVERAGE PERFORMANCE OF THE POST_CN COHORT (THE SD IS PLOTTED IN GREY).....	4-25
FIGURE 4-12: SIMPLEX CO-ORDINATE REPRESENTATIONS OF THE BOEC FOR THE POST_CN CLASSIFIED WITH THE POST_GRA COHORTS	4-26
FIGURE 4-13 : KINEMATIC WAVEFORMS FOR THE AVERAGE WALKING PERFORMANCE AND ITS SD FOR ONE GAIT CYCLE ON THE WD BEAM. THE BOLD BLACK LINES REPRESENT THE AVERAGE PERFORMANCES OF THE POST_GRA COHORT (THE SD IS PLOTTED IN THIN BLACK LINES); THE DOTTED LINES REPRESENT THE AVERAGE PERFORMANCE OF THE POST_CN COHORT (THE SD IS PLOTTED IN GREY).....	4-27
FIGURE 4-14: SIMPLEX CO-ORDINATE REPRESENTATIONS OF THE BOEC FOR THE POST_LE CLASSIFIED WITH THE POST_GRA COHORTS	4-28
FIGURE 4-15: SIMPLEX CO-ORDINATE REPRESENTATIONS OF THE BOEC FOR THE POST_LE CLASSIFIED WITH THE POST_GRA AND POST_CN COHORTS.	4-29

FIGURE 5-1: QTM SCREEN SHOTS OF THE THREE DEFINED RIGID BODIES, A) TRUNK, B) PELVIS AND C) UPPER BODY; USED TO INVESTIGATE HUMAN POSTURE DURING GAIT.	5-5
FIGURE 5-2: KINEMATICS WAVEFORMS REPRESENTATIVE OF <i>ROLL</i> , <i>PITCH</i> AND <i>YAW</i> ROTATIONS OF THE THREE RIGID BODIES (A) PELVIS; (B) TRUNK AND (C) UPPER-BODY. ON THE THREE WALKWAYS: WDW =SOLID LINE; NRW =DOTTED LINES AND GRW = DASHED LINES.....	5-10
FIGURE 5-3: TRUNK KINEMATICS WAVEFORMS COMPARING THE MALE (MEAN=SOLID LINES, SD=LIGHT GREY LINES) AND FEMALE (MEAN=DASHED LINES; SD=DARK GREY LINES) <i>ROLL</i> , <i>PITCH</i> AND <i>YAW</i> ROTATIONS ON THE A) WDW, B) NRW AND C) GRW	5-15
FIGURE 5-4: PELVIS KINEMATICS WAVEFORMS COMPARING THE MALE (MEAN=SOLID LINES, SD=LIGHT GREY LINES) AND FEMALE (MEAN=DASHED LINES; SD=DARK GREY LINES) <i>ROLL</i> , <i>PITCH</i> AND <i>YAW</i> ROTATIONS ON THE A) WDW, B) NRW AND C) GRW.	5-16
FIGURE 5-5: UPPER BODY KINEMATICS WAVEFORMS COMPARING THE MALE (MEAN=SOLID LINES, SD=LIGHT GREY LINES) AND FEMALE (MEAN=DASHED LINES; SD=DARK GREY LINES) <i>ROLL</i> , <i>PITCH</i> AND <i>YAW</i> ROTATIONS ON THE A) WDW, B) NRW AND C) GRW	5-17
FIGURE 8-1: CAMERA MAP AND CALIBRATION FRAME POSITION	B-6
FIGURE 8-2: MAKER PLACEMENT ON THE BEAM	B-7
FIGURE 8-3 MARKERS ATTACHED TO THE RATS BODY A) APPENDICULAR ASPECTS OF THE RATS SKELETAL , B) HEAD, MID-SPINE AND BACK- SPINE AND C) ON THE 4 PAWS USING CABLE TIES.....	B-7
FIGURE 8-4 CABLE-TIE AND MAKER CONFIGURATION	B-7
FIGURE 8-5: CAMERA MAP AND CALIBRATION FRAME POSITION	B-10
FIGURE 8-6: ANTERIOR MAKER PLACEMENTS.....	B-11
FIGURE 8-7 POSTERIOR MARKER PLACEMENT	B-12
FIGURE 8-8: EXPORT TO 6DOF	C-21
FIGURE 8-9: WAKRSPACE DEFINE	C-21
FIGURE 8-10: WORKSPACE TRANSLATE.....	C-22
FIGURE 8-11: QTM EXPORT 6DOF	C-22
FIGURE 8-12:PD 6DOF KINEMATIC WAVEFORMS ALONG THE WIDE BEAM	D-1
FIGURE 8-13: PD 6DOF KINEMATIC WAVEFORMS ALONG THE GRADUATED BEAM.....	D-2
FIGURE 8-14: PD 6DOF KINEMATIC WAVEFORMS ALONG THE NARROW BEAM.....	D-3
FIGURE 8-15: HUMAN 6DOF UPPER BODY	D-4
FIGURE 8-16: HUMAN 6DOF TRUNK.....	D-5

FIGURE 8-17: HUMAN 6DOF PELVIS D-6

FIGURE 8-18: HUMAN 6DOF UPPER BODY D-7

FIGURE 8-19: HUMAN 6DOF TRUNK..... D-8

FIGURE 8-20: HUMAN 6DOF PELVIS D-9

FIGURE 8-21: HUMAN 6DOF UPPER BODY D-10

FIGURE 8-22: HUMAN 6DOF TRUNK..... D-11

FIGURE 8-23: HUMAN 6DOF PELVIS D-12

LIST OF TABLES

TABLE 1-1: ASSESSMENT MOTOR BEHAVIOURAL TEST AVAILABLE AT THE CARDIFF BRG	1-9
TABLE 2-1: SUMMARY OF MARKER PLACEMENT.	2-12
TABLE 2-2: DIMENSION DEFINITIONS OF THE ELEVATED BEAM AND THE HUMAN WALKWAY	2-14
TABLE 2-3: SUMMARY OF HUMAN MARKER PLACEMENT	2-19
TABLE 2-4: DEFINITIONS OF <i>ROLL PITCH</i> AND <i>YAW</i>	2-36
TABLE 2-5: RAT AND HUMAN MA PROTOCOLS	2-47
TABLE 3-1 TEMPORAL GAIT PARAMETERS COMPARING THE PNL AND CNL COHORTS ON THE GR, NR AND WD BEAMS (RFL=RIGHT FORELIMB, LFL=LEFT FORELIMB, RHL=RIGHT HINDLIMB, LHL=LEFT HINDLIMB). THE RESULTS ARE EXPRESSED AS MEAN \pm SME	3-8
TABLE 3-2: THE MEAN ROM (DEGREES) FOR <i>ROLL</i> , <i>PITCH</i> AND <i>YAW</i> DURING LOCOMOTION ALONG THE WD, NR, AND THE THREE ZONES ON THE GR BEAM FOR THE PNL AND CNL COHORTS; SIGNIFICANT DIFFERENCES (* P<0.05) WERE FOUND BETWEEN THE CNL AND PNL ANIMALS FOR <i>ROLL</i> ON THE WD BEAM AND <i>YAW</i> ON THE GR BEAM (ZONE 1).	3-15
TABLE 3-3: TAIL POSITIONS EXPRESSED AS A PERCENTAGE OF ALL ANALYSED GAIT CYCLES AS EITHER STRAIGHT BEHIND THE RAT'S BODY ON BEAM OR RIGHT OR LEFT OF THE RAT'S BODY ASSISTING POSTURAL BALANCE BY TOUCHING THE BEAM AND THE LEDGE	3-20
TABLE 3-4: POSITION OF ALL THE FOUR LIMBS WAS RECORDED AS EITHER 'LIMB ON THE BEAM' (= 1) OR 'LIMB ON THE LEFT OR RIGHT LEDGE' (= 0) AND IS PRESENTED AS A PERCENTAGE OF ALL GAIT CYCLES ANALYSED PER RUN.	3-20
TABLE 4-1: KINEMATIC PARAMETERS OF THE RATS FOR MA1 (PRE_PREFIX) AND MA2 (POST_PREFIX) SHOWING TEMPORAL AND POSTURAL GAIT PARAMETERS FOR THE CN; LE AND GRA COHORTS WHILE WALKING ALONG THE BEAM. WHERE LFL= LEFT FORE LIMB, LHL= LEFT HIND LIMB, RFL= RIGHT FORE LIMB, RHL=RIGHT HIND LIMB. THE RESULTS ARE EXPRESSED AS MEAN \pm SME OF EACH COHORT.	4-12
TABLE 4-2: RANGE OF MOTION OF THE RATS FOR MA1 (PRE_PREFIX) AND MA2 (POST_PREFIX) SHOWING POSTURAL GAIT PARAMETERS IN TERMS OF ROLL, PITCH AND YAW ANGLES FOR THE CONTROL (CN); LESION (LE) AND GRAFT (GRA) COHORTS WHILE WALKING ALONG THE BEAM. THE RESULTS ARE EXPRESSED AS MEAN \pm SEEM OF EACH COHORT)	4-15
TABLE 5-1: TEMPORAL PARAMETERS COMPARING THE WDW, NRW AND GRW. THE RESULTS ARE EXPRESSED AS MEAN \pm SD OF BOTH THE RIGHT AND LEFT LIMBS.	5-7
TABLE 5-2: POSTURAL PARAMETERS COMPARING THE WDW, NRW AND GRW. THE RESULTS ARE EXPRESSED AS MEAN \pm SD FOR THE <i>ROLL</i> , <i>PITCH</i> AND <i>YAW</i> ROM ANGLES.	5-8
TABLE 5-3: TEMPORAL PARAMETERS COMPARING THE MALE AND FEMALE COHORT ALONG THE WDW, NRW AND GRW. THE RESULTS ARE EXPRESSED AS MEAN \pm SD OF BOTH THE RIGHT AND LEFT LIMBS.	5-12

TABLE 5-4: MEAN \pm SD POSTURAL PARAMETERS COMPARING THE MALE AND FEMALE COHORTS DURING GAIT ALONG THE WDW, NRW AND GRW FOR THE <i>ROLL, PITCH AND YAW</i> ROM VALUES OF THE TRUNK RIGID BODY.	5-13
TABLE 5-5: MEAN \pm SD POSTURAL PARAMETERS COMPARING THE MALE AND FEMALE COHORTS DURING GAIT ALONG THE WDW, NRW AND GRW FOR THE <i>ROLL, PITCH AND YAW</i> ROM VALUES OF THE PELVIS RIGID BODY.	5-13
TABLE 5-6: MEAN \pm SD POSTURAL PARAMETERS COMPARING THE MALE AND FEMALE COHORTS DURING GAIT ALONG THE WDW, NRW AND GRW FOR THE <i>ROLL, PITCH AND YAW</i> ROM VALUES OF THE UPPER BODY RIGID BODY.	5-14
TABLE 8-1: LIMB AND TAIL POSITIONS ON THE GR BEAM.....	C-23
TABLE 8-2: LIMB AND TAIL POSITION ON THE NR BEAM.....	C-24
TABLE 8-3: LIMB AND TAIL POSITION ON THE WD BEAM	C-25
TABLE 8-4: BOEC VALUES FOR THE PRE_CN COMPARED TO PRE_GRA AND PRE_LE DATASET	F-4
TABLE 8-5: BOEC VALUES FOR THE PRE_GRA COMPARED TO PRE_CN AND PRE_LE DATASET	F-5
TABLE 8-6: BOEC VALUES FOR THE PRE_LE COMPARED TO PRE_GRA AND PRE_CN DATASET	F-6
TABLE 8-7: BOEC VALUES FOR THE PRE_CN COMPARED TO POST_CN DATASET	F-7
TABLE 8-8: BOEC VALUES FOR THE PRE_GRA COMPARED TO POST_GRA DATASET.....	F-7
TABLE 8-9: BOEC VALUES FOR THE PRE_LE COMPARED TO POST_LE DATASET	F-8
TABLE 8-10: BOEC VALUES FOR THE POST_CN COMPARED TO POST_GRA DATASET.....	F-8
TABLE 8-11: BOEC VALUES FOR THE POST_LE COMPARED TO POST_GRA DATASET.....	F-9
TABLE 8-12: BOEC VALUES FOR THE POST_LE COMPARED TO POST_CN DATASET	F-9

CHAPTER 1

1. Introduction and literature review

1.1. Introduction

Three dimensional (3D) motion analysis (MA) is a useful tool that provides highly sensitive, non-invasive detection and evaluation of many patho-physiological features, such as those occurring in Parkinson's disease (PD), Huntington's disease (HD), stroke, neuromuscular and skeletal muscle diseases (Whishaw et al., 2002; Schallert, 2006,; Madete et al., 2010,; Madete et al., 2011). Animal models of neurodegenerative diseases such as PD and HD enable us to understand the underlying pathology and offer potential therapeutic treatments. These models are very instrumental in providing an insight to how diseases may be managed and treated, by performing a range of functional and behavioural studies specific to the symptoms presented in the disease.

Behavioral and functional studies that involve the use of animal models to study diseases that affect motor abilities, such as PD and stroke, have been mainly non-automated and subjective (Whishaw et al., 2002; Schallert and Hall, 1988). This thesis approaches animal data acquisition from a biomechanics point of view using 3DMA techniques. By calculating 3D co-ordinate data of reflective markers placed at intrinsic locations on the subject, it's possible to analyse time and distance variables from the position and location of segments and bodies during gait.

The thesis provides a step by step outline as to how a novel protocol was developed in conjunction with the Brain Repair Group (BRG) at Cardiff University. The BRG

provided full support during the data collection process and decisions were made in-line with suggestions from them as experts in animal and brain research. This was the first collection of this kind at Cardiff University.

The results of the current research project have an impact in the area of animal brain studies as it allows for further validation of the animal models. The study provides a basis for correlation of gait data and thus proof of homology with human patients (Whishaw et al., 1992, and 2002). As a result, a better understanding of therapeutics and treatment plans can be achieved.

The first Chapter presents a brief background as to why animal models are important in brain research; how the brain controls movement (more specifically, gait); and what happens when the control processes are disrupted, with focus made on PD and stroke. A detailed review, providing insight into current research carried out in the areas of gait analysis of PD and stroke for both humans and animal models of the disease is provided. The remainders of the chapters introduce a novel 3DMA protocol for quantifying locomotion in rats and humans followed by the results from studies carried out on two separate groups of rats (PD and Stroke) and one group of healthy humans.

1.2. Background

1.2.1. Brain storming

This project was developed to introduce alternative ways to utilise the motion analysis techniques developed at the Cardiff School of Engineering. Behavioural studies involving animals at the Cardiff BRG are regularly performed using tests that examine the behaviour of rats. Each study is developed to test different aspects of the animals' behaviour and function for example paw reaching studies to evaluate impairments in compensatory adjustments (Miklyeva et al., 1994).

Initially, a brainstorm into numerous scenarios and protocols that combined the use of the motion capture system with animal behavioural studies were investigated. The final outcome would allow assessment of animal motion and test human subjects under the same testing conditions.

Animal models (in this case, rats) of neurological disease are designed to test reflexes usually present from birth that may be lost due to certain neurological conditions. For example, the righting reflex is tested by placing the rat on its back and measuring the time taken for it to return back on all fours (right itself). This ability may be lost due to neurological conditions or motor impairment (Miklyeva et al., 1995). In addition, stimuli such as touch, vision or sound, can be used to test neurological reflexes as the rat's body may flinch to the sound of a loud noise such as a metal clicker, or the rat may blink when approached with a cotton bud (Woodlee et al., 2008). The head may also turn when the whiskers are touched with a cotton bud. In a similar test, the rat is held and its whiskers are brushed against the edge of a table as the rat is lowered. This gives the rat the sensation of falling and its

automatic instinct should be to try and place its forepaw on the table to stop its “fall”. (Woodlee et al., 2008).

In order to use the 3D motion capture software the thesis concentrates on the motor functions presented by the rats and not reflexes. Different levels of activity can be measured to give an idea of how greatly the animal is affected by the neurological condition present. The open field test, (Pellis et al., 1987, Miklyaeva et al., 1995, Rochester et al., 1994) for example looks at anxiety as the rat is placed in a set volume for 10 minutes where its activity is monitored and a trace of the rat’s position throughout can be plotted to show a difference between high levels of activity and lower levels of activity.

A cylinder test looks at the rats’ need to explore its surroundings when placed in a new environment (Lundblad et al., 2002). The rat is placed in the cylinder for a set length of time and the number of rotations and paw placements can be recorded by hand. The rat will rear up and place one of its paws, either left or right, on the Perspex cylinder. It will also rotate to investigate all areas of its new surroundings. When combined with motion capture, the open field test and the cylinder tests do not present any constant variables to quantify rat motion.

The paw reaching test investigates skilled forelimb reaching and forelimb preference. Pellets are placed on steps (Figure 1-1), the top steps being easiest to reach by the rat, the rat stands on the beam and reaches down to pick up the food pellets. Once the top pellets have run out, the rat has to reach lower to the harder to reach steps. The paw reaching apparatus provides a number of variables; trajectories of paw reach, speed in which the rat reaches for the pellets and upper body orientation

within the apparatus. This approach could possibly be incorporated within a motion capture system.

Unlike the cylinder and the open field tests, the setup could be modified for human testing. An initial design is shown here in Figure 1-2 the subjects would sit on the chair with their hands reaching to collect pellets on the steps, similarly, the top ones being easiest to reach.



Figure 1-1: Staircase paw reaching apparatus from the Cardiff Brain Repair Group

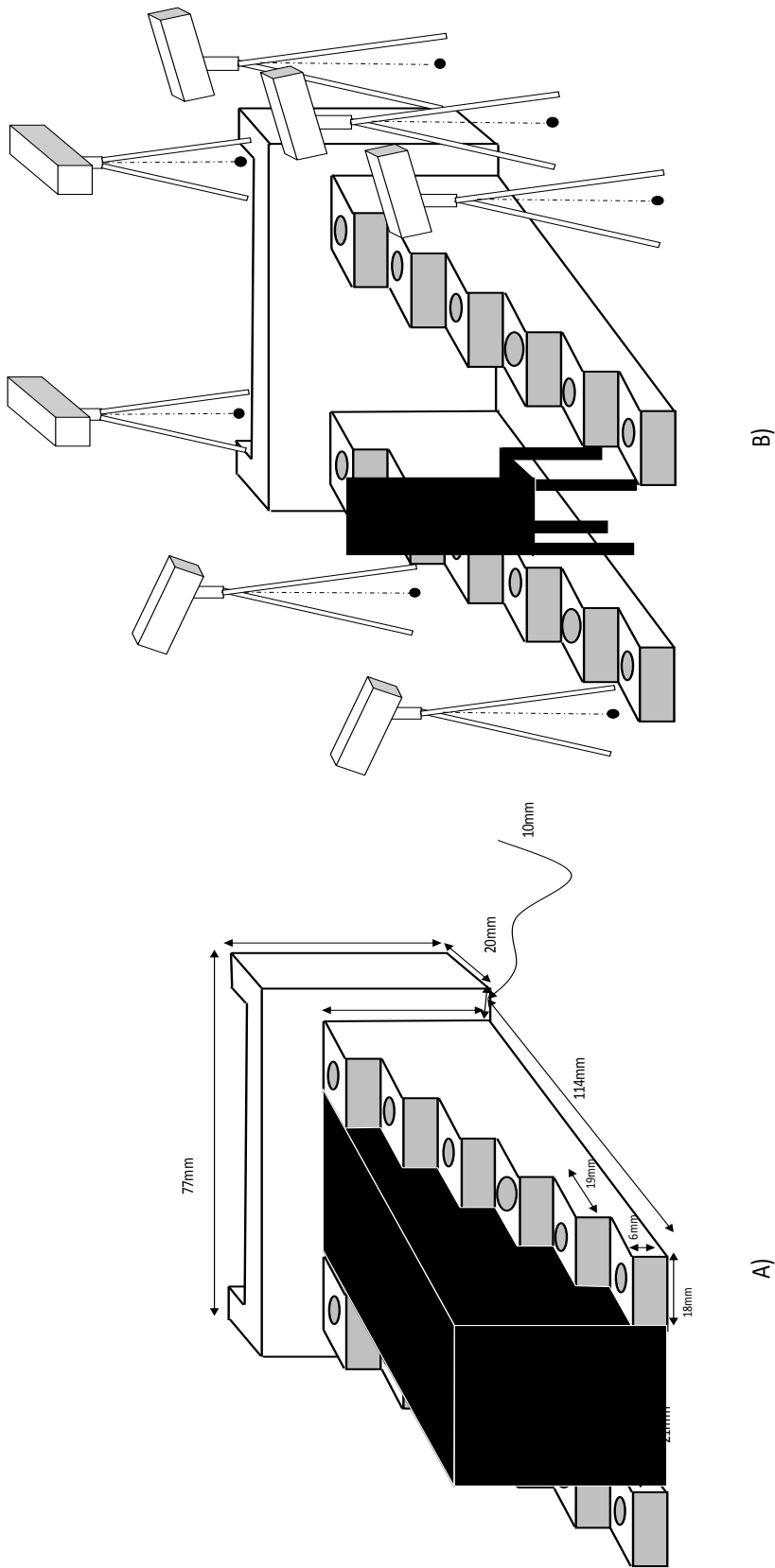


Figure 1-2 :Initial design to mimic the staircase apparatus to be used test human reaching (A) rat apparatus (B) interpreted human apparatus

A pilot project that assessed reaching of five volunteers was carried out with a simplified apparatus shown here in Figure 1-3. Although human data acquisition was possible, the rat motion capture attempt introduced difficulties in data acquisition in that the Perspex glass hindered accurate representation of the data post analysis, and removing the glass meant losing the variables for the animal study.

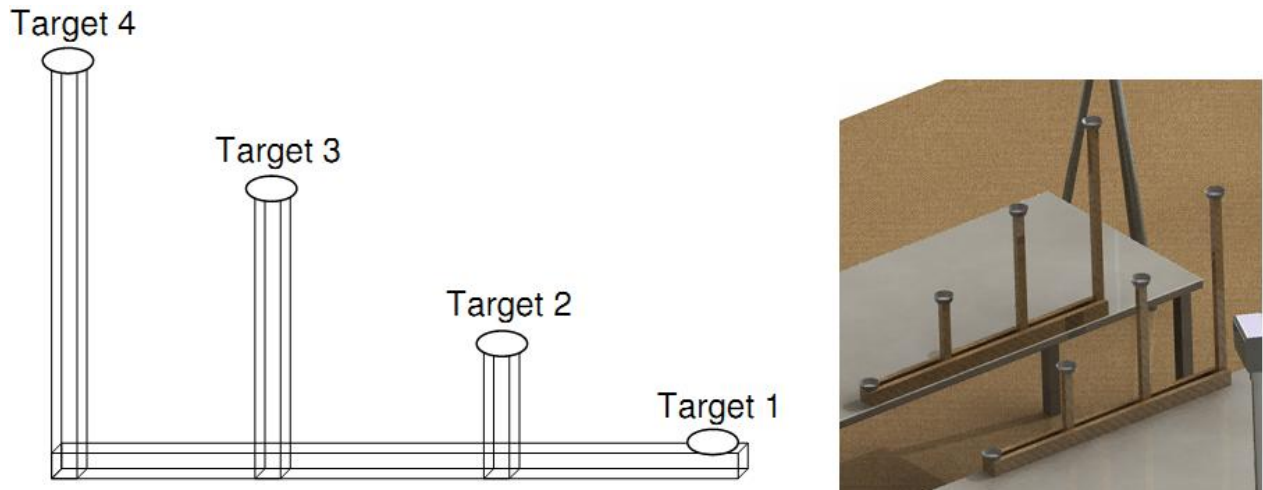


Figure 1-3: Human reaching experiment design carried out while the subject was standing

Two further experiments were investigated for rat data collection. The accelerating rotarod (Ogura et al., 2005) and the balance beam (Allbutt et al., 2005, Goldstein et al., 1990, Domingo et al., 2009) test. The two apparatus (Figure 1-4) assess balance and coordination as the rat walks. The rotarod tests motor coordination and balance as the rat walks at the same speed that the bar is rotating and while it balances at the top. As the speed gradually increases it becomes harder for the rat to stay on, and so may fall off onto a trigger plate which stops the timer so the length of time the rat is able to balance is recorded. This is however difficult to translate to a human study and limited variables can be collected using motion capture techniques.



Figure 1-4: Beam and rotarod apparatus

The balance beam on the other hand, involves walking in a straight line on a defined length and width which can be performed by human subjects. In the animal test, following training, the rat is placed on one end of the beam and walks along to the other end on a beam where a dark box that contains treats is located. Healthy rats perform the task without difficulties; however rat models will find it harder to balance and may have to take more steps along the beam so the total time taken to reach the end will be greater.

At the Cardiff BRG the beam used is graduated, the beam gets narrower as the rat approaches the box making the task harder the closer they get to the end. This helps to distinguish the differences between healthy and transgenic rats as the transgenic rats may lose their footing as they get closer to the end. This test introduced a number of variables that could be analysed using the motion analysis system. Furthermore it allowed translation into a human study of balance and coordination during gait.

The elevate beam was chosen to carry out the project. The next steps of the study experimented on different scenarios in order to establish the best motion capture setup for the study. This included camera and marker protocol for optimum system potential. Ideally marker placement needed to be non-invasive and representative of the rats' movements being investigated. The placement method had to be repeatable and accurate. The tests limitations and accuracy are summarised in Table 1-1.

Table 1-1: assessment motor behavioural test available at the Cardiff BRG

Motor task behavioural tests	Limitation	Accuracy	Cost in addition to motion capture equipments
Open field test	Rat's keeps stopping to groom or feed and with no motivation to walk in a straight line Can't be translated to human study	gait is not cyclic therefore unable to achieve accuracy	Price of open field
Cylinder test	No motion capture variables Can't be translated to human study	Rat movements are not constant	Price of Perspex glass
Paw reaching	Limited amount of variables, and hindrance of the Perspex glass	Accurate in determining upper body motion of human but not accurate in the rat study	Price of stair apparatus
Accelerating rotarod	Can't be translated to human study	Accurate timing parameters	Price of the rotarod
Elevated beam	Elevation can't be translated to human study but width and length can		Price of elevated beam

In rat studies, the skin movement artefact, where the skin displaces relative to the bones and soft tissue movement reduces the accuracy of marker placement studies Muir and ebb (2000) and Filipe et al., (2006) quantified the magnitude of skin displacements during marker based motion analysis studies. Filipe et al., (2006) collected data from 10 Wistar adult rats and performed kinematic recording using a marker based motion system on the lateral side on the left hindlimb. They found there is a considerable skin movement artefact by comparing the knee marker and the knee position estimate during a step cycle. It was concluded that these large

errors can decrease data reliability in the research of rat gait analysis. With this in mind, the protocol development focussed on achieving relative motion and trajectory data rather than joint motion. The protocol, including marker choice and placement are discussed in Chapter 2.

The initial stages of the study investigated the various potential experimental protocols based on the behavioral test used at the Cardiff BRG. As described, the paw reaching test did not produce sufficient data for analysis therefore the apparatus chosen was the balance beam. In addition marker placement techniques were explored and a technique was designed that investigated relative motion rather than joint motion during gait.

The results of the current research project have an impact in the area of animal brain studies as it allows for further validation of the animal models. The study provides a basis for correlation of gait data and thus proof of homology with human patients (Whishaw et al., 1992, and 2002). As a result, a better understanding of therapeutics and treatment plans can be achieved.

The first Chapter presets a brief background as to why animal models are important in brain research; how the brain controls movement (more specifically, gait); and what happens when the control processes are disrupted, with focus made on PD and stroke. A detailed review, providing insight into current research carried out in the areas of gait analysis of PD and stroke for both humans and animal models of the disease is provided. The remainder of the chapters introduces a novel 3DMA protocol for quantifying locomotion in rats and humans followed by the results from studies carried out on two separate groups of rats (PD and Stroke) and one group of healthy humans.

1.2.2. Rat models

Different types of neurological disorders are induced in healthy animals with rats being the most commonly used species. Despite rats having a brain that is 15 times smaller than the human brain, they have similar neurological, sensory and motor systems to humans (Whishaw et al., 2003a). However, the question remains whether “artificially induced” rat models are accurate representative models of the real naturally occurring disorder observed in humans. This is a dilemma that has been a topic of much debate for many years and requires careful analysis of behaviour and function for each disorder under study. Although not all aspects of the modelled neuro-degenerative disorders can be investigated, these models are useful as they exhibit similar motor behaviour to patients with the disease.

1.2.3. The Gait Cycle

A gait cycle is the sequence of events from the time a limb is in contact with the floor to when it comes into contact with it again i.e., heel strike to heel strike. It is divided into stance and swing phases (Figure 1-5).

1. Stance phase: The term used to designate the entire period of time during which the foot is on the ground. It begins with initial contact (heel strike) followed by limb flexion to support body weight and finally extension to push the body forwards.
2. Swing phase: The time the foot is in the air from limb advancement. It begins when the foot is lifted from the floor (toe off); followed by the limb moving forwards relative to the body and finally extends in preparation for contact with the ground (heel strike).

A full gait cycle is described as one stride. A stride consists of two steps; defined as the interval between initial contacts by the left then the right foot. The rates of repetitions of a stride are a primary determinant of gait speed with a relationship that is linear in healthy individuals. The steps, rather than the strides, are counted to determine the step rate known as the **cadence**. Gait Parameters i.e., **stance time**, **swing time**, **stride length**, **speed** and **cadence** are important variables used to characterise normal and pathological gait.

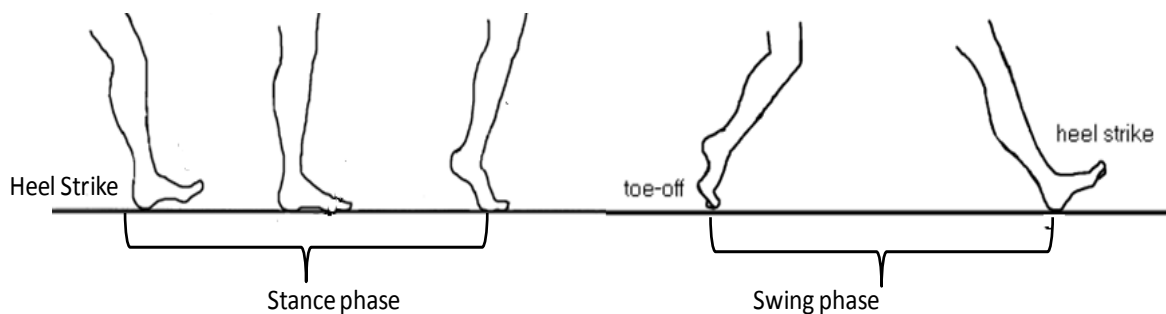


Figure 1-5: One human gait Cycle

In the assessment of one gait cycle for rats, the limb that moves from heel strike to heel strike at a given period of time is known as the “*reference limb*”. During stance phase, the reference limb flexes to support the rats body weight (heel strike), then extends to push the rat forward (toe off). The limb then enters swing phase where it moves forward relative to the length of the rat’s body and finally extends in preparation for contact to the ground for the subsequent stance phase (Whishaw and Kolb, 2005).

Normally 60% of the cycle for both rats and humans represents the **stance phase**; and the remaining 40% is represented by the **swing phase**. The timing slightly varies depending on the speed. The relationship between speed and phase time is inversely related; that is, both total swing time and stance time are shortened as gait

speed increases. In humans there is an interval when both feet are in contact with the ground known as double stance, but is reduced with faster walking and is eventually eliminated when the person is in running mode.

In rats, the stance phase shortens with increasing speed where as swing phase changes very little. Unlike humans walking, rats maintain a crouched limb posture at all speeds providing increased stability. Limb coordination changes with speed; walking is defined at <55cm/s, trotting at 55-80cm/s and galloping at >80cm/s (Gillis and Biewener, 2001). In the current studies only walking was investigated.

1.2.4. Postural control during gait

Posture is defined as the orientation of a body segment. This can be relative to the gravitational vector coordinate system (angular measure from the vertical axis) or to the 3D orthogonal vector system. Maintaining posture in a defined reference system relative to the gravitational vector is important for stability during gait (Winter, 1995). During human gait, muscle action of the neck and trunk serve to maintain orientation and neutral alignment of the spine, while the pelvis acts as the link between the trunk and the mobile unit made up of the two limbs. Muscles in the pelvis help move the pelvis asynchronously in all three planes during gait; *roll* in the sagittal plane, *pitch* in the frontal plane and *yaw* in the transverse plane to maintain balance especially during single limb support.

A common symptom of patients with deficient motor function is postural instability. The term defines the inability to control the orientation of body segments relative to the gravitational vector (Bishop et al., 2006, Rochester L Fau - Hetherington et al., 2004). Research into posture during gait is helpful in revealing data that may help in predicting fall risk and in documenting recovery of stability (Woollacott and

Shumway-Cook, 2002, Adkin et al., 2005). The current study investigates body angular rotations as an indirect measure that can be quantified to analyse postural instability (Madete et al., 2011). Similar parameters during animal gait that are used to monitor subtle changes in posture can be applied.

1.2.5. Brain function during gait

The mechanisms that allow the complexity of human and rat gait cycles to occur flawlessly in the coordination of movement of all the limbs occurs in the brain. Brain function underlying motor control is divided into multiple processing levels that include the spinal cord, the brain stem, the cerebellum, the cerebral cortex and the basal ganglia (Figure 1-6).

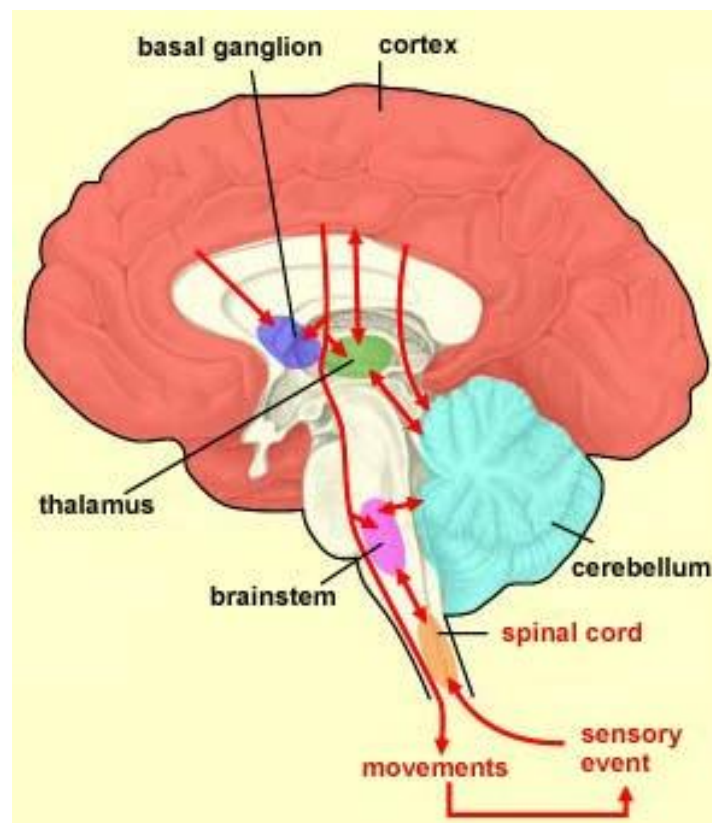


Figure 1-6: The cross section of a brain; the cortex, the brain stem and the spinal cord are the three main levels of control within the central nervous system (adapted from Dubuc, 2002)

The cortex, the brain stem and the spinal cord are the three main levels of control within the central nervous system. During movement, signals pass from the brain's cortex, via the brain stem and spinal cord, to the muscles, which then contract. Other signals pass to the basal ganglia and the cerebellum to either damp or increase the pathway signal thus modulating movements, as illustrated in Figure 1-6. A disruption of any of the systems involved in movement results in abnormal human gait, where it may lead to neurodegenerative conditions and movement disorders such as those exhibited in PD and stroke.

1.2.6. Parkinson's disease

Parkinson's disease (PD) is the second most common neurodegenerative disorder after Alzheimer's, affecting at least 2% of the population aged 65 years and older (de Lau and Breteler, 2006, Gotz and Ittner, 2008). PD is caused by the degeneration of substantia nigra, a structure located in the basal ganglia, resulting in loss of dopamine. Dopamine is a neurotransmitter that damps the signal pathways to reduce muscle tone and allow smooth movements (Field et al., 2006). This loss of dopamine leads to symptoms such as muscle tremors, rigidity, slow movements and difficulty initiating physical activity (Penney and Young, 1983). Many symptoms expressed in PD are progressive and it may take between 5 and 20 years for a patient to exhibit all of these symptoms.

1.2.6.1. How PD affects gait in humans.

Abnormal gait caused by PD is characterised by a short stride length, a reduced walking speed, an abnormal cadence and a leaned forward trunk (Van der Burg et al., 2006). Impaired gait causes instability in patients that affects their ability to adjust their walking patterns. This in turn leads to an impaired forward motion and to an

increased risk of frequent falls. This imbalance eventually results in a decreased executive function leading to a condition known as “freezing of gait” (Plotnik and Hausdorff, 2008, Woollacott and Shumway-Cook, 2002). Therefore, PD patients tend to walk with a more cautious gait exhibiting compensatory behaviour in an attempt to improve their stability (Latt et al., 2009, Woollacott and Shumway-Cook, 2002).

The cause of neuro-degeneration is not known and therefore current available treatments target the symptoms and aim to bring support and comfort to the patient. Most treatments are still in their infancy and with an aging population; there is an increased need for research to further understand the disease.

1.2.6.2. How PD affects gait in rat models

Animal models of PD have been developed to exhibit characteristics similar to those found in patients, e.g. shorter steps and reduced toe clearance which reflects shuffling of gait in humans (Metz et al., 2005, Klein et al., 2009). To investigate the clinical condition of PD, the most commonly used model is the unilateral injection of the neurotoxin 6-hydroxydopamine (6-OHDA) into the rat medial forebrain bundle (MFB) ;(Ungerstedt, 1968). This injection produces dopamine depletion that results in motor deficits that are similar to those in human PD (Cenci et al., 2002, Henderson and Watson, 2003, Iwaniuk and Whishaw, 2000, Whishaw et al., 1992).

Unilaterally lesioned (hemi-parkinsonian) rats show motor deficits on the side contralateral to the lesion. The ipsi-lateral side serves as an internal control. Furthermore, these rats show an almost complete neglect of the contra-lateral side, and conversely, they are more responsive to stimuli on the ipsi-lateral side. Body weight bearing and body posture are compensated with the healthy ipsi-lateral side (Miklyaeva et al., 1995).

1.2.7. Stroke

A stroke is caused by an interruption of blood supply to the brain due to blocked or damaged arteries (anterior, middle and posterior) or their branches. An estimated 150,000 people suffer from stroke in the UK each year and it accounts for around 53,000 deaths per annum (Wolfe et al., 1996). Over 300,000 people are living with moderate to severe disabilities following a stroke, such as severe loss of motor control and language (Adamson et al., 2004).

Strokes are either ischemic (80% of population) or haemorrhagic. Following an ischemic stroke, a blockage of the vessel causes the surrounding tissue to be affected leading to a complex set of events, (Kolb and Cioe, 2000). The location and extent of the damage in the brain plays an important part in determining the observed behavioural and functional symptoms (Van der Staay et al., 1996, Corbett and Nurse, 1998). Stroke symptoms affect only one side of the patient (depending on what side of the artery is blocked) and can be reduced with good post stroke rehabilitation (depending on the age of the patient). Ischemic stroke can be treated pharmacologically up to 3 hours from the episode occurring by reducing the size of the clot to allow blood to flow to the affected region. Post stroke rehabilitation is the only alternative after the 3 hour window.

Haemorrhagic stroke occurs when weak vessels have aneurysms that eventually rupture, mostly due to symptoms of hypertensive small-vessel disease. In some cases, underlying problems such as vascular malformations or infarcts into which secondary haemorrhage has occurred, may lead to stroke. The prognosis is worse than ischemic, with a 1 month mortality approaching 50% (Donnan et al., 2008, Auer and Sutherland, 2005).

1.2.7.1. How Stroke affects Gait in humans

Similar to PD patients, spatio-temporal gait and posture are affected. Patients walk more slowly than average healthy subjects. Their gait cycle is characterised by a low stride length, low cadence, a longer stance phase, an increased double support times and toe drag during the swing phase (De Bujanda et al., 2004, Olney et al., 1994, Shumway-cook and Woollacott, 1995). Unlike PD, stroke symptoms affect only one side of the patient and can disappear with good post stroke rehabilitation (depending on the age of a patient).

The characteristics of human ischemic stroke are very diverse, where the location of the damage plays an important role in determining the observed symptoms (Van der Staay et al., 1996, Corbett and Nurse, 1998). This thesis focuses only on ischemic stroke of the middle cerebral artery (MCA), as this is the most frequently occluded artery in humans and is the most common model used in rodents. The lack of blood supply caused by the blockage of the MCA, causes damage to the largest branch of the internal carotid which supplies a portion of the frontal lobe, the lateral surface of the temporal and parietal lobes, including the primary motor and sensory areas of the face, throat, hand and arm and in the dominant hemisphere, the areas for speech.

1.2.7.2. How stroke affects gait in rats

This thesis considers a focal model known as MCA occlusion (MCAO) model, where a reversible occlusion around the MCA was performed. MCAO is a good representation of the pathology observed in human stroke victims and results in motor deficits similar to those in human stroke and is applied to only one brain hemisphere leading to a left-right motor imbalance. Therefore motor deficits are observed on the side contra-lateral to the occlusion. The duration of the MCAO can

be as short as 30 minutes (Shen and Wang, 2010) although some studies perform it for as long as 3 hours (Lim et al., 2008). There are advantages and disadvantages to the difference in duration of the occlusion. The longer the duration the larger the infarction caused. This difference can be seen in both pathology and behaviour, i.e., motor deficits increase with an increase in the infarction size (Wegener et al., 2005).

1.3. Literature Review

In the following sections, a literature review of the studies that have used two dimensional (2D) and 3DMA techniques to analyse gait on human patients with PD and stroke and associated animal models are described. The review also discusses methods used to quantify temporal gait and posture of both species.

1.3.1. Human based motion analysis

Clinical human gait analysis plays an important role in understanding the pathology of various diseases. In the early nineties, motion was quantified using a carefully designed apparatus to assess gait in terms of stride by stride analysis. Blin et al., (1990)) used a device attached to the foot to measure longitudinal displacement of both feet during locomotion and function to assess gait in subjects with PD. Each foot was attached to a separate string as the subject walked down a pulley system. Movement was recorded in the form of an electric signal via a pulley linked to a potentiometer. Variables were measured over 10m and included stride length, gait cycle, stance, swing, double support times, stride, and swing velocity. They found that PD patients had significantly shorter stride length and a longer stride time differences compared to an aged matched cohort. The method used was simple and practical; however the strings attached to the feet may have caused discomfort and as a result normal gait might not have been achieved.

With technological advances; current methods such as incorporating sensors, foot switches, and reflective markers combined with high speed cameras and computer systems for analysis; the same level of practicality can be achieved. In addition these methods produce data with an increased sensitivity and accuracy.

Sensors allow mobile and wireless clinical gait analysis. Takeda et al., (2009) used sensors that consisted of wearable units placed on the lower limb of the patients (both thighs and both shanks). The advantage of this system is that one sensor unit can measure the acceleration and the angular velocity along three orthogonal axes simultaneously. The study goes further to investigate the difference between sensor placements with a marker placement system and found that there was a high correlation (values of above 0.72.) between the two. However, their study did not investigate cyclic gait over a long period of time and it assumes constant velocity which is not true, especially with patients that have difficulties in gait.

Foot switches are a convenient and inexpensive way of obtaining temporal and pressure based gait measurements. They work by either compression closing or using force sensitive resistor switches, usually configured as thin insoles. They can be placed between the foot and shoe or taped to the bottom of a bare foot. Bond and Morris, (2000) investigated the effects of goal-directed secondary motor tasks on gait in healthy subjects and subjects with PD using foot switches. Patients walked on a 15m walkway and motion was measured in three conditions; preferred walking, walking whilst carrying a tray, and walking whilst carrying a tray with four glasses. The spatial and temporal characteristics of the foot pattern were measured using commercially available clinical stride analyser, which consisted of insole switches placed under the heel with the data logger placed on the waist. They found that PD patients walked slower, had shorter steps and whilst carrying a tray with four glasses on it, they were slower and showed a deterioration of gait compared to the other two scenarios. This study showed that gait analysis provided accurate representation of data and allowed for a comparison between two cohorts on three different scenarios.

A force plate measures the ground reaction forces (GRF) exerted during stepping, which is a measurement used to determine joint forces and moments. Using GRF as a variable for gait analysis provides a measure of how well the subject handles weight bearing and balance. It can be monitored by using force plates or in sole devices. A study by Chastan et al., (2009), performed a biomechanical analysis to monitor gait and balance disorders in PD patients to observe their ability to actively brake the fall of centre of gravity. The step length, peak progression velocity of the first step, and vertical velocity of the centre of gravity using force platform was measured. The study found that the decreased step length and velocity, characteristic of PD, mainly result from degeneration of central dopaminergic systems. The results from this study, combined with clinical evaluation showed the strength of MA as a vital research tool for bio-scientists. The data obtained from such studies can be used for further calculations of measuring new parameters such as the braking capacity, which is important when assessing risks of falls and postural stability associated with PD patients.

Another method used to acquire force data is by using force insoles or gait mats. Hausdorff et al., (1998) investigated stride -to- stride variations of the gait cycle in PD patients and in Huntington's disease patients (HD). The subjects walked with a normal pace up and down a 77m long hallway for 5 minutes. A self determined pace was chosen for the healthy subjects because walking variability was minimised. Gait parameters were measured using force sensitive insoles that produced a measure of the force applied to the ground during gait. The variables measured were stride time, swing time, percentage swing time, double stance, percentage double stance and step time and gait speed. They found all measures of stride-to-stride gait variability

were significantly increased in PD patients to those observed in control subjects and the degree of variability correlated with disease severity (Hausdorff et al., 1998)

1.3.2. 3D Marker Based Human Motion Analysis

Calculation of both gait and posture requires 3D techniques where coordinate data is transformed into accurate positions and locations of segments and bodies. 3DMA comprises of two or more video cameras to track reflective markers placed on a subject. Provided 2 or more cameras record a markers location, 3D coordinates can be calculated. 3DMA has been shown to be practical and accurate in determining temporal and postural gait in healthy subjects and patients with neurodegenerative disorders (Jansson et al., 1998, Sofuwa et al., 2005).

3DMA studies on PD patients have investigated changes in motion following rehabilitation and have attempted to understand the characteristics of early onset PD (Peppe et al., 2007, Ferrari et al., 2008). Studies also include those that have investigated the effects of different treatments and therapeutic solutions (Jansson et al., 1998, Sofuwa et al., 2005)

Ferrarin et al., (2006) tested onset PD patients and their controls following a protocol consisting of 3 different tests which were, steady-state walking, turning while walking and initiation of gait. A force platform was positioned in the middle of a long walkway to record foot ground reaction force during walking. Kinematics data was recorded using an optoelectronic system consisting of 9 cameras located around a calibrated volume with a sampling rate of 60 Hz. They found that although PD patients did not differ from controls in steady state walking, significant differences emerged in gait initiation and turning strategies and therefore small differences in gait were quantified.

Peppe et al., (2007) quantified motion following rehabilitation of PD disease patients using 3DMA. They found that marker based MA highlighted a statistically significant difference between controls and PD patients, or in the same PD patients before and after the motor rehabilitation program. They confirmed that gait analysis provides objective outcome measures of a rehabilitation program

Jansson et al., (1998) compared single dose effect of two different forms of 200 mg l-dopa on the motor performance of eight patients with PD. Patients had gone without their ordinary anti-parkinsonian medication and food intake for 12 hours prior to testing. The patients' motor performance was recorded with an opto-electronic camera system. They found that the dispersible drug has a much faster and more constant onset of action than the standard drug preparation (25 vs 46 min.). The effect duration and the effects on motor performance were otherwise the same. Similarly, Sofuwa et al., (2005), compared gait parameters in PD patients during the on-phase of medication cycle with those of healthy elderly control subjects. They found that the PD patient's spatiotemporal results showed a significant reduction in step length and walking velocity compared with the control group.

Stroke studies place their emphasis on the effects of post-stroke rehabilitation. 3DMA is a valid tool for evaluating changes in patients with stroke as the therapy progresses by monitoring of patients after various motor rehabilitation programs (Yavuzer et al., 2008, Peppe et al., 2007, McCain and Smith, Mulroy et al., 2003). McCain et al., (2008) investigated the impact of locomotor treadmill training as a form of rehabilitation after stroke. They measured increased knee flexion during swing and absence of knee hyperextension in stance. In addition, more normal ankle kinematics at initial contact and terminal stance were observed following the rehabilitation

regime. Improved gait symmetry was confirmed by measures of single support time, hip flexion at initial contact, maximum knee flexion, and maximum knee extension during stance. This study concluded that application of locomotor treadmill training with partial body weight support before over ground gait training may be more effective in establishing symmetric and efficient gait in adults' post-acute stroke than traditional gait training methods in acute rehabilitation.

In a study by Jonsdottir et al., (2009), 39 adults were analysed to investigate the effect of speed on gait. They aimed to understand the underlying dynamic resources that determine an individual's speed of walking by performing quantitative gait analysis. The marker based gait analysis system was coupled with a force platform and an Electromyograph (EMG) system. Patients walked at two speeds: their preferred speed and as fast as they could. They found that at both speeds, stroke individuals tended to walk at higher cadence and with shorter stride length. At the preferred speed the investigated parameters for all patients were mostly within the normal profile. The results indicate that to increase gait speed, patients with loss of function on one side (hemi-paretic) have different functional resources needed to produce work of the ankles and hips compared to healthy subjects to draw from, and these vary from individual to individual. This study shows that 3DMA can be used to investigate cadence, stride length and enable discrete difference in function to be quantified.

Temporal and spatial parameters may be acquired simultaneously in different situations using 3DMA (Nadeau et al., 1999, De Bujanda et al., 2004). Lateral displacements and lateral acceleration of the shoulders and pelvis of hemi-paretic patients was assessed (De Bujanda et al., 2004). Three walking speeds were tested:

slow, natural, and fast speeds. They found that stroke patients had larger lateral displacements and accelerations compared to the control group when walking at similar speeds. Results also indicated that accelerations were greater on the affected side, whereas single stance percentages were greater on the non-paretic side. The data were almost symmetric for the control subjects.

Numerous variables can be investigated using MA; which vary depending on the nature of the study. Nadeau et al., (1999) combined the use of marker based analysis with force plate data to determine whether plantar-flexor weakness is among the factors preventing stroke subjects from walking at faster speeds. On the contrary, Roerdink and Beek, (2011) sought to understand directional variations in step-length asymmetry in terms of asymmetries in forward foot placement relative to the trunk and trunk progression.

1.3.3. Non -marker based rat motion analysis

Animal MA studies dates back to the early 19th century, where a photographer named Muybridge was commissioned to prove the concept that horses have all hooves off the ground during a gallop using a 12 still camera system (Muybridge, 1899). Studies on animal MA were generally limited to two planes and post analysis was laborious and time consuming as it involved frame by frame analysis and digitising to visualise the motion. Currently, dynamic animal studies using different apparatus, e.g. ladders, treadmills or flat surfaces are well established (Couto et al., 2008b, Canu et al., 2005). The data acquisition techniques vary depending on the output and parameters under investigation. Both 2D and marker based 3D methods of analysis have advantages and limitations depending on the required outcomes and their application.

Most 2D rat gait studies use the principle of paw contact analysis. The simplest approach is paw print analysis where ink is painted on the paws of the animal as it walks along a marked path (Brown and Taylor, 2005, Fan et al., 2008, Ackland et al., 2010). This approach provides instant and visible paw contact and the ability to produce temporal gait parameters of all four limbs simultaneously (Figure 1-7). However, faint footprints may be produced when affected paws are un-weighted and smearing may also occur caused by toe drag (Wang et al., 2008).

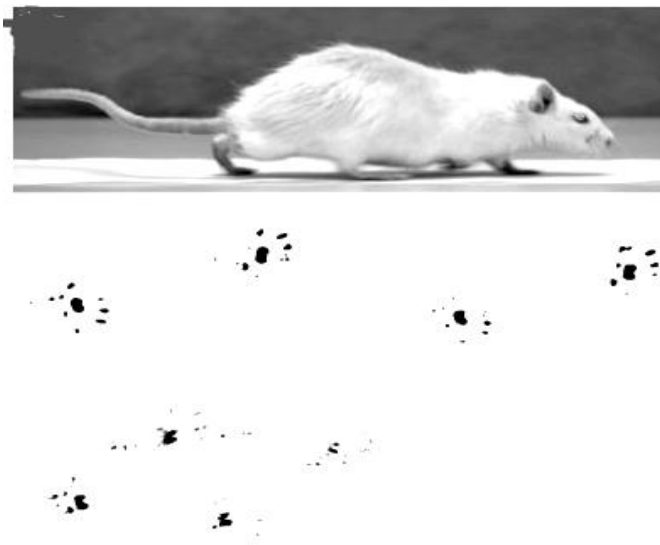


Figure 1-7: Example of paw print analysis from Metz et al 2005

Recently footprint analysis has been computerised in the form of the CatWalk method, an example output is illustrated in

Figure 1-8. CatWalk is a program based technique, which has been found to improve paw contact analysis (Koopmans et al., 2007, Hamers et al., 2006, Vrinten and Hamers, 2003). Movement is recorded in a specialised chamber thus limiting versatility of the environment; therefore movement cannot be performed on a ladder or a beam.

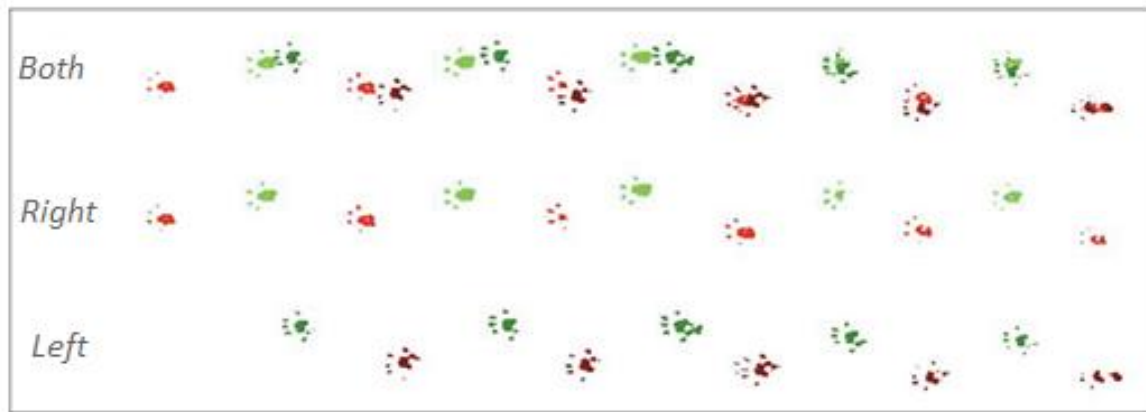


Figure 1-8: Catwalk output example from Hamers et al in 2006, the colours are normally assigned by the program, Green= right, Red= left, light = fore and Dark = hind.

Rat gait studies that do not involve ink printing or CatWalk, such as the one carried out by (Coulthard et al., 2002), record the gait cycle as the rats walk along a Plexiglas chamber fitted with a central glass floor that has a mirror which allowed paw-floor contacts to be viewed at the same time as conventional lateral animal motion. Coulthard et al used video data acquisition method (camera's frequency of 25 frames per second) to convert the number of frames for which a particular event was into a period of time in seconds. Therefore, temporal parameters such as stride length, stride time, swing time, single stance time, and the dual stance time can be analysed.

Other technologies include the use of Tekscan pressure mat systems (Tekscan, South Boston) to monitor deviations in gait (Boyd et al., 2007). Using the pressure of the rat's paw when in contact with the mat, the system allows gait analysis from in built sensors on a Plexiglas tunnel to record the force applied as the animal walks. Another specialised gait analysis tool is Treadscan, (Clever Sys. Inc. Reston, VA, USA). It allows the calculation of stance time, swing time, stride length and running speed as the animal runs on a transparent treadmill (Simjee et al., 2007).

The use of 2D MA techniques to investigate rat gait parameters are favoured since only one inexpensive camera is used and less data needs to be acquired. This review shows that 2D analysis techniques that combine the use of technologies in conjunction with already existing behavioural studies improve their accuracy and repeatability. Nevertheless, these motion studies fail to measure important variables; such as orientation in 3D space and relative motion of segments and bodies that are essential for determining asymmetry, instability and postural control during gait (Couto et al., 2008).

1.3.4. Marker based rat motion analysis

Temporal and postural parameters in three planes can be recorded using 3DMA techniques thus increasing the scope of the amount of variables that can be used to investigate a given function and behaviour. It is a useful method to determine limb motion during locomotion as it allows the quantification of locomotor parameters, which are only qualitatively evaluated by visual examination (Canu et al., 2005).

3DMA techniques reviewed earlier for human MA are not commonly used for animal locomotion because unavoidable skin movement artefacts, that affect the accuracy of the measurements, leads to the need to shave the fur off animals, making the procedure invasive (Filipe et al., 2006). Nevertheless, previous studies have successfully (

Figure 1-9) used this method to investigate temporal and spatial parameters as well as angular displacement of joints during locomotion in versatile environments (Garnier et al., 2008, Metz et al., 1998, Canu and Garnier, 2009, Canu et al., 2005, Couto et al., 2008b).

Metz et al., (1998) described the effects of a brain occlusion on hindlimb function. They observed severe impairments in trunk instability, lateral shifts in weight support, toe dragging, and hindlimb exo-rotation. Their study stressed the need for extremely sensitive methods, such as 3DMA, and sensitive behavioural tasks to enable detection of parameters for hindlimb function.

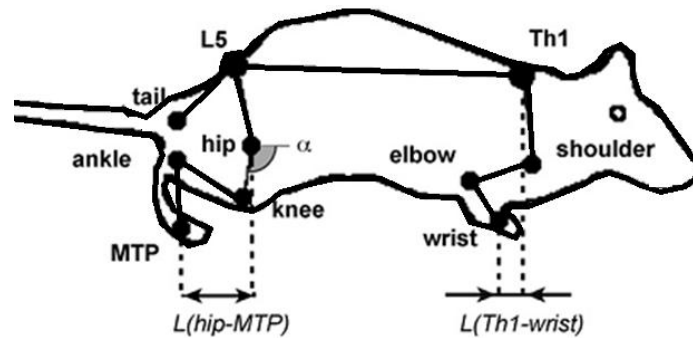


Figure 1-9: Successful marker placement on rats in a study by Garnier et al 2008.

Couto et al., (2008b) used marker based MA to determine hind limb kinematics on a treadmill for spinal cord injured rat models. They used 2mm hemispheric markers, covered by adhesive reflective tape. The markers were placed on the skin over five anatomical landmarks on the lateral side of the left hind limb. Kinematics data was collected after shaving around the left hind limb to improve the visual image obtained for analysis. The set up, shown here in Figure 1-10, included three high-speed digital cameras strategically positioned around the left hindlimb to minimize marker occlusion and maximize resolution. The angle measurements were taken at the flexor side of each joint. They found significant difference between 2D data and 3D joint angular motion. They concluded that maximal precision and accuracy of the kinematic data in 3D and also found that 2D methods cannot be used to determine the external or internal rotations of the foot because this movement occurs in the transverse plane.

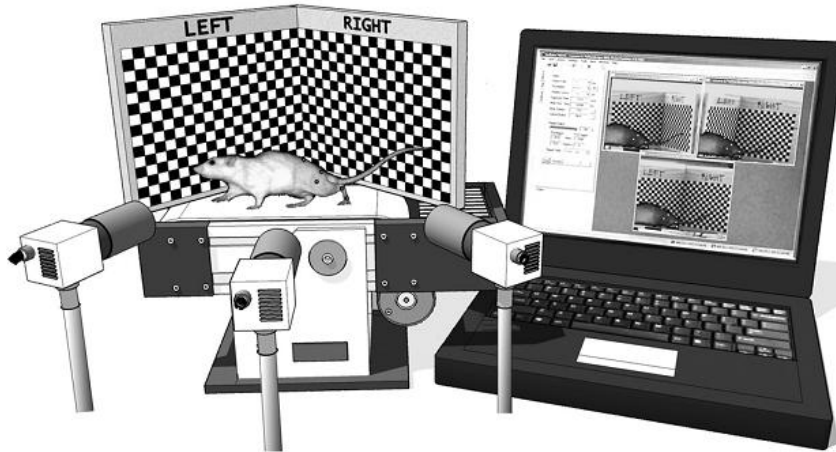


Figure 1-10 : Experimental set up for (Couto et al., 2008b); three high speed cameras were positioned around the hindlimb to minimize marker occlusion and maximise resolution. Reflective markers placed on the left hindlimb of the rat are shown.

Garnier et al., (2008) studied qualitative and quantitative locomotion characteristics in different modes of locomotion. They performed a 3DMA kinematics analysis of both hind and forelimb during over ground and ladder walking. Movements of the right hind and forelimb were evaluated using a 3D optical analyser, and EMG of the soleus and tibialis anterior muscles was synchronously recorded. Their results showed that kinematic and electro-myographic characteristics of locomotion are dependent on the type of support and that changes were more obvious for hind-limb rather than for fore-limb. In addition, they also found that velocity and stride length were lower on the ladder than on the runway.

As the literature above suggests, measurements and apparatus vary depending on the condition and behaviour being investigated. It emphasizes the need of a simple and practical 3DMA analysis protocol that can be modified according to the experimental conditions by improving on the more simple approaches and simplifying more invasive ones.

1.4. Aim and Objectives

Animal models of neurological diseases are commonly used to test new therapies as well as to understand behaviour and function following an onset of the neurological disease. **The aim of this thesis was to develop a practical, non-invasive and sensitive three dimensional motion analysis technique to investigate animal and human temporal and postural gait parameters.**

To achieve this, four key objectives were explored:

1. Development of a novel technique for the measurement of temporal and postural parameters of an animal model of Parkinson's disease.
2. Application of the developed technique on an animal model of stroke, and the utilisation of the classifier, based on the Dempster-Shafer theory, for data processing to characterise stroke model gait.
3. Expansion of the novel technique for the analysis of temporal and postural parameters of humans.
4. Correlating temporal and postural parameters of the animal and humans from the developed protocols.

This thesis describes the first study to emerge from links established between Cardiff School of Engineering and the School of Biosciences' BRG. It is hoped the outcomes will contribute to the validation of the rat as an animal model of PD and stroke and further increase understanding of the diseases in terms of behaviour and function during gait.

1.5. Thesis Summary

The use of motion capture at MAL Cardiff School of Engineering has long been associated with orthopaedics research, especially in the classification of osteoarthritic knee function. In the last few years, the research has included gait analysis after total hip replacement, functional analysis of the shoulder complex and the quantification of skin deformation. The MAL performs MA studies using Qualisys motion capture system (Qualisys, Sweden) to record human movement data. The set-up comprises of optoelectronic cameras and tracking software that allows fast and precise collection of 3D and 6DOF data in real time.

The study applies an available animal behavioural test, established in the BRG lab, in combination with MA techniques, used at the School of Engineering to develop a protocol that analyses animal model behaviour, whilst being translatable to human data collection. The chapters of this thesis are designed to demonstrate the use of the developed MA protocol in the data acquisition of rats and humans during over-ground locomotion in 3D.

Chapter 2 introduces the 3D marker based MA methods that were used to measure locomotion along an elevated beam for the animal models and the healthy human cohort. Data was collected in two laboratories and processed using Qualisys (Sweden) proprietary software, Qualisys Track Manager, and a custom developed software in Matlab (Mathworks, USA) and C++ (eclipse platform). Gait was presented in terms of temporal distance parameters and kinematic waveforms for the postural rotations during locomotion. In addition, a description of the DS classifier

method to further investigate changes in gait following MCAO lesion and graft are also described in this chapter.

Initial protocol development began with a cohort of five rats that were models of HD. They were used to test the possibility of using the MA system to measure a rat's gait cycle while walking on an *elevated beam*. The elevated beam is an established apparatus that is used to monitor foot falls and posture during gait. The results from this initial study were inconclusive. However, the process revealed the many obvious challenges of working with animal models and that the elevated beam was an ideal apparatus for gait analysis.

Chapter 3 presents the results following successful data processing from a group of ten rat models of PD used to further refine the protocol. The study builds on two published journal papers that were previously presented in three conferences. The PD model study successful lead to two publications in peer review journals (Madete et al., 2010, Madete et al., 2011). **Chapter 4** further describes how the protocol was successfully applied to a large cohort of stroke rat models before and after lesion surgery, and before and after embryonic grafting. **Chapter 5** demonstrates how the protocol was further modified to accommodate a group of healthy human subjects. **Chapter 6** outlines an overall discussion comparing and contrasting human and animal gait data. **Chapter 7** provides a set of conclusions which can be drawn from this work and provides directions for future work.

CHAPTER 2

2. Protocol development

2.1. Introduction

Motor impairments in rodent models of neuro-pathological diseases are traditionally analysed in two dimensions (2D) as well as other subjective methods such as digital video analysis and paw print analysis (Brown et al., 2005, Fan et al., 2008, Klein et al., 2009, Fan et al., 2008 Coulthard et al., 2002). Recently, objective and quantitative gait measurements for rat models of disease have been collected using three dimensional (3D) motion analysis (MA) techniques (Canu et al., 2005, Metz et al., 1998, Couto et al., 2008b). The approach has been extensively used to analyse gait patterns in humans (Whatling et al., 2008, Whatling and Holt, 2010, Jones and Holt, 2008, Peppe et al., 2007, De Bujanda et al., 2004, Nadeau et al., 1997).

Acquisition of rat gait patterns is challenging, with techniques ranging from simple paw print analysis to complicated electrode implantation, all these techniques are viable and effective. However it is difficult to effectively reproduce them for human gait analysis. This study presents a protocol that will explore the application of motion analysis (MA) to quantify temporal parameters, motor asymmetry and stability in rats and humans. In order to achieve the aim of the project the designed protocol intends to investigate rat locomotion in terms of swing time, stance time, stride length, speed and cadence in addition to quantifying balance parameters. Such animal measurements can then be directly compared with human measures to explore correlations between the two species using a generic data acquisition system.

Animal model behavioural studies of function tests used at the Cardiff Brain Repair Group (BRG) are vast. The tests were investigated and a suitable study was found that allowed for MA of rats and humans. The 'elevated beam, a test that investigates balance during gait of rat models, was chosen for its ability to produce reproducible results and variable. The test can also be interpreted and translated into a trial that achieves similar outputs in human subjects for the purpose of correlative studies and cross validation of the rat models of disease. The developed rat and human protocols and future outputs will be combined with other behavioural and functional studies e.g. paw reaching, as part of an ongoing research programme with the BRG.

To the author's knowledge, performing human and rat gait analysis under the same testing condition hasn't been performed before. A study by Whishaw et al., (1992) investigated homologous behaviour between rats and humans to analyse skilled reaching. They concluded that similarities between rats and humans strengthen the generalisation made in neuroscience rat model studies.

This Chapter aimed to apply the 3D marker based MA (3DMA) techniques, established for human motion studies in the MA Laboratory (MAL) at the Cardiff School of Engineering, to record and analyse rat locomotion. A novel rat 3DMA protocol was developed using an optoelectronic motion capture system to quantify temporal gait parameters and postural adjustments (protocols available in Appendix B and C).

The design of the protocol focused on the sensitivity and versatility of the motion capture system to record practical and non-invasive data, whilst achieving a high standard of accuracy. This Chapter outlines the process of developing a working protocol and discusses the validation of the new MA technique in quantifying rat and

human forward locomotion. The challenges encountered during protocol development have also been addressed.

This chapter describes the development of the following protocols:

1. Rat gait analysis protocol using marker based MA techniques. The walking trial was over-ground on three elevated beams of different widths.
2. Human gait analysis protocol adapted from the rat gait analysis. The walking trial was also over-ground on specifically designed walkways of different widths.

A description of details of the equipment used, camera layouts, calibration procedure, marker placement and an outline of the data collection and processing protocol is provided. This is the first study that aimed to investigate quantification of over-ground locomotion in rats by using optoelectronic methods for comparison purposes with human gait. A motion capture set up was established at the School of Biosciences to record rat gait on the elevated beam apparatus and the adapted approach. Data collection to provide similar movement analysis in healthy human subjects was at the MAL at the School of Engineering

2.2. Data Collection

2.2.1. Qualisys motion analysis system

3D movement was recorded and tracked using an array of Qualisys PROreflex MCU cameras and its proprietary software Qualisys Track Manager, (QTM) (Qualisys, Sweden). Each camera contains infrared emitting diodes that capture 2D coordinate data of reflective markers positioned in their line of view. A series of more than two cameras positioned strategically and calibrated, converts the 2D data into 3D using inbuilt algorithms in QTM. The produced data can be adapted to accommodate different movement scenarios and characteristics and later exported.

2.2.2. Calibration

The calibration procedure was performed according to the software specifications. A calibration kit consisting of two parts: an L-shaped reference structure (frame) and a calibration wand was used. The frame consists of a metal bar with four markers attached which define the origin and orientation of the laboratory coordinate system (Figure 2-1a). This is then placed in a position that allows all cameras in the system to view all four markers. The wand is a T-shaped metal stick with two markers attached on either end of the horizontal T at a known distance apart which defines the capture volume (Figure 2-1b).

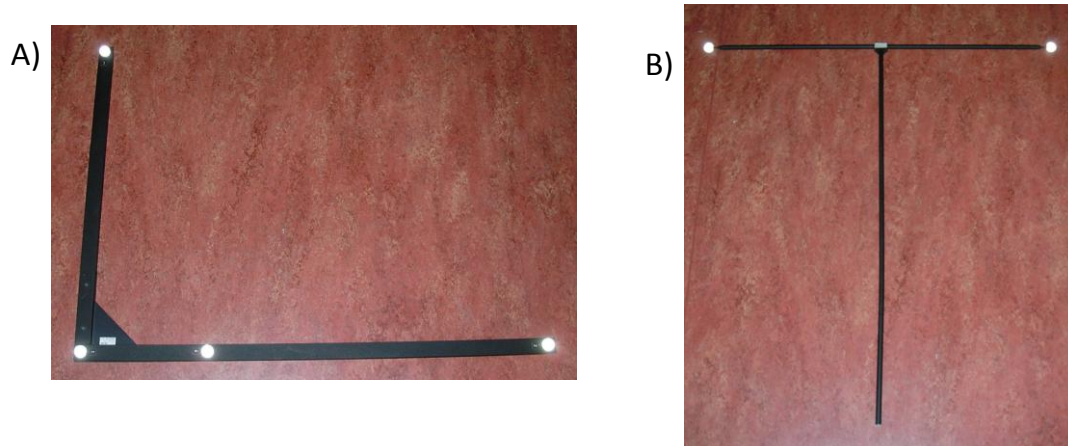
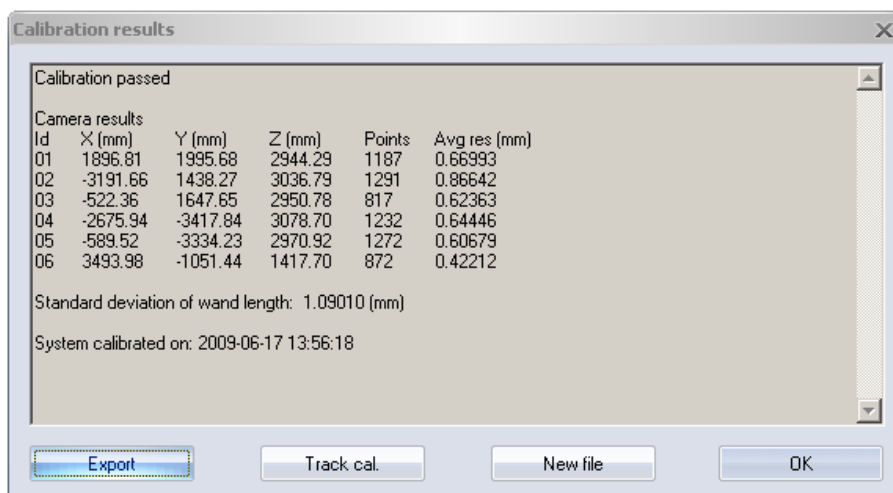


Figure 2-1: Calibration kit A) 'L' shaped frame and B) 'T' shaped wand

To perform a system calibration, the wand is moved in the measurement volume in all three directions while QTM records its motion for between 10 and 20 seconds. Each camera's position and orientation is extracted by evaluating the camera's view of the wand during the calibration. A passed calibration (depending on the study being carried out) increases the system accuracy and is indicative of a good camera position for the required volume. An accepted calibration for this study shows each camera with an average residual of less than 1 mm, as shown in Figure 2-2.



Id	X (mm)	Y (mm)	Z (mm)	Points	Avg res (mm)
01	1896.81	1995.68	2944.29	1187	0.66993
02	-3191.66	1438.27	3036.79	1291	0.86642
03	-522.36	1647.65	2950.78	817	0.62363
04	-2675.94	-3417.84	3078.70	1232	0.64446
05	-589.52	-3334.23	2970.92	1272	0.60679
06	3493.98	-1051.44	1417.70	872	0.42212

Figure 2-2: Calibration results

2.2.3. Protocols

The rats and human data collection protocols are described in sections as follows:

1. Ground (Elevated beam apparatus for rats and walkway for humans)
2. Cameras and calibration
3. Marker placement
4. Walking trials

2.2.3.1. Rat Protocol

Elevated beam apparatus

Behavioural studies at the Cardiff BRG include several tests that study the effect of neurodegenerative disorder in rats and mice. In order to carry out a successful motion capture session a test that would be compatible for use with the system had to be chosen. The options presented to us included the 'elevated beam' that tested balance, the 'cylinder test' that tested balance and the 'open field' test that investigated exploration reflexes present in the rats since birth and 'paw reaching' to monitor upper body balance and speed of reaching with food rewards.

As discussed in Chapter 1 the 'elevated beam' was chosen as it allowed for the analysis of multiple variables, i.e., body orientations and temporal parameter during gait. The camera set up was easily placed in the volume of the beam, and there were no interference in the line of view of the camera, as in the paw reaching apparatus and the cylinder apparatus that were surrounded by Perspex. The 'elevated beam' allowed the capture of continuous gait, similar to studies carried out on human subjects walking a defined length.

The 'elevated beam' (Figure 2-3) is typically used to monitor forward locomotion and limb coordination of rodents by scoring foot faults (slips) as the rat walks along it. This technique is a highly sensitive and accurate method to evaluate motor deficits in models of neurodegenerative diseases (Schallert et al., 2006). The current study utilised the 'elevated beam', to quantify parameters of gait and posture during forward locomotion. The relative position of the head, the tail and all the four paws was manually recorded.



Figure 2-3: Elevated beam (Graduated)

The graduated (GR) beam was first described by Schallert et al., (2006) as a 1.65 m long beam with three 45 cm zones (Figure 2-4). The GR beam is tapered, i.e. each consecutive zone is narrower than the previous, thus has increased difficulty as the rat walks along the tapered section.

A resting box was placed at the end of the beam for the rat to rest in between walks. The beam has 2 cm wide ledges, located 2 cm below the upper surface of the beam. These allowed the rats to place their limbs off the beam and recover from foot slips and provided an aid to deal with the increasing difficulty of the beam.

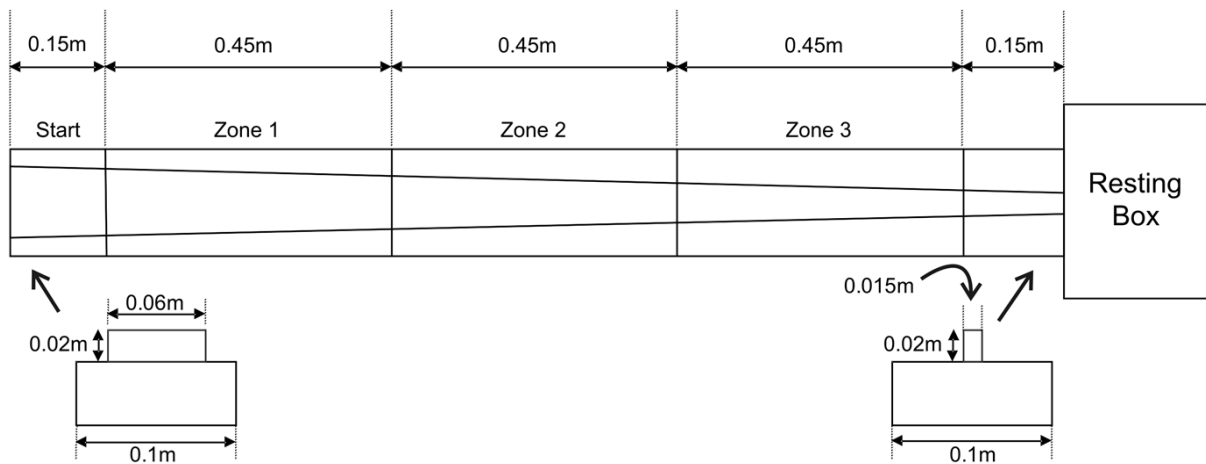


Figure 2-4: The plan view of the GR beam showing the narrowing of the beam towards the resting box and the three zones used to calculate zonal speed

Two additional beams, a wide (WD) beam and a narrow (NR) beam, were constructed with specifications derived from the GR beam: The WD beam had the same dimensions as the wide section of the GR beam and the NR beam as the narrow end of the GR beam. All three beams are shown in Figure 2-5.

The WD beam was introduced to test the hypothesis that the ledge, present in the GR and NR beams, provides a crutch for the rats as the walkway becomes more difficult. The beam is wide enough to accommodate the entire base of support and all four limbs of the rats. Consequently, the NR beam was introduced to test whether foot faults observed were inevitable coincidence or developed compensatory strategies due to the deficit.

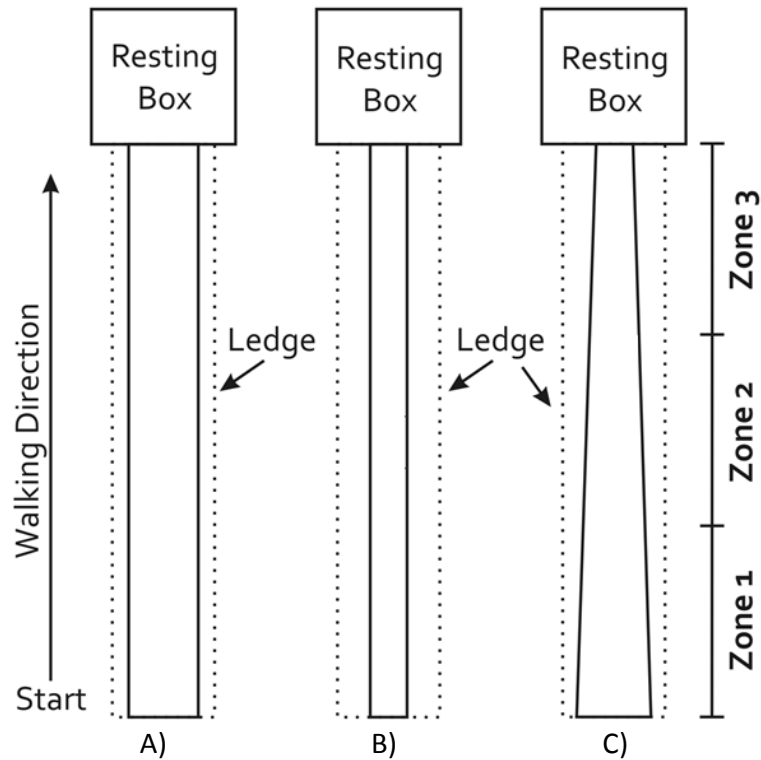


Figure 2-5: Aerial view of the three different beams A) WD beam, B) NR beam and C) GR beam

Cameras and calibration

A camera set up was chosen that did not cause frequent marker drop out and allowed the production of acceptable 3D data for analysis. The set up included seven *Qualisys* cameras to ensure full recording as the rats moved along the 1.65m beam. The camera positions and the directions are shown in Figure 2-6. The camera set-up allowed the collection of eight to ten gait cycles for each limb. Marker position was sampled at 60Hz. The calibration frame was placed on the beam and the 300 mm wand calibration was waved for 10 seconds.

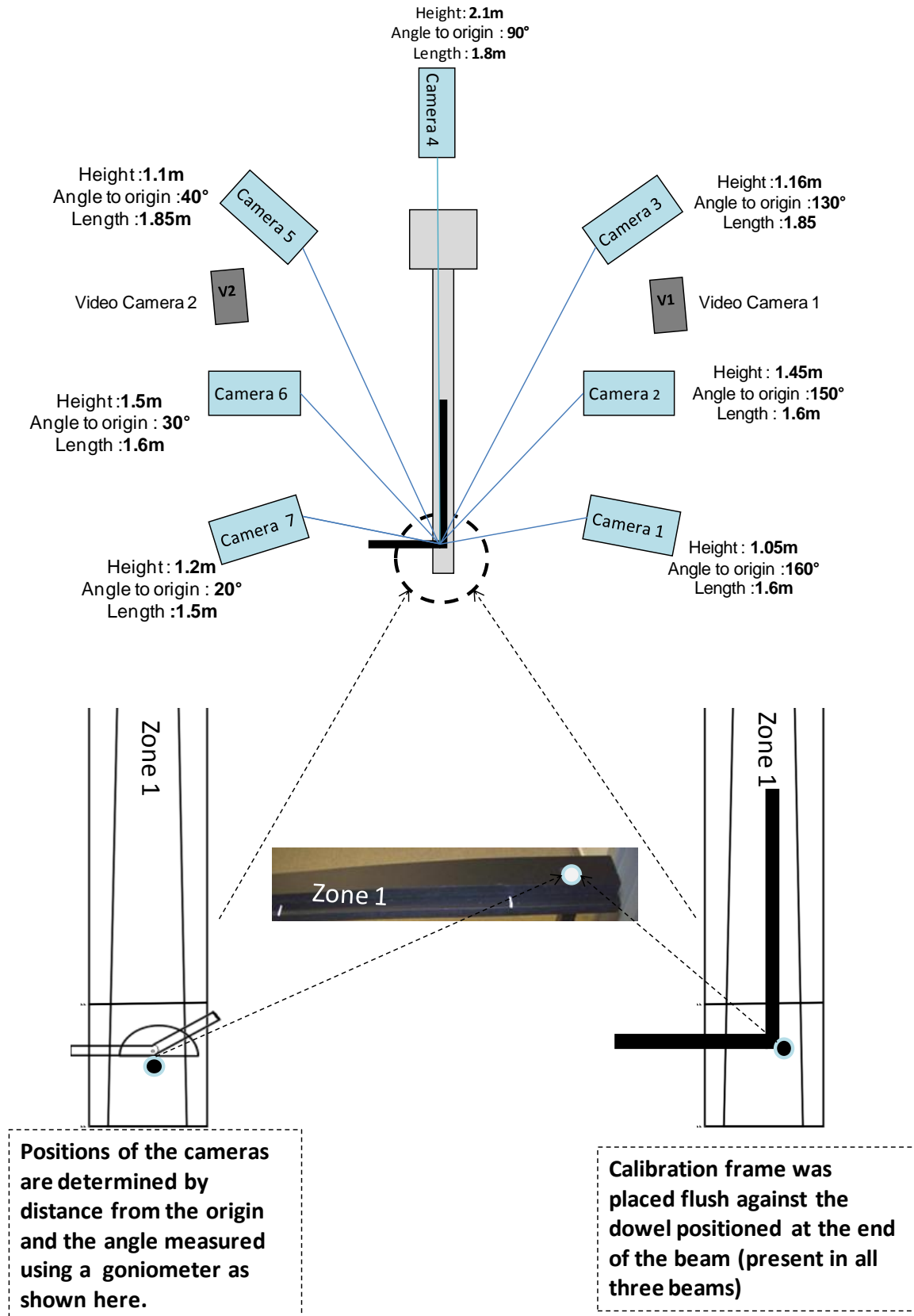


Figure 2-6: Camera map and calibration frame position

Marker placement

There are no known marker placement standards for rat gait studies. Due to the rats' fur coat, pliable moving skin, and size, the rats' physique and small skeletal structure, finding distinctive bony landmarks is difficult.

Two types of markers were explored:

1. Retro-reflective tape cut into strips or into circles (using a paper punch) and stuck directly on the rat.(Mahmud et al., 2010)
2. Spheres of 2.5mm and 5mm diameter made from plastic and covered with retro- reflective tape (Madete et al., 2010).

Placing reflective tape directly on the rat's body reduced 3D tracking accuracy due to the length of the fur. Therefore, the 5mm spheres were the preferred method since the markers were large enough not to be covered by the fur, and small enough to allow filming without infringement.

Markers were located relative to underlying anatomical bony landmarks used to identify the four limbs and the rats' body are described in Table 2-1 and in Figure 2-7.

Circular reflective markers were placed on the skin cover:

1. One marker on the **middle of the skull** to identify head motion
2. Four markers on the appendicular aspects of the rat skeletal structure
 - a. A marker on each **Acromium**
 - b. A marker on each **Greater Trochanter**
3. Along the vertebrae
 - a. A marker on the second **Thoracic vertebrae**
 - b. A marker on the **Sacrum**

4. Above each **Calcaneus** using cable ties.

Cable ties were used to fasten the markers on the four paws; all the remaining markers were securely fixed to the rat using double sided tape. Additional markers were placed along the length of the beam to identify relative motion of the rat and to illustrate the effect of the varying width of the GR beam width on rat motion.

Table 2-1: Summary of marker placement.

Location	Number of markers
Above the Calcaneus.	1x4
Thoracic Vertebrae	2
Skull	1
Greater Trochanter	1x2
Achromium	1x2

The protocol provided a practical, sensitive and non-invasive method that allows for the analysis of representative gait parameters rather than accurate joint rotations measurements.

Walking Trials

A licensed member of staff from the Brain Repair Group (BRG) trained and tested the rats to walk along the beams. Following camera set, calibration and marker placement described earlier; gait analysis data was recorded while rats walked along the three different beams.

Walking trials were performed in the following order: rats were placed on the wide end of the GR beam to begin testing. The rats walked along the tapered beam towards the resting box. The GR beam was then replaced with a NR beam using the same set-up. This procedure was then repeated for the WD beam as control run. A minimum of three continuous walking were obtained per recording. Trials in which

the rat stopped along the beam at some point before it reached the resting box were excluded from the results. Analysis included at least two runs from each rat that included at least five consecutive gait cycles without any stops. This provided the minimum number of steps that must be recorded to eliminate deviant kinematic curves (Duhamel et al., 2004).

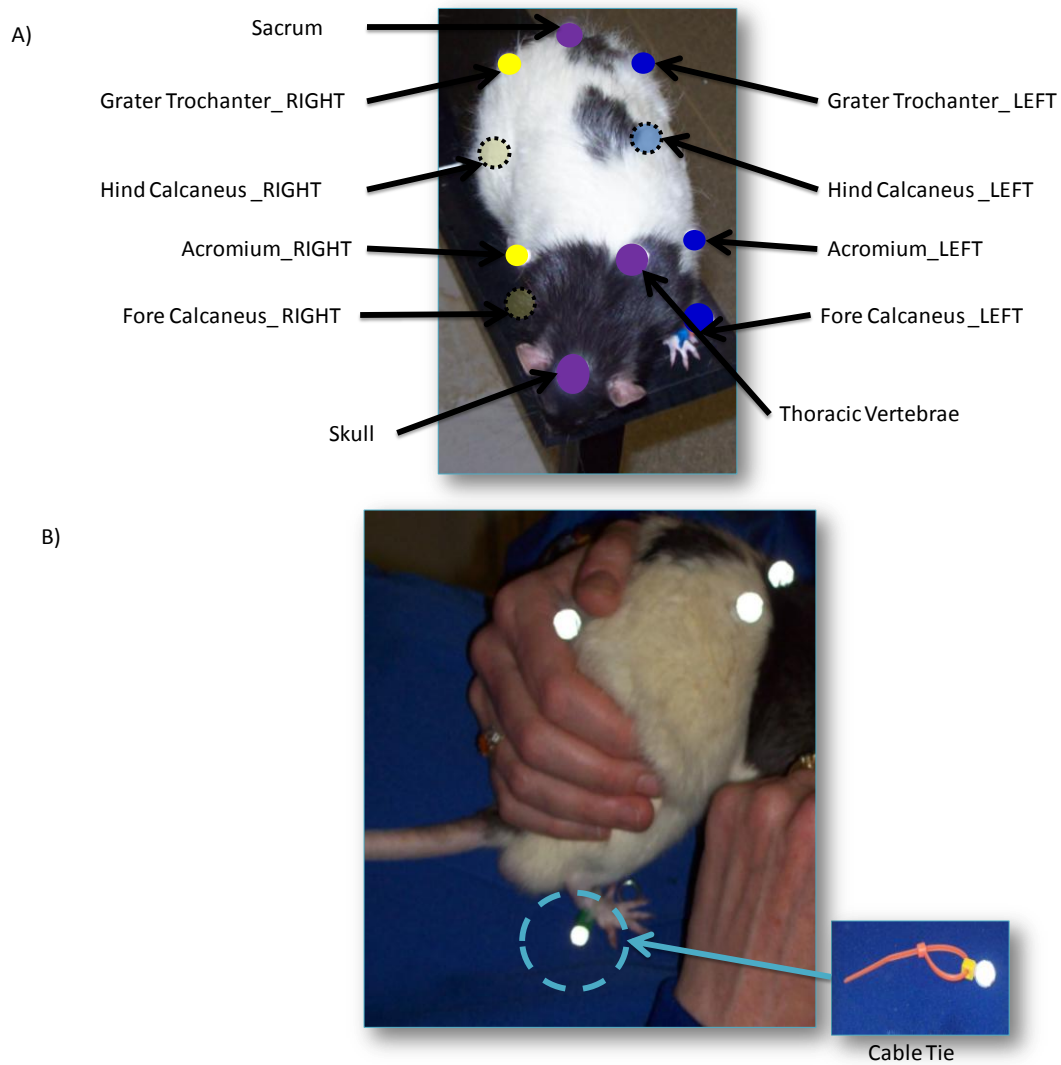


Figure 2-7: A) Rat marker positions B) use of cable ties to fasten markers on limbs.

2.2.3.2. Human protocol

Walkway

The walkway used for the human protocol was adapted from the elevated beam apparatus. The elevated beam was designed to examine stability and balance in rats as they walked along the elevated beam. Shown in Table 2-2 and illustrated in Figure 2-8 are the scaling procedure from the elevated beam into the scaled human walkway.

Table 2-2: Dimension definitions of the elevated beam and the human walkway

	Rat	Human
Base of Support	2cm (Gabriel (2007))	18cm(Seidel (2002))
Width	6cm	54cm
Entire Length	165cm	1765cm
Zone 1	6	54
Zone 2	4.5	40.5
Zone 3	3	27

From Table 2-2, data from literature illustrate that a healthy human's base of support is nine times larger than that of the rat, thus all the dimensions of the walkway was scaled up by a factor of nine

The base of support of healthy humans is around 18cm (Seidel et al., 2001), thus allowing for an approximate width of 54cm. The average stride length of a human subject is approximately 1.5m (Beauchet et al., 2009); therefore the length of the walkway was set to 8m. The length of the walkway was based on acquiring five complete gait cycles during testing since the size of the lab at Cardiff School of Engineering did not allow for ten gait cycles. The zone widths were also determined by the 1:9 ratios.

To keep the protocol generic and to test for dual tasking in humans, three different variations of the walkway (graduated walkway (GRw); wide walkway (WDw); and narrow walkway (NRw) were used. The WDw had the same width as the wide section of the GRw; and the NRw as the narrow end of the GR walkway. The NRw and GRw were also developed to identify important postural and balance attributes during gait as expressed by human subjects, both in healthy and diseased subjects. Dimensions were defined as shown in Figure 2-8.

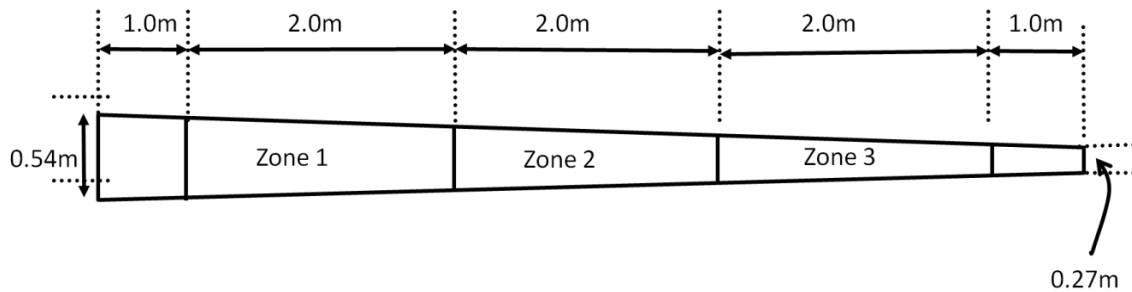


Figure 2-8: Graduated walkway showing dimensions

Cameras and calibration

Twelve analysis ProReflex MCU cameras were used to record subjects' gait cycles at 60 frames per second, as they walked along the 8m walkway in the MAL at the Cardiff School of Engineering (Figure 2-9).

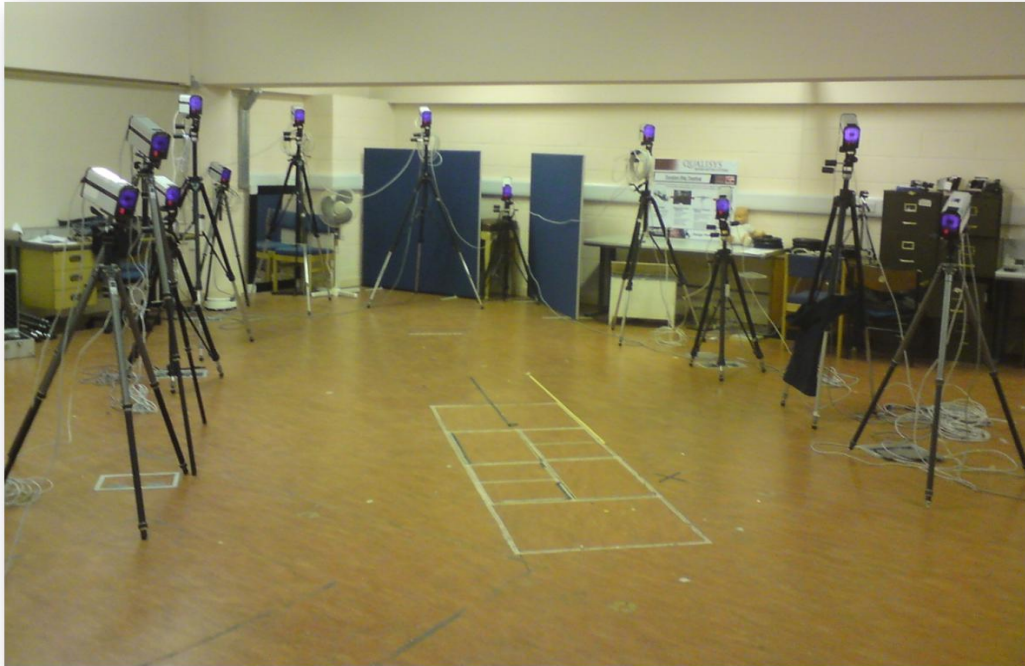


Figure 2-9: Cardiff University Motion Analysis Laboratory with a 12 camera set up.

A map of the camera layout and the position calibration frame is shown in Figure 2--10. An “*extended*” calibration was carried out due to the extent of the volume required for filming. This method allows for situations where the calibration frame cannot be viewed by all the cameras. It works on the idea that if the neighbouring camera has a view of the frame, the overlapping field of view of the two cameras allows both cameras to be calibrated when the wand was waved (Figure 2-11). Calibration was carried out for 15 seconds using a 700 mm calibration kit.

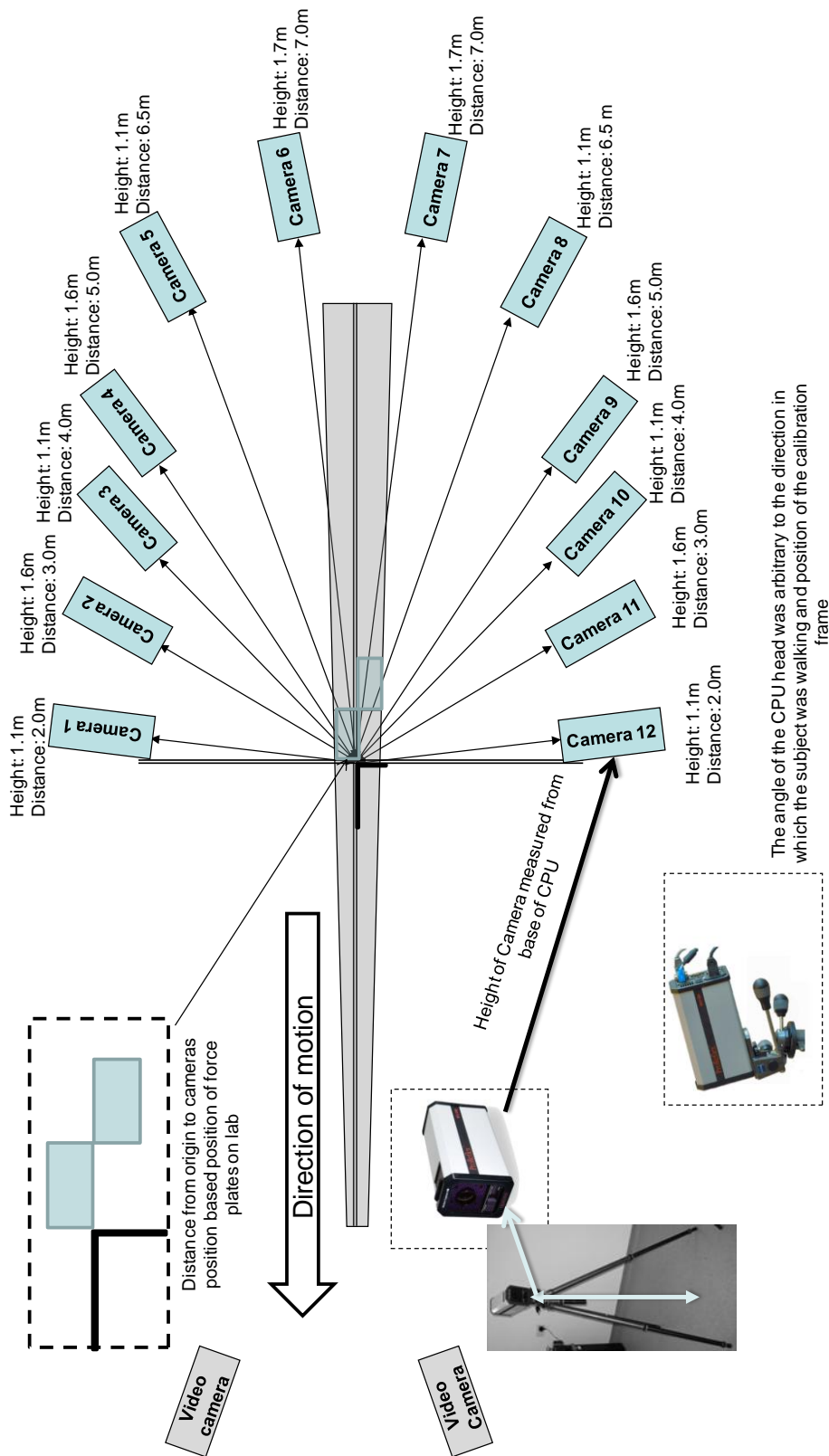


Figure 2--10: Camera set up including the height and the distance from origin of each camera and position of the calibration frame during extended calibration.

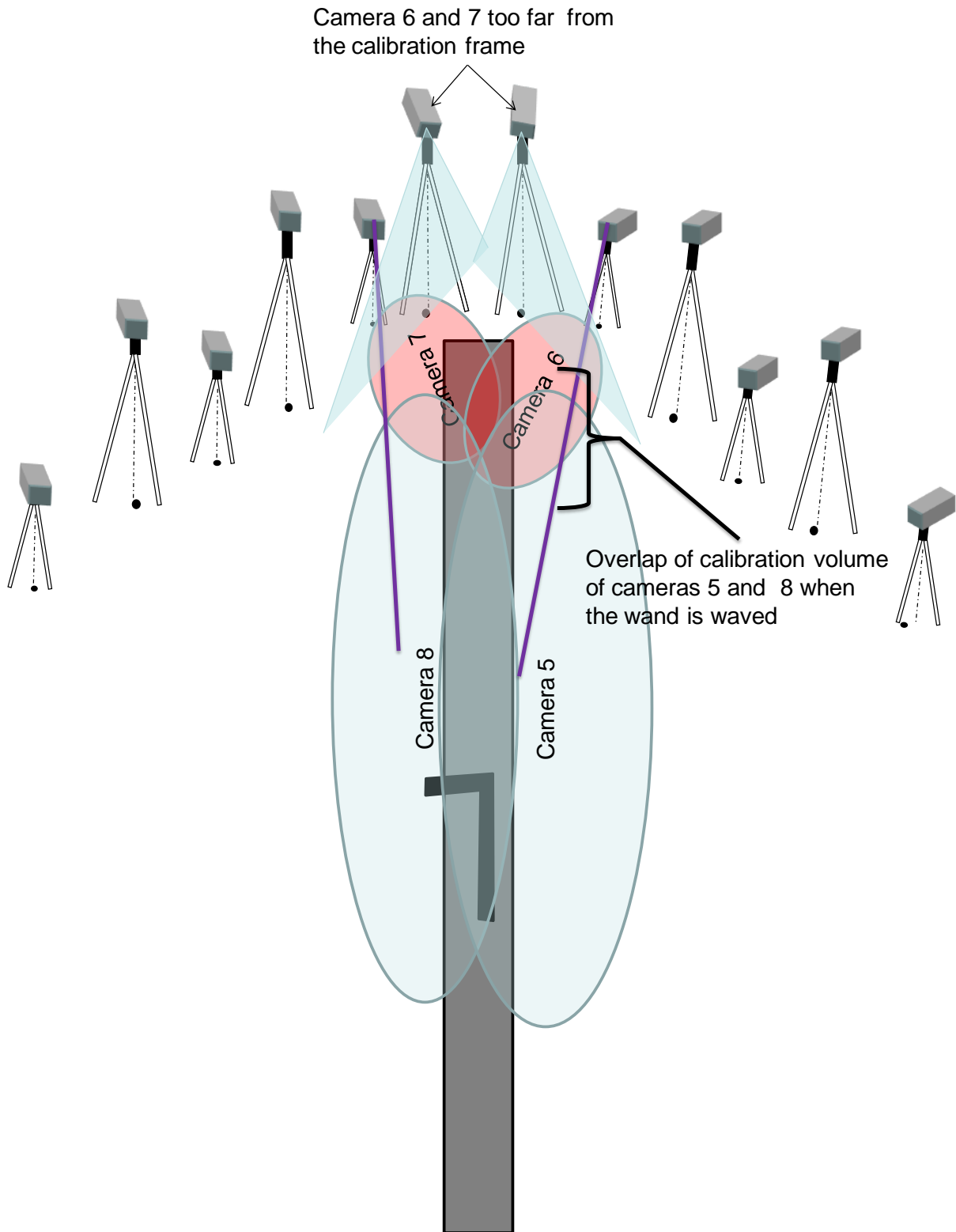


Figure 2-11 : Extended calibration

Human Marker placement

Marker placement was designed to allow the recording of temporal gait parameters and postural body rotations of the trunk. Marker positions mirrored those established in the rat study. Twenty 15 mm retro-reflective markers were positioned as described in Table 2-3 and Figure 2-12. Markers are representative of the trunk, head, feet, and hand motion during gait. Markers were attached using double sided tape. A marker cluster used to observe head motion was placed on the head and was held using a head band. Markers were also placed along the length of the walkway to identify relative motion of the subject and to illustrate the effect of the varying width of the GRw width on motion.

Table 2-3: Summary of human marker placement

Location	Number
Head and a marker cluster	1 x 5
Acromium	1 x 2
Greater Trochanter.	1 x 2
Head of radius	1 x 2
Lateral Epichondyle of the humerous	1 x 2
7 th Cervical vertebrae	1
1 st lumbar vertebrae	1
Lateral Epichondyle	1 x 6
Calcaneaus	1 x 2
1 st metatarsal	1 x 2

The placement was aimed to be as similar as possible to the one used for rat gait analysis and were placed on specified locations throughout the body that allowed for the cameras to capture markers during gait for the entire length of the walkway. The new approach was shown to be practical and allowed the best correlation of data with the rat results.

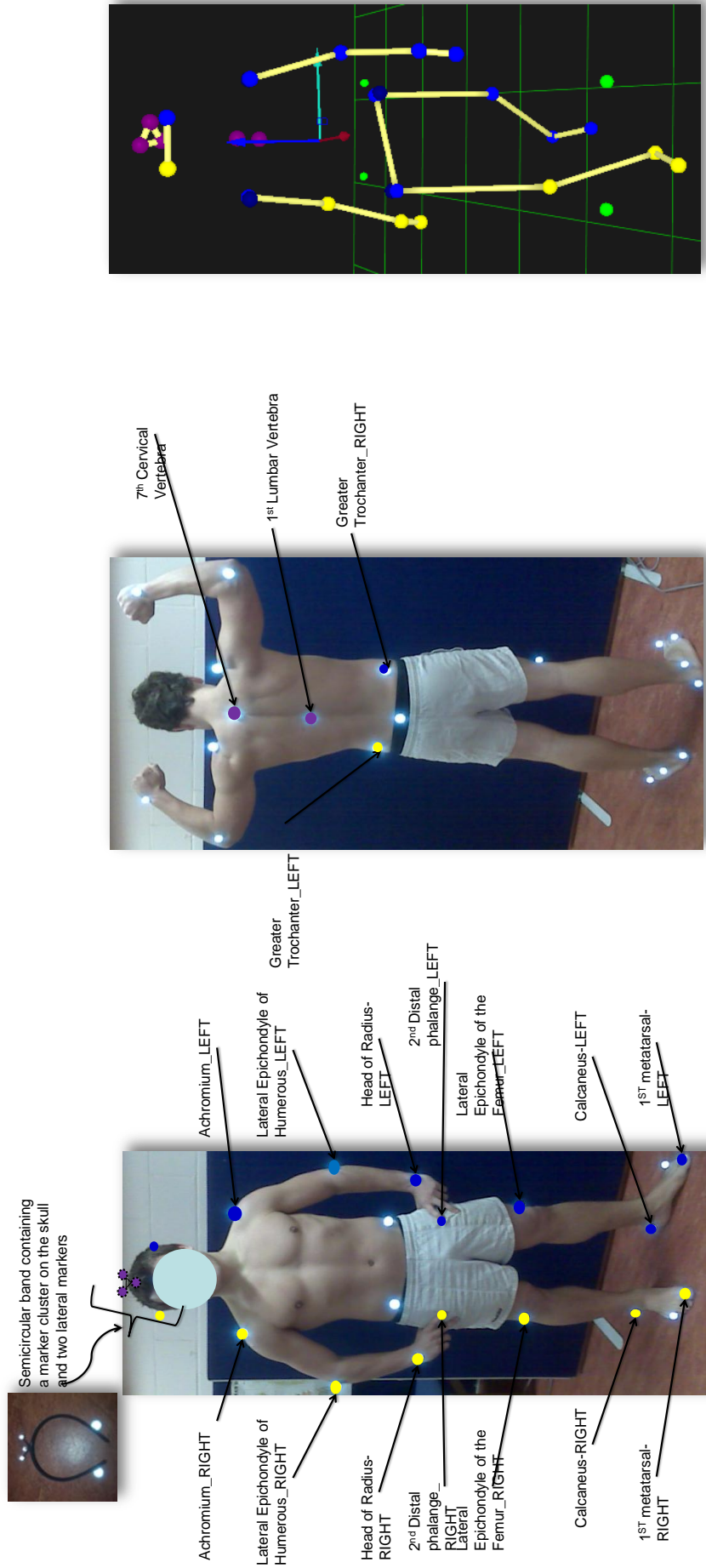


Figure 2-12: Human subjects marker placements (the dashed lines indicating posterior markers)

Human Walking trial

Subject walked along the defined walkway starting with the GRw; followed by the NRw and finally the WDw in the direction shown in Figure 2--10. A ‘good’ walk included a minimum of five consecutive gait cycles that had no marker drop outs or inconsistent steps. Figure 2-13 shows a QTM recording of a successful walking.

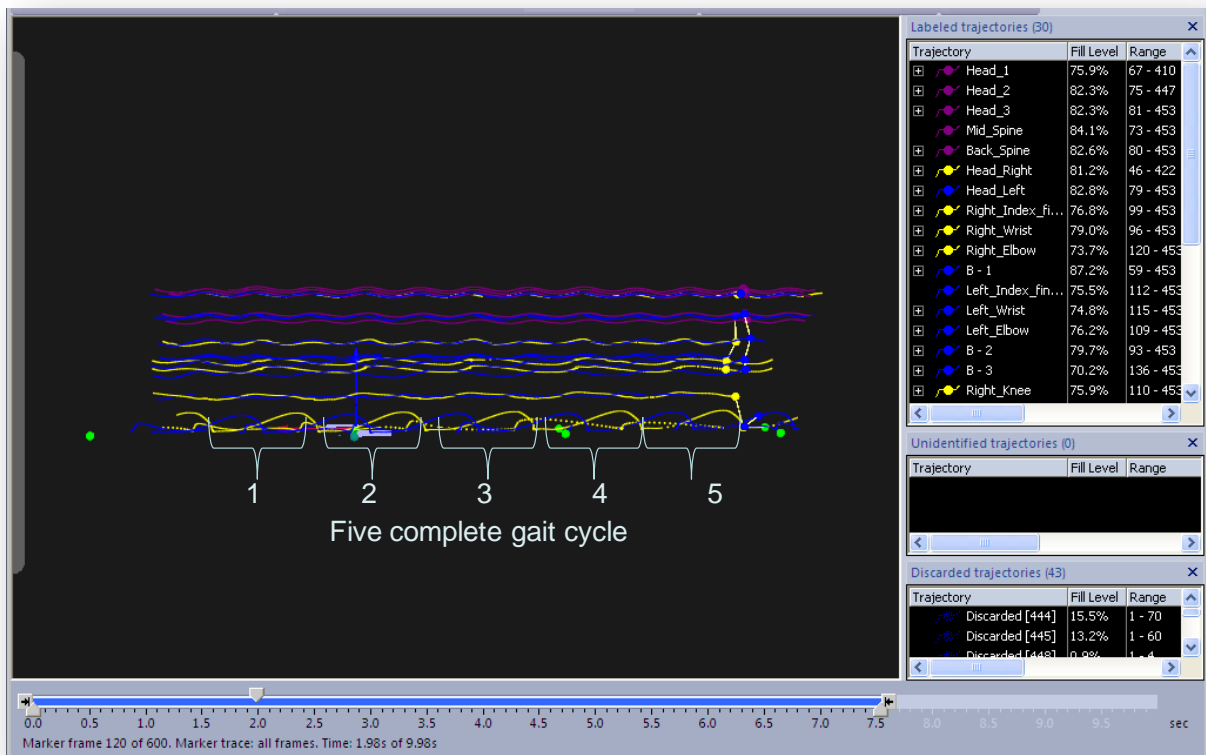


Figure 2-13: Healthy human walking output from QTM showing five gait cycles of the left limb

2.3. Data Processing

3D and 6DOF coordinate data was obtained by tracking markers in QTM. The tracking involved identifying the markers for each trial accurately. A one second recording produced 60 frames of data. Data was exported to excel for post analysis. The **temporal gait parameters** analysed were cadence, speed, swing time, stance time and stride length; and for the **postural parameters**; *roll, pitch and yaw* angles, limb position and tail position.

This section describes data processing methods applied to the rat walking trial results, summarised in Figure 2-14. The same methods of analysis were applied to the data from the human walking trial since the same output variables were acquired except for the tail position and paw placement data.

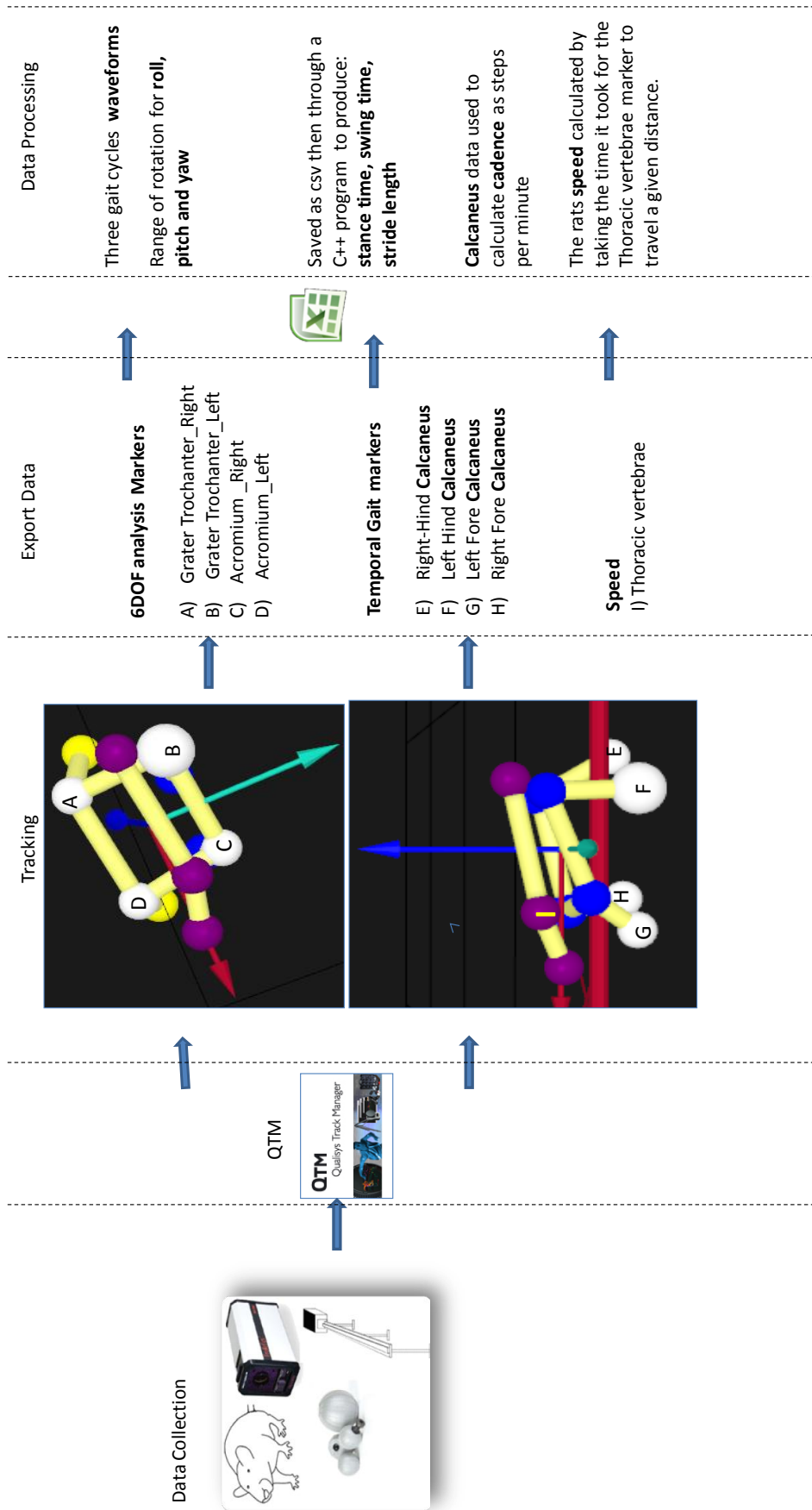


Figure 2-14: Processing data from the rat waking trial. The method was also applied to the human walking trial since similar protocol was used, similar output were achieved.

2.3.1. Temporal Gait parameters

The Cadence is the number of steps taken in a given time, the usual units being steps per minute. Complete cycles are counted, and since a cycle consists of two steps, the cadence is a measure of half cycles. Cadence was calculated by counting the number of steps taken by each limb in 60 seconds using Equation (2-1).

$$\text{Cadence (steps per minute)} = \frac{\text{steps counted} \times 60 \times 60}{\text{Number of frames (on QTM)}} \quad (2-1)$$

Where 60 x 60 refers to 60 seconds per minute and 60 frames of data in a second.

The speed of walking in the distance covered by the whole body in a given time in meters per second. Speed was calculated from the coordinate data of the marker placed on the second thoracic vertebra marker using Equation (2-2).

$$\text{Speed (m/s)} = \frac{\text{Distance (mm)} \times 60 \times 1000}{\text{Number of frames}} \quad (2-2)$$

Where 60 and 1000 are conversion factors (60 frame /s and 1000 mm in a meter).

2.3.1.1. Swing Time, Stance time an stride length

A custom developed C++ program (Eclipse platform, 2009) was used to calculate swing time, stance time and stride length. Calculations were applied to the paw trajectory data using the *Analyse* function in the *trajectory info window* menu in QTM. The magnitude of the position vectors along the three axes (x, y and z) were exported for analysis. The positions of the four paw markers were plotted as shown in Figure 2-15 . Data was saved as a CSV file; ensuring that there were no empty cells and that all the four columns were of the same length. A zero value to any empty cell at the end of the graph was inserted and the author ensured the exported data had complete trajectories.

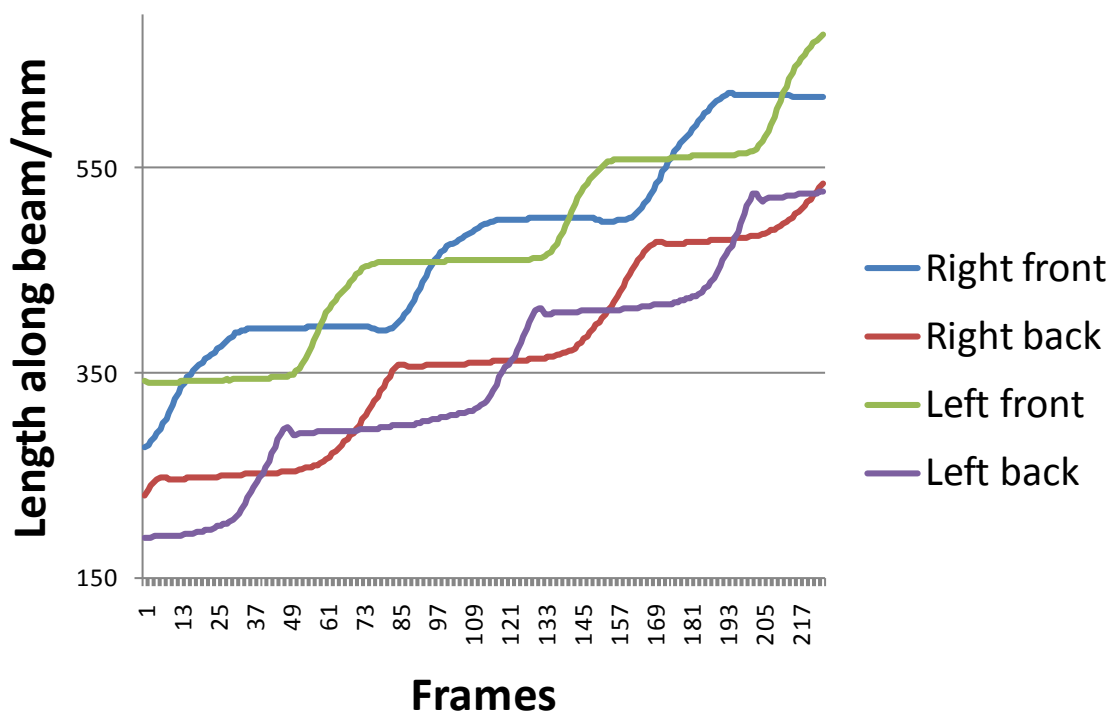


Figure 2-15: Excel output for three gait cycles from exported data

Stance time

Stance phase was defined as the entire period during which the paw is on the beam. From the illustrated curve in Figure 2-16, stance phase is representative of the points where there is little or no change in the 'y' axis. The maximum value (*maxdy*) and the minimum value (*mindy*) in the period where there is no change in 'y' was defined as *paw strike* and *toe off* respectively. Stance time was calculated using Equation (2-3).

$$\text{Stance Time} = (\text{maxdy} - \text{mindy})$$

(2-3)

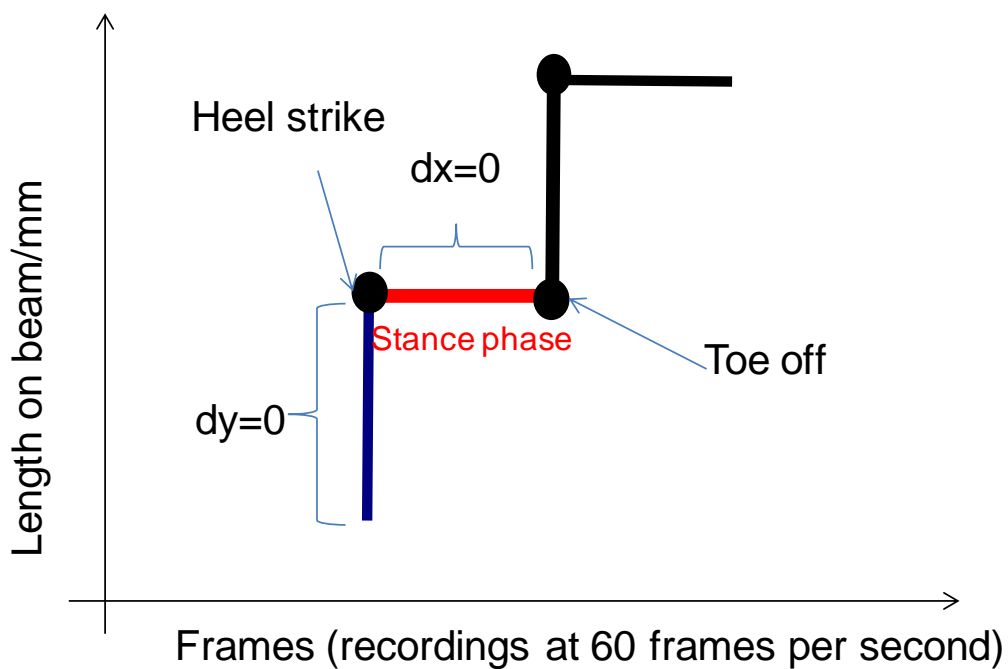


Figure 2-16: Example of one gait cycle with annotations used to calculate stance time

Swing time

Swing phase was defined as the entire time the paw is in the air. During swing phase there is little or no change in the 'x' axis (Figure 2-17). The maximum value (*maxdx*) and the minimum value (*mindx*) in the period where there is no change in 'x' is defined as *toe off* and *paw strike* respectively. Therefore swing time is calculated by taking the difference in frames between *maxdx* and *mindx* using Equation (2-4).

$$\text{Swing Time} = (\text{maxdy} - \text{min dy})$$

(2-4)

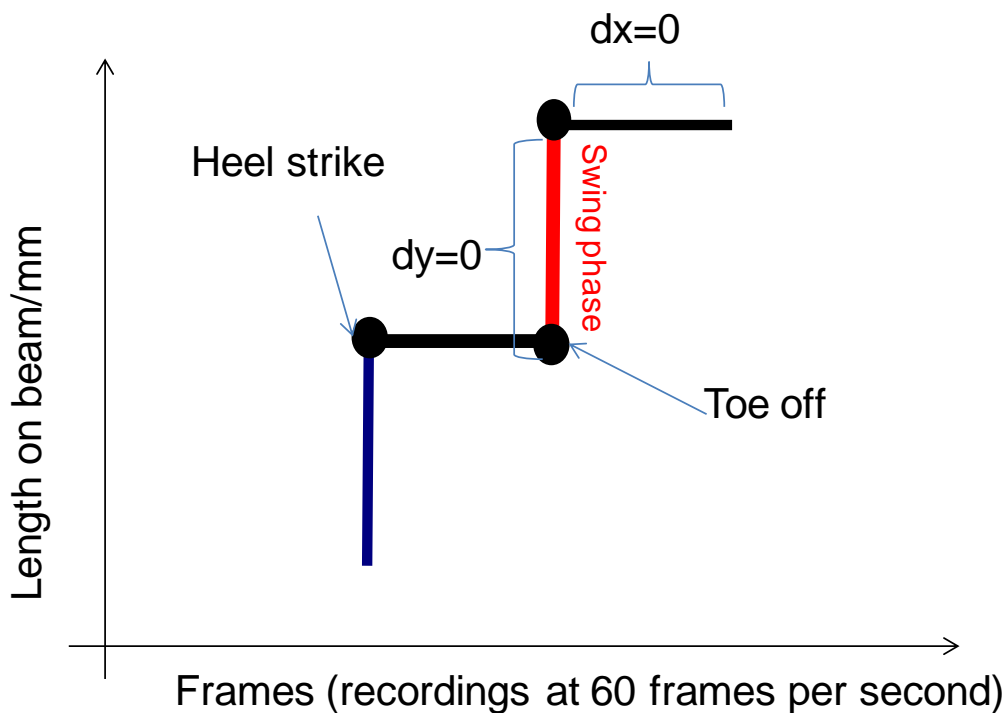


Figure 2-17: Example of one gait cycle with annotations used to calculate swing time

Stride length

Stride length is the distance that the paw travels between two sequential initial contacts with the beam by the same limb. A stride is equivalent to the rats gait cycle and is based on the actions of one limb. From the curve in (A) the stride length can be calculated. The difference in mm between *maxdy* and *mindy* (*stance length*) and between *maxdx* and *mindx* (*swing length*) are used to calculate the stride length using Equation (2-5).

$$\text{Stride length} = \sqrt{(\text{swing length})^2 + (\text{stance length})^2}$$

(2-5)

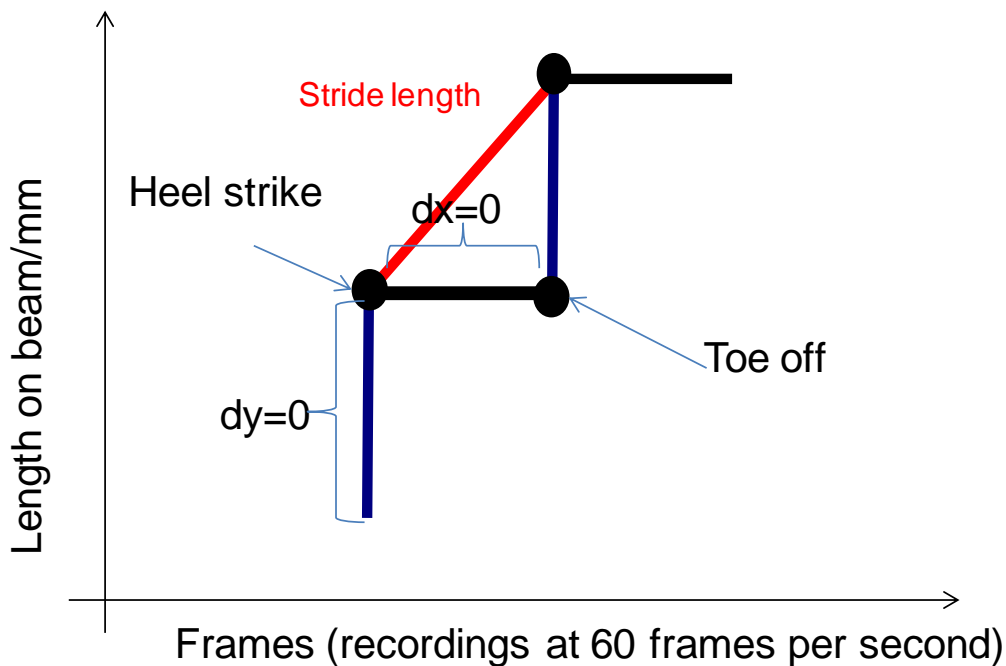


Figure 2-18: Example of one gait cycle with annotations used to calculate Stride length

2.3.2. Postural Parameters

2.3.2.1. Roll, Pitch and Yaw

The orientation of a “rigid body” was defined from the coordinate data of four markers placed on the appendicular aspects of the rat’s skeleton (Figure 2-19). The following section describes the steps used to transform x , y and z coordinate data into axes on the “rigid body” in QTM to thus define body orientation during walking.

The motion of the rigid body is in reference to an origin in a Global Reference System (GRS) defined during calibration. The rigid body provides an axis system known as local reference systems (LRS). Therefore, the GRS is established on the walking ground and the LRS was established at the geometrical centre of the rigid body.

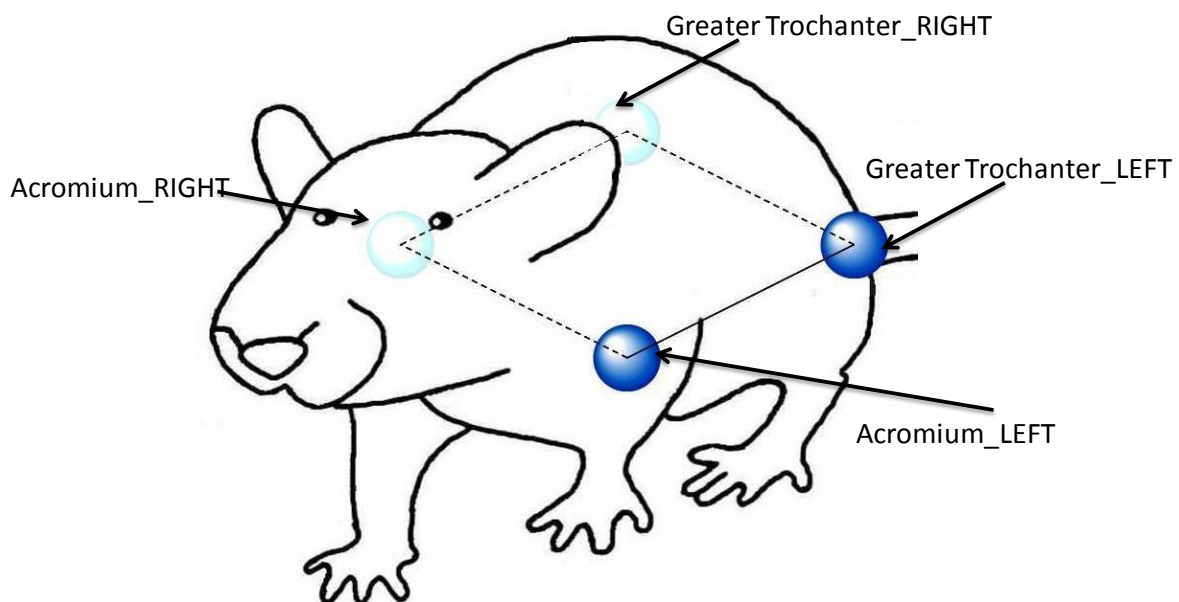


Figure 2-19: Defining a rigid body for 6DOF calculations of the *roll*, *pitch* and *yaw*

2.3.2.2. Rotation of Axes

Qualysis track manager w/s used to calculate the body orientation by analysing rotational angles.

The following steps are followed to calculate the rotational angles from marker trajectory data in QTM. The angles are applied to the local coordinate system in the order: roll, pitch and finally yaw. A positive rotation is defined as clockwise rotation when looking in the direction of the axis. On a rigid body these rotations are defined as:

1. Rotation around the GRS X-axis is called roll.
2. Rotation around the GRS Y-axis is called pitch.
3. Rotation around the GRS Z-axis is called yaw.

Therefore to find the rotation of a rigid body with given roll, pitch and yaw angles from QTM, apply first roll, then pitch and finally yaw. For example, Figure 2-20 illustrates a LRS (x, y and z) established at the geometric center of a rigid body ((six degrees of freedom (6DOF) body,, which is in alignment with the GRS (X, Y and Z).

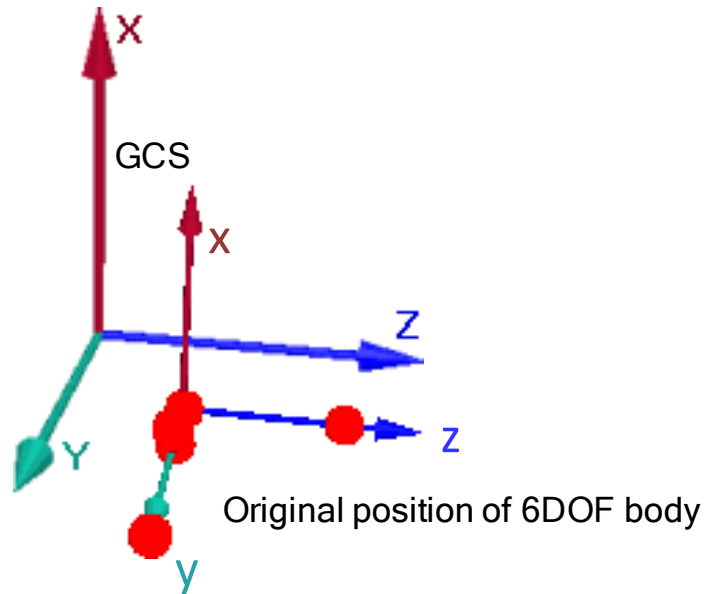


Figure 2-20: Original position of 6DOF in the GRS

1. First the LRS is rotated around the X-axis (roll) with an angle θ to the new positions y' and z' of the Y- and Z-axis as in Figure 2-21.

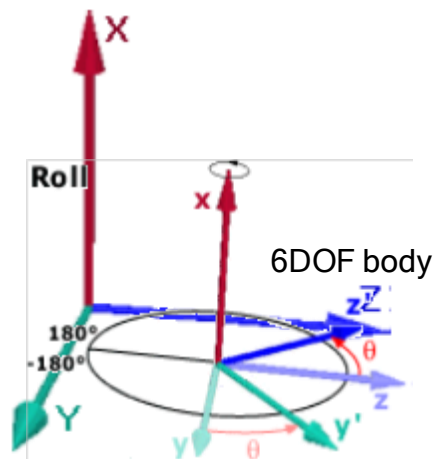


Figure 2-21: rotation around the X-axis

2. After the roll the local coordinate system rotates around the Y-axis (pitch) with the Y-axis in its new position as in Figure 2-22. The X- and Z-axis is rotated with an angle ϕ to the new positions x' and z' .

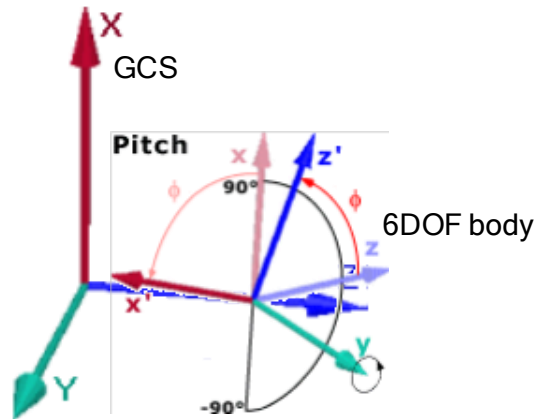


Figure 2-22: Rotation around the Y- axis

3. Finally the local coordinate system is rotated around the Z-axis (yaw) with the Z-axis in its final position as in The X- and Y-axis is rotated with an angle ψ to the new positions x' and y' .

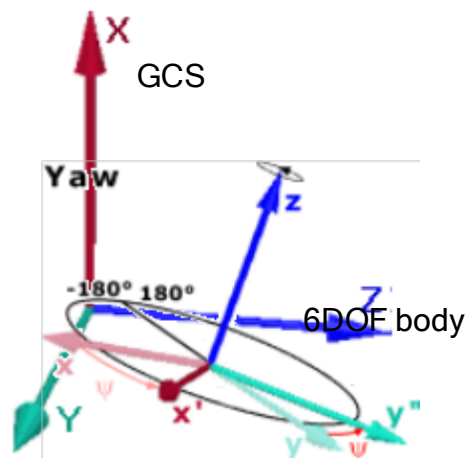


Figure 2-23: Rotation around the Z- axis

After the rotations the rigid body has a new orientation in reference to the GRS as shown in Figure 2-24.

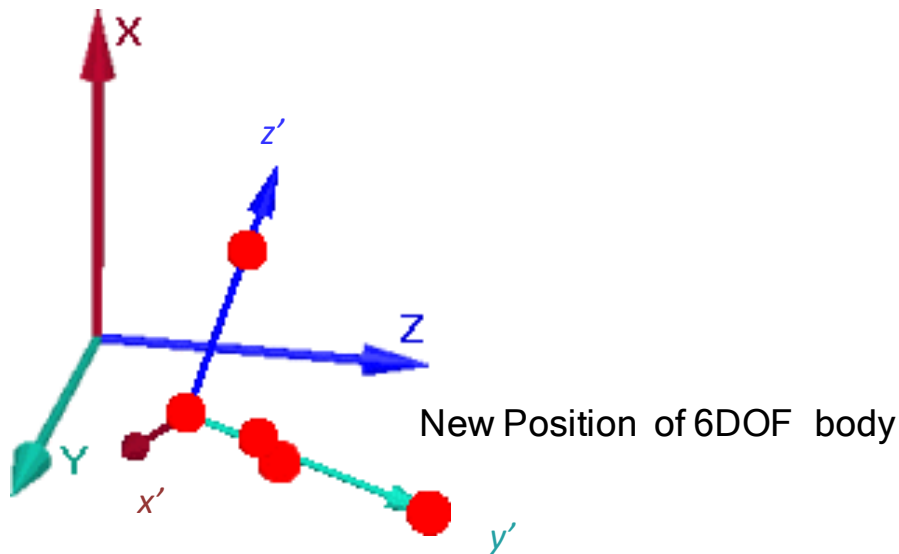


Figure 2-24: New 6DOF position in the GRS.

QTM uses the rotation matrix internally to describe the rotation of rigid bodies, and when exporting 6DOF to TSV files the rotation matrix is included for all bodies in all frames, together with roll, pitch and yaw angles.

Euler angles (rotation angles) are the way that QTM shows the rotation of a 6DOF body. It is also how you enter any rotation that should be applied to a global or a local coordinate system. It is therefore important to understand how Euler angles work to be able to use 6DOF data correctly. Euler angles are a method to define the rotation of a body. The rotation angles are transformed into rotation matrix as follows:

The defined position of the rigid body is used to compute **P**-origin, the positional vector of the origin of the LRS in the GRS, and **R**, the rotation matrix which describes the rotation of the rigid body. The rotation matrix (**R**) can then be used to transform a position **P**-local (e.g. $x'1$, $y'1$, $z'1$) in the LRS, which is translated and rotated, to a position **P**-global (e.g. $x1$, $y1$, $z1$) in the GRS. The following (2-6) is used to transform a position:

$$P_{global} = R - P_{local} + P_{origin}$$

(2-6)

The rotation angles are calculated from the rotation matrix (**R**), by expressing it in the three rotation angles: roll (θ), pitch (ϕ) and yaw (ψ). To begin with the rotations are described with individual rotation matrixes: R_x , R_y and R_z . The resulting three rotation matrixes are then as shown in (2-7,-(2-8 and (2-9:

$$R_x = \begin{bmatrix} 1 & 0 & 0 \\ 0 & \cos\theta & -\sin\theta \\ 0 & \sin\theta & \cos\theta \end{bmatrix}$$

(2-7)

$$R_y = \begin{bmatrix} \cos\phi & 0 & \sin\phi \\ 0 & 1 & 0 \\ -\sin\phi & 0 & \cos\phi \end{bmatrix}$$

(2-8)

$$R_z = \begin{bmatrix} \cos\psi & -\sin\psi & 0 \\ \sin\psi & \cos\psi & 0 \\ 0 & 0 & 1 \end{bmatrix}$$

(2-9)

The rotation matrix (**R**) is then calculated by multiplying the three rotation matrixes. The orders of the multiplications below means that roll is applied first, then pitch and finally yaw

$$R = R_x R_y R_z = \begin{bmatrix} r_{11} & r_{12} & r_{13} \\ r_{21} & r_{22} & r_{23} \\ r_{31} & r_{32} & r_{33} \end{bmatrix} =$$

$$\begin{bmatrix} \cos\phi \cdot \cos\psi & -\cos\phi \cdot \sin\psi & \sin\phi \\ \cos\theta \cdot \sin\psi + \cos\psi \cdot \sin\theta & \sin\phi & \cos\theta \cdot \cos\psi - \sin\theta \cdot \sin\phi \cdot \sin\psi & -\cos\phi \cdot \sin\theta \\ \sin\theta \cdot \sin\psi - \cos\theta \cdot \cos\psi \cdot \sin\phi & \cos\psi \cdot \sin\theta + \cos\theta \cdot \sin\phi \cdot \sin\psi & \cos\theta \cdot \cos\phi \end{bmatrix}$$

(2-10)

(2-11 to (2-13 are then used to calculate the rotation angels from the rotation matrix:

$$\mathbf{Pitch: } \phi = \arcsin(r_{13}) \tag{2-11}$$

$$\mathbf{Roll: } \theta = \arccos \frac{r_{33}}{\cos \phi} \tag{2-12}$$

$$\mathbf{Yaw: } \psi = \arccos \frac{r_{11}}{\cos \phi} \tag{2-13}$$

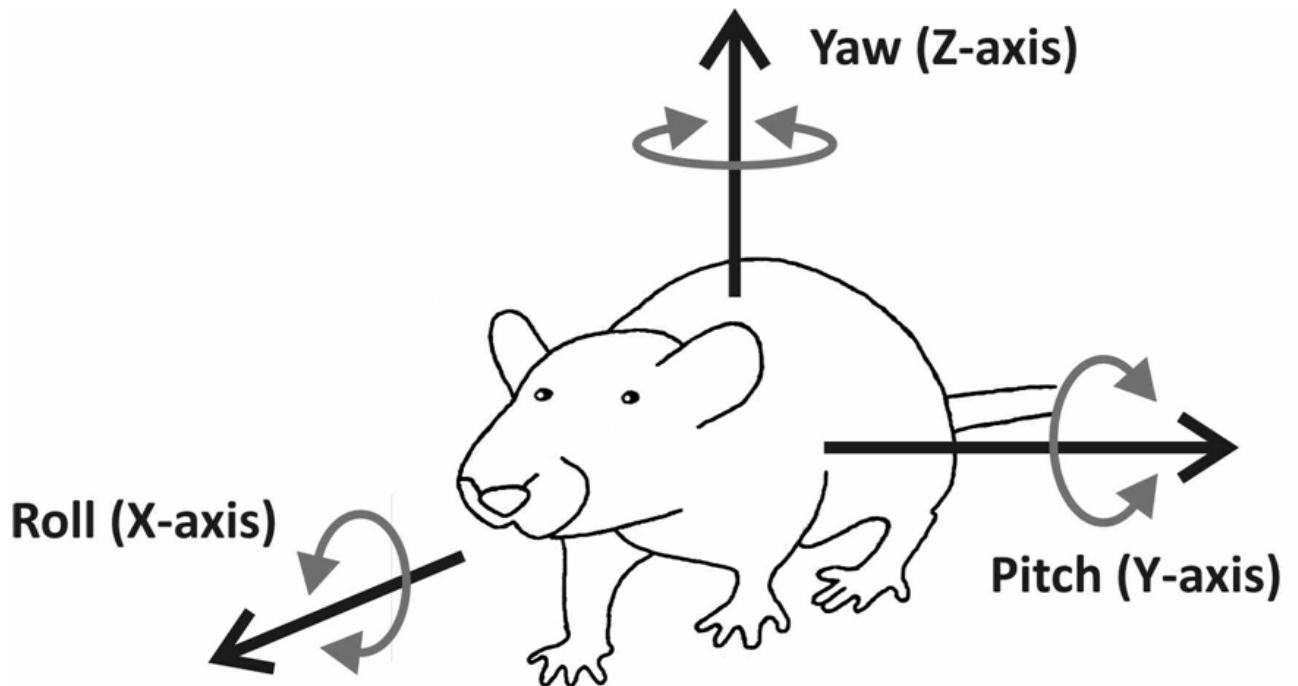
The rotation angles of a rigid body are defined as:

1. Rotation around the X-axis is called *roll*.
2. Rotation around the Y-axis is called *pitch*.
3. Rotation around the Z-axis is called *yaw*.

Positive rotation is defined as clockwise when looking in the direction of the axis. The angles are applied to the local reference system of the rigid body in the order: *roll*, *pitch* then *yaw*. These rotation angles are defined starting with the 6DOF body which is in alignment with the GRS . The postural rotations of the defined rigid body are illustrated in Figure 2-25. *The roll, pitch and yaw* are representative of body rotations of the rat during gait defined in Table 2-4.

Table 2-4: Definitions of *roll pitch* and *yaw*

Roll	Motion of the body during walking in the axis parallel to the beam, x-axis. On the plane perpendicular to the beam, z-y plane showing the body rotation of the rat from side to side
Pitch	Motion of the body during walking in the axis perpendicular to the beam, y-axis On the plane parallel to the beam, x-z plane. showing how much the animal is rotating the body up and down the beam
Yaw	Motion of the body during walking in the axis perpendicular to the beam. x-axis on the plane perpendicular to the beam, x-y plane showing body rotations from left to right as the rat walks to right

Figure 2-25: Illustrations of *roll pitch* and *yaw*

2.3.3. Limb and paw placements analysis

Limb placement data was analysed during locomotion by observing video files recorded using standard 2D video analysis (Sony camera, Japan) in QTM software.

Two parameters were analysed:

1. Tail position: Monitored and recorded as straight, left or right (Figure 2-26 B) and converted into percentages over the entire beam.
2. Position of limb on either the beam or the ledge (Figure 2-26 B): The four limbs were observed individually for each trial. A score of '1' was given if the limb was placed on the beam and '0' if it was placed on the ledge. The number of '1s' and '0s' acquired for each rat was averaged and expressed as a percentage ('foot-slips'). Scoring can be found in Appendix C.

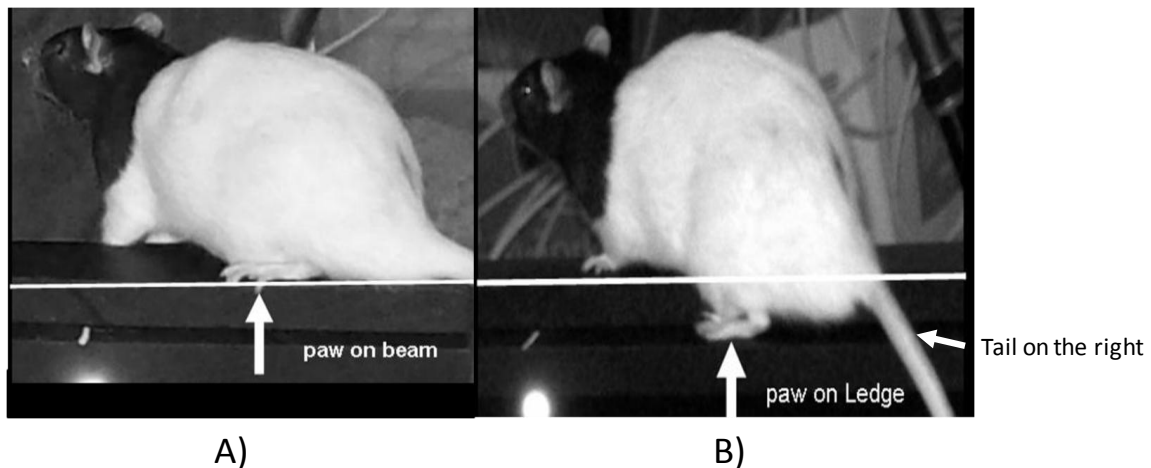


Figure 2-26: Paw position along the beam was scored as either, A) on the beam or B) on the ledge. B) Also reveals a tail positioned on the right.

2.3.4. Statistical and Error Analysis

Data was analysed using GenStat and using SPSS 16 for Windows. Temporal gait parameters and ROM rotations were acquired for animal and human trials. Differences of temporal and postural gait parameters were assessed by ANOVA ($p < 0.05$) where ($F_{1, \text{degrees of freedom}}$) followed by a SIDAK post hoc test.

The inter-trial repeatability of gait parameters was calculated by the one-way random intra-class correlation coefficient (ICC) and the 95% confidence interval (CI) of the ICC, using one-way ANOVA (Oken et al., 2008). The evaluation criteria and standards for ICC values are accepted as follows: values ≥ 0.75 represent excellent repeatability, 0.4-0.74 represents adequate repeatability, and values ≤ 0.40 represent poor repeatability.

2.3.5. Classification using Dempster-Shafer theory (DST)

The classification method was developed and is currently employed at Cardiff University (Jones et al., 2006, Whatling et al., 2008). It is based around the Dempster-Shafer theory (DST) of evidence. The tool uses mathematical probability to quantify objective data and provides a means of interpreting several data sets simultaneously. This method of classification was initially used to differentiate between the characteristics of non pathological and osteoarthritic knee function (Jones et al., 2006) and has subsequently been used to classify hip function and total knee replacement function (Whatling and Holt, 2010).

The DST helps to deal with conflicting data produced from motion analysis by assigning levels of support to each measurement variable; taking each piece of evidence to classify the data presented. The DST-based classifier transforms the walking data into a set of belief values based on the hypothesis tested and input parameters. The belief values are then represented as a unique point on a simplex plot to visually represent final classification of walking abilities. Visual representation enhances the appeal to the method and provides a tool that can be used to understand behavioural outcomes objectively.

2.3.5.1. DST Classification method

A summary of the classification method (summarised in Figure 2-27) from (Jones et al., 2004) and (Whatling et al., 2009) and is described here using POST_CN and POST_LE comparison as an example. Rat gait data is transformed into a set of three belief values THAT FORM THE Body of Evidence (BOE):

1. A belief that the rat has normal gait (*POST_CN*)
2. A belief that the rat has gait that is characteristic of a model of stroke (*POST_LE*)
3. An associated level of uncertainty $m(\theta)$.

These are represented as points on a simplex plot to give a visual representation of rat gait. The belief value for each point is proportional to the distance of the point from each side of the equilateral triangle, e.g., the closer the point is to the vertex labelled CN the greater is the belief that the subject has a normal gait. The classification method consists of five stages.

1. Conversion of input variables into confidence factors
2. Conversion of confidence factors to BOE
3. Visualisation of BOE using simplex plots
4. Combination of individual BOE
5. Classifications based on the final combined BOE

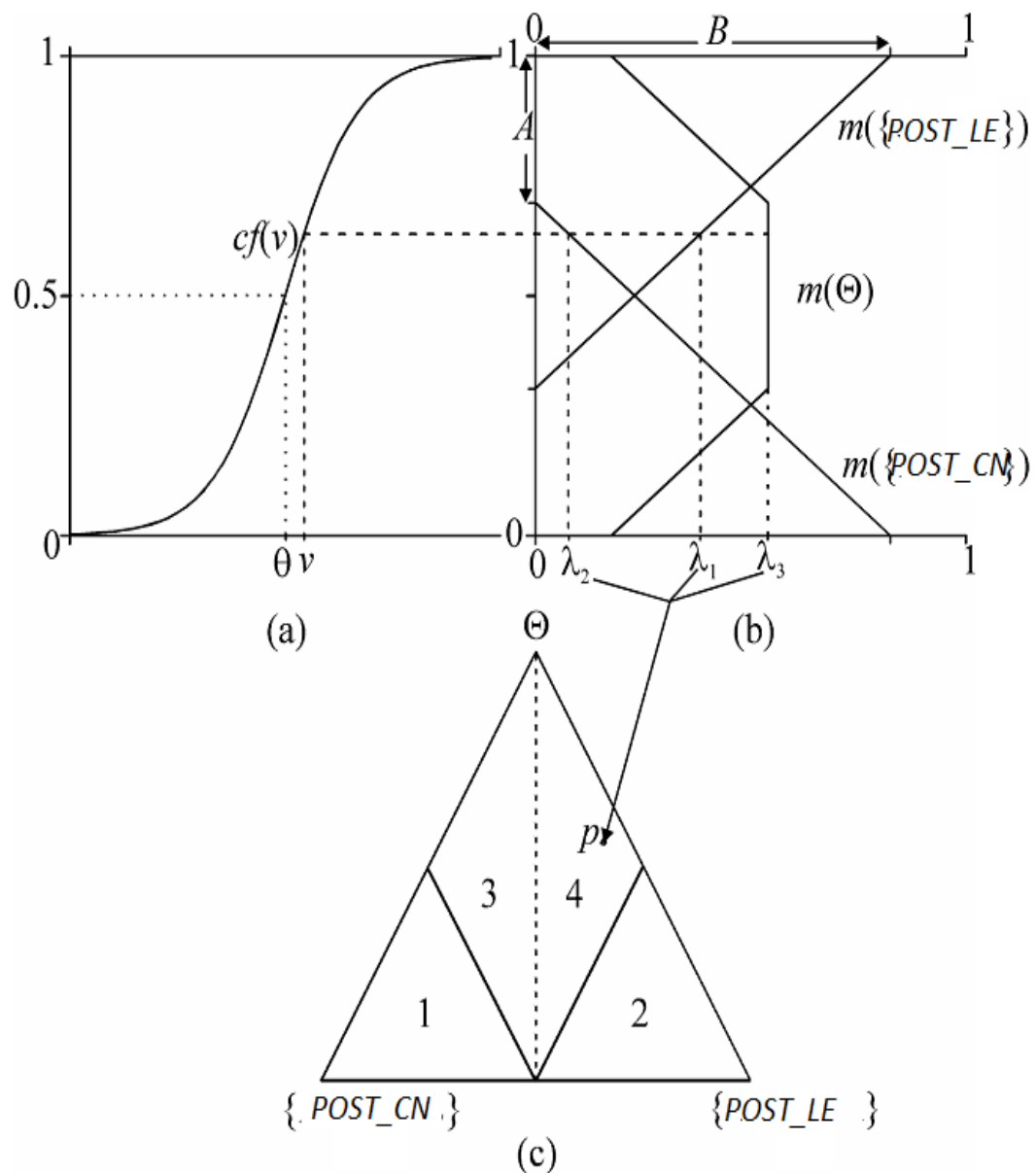


Figure 2-27: The classification method showing the interaction of its three main stages.(a) Conversion of input variable, v , into confidence factor $cf(v)$ using the sigmoid function. Θ is the value of v for which $cf(v) = 0.5$. (b) Conversion of confidence factor into body of evidence (BOE) (c) Conversion of the BOE into its simplex coordinate, denoted by the point p (adapted from Beynon et al., 2002). The simplex plot is divided into four regions: 1 denotes the dominant POST_CN classification region; 2 denote the dominant POST_LE classification region; 3 denote the non-dominant POST_CN classification region and 4 denotes the non-dominant POST_LE classification regions. The dotted vertical line is the decision boundary.

Conversion of input variables into confidence factors (From Jones et al 2004)

The first stage of the classification procedure is to standardise each input or characteristic measurement, v , to a value on a scale of 0-1. The transformed variable is defined as a confidence factor f ($cf(v)$) and represents a level of confidence in (or not in). The $cf(v)$ must satisfy the following criteria (adapted from Safranek et al., 1990):

1. $cf(v)$ is a monotonic function
2. $cf(v) = 1$ if the measurement implies certainty in {POST_CN}
3. $cf(v) = 0$ if the measurement implies certainty in {POST_LE}
4. $cf(v) = 0.5$ if the measurement favours neither {POST_LE} nor {POST_CN}

The input variable is transformed into a confidence factor using the sigmoid function in Equation (2-14)

$$cf(v) = \frac{1}{1 + e^{-k(v-\theta)}} \quad (2-14)$$

Where θ is the value v for which $cf(v)=0.5$. The mean value v is used so that θ is not biased towards either group. The k parameter adjusts the steepness of the sigmoid function (see Figure 2-28). to reflect the nature of the spread of the data.

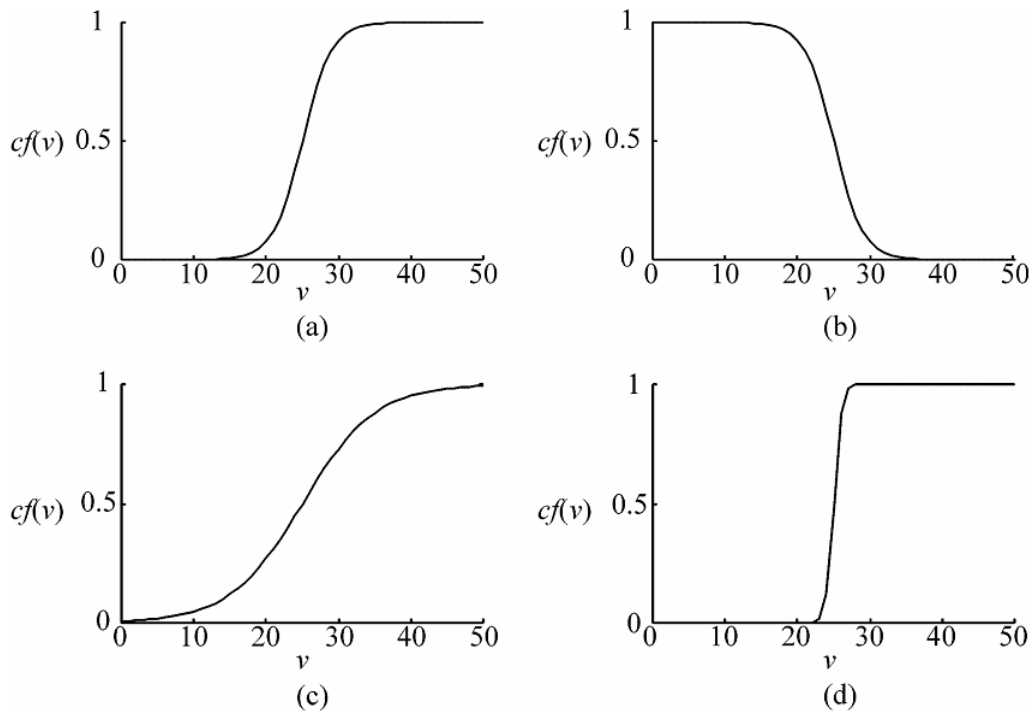


Figure 2-28: Influence of k on confidence factor (a) positive association ($k = 0.25$) (b) negative association ($k = -0.25$) (c) small absolute value of k ($k = 0.2$) (d) large absolute value of k ($k = 2$) (adapted from jone 2004)

Conversion of confidence factors to BOE

The $cf(v)$ is converted into a characteristic body of evidence (BOE). The BOE is a set of belief values which expresses the degree to which the evidence confirms each hypothesis.

1. $m(\{\text{POST_CN}\})$ the degree of belief in the gait being $\{\text{POST_CN}\}$
2. $m(\{\text{POST_LE}\})$ the degree of belief in the gait being $\{\text{POST_LE}\}$
3. $m(\{\text{POST_CN}\} \{\text{POST_LE},\}) = m(\emptyset)$ the degree of belief in either the rats gait being $\{\text{POST_CN}\}$ or $[\text{POST_LE}]$.

The value $m(\{\text{POST_CN}\};\{\text{POST_LE}\})$ is the associated uncertainty and represents the value which cannot be assigned to $\{\text{POST_CN}\}$ or $\{\text{POST_LE}\}$.

The sum of the belief values in a BOE is 1 as in Equation (2-15) i.e

$$m(\{\text{POST_LE}\}) + m(\{\text{POST_CN}\}) + m(\{\text{POST_LE}, \text{POST_CN}\}) = 1.$$

(2-15)

The belief values are defined in Equation(2-16, (2-17 and (2-18 as follows (Whatling)

$$m(\{\text{POST_LE}\}) = \frac{B}{1-A} cf(v) - \frac{AB}{1-A}$$

(2-16)

$$m(\{\text{NORM}\}) = \frac{-B}{1-A} cf(v) + B$$

(2-17)

$$m(\Theta) = 1 - m(\{\text{NORM}\}) - m(\{\text{POST_LE}\}) = \frac{1-A-B}{1-A}$$

(2-18)

Where A is the dependence of $m(\{\text{POST_LE}\})$ of the confidence factor and B is the maximal support that can be assigned to $m(\{\text{POST_LE}\})$. The assignment of the values of A and B is dependent on the general limits of uncertainty $[\Theta_L, \Theta_U]$ allowed for the individual input variables. The values of A and B are expressed in Equations (2-19 and (2-20 as:

$$A = \frac{\Theta_U - \Theta_L}{1 + \Theta_U - 2\Theta_L}$$

(2-19)

$$B = 1 - \Theta_L$$

(2-20)

2.3.5.2. Combination of individual BOE

BOE's combined using the Dempster's rule into a final combined $BOE(BOE_c)$ to offer evidence to support the classification of the input variables. In the case where only two exhaustive outcomes exist, POST_LE and POST_CN, the combination of two independent BOE $m_i(.)$ and $m_j(.)$ is given by the following three formulaic expressions in Equations (2-21), (2-22)(2-23). The BOE_c comprises the same functions as in the individual BOE namely {POST_LE}, {POST_CN} and(Θ).

$$(m_i + m_j)(\{POST_LE\}) = m_c(\{POST_LE\})$$

$$= \frac{m_i(\{POST_LE\})m_j(\{POST_LE\}) + m_j(\{POST_LE\})m_i(\Theta) + m_i(\{POST_LE\})m_j(\Theta)}{1 - (m_i(\{POST_CN\})m_j(\{POST_LE\}) + m_i(\{POST_LE\})m_j(\{POST_CN\}))}$$

(2-21)

$$(m_i + m_j)(\{POST_CN\}) = m_c(\{POST_CN\})$$

$$= \frac{m_i(\{POST_CN\})m_j(\{POST_CN\}) + m_j(\{POST_CN\})m_i(\Theta) + m_i(\{POST_CN\})m_j(\Theta)}{1 - (m_i(\{POST_CN\})m_j(\{POST_LE\}) + m_i(\{POST_LE\})m_j(\{POST_CN\}))}$$

(2-22)

$$(m_i + m_j)(\Theta) = m_c(\{\Theta\}) = 1 - (m_c(\{POST_LE\}) - m_c(\{POST_CN\}))$$

(2-23)

2.3.5.3. Visualisation of BOE using simplex plots

Given the expressions $m(\{POST_LE\}) = \lambda_1$, $m(\{POST_CN\}) = \lambda_2$ and $m(\Theta) = \lambda_3$, a simplex coordinate is used to represent this set of belief values as a single point on the simplex plot (see Figure 2-27). The simplex plot is an equilateral triangle within which lies a point. This point exists such that the distance from p to each of the sides of the equilateral triangle is equal in the same proportion as the ratios of the values λ_1, λ_2 and λ_3 .

There exists a central boundary at the centre where $m(\{POST_CN\}) = m(\{POST_LE\})$. To the left is the area where the belief that the gait is normal i.e., $m(\{POST_CN\}) > m(\{POST_LE\})$. And to the right of the boundary the belief that the rats have a gait that is characteristic of stroke rats, i.e., $m(\{POST_LE\}) > m(\{POST_CN\})$. Region 1 is the area of dominant POST_CN, 2 is for dominant POST_LE, region 3 non-dominant POST_CN function and region 4 non-dominants POST_LE. the simplex plots provide a method of visualising gait data. With numerous data and numerous of groups to compare, visualisation is useful in comparing the three groups of rats in this study (see Figure 2-27)..

2.3.5.4. Evaluating accuracy

The final stage of classifier design is performance evaluation through examination of its error or misclassification rate. This evaluation method is discussed in (Jones, 2004, Jones et al., 2006). The classifier is trained using a set of cases and the error rate is calculated using the same cases that were used to design the classifier (Jones, 2004). The true error rate is estimated using the hold-out method (Jones, 2004) where a set number of cases are assigned to the training group and the remainder to the testing group.

The classifier is trained on the cross-validation method known as the leave-one-out method, where the classifier is trained on N training cases and tested on the remaining one test case. This process is repeated N times. The leave-one-out error rate is then defined as the average test case error rate. This method overcomes the issue of inefficient use of the data since every case is used in testing and each time every case save one is employed as a training case.

2.4. Comparing Human and rat protocol

Protocols were designed to measure human and rat gait patterns accurately using the same measurement system of 3DMA. Differences of the two developed experimental protocols, one for rat and one for human motion capture are summarised in Table 2-5.

Table 2-5: Rat and human MA protocols

	Rat MA	Human MA
Apparatus-dimensions based on rats stride length and base of support during gait	1.65m elevated beam	8m Flat walkway
Camera system–Qualisys ProReflex MCU's	7 cameras calibrated using 300mm kit	12 cameras calibrated using 700mm kit
Retro-Reflective markers	11 on rat and 8 to define the beam	20 on the human and 8 on the walkway
Gait cycles achieved	More than 10	Between 4-6

The human protocol required a larger space, more cameras and more markers to acquire the required number of gait cycles (i.e., 5) than the rat protocol.

2.4.1. Cameras and calibration

To optimise the use of the Qualisys system, camera set up and calibration is very important. Data recording for the rat study was carried out at the School of Biosciences. This was the first time MA techniques were performed across disciplines at the School. The rat protocol involved a 7 camera set up where the cameras were placed around the apparatus to capture data of the whole rat as it walked along the beam the room size and space was not a problem.

Data acquisition of human multiple gait cycles had not been performed at Cardiff University MA Laboratory and due to the size of the room this proved to be a

challenge. To achieve maximum use of the space, 12 cameras were used facing towards the calibration frame. This only allowed the capturing of data at the posterior region of the subject from the start of the walkway to finish. However, the required number of gait cycles could be recorded.

Setting up the cameras was time consuming because camera positions, cable connections, aperture and focus had to be adjusted for each session. The time it took to set up varied depending on the calibration success rate, with the rat calibration having a better calibration rate since all the cameras were focussed at the same volume around the beam. Calibration and set up took longer for the human setup because of the need to carry out an extended calibration, in addition to the numerous cameras and the larger room to work with.

Once the cameras were calibrated, the data collection process was faster for the healthy human subjects since they were able to respond to commands from the researcher and walk along from one end of the walkway to the other without destruction. On the other hand, with rats, marker placement took longer since they were fidgeting while walking and their gait was sometimes unpredictable, However some rats walked without stopping while others would stop and groom before continuing, therefore repeated measurements were necessary to record at least two good walks along the beam.

2.1. Data processing

The purpose of the developed protocol in Chapter 2 was to explicitly compare rat to human gait parameters. To achieve this, similar data processing methods were necessary to measure similar outputs. Each group, that is rats and human, produced similar data patterns which allowed for similar analysis. Assessment of gait to analyse behaviour is essential since this is a common behaviour in both rats and humans. Rat gait studies are used as a paradigm for the experimental study of control and recovery of function after injury in the expectation that results are generalized to humans.

The movements were recorded and analysed using 3DMA to capture frame-by-frame Cartesian data of markers using Qualisys Track Manager (QTM). The measurements are written into text format and exported for post-processing in Excel and Matlab, the process is described in Chapter 2. Two programs were written, one to transform foot and paw trajectories into temporal gait parameters, and the other to transform body rotation kinematic waveforms into the postural data for one gait cycle.

2.2. Outputs

2.2.1. Temporal parameters

Both humans and rats were required to walk over-ground for a length that allowed the capture of five continuous gait cycles. Both trials were practical, non invasive and there were no constraints or hindrance to walking. The limb movement pattern of the rats and the humans during gait appeared very similar. Outputs from QTM of

comparable patterns during locomotion are given in Figure 2-29 and Figure 2-30, for the rats and humans respectively.

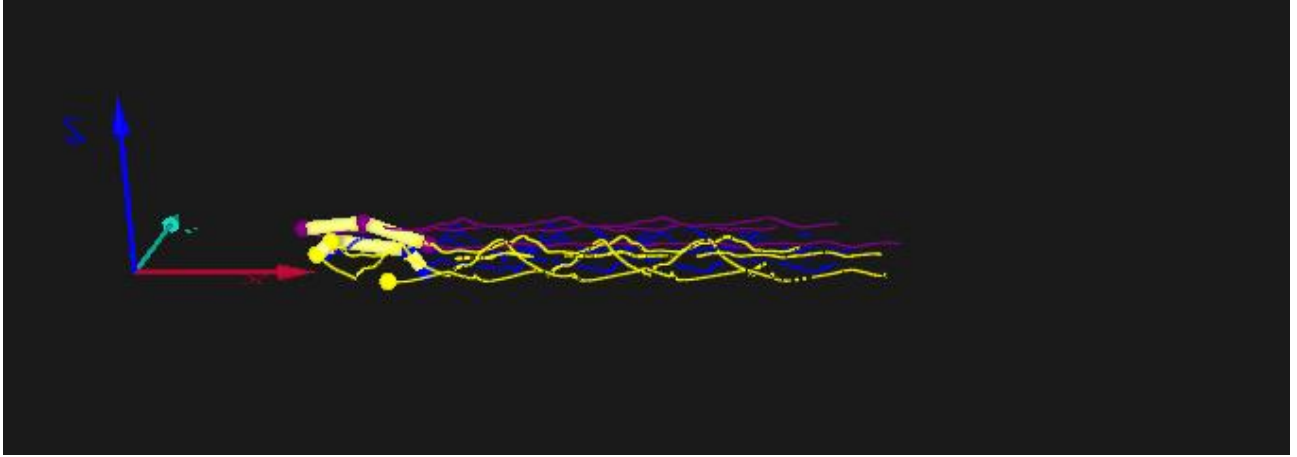


Figure 2-29: Output data from QTM for the rats walking trial showing five gait cycles.

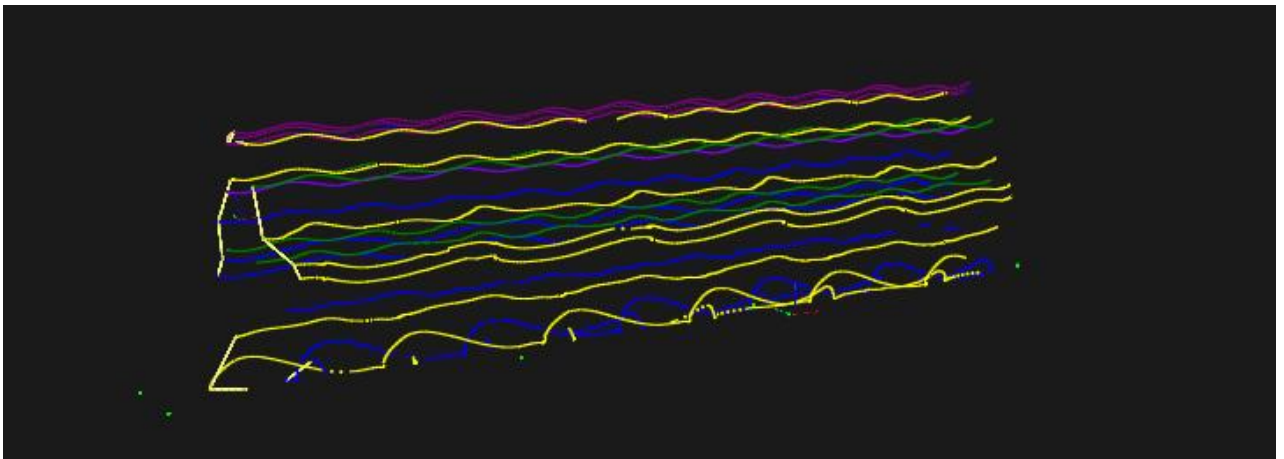


Figure 2-30: Output data from QTM for the human walking trial showing five gait cycles.

In general, rats walked with a lateral gait where two limbs were in contact with the ground at any given time (the order of limb contact in one stride was left hindlimb (LHL), left forelimb (LFL), right hind limb (RHL) and right forelimb (RFL)), whereas the human walking pattern was so as only one limb was in contact with the ground at any one time. The output data had similar patterns of trajectories as illustrated with an example of healthy rats in Figure 2-31 and healthy humans.

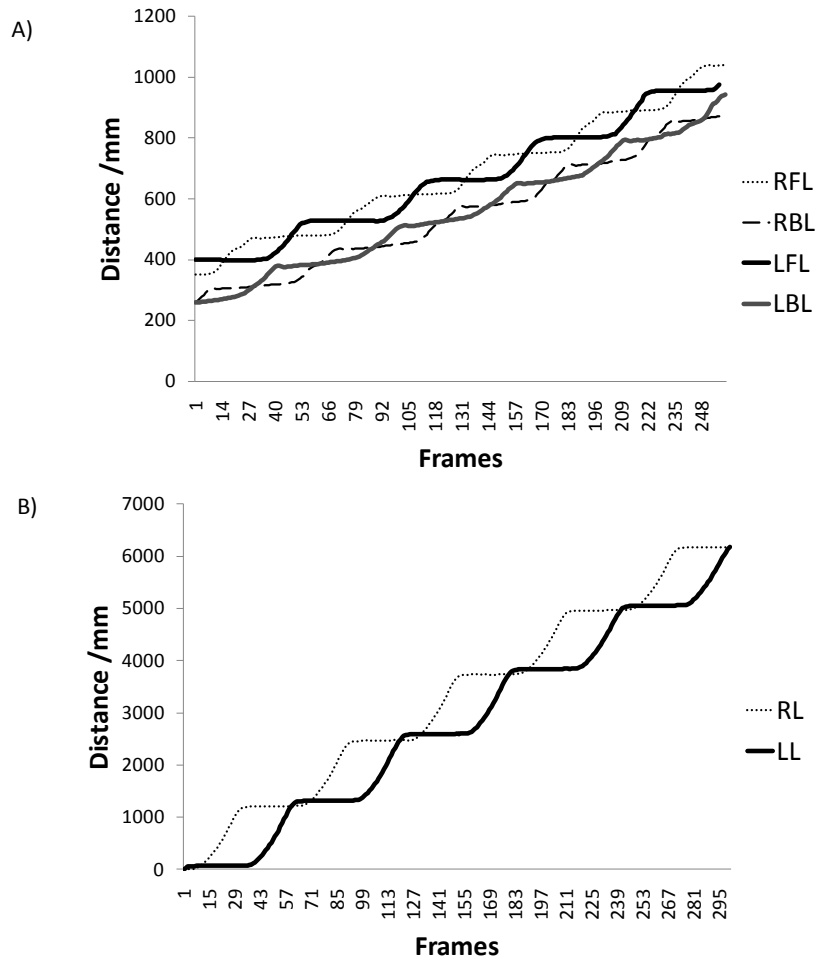


Figure 2-31: A) Rat gait trajectories for all four limbs and B) Human gait trajectories for all four limbs

As illustrated in the two figures, the human subjects walked along on a distance of 7m (Figure 2-31B) while rats require just under 1m length (Figure 2-31A) to record 5 cycles.

2.2.2. Postural parameters

Postural control during gait was also described and discussed for each studied cohort (Figure 2-32 to Figure 2-34 for *roll*, *pitch* and *yaw* respectively). Human postural studies (Chapter 5) describe body rotations of the upper body (shoulders and spine) trunk (shoulders and pelvis) and pelvis to evaluate which of the three body rotation presented patterns that were similar to the rat rotations during gait.

Kinematic waveforms of body rotations revealed that during one gait cycle, body orientation is towards the weight bearing limbs for both species.

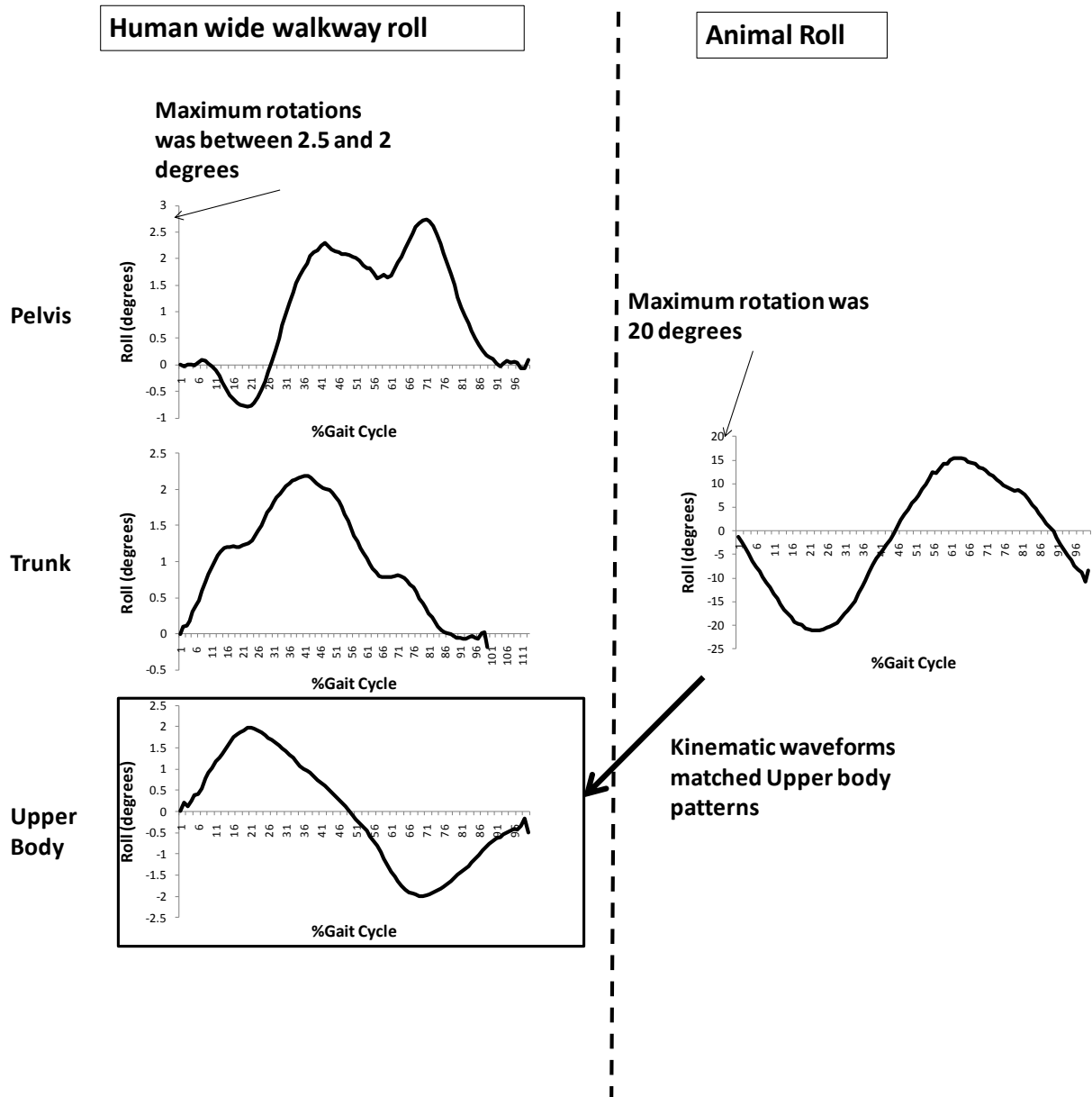


Figure 2-32: The *roll* of the body from left to right during one gait cycle which involves rotations towards the side of limb weight bearing during gait for both species.

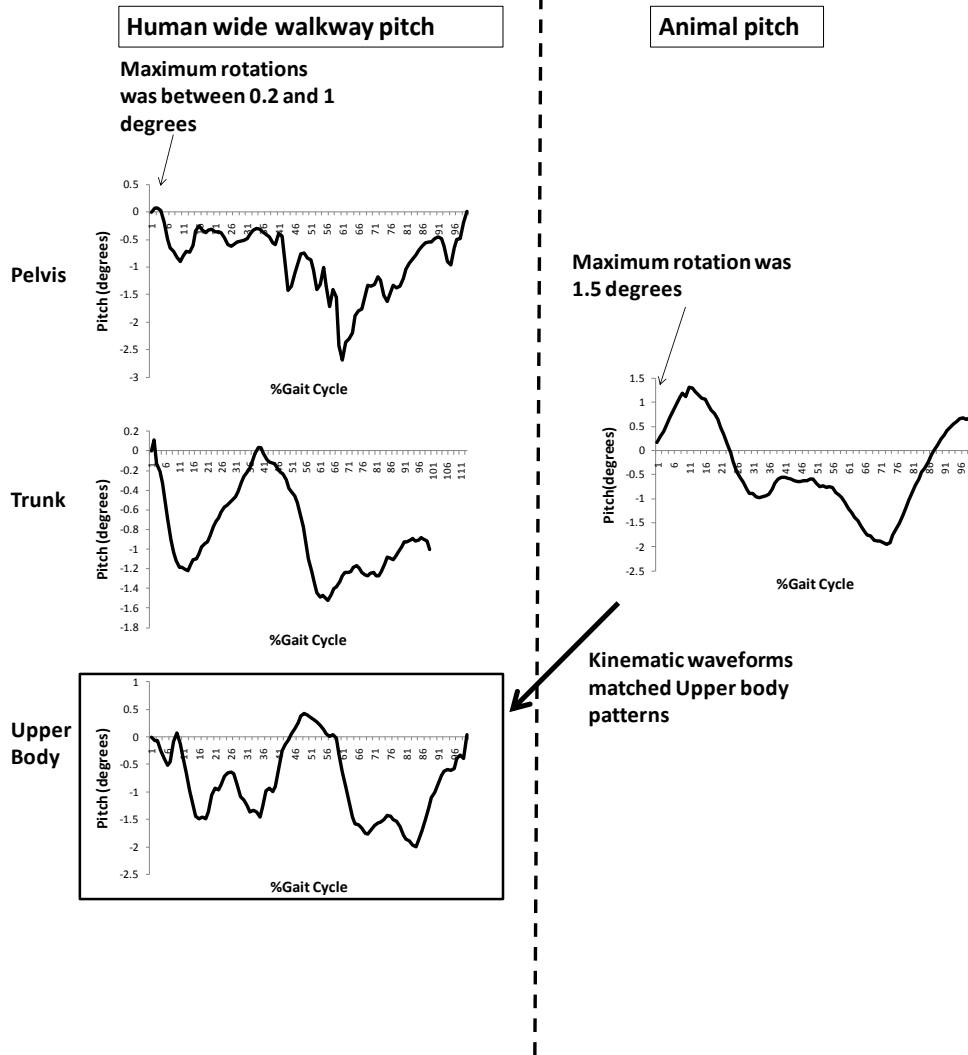


Figure 2-33: Pitch rotation representative of the vertical axial displacements with the human upper body rotations matching the pattern of the animal motion of a double sinusoidal path.

These represent two cycle of downward and upward displacement in each stride of the right and left steps. The two dips occur during periods of double limb support each followed by a progressive rise above zero degrees due to the two single support intervals during terminal stance and late mid swing.

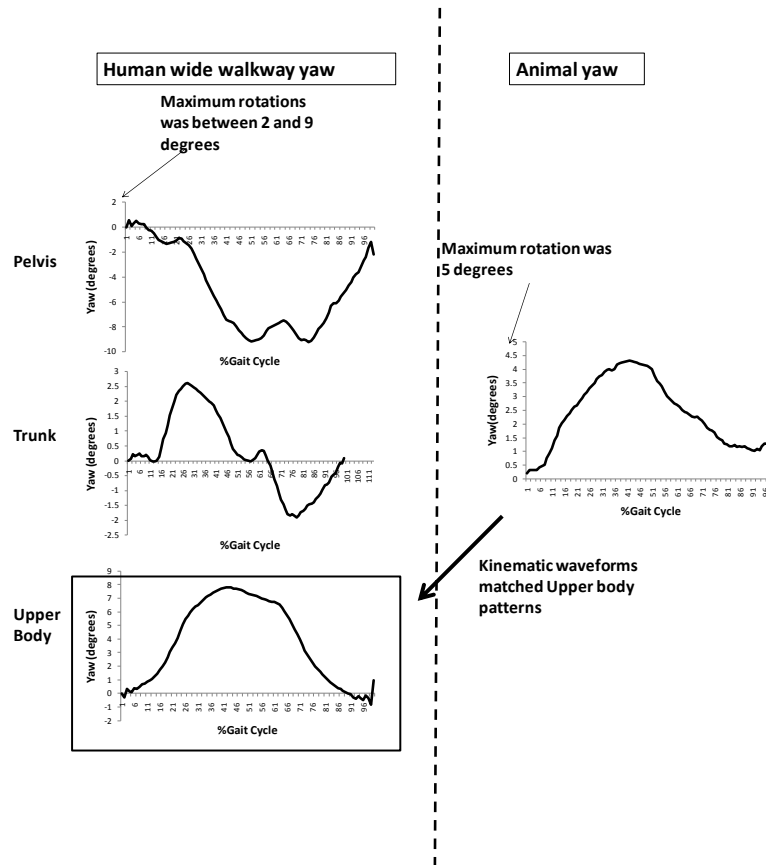


Figure 2-34: Yaw lateral displacement towards the side of the supporting limb is illustrate in the upper body waveforms and the animal waveforms. Displacements occur during single stance as the limb support shifts from the left to right limbs. Maximum displacement is at around 50% gait cycle during double limb with

The developed protocol has demonstrated a protocol that enables the measurements of gait on a defined walkway for both rat and human subjects. This chapter has introduced and described the new protocol for both data collection and processing in detail. The data collection protocol for rat motion capture has achieved a level of practicality that was non-invasive, and in turn producing accurate results illustrated from the error analysis and repeatability tests on marker placements. In addition a new human marker based motion analysis protocol was designed to incorporate the marker set and gait cycles of those of the rat's protocol, incorporating the available volume and similar marker set as the rat protocol. Results and discussions based on this chapter are given in Chapters 3 to 5.

CHAPTER 3

3. Quantifying locomotion of Parkinson's disease rats

This chapter investigates the novel application of the motion analysis protocol developed in Chapter 2 as a tool for assessing the outcome of unilateral lesion surgery on a rat model with Parkinson's disease (PD). A brief introduction to the study, followed by the results of five unilaterally lesion rats and five controls as they walked along an elevated beam is provided.

3.1. Introduction

Animal models of PD (in this case rats) have been reported to exhibit characteristics similar to those found in human patients (Metz et al., 2005, Klein et al., 2009, Whishaw et al., 1992). To investigate the clinical condition of PD, the most commonly used model is the unilateral injection of the neurotoxin 6-hydroxydopamine (6-OHDA) into the rat medial forebrain bundle; (Ungerstedt, 1968).. This injection produces dopamine depletion that results in motor deficits that are similar to those in human PD (Cenci et al., 2002, Henderson et al., 2003, Iwaniuk and Whishaw, 2000, Whishaw et al., 1992).

The Rats with unilateral lesion (hemi-parkinsonian) show motor deficits on the opposite side (contra-lateral) of the lesion. The ipsi-lateral side serves as an internal control. These rats show an almost complete neglect of the contra-lateral side, and conversely are more responsive to stimuli on the ipsi-lateral side while body weight

bearing and posture are compensated with the healthy ipsi-lateral side (Miklyeva et al., 1995).

Previous behavioural studies on rat model of PD to investigate the outcome of the lesion surgery have either been qualitative and descriptive; for example (Whishaw et al., 2003b) analysed behaviour of PD models using rating scales of stepping behaviour to indicate that the hemi-Parkinson rats were chronically impaired in their posture and in the use of the contra-lateral limbs; or invasive such as in EMG studies where electrode are implanted into the skin surface (Metz et al., 2005). Therefore there is a need for a simple, practical and objective tool that would allow for the assessment of the motor deficits expressed in PD models and furthermore, generate results that are comparable to human studies (Whishaw et al., 1992)

3.2. Methods

3.2.1.1. Data collection

Ten adult male Lister Hooded rats (Charles River, UK) were tested in accordance with the United Kingdom Animals (Scientific Procedures) Act, 1986. The rats were older and slower than the average rat used for behavioural studies. They were housed in standard cages in groups of five animals in a temperature-controlled environment ($23.0 \pm 0.3^{\circ}\text{C}$) on a 14 h light: 10 h dark schedule. Food and water was provided *ad libitum*. The animals were divided into two cohorts: five rats underwent the unilateral partial nigrastraital lesion (PNL) surgery while other five rats were non-operated control rats (CNL).

All the surgeries were carried out by a member of licensed member of the Brain Repair Group. All PNL rats were anesthetized with isoflurane (Abbott,

Queensborough, UK) and were stereotactically injected with 6-OHDA (3 µg/µl in 0.2 mg/ml ascorbic acid in 0.9 % sterile saline; Sigma, Poole, UK) into the right MFB using a 30-gauge cannula (Ungerstedt, 1968).. Lesion coordinates were set in mm (Kirik et al., 1998): tooth bar -2.3, anterior / posterior -4.4, lateral -1.0, dorso-ventral -7.8. Injection volume was 3 µl and the injection rate was 1 µl/min. The cannula was left in place for 3 min before withdrawal followed by cleaning and suturing of the wound.

Six weeks post surgery; all animals were habituated to walk along three elevated beams. Three dimensional (3D) Cartesian data of markers attached to the rat were acquired whilst they walked along wide (WD), a narrow (NR) and a graduated (GR) beams using a Qualisys optoelectronic camera system as described in detail in Chapter 2. The beams were equally divided into three sections called *zones*.

The following hypotheses were investigated:

1. Rat models of PD show differences in gait variables compared with their controls while walking over-ground
2. Rat models of PD show differences in gait variables on the limbs contra-lateral to surgery compared to the ipsi-lateral side while walking over-ground on a WD, NR and GR elevated beams.
3. Rat models of PD show differences in gait variables while walking on beams of different widths.

3.3. Data Processing

3.3.1.1. Temporal gait parameters

Temporal gait parameters were quantified by calculating the positional vectors of the markers attached to the four limbs of the rat as described in Chapter 2. The data was input into custom developed software that calculated the stance times, swing times, stride length, speed and cadence for comparisons between the PNL and CNL while walking along the three elevated beams. The data was recorded as the average values of two walking trials for each animal, and the average taken for all the rats from each cohort.

3.3.1.2. Postural gait parameters

Postural instability was also quantified by calculating the rat's body displacement and orientation using Euler angles from markers placed on appendicular parts of the rat's skeletal structure as described in Chapter 2. These markers effectively define a "rigid body" attached to the trunk and enable six degrees of freedom (6DOF) calculation as displacement angles defined as the *roll*, *pitch* and *yaw*. Data was acquired as the rats were walking along three different beams (WD, NR and GR). The displacements were recorded as average range of motion (ROM) angles and generating kinematic waveforms for both cohorts.

Range of Motion

The mean range of motion (ROM) for *roll*, *pitch* and *yaw* rotations were calculated comparing the three beams and the PNL and CNL cohorts. On the WD and NR beams the ROM mean performance was calculated for three gait cycles for each animal in the central section of the beams (zone 2); on the GR beam, the mean ROM was calculated for three gait cycles in each zone.

Kinematic waveforms

The 6DOF displacement was also illustrated as kinematic waveforms in order to visually represent the changes in posture occurring during gait and the strategies that PD rats adopt. The waveforms represent one gait cycle (left forelimb taken as reference) calculated as the average of three gait cycles taken along the central section of the beams. The mean waveform of the three cycles were resample to 100 data points and the average of each cohort was used to compare the differences presented on the beam.

The differences in the kinematic waveforms of *roll*, *pitch* and *yaw* rotations between the two cohorts were examined in order to understand changes in gait and postural strategies in hemi-parkinsonian rats. To compare the patterns of rotations for the two cohorts, the mean of three gait cycles (left forelimb as the reference limb) along the central section of the beam (zone 2) was calculated for the WD and NR beams. For the GR beam, the patterns of rotation were compared within each zone: the means of two gait cycles within zone 1 and three gait cycles within zones 2 and 3 were calculated respectively (Raw kinematic waveforms can be found in Appendix D).

3.4. Results

3.4.1. Temporal Gait Parameters

Temporal gait parameters were considered for comparisons between:

1. The PNL and CNL cohorts
2. The ipsi-lateral and contra-lateral limbs on the PNL cohort
3. The three beams.

An ANOVA ($p < 0.05$) statistical analysis was performed for the 10 animals to evaluate the differences between their gaits following motion analysis along an elevated beam.

3.4.1.1. PNL and CNL

This section compares the data from PNL and CNL rats to illustrate the effect of unilateral lesion surgery on gait. The mean and standard mean errors for the temporal gait parameters of the rat models and their controls were recorded in Table 3-1 and illustrated in Figure 3-1, Figure 3-2 and Figure 3-3 for the WD, NR and GR beam respectively, where the RFL=right forelimb, LFL=left forelimb, RHL=right hindlimb, LHL=left hindlimb.

The main observations comparing the PNL with the CNL cohort were as follows: the PNL cohort showed

1. Lower forelimb cadence for the hind limbs for all three beams.
2. Slower walking speed for the three beams.
3. Longer swing time on the NR and GR beams.
4. Shorter swing times on the WD beam except the LFL
5. Longer stance time on the WD and GR beams with the exception of the RFL in the WD beam.
6. Shorter stance time on the NR beam
7. Shorter stride lengths on all three beams with the exception of the RBL, LBL, RBL on the WD, NR and GR beams respectively.

The observations that were found to be significantly different for beam width and limb interactions were that the PNL cohorts showed:

1. Slower walking speed, lower hindlimb cadence ($F_{1,1} = 6.08$), smaller forelimb stride length on the WD beam ($F_{1,1} = 35.08$),
2. Faster walking speed, lower forelimb cadence ($F_{1,4} = 22.94$) and a longer forelimb stance time ($F_{1,4} = 9.07$) on the GR beam,
3. Lower hindlimb cadence ($F_{1,1} = 20.25$), Longer hindlimb stance time ($F_{1,1} = 9.73$) and lower forelimb stride length ($F_{1,1} = 18.25$) on the NR beam

There were no interactions between the right and left limbs in the two groups.

Table 3-1 Temporal gait parameters comparing the PNL and CNL cohorts on the GR, NR and WD beams (RFL=right forelimb, LFL=left forelimb, RHL=right hindlimb, LHL=left hindlimb). The results are expressed as mean \pm SME

Variable	Limb	Wide Beam (WD)			Narrow Beam (NR)			Graduated Beam (GR)		
		CNL (n=5)	PNL (n=5)	CNL (n=5)	PNL (n=5)	CNL (n=5)	PNL (n=5)	CNL (n=5)	PNL (n=5)	
Cadence (steps per minute)	RFL	190.91 \pm 33.40	147.27 \pm 41.36	175.00 \pm 17.68	(131.25\pm31.46)*	214.62 \pm 26.51	(138.46\pm19.58)*			
	LFL	190.91 \pm 33.40	152.73 \pm 31.10	150.00 \pm 25.00	(133.20\pm31.51)*	200.77 \pm 34.85	(149.54\pm15.17)*			
	RHL	185.45 \pm 35.56	(141.82\pm29.88)*	150.00 \pm 30.62	131.25 \pm 31.46	173.08 \pm 26.51	149.54 \pm 15.17			
	LHL	190.91 \pm 33.40	(141.82\pm35.56)*	140.00 \pm 22.36	118.75 \pm 12.50	214.62 \pm 26.51	138.46 \pm 27.69			
Speed cm/s	Entire beam	15.94 \pm 2.42	(9.87\pm3.24)*	11.91 \pm 2.42	8.51 \pm 3.21	10.89 \pm 2.93	(6.70\pm2.03)*			
	Zone 1	12.78 \pm 5.48	13.75 \pm 0.54	12.16 \pm 1.24	9.71 \pm 2.51	11.41 \pm 1.53	(6.27\pm2.91)*			
	Zone 2	20.30 \pm 3.70	(9.38\pm2.26)*	14.47 \pm 1.52	11.18 \pm 1.80	13.38 \pm 1.76	8.65 \pm 3.52			
	Zone 3	19.06 \pm 2.55	14.22 \pm 4.05	13.98 \pm 1.57	(9.64\pm0.97)*	9.80 \pm 1.43	10.08 \pm 3.39			
Swing time (ms)	RFL	181.67 \pm 20.92	169.67 \pm 25.51	189.67 \pm 66.35	115.41 \pm 64.71	141.83 \pm 36.12	148.67 \pm 15.06			
	LFL	184.00 \pm 23.65	187.00 \pm 30.12	199.00 \pm 13.00	141.49 \pm 83.89	163.56 \pm 29.25	185.58 \pm 25.83			
	RHL	227.33 \pm 27.25	227.00 \pm 60.04	251.33 \pm 37.26	159.61 \pm 95.16	186.39 \pm 83.46	208.86 \pm 46.47			
	LHL	260.33 \pm 52.97	240.33 \pm 37.11	253.92 \pm 55.10	183.16 \pm 104.57	193.44 \pm 40.79	224.83 \pm 30.95			
Stance time (ms)	RFL	595.78 \pm 180.20	526.33 \pm 163.87	397.08 \pm 98.39	467.10 \pm 277.16	416.67 \pm 110.89	(651.08\pm196.93)*			
	LFL	440.08 \pm 126.18	535.83 \pm 147.61	426.75 \pm 131.73	398.64 \pm 297.77	453.33 \pm 100.08	(651.58\pm64.96)*			
	RHL	454.33 \pm 201.07	548.00 \pm 128.83	453.50 \pm 169.08	(434.65\pm248.22)*	530.33 \pm 154.97	660.61 \pm 167.49			
	LHL	477.39 \pm 149.74	554.67 \pm 237.14	329.75 \pm 141.41	(385.86\pm248.23)*	460.33 \pm 152.77	760.00 \pm 309.66			
Stride length (mm)	RFL	105.03 \pm 12.38	(83.92\pm18.27)*	96.57 \pm 14.96	(58.61\pm35.32)*	88.78 \pm 46.88	72.53 \pm 17.53			
	LFL	105.25 \pm 12.08	(82.62\pm19.26)*	87.27 \pm 2.55	(52.87\pm32.14)*	80.94 \pm 23.54	70.75 \pm 15.25			
	LHL	107.95 \pm 14.23	108.38 \pm 29.98	100.86 \pm 11.19	76.94 \pm 53.10	77.36 \pm 26.41	92.72 \pm 41.20			
	LHL	105.94 \pm 14.35	83.88 \pm 20.09	83.88 \pm 25.14	78.70 \pm 73.70	102.04 \pm 50.01	74.12 \pm 14.18			

Significant difference * p<0.05

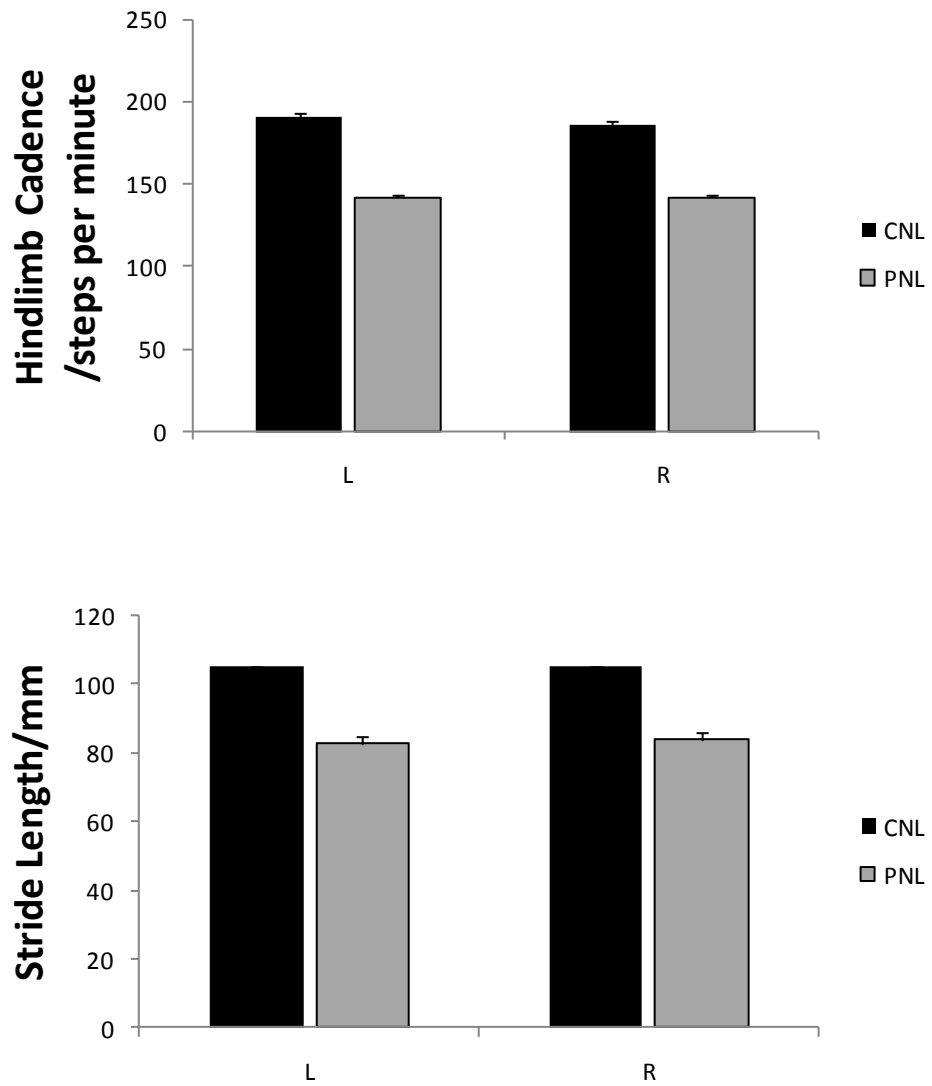


Figure 3-1 : Temporal parameters that were found to be significantly different between the PNL and CNL cohorts while walking along the WD beam. The results are expressed as bar charts of the mean of each cohort with standard mean error

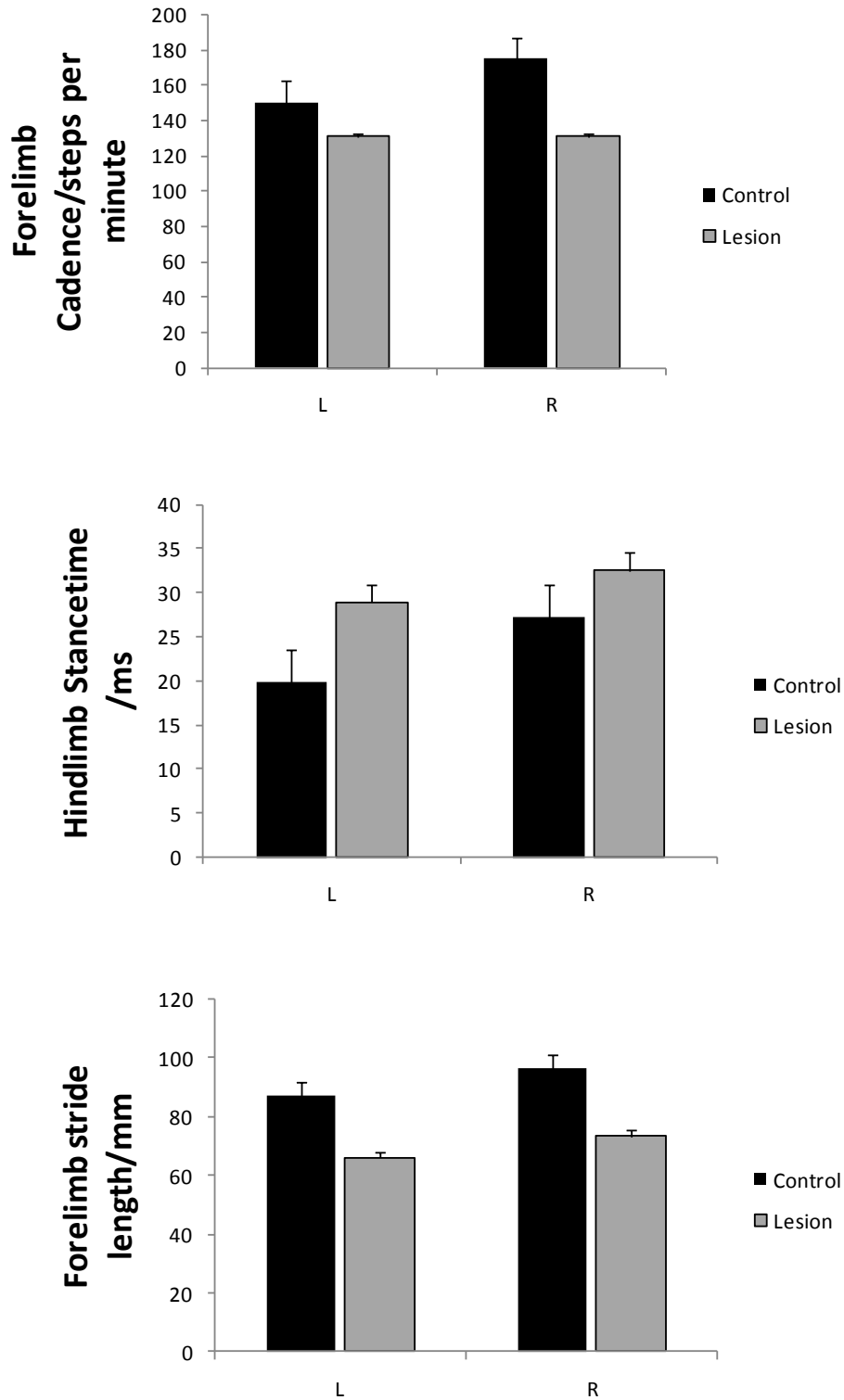


Figure 3-2 : Temporal parameters that were found to be significantly different between the PNL and CNL cohorts while walking along the NR beam. The results are expressed as bar charts of the mean of each cohort with standard mean error bars

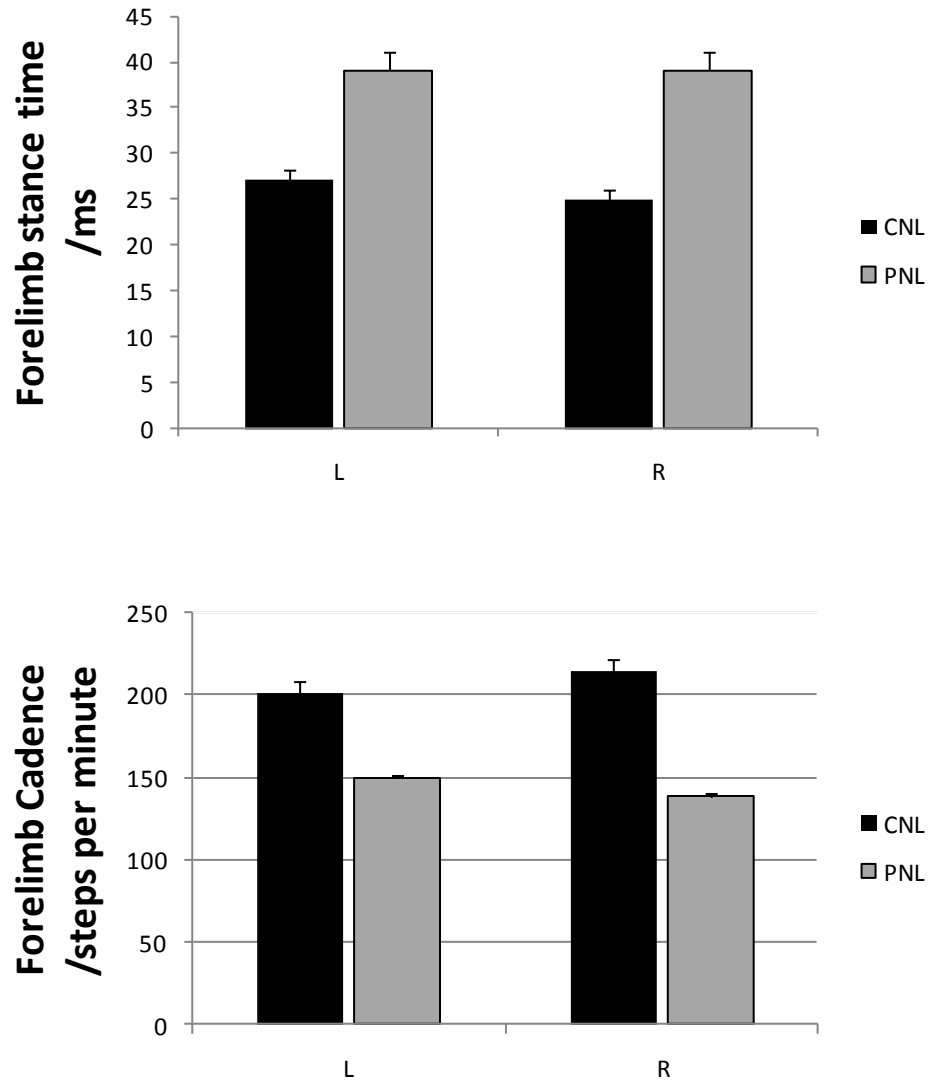


Figure 3-3 : Temporal parameters that were found to be significantly different between the PNL and CNL cohorts while walking along the GR beam. The results are expressed as bar charts of the mean of each cohort with standard mean error bars

3.4.1.2. Comparing contra-lateral and ipsi-lateral limbs

The comparisons between the left (impaired) and right (healthy) sides for the PNL cohort showed that there was no interaction between the side and the three beams, i.e., the different beams had no effect on the data from the sides. The following differences were noted comparing the left and the right sides:

1. Cadence was similar between the right and left side of the rats (Forelimb = $F_{1,4} = 0.23$, $P=n.s.$; and hindlimb = $F_{1,4} = 0.26$, $P=n.s.$)
2. Longer swing times during gait on the left than on the right forelimb and hindlimb showing a slight asymmetry (forelimb = $F_{1,4} = 8.82$, $P<0.05.$; and hindlimb = $F_{1,4} = 3.46$, $P=n.s.$)
3. Longer left forelimb and left hindlimb stance times during gait. These differences were not statistically significant (forelimb = $F_{1,4} = 2.01$, $P=n.s.$; and hindlimb = $F_{1,4} = 0.15$, $P=n.s.$)
4. Shorter forelimb and hindlimb stride lengths while walking. These differences were not (forelimb = $F_{1,4} = 1.21$, $P=n.s.$; and hindlimb = $F_{1,4} = 0.52$, $P=n.s.$)

Although the differences were not significant on most variables, these set of comparisons were included to test the null hypothesis that asymmetry exists between the left and right side due to unilateral surgery that is meant to affect the contra-lateral side only.

3.4.1.3. Comparing beams

The mean and SME for the temporal gait parameters for all animals as they walked along the three beams were analysed.

In general for the CNL cohort walked along the;

1. GR beam with a higher cadence than along WD and NR beams.
2. WD beam faster than on the GR and NR beam
3. GR beam with shorter swing time than along WD and NR beams. The times were longer on the NR beam than on the WD beam.
4. NR beam with the shortest stance time than along WD and GR beams
5. WD beam with long stride length compared to the GR and NR

PNL rats walked along the:

1. GR beam with a higher cadence than along WD and NR beams.
2. WD beam faster than on the GR and NR beam
3. NR beam with shorter swing time compared to the WD and GR beams
The times were longer on the WD beam than on the GR beam.
4. GR beam with longer stance time compared to the WD and NR beams
5. WD beam with long stride length compared to the GR and NR

It was found that there was a significant effect of the beams width on:

1. Forelimb and hindlimb cadence (forelimb = $F_{1,8} = 5.70$; and hindlimb = $F_{1,8} = 27.98$). A post hoc analysis revealed that the difference was significant between the WD and NR beams and between the GR and NR beams.

2. Speed where $F_{1,2} = 6.52$, a post hoc analysis revealed that the difference was significant between the WD and GR beam.
3. There was a significant interaction between the PNL and CNL cohorts for the *roll* ROM ($F_{1,2} = 4.64$) and the forelimb swing time ($F_{1,4} = 3.53$).

3.4.2. Postural gait Parameters

The *roll* ROM was significantly higher in the PNL cohort while walking along the WD beam. Table 3-2 displays mean *roll*, *pitch* and *yaw* ROM on the GR beam calculated during motion along each zone 1, zone 2 and zone 3 independently. The mean *roll* ROM in zone 1 was found to be significantly less for the PNL cohort. The mean *pitch* ROM in zone 2 was less in the CNL cohort compared to the PNL cohort. All other ROMs in zones 1 and 2 were found to be similar. In zone 3, where the beam has reduced its width to the width of the NR beam, the *roll* ROM showed a non significant trend towards being higher for the CNL cohort compared to the PNL cohort; however, no significant differences were found. It is noteworthy that the *yaw* ROM displayed a particularly large standard variation in all three zones.

3.4.2.1. Kinematic waveforms

Figure 3-4 shows mean kinematic rotations along the WD beam; The PNL cohort produced a more positively biased *roll* and *yaw* ROM, i.e. they **leaned** to the right (healthy) side while **turning** towards the left during gait. Figure 3-5 represents mean rotations along the NR beam. The CNL and PNL cohorts used similar patterns of motion. Analysing the two cohorts, there was no bias towards either side for the *roll* and *pitch* ROM. The PNL cohort walked with a negative *yaw* ROM, i.e. they turned towards the right (healthy) side.

Figure 3-6 displays rotations in zones 1, 2 and 3 for the GR beam. The CNL cohort produced a negatively biased *roll* ROM. The PNL cohort walked with a positive *roll* ROM, i.e. they leaned to the right (healthy) side, which is related to the tail to the right. Both *pitch* and *yaw* rotations showed a positive bias compared to the CNL cohort. Note the increasing variations in zone 2 and 3 as the width of the GR beam decreases.

Table 3-2: The mean ROM (degrees) for *roll*, *pitch* and *yaw* during locomotion along the WD, NR, and the three zones on the GR beam for the PNL and CNL cohorts; significant differences (* $p < 0.05$) were found between the CNL and PNL animals for *roll* on the WD beam and *Yaw* on the GR beam (zone 1).

Beam	Postural ROM/degrees	CNL	PNL
WD	Roll	22.41±4.51	27.01±5.10*
	Pitch	12.50±3.84	12.95±3.90
	Yaw	12.36±2.38	13.19±2.53
NR	Roll	27.52±5.01	24.94±2.25
	Pitch	16.24±2.41	13.66±4.37
	Yaw	15.62±2.36	13.87±4.08
GR_Zone1	Roll	28.60±10.11	25.26±11.77
	Pitch	11.14±2.00	8.48±2.06
	Yaw	11.50±2.37	7.88±3.093*
GR_Zone2	Roll	24.41±4.24	25.17±1.964
	Pitch	11.29±1.23	10.66±1.391
	Yaw	13.53±2.76	13.03±6.132
GR_Zone3	Roll	24.16±3.317	24.76±2.8
	Pitch	12.91±3.549	15.82±4.2
	Yaw	15.06±3.718	14.84±5.6

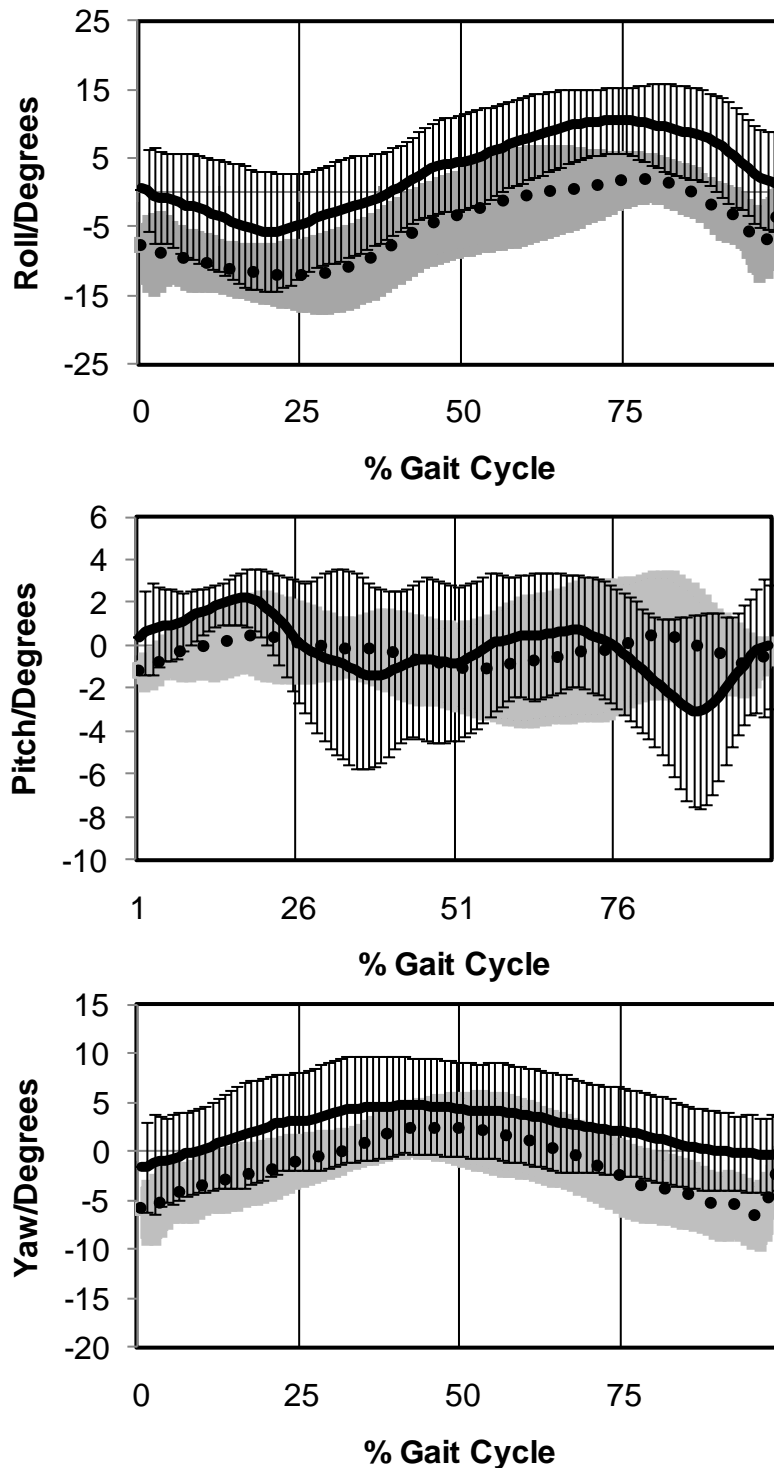


Figure 3-4: Kinematic waveforms for the average walking performance and its SD for one gait cycle on the WD beam. The bold black lines represent the average performances of the PNL cohort (the SD is plotted in thin black lines); the dotted lines represent the average performance of the CNL cohort (the SD is plotted in grey).

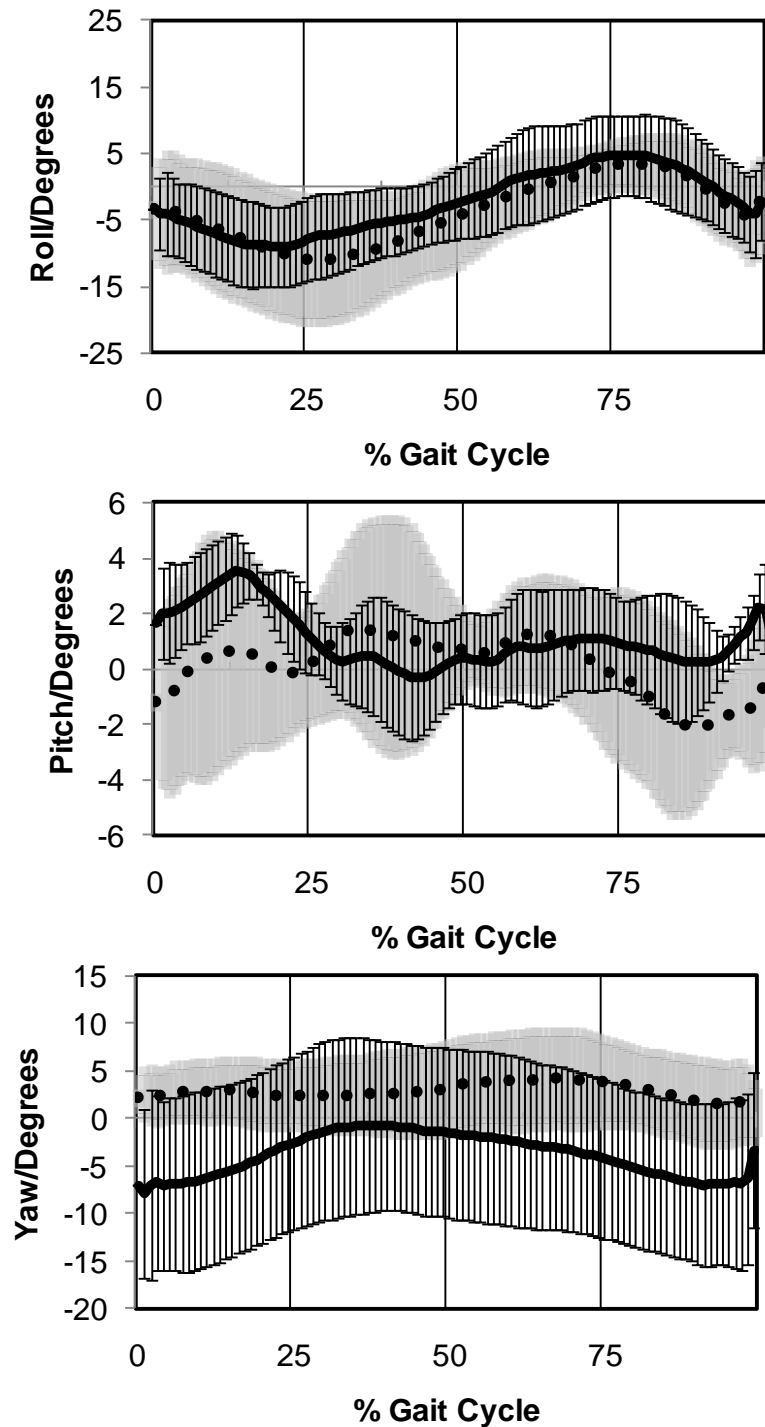


Figure 3-5: Kinematic waveforms for the average walking performance and SD for one gait cycle on the NR beam. The bold black lines represent the average performances of the PNL cohort (the SD is plotted in thin black lines); the dotted lines represent the average performance of the CNL cohort (the SD is plotted in grey).

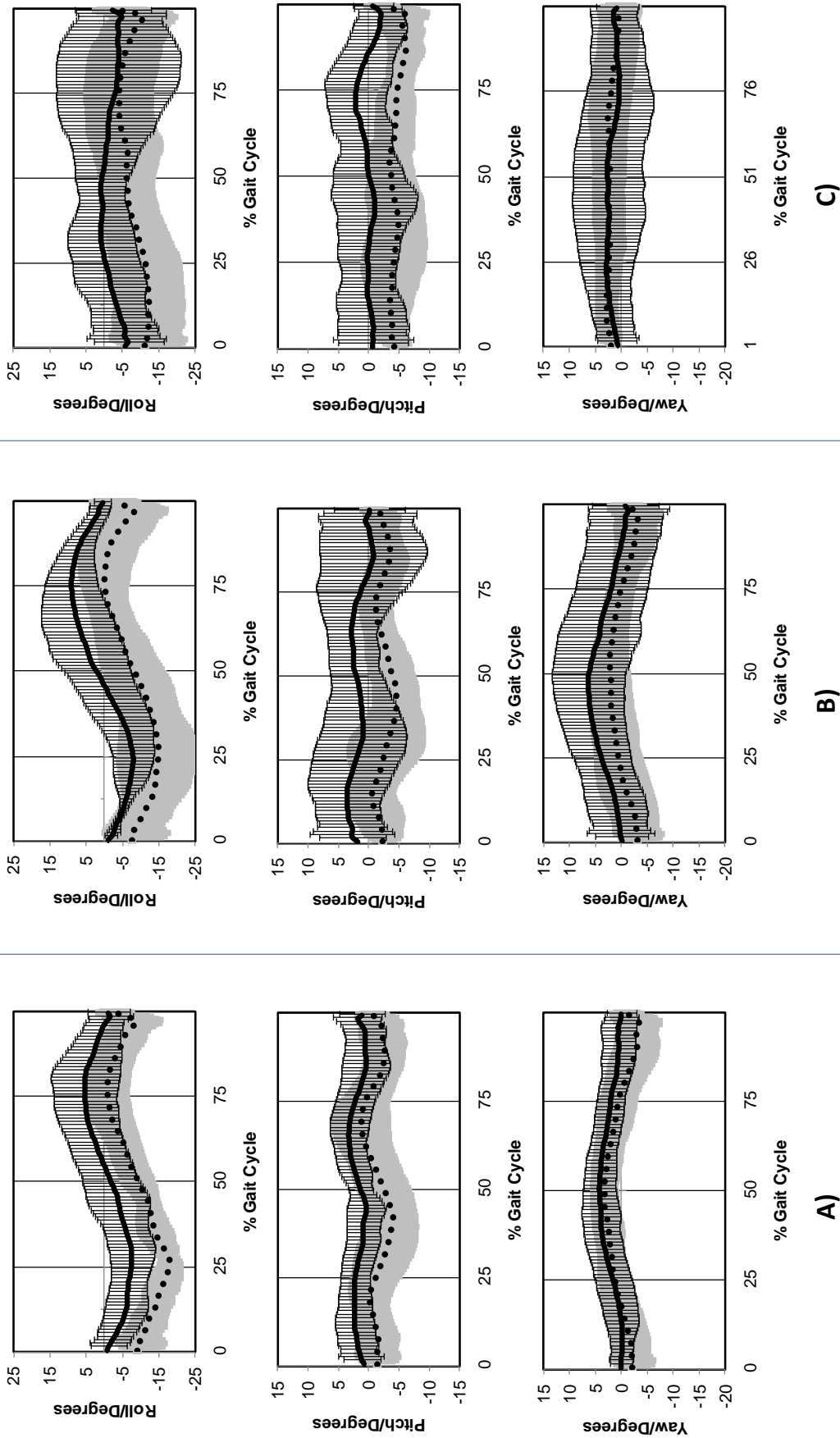


Figure 3-6: Kinematic waveforms for the average walking performance and its SD for one gait cycle on the GR beam A) zone 1, B) zone 2 and C) zone 3. The bold black lines represent the average performance of the PNL cohort (the SD is plotted in thin black lines); the dotted lines represent the average performance of the CNL cohort (the SD is plotted in grey)

3.4.2.2. Tail and limb position

Tail position was recorded as *straight*, *right* or *left* during locomotion on the beam Table 3-3. The main difference in tail position between the two cohorts is demonstrated by the PNL cohort walking with their tail mainly to the *right* (healthy) body hemisphere on the WD, NR and GR beams. However, one animal of the PNL group developed a different strategy while crossing the WD beam where the tail was always on the left, compensating for having both the right fore and hind limbs always on the right ledge (instead of on the beam).

Limb position of all the four limbs was observed and recorded as either 'limb on the beam' (= 1) or 'limb on the ledge' (left or right; = 0). On the WD beam, the CNL rats placed their limbs on the beam while walking along the beam at all times (100%), whereas the PNL rats placed their limbs only with an 85% success rate on the beam (Table 3-4). On the NR beam, all the rats in the CNL and PNL cohorts walked on the beam with a 50% success rate. On the GR beam, all rats in both cohorts walked with their limbs on the beam in zones 1 and 2 (90 - 100 %), whereas in zone 3, 25% of the CNL and 35% of the PNL rats used the ledge with their left limbs.

Table 3-3: Tail positions expressed as a percentage of all analysed gait cycles as either straight behind the rat's body on beam or right or left of the rat's body assisting postural balance by touching the beam and the ledge

Beam	Tail Position	CNL/%	PNL/ %
WD	Straight	80	20
	Right	0	40
	Left	20	40
NR	Straight	0	0
	Right	60	100
	Left	40	0
GR-Zone 1	Straight	40	40
	Right	0	60
	Left	60	0
GR-Zone 2	Straight	0	40
	Right	0	60
	Left	100	0
GR-Zone 3	Straight	0	0
	Right	40	100
	Left	60	0

Table 3-4: Position of all the four limbs was recorded as either 'limb on the beam' (= 1) or 'limb on the left or right ledge' (= 0) and is presented as a percentage of all gait cycles analysed per run.

Beam	Limb Position	CNL/%	PNL/%
WD	Beam	100	85
	Right Ledge	0	12
	Left Ledge	0	3
NR	Beam	50	50
	Right Ledge	25	25
	Left Ledge	25	25
GR-Zone 1	Beam	90	95
	Right Ledge	0	0
	Left Ledge	10	5
GR-Zone 2	Beam	100	100
	Right Ledge	0	0
	Left Ledge	0	0
GR-Zone 3	Beam	75	65
	Right Ledge	10	10
	Left Ledge	25	35

Repeatability of assessed gait parameters was excellent (ICC >0.890), except for temporal parameters along the WD beam for the CNL cohort (ICC 0.283) and the PNL cohort (ICC 0.446) ,

3.5. Discussion

This chapter presents quantitative assessment of 3D temporal gait parameters as well as speed and postural adjustments during over-ground locomotion of healthy and hemi-parkinsonian Lister Hooded rats. The comparison of lesion and control animals indicates that animal MA can provide a measure of different behaviour and functional characteristics of all four limbs. Five different variables were tested for significant differences between the two cohorts; body asymmetry was quantified between the impaired and the healthy side within the PNL cohort and the effects of varying the width of the beam on speed was also measured.

Numerous methods have been suggested to study locomotion of rats with PD lesions, both in 2D and in 3D. However, few were performed with intention to correlate motor performance of patients with their respective animal models. For this reason, the current study was established using 3D MA techniques to evaluate functional aspects of PD during over-ground walking on three different elevated beams.

The PNL animals with unilateral dopamine depletion show impairments that are homologous to PD patients (Whishaw et al., 1992, Metz et al., 2005) and present the motor deficit on the side contra-lateral to surgery, in this case impairment was on the left side. For the current study, expected asymmetry was observed and quantified for the PNL animals, affecting stance and swing times as well as cadence. Speed of

movement along the beams has also been shown to be slower following lesion surgery, caused by delayed initiation and processing of motion (Lundblad et al., 2002). In the current study the average crossing speeds of the three beams was found to be lower for the PNL cohort.

Results from this study support the view of Metz et al., (2005), Miklyaeva et al., (1995), and Pinna et al., (2007), that, compared to the CNL cohort, the PNL cohort walks more slowly with a longer stance time and swing time, indicating that the animals consistently remain in stance for longer period of time in all four limbs, resulting in lower cadence and a shorter stride length. The latter was significantly shorter in the PNL cohort for the impaired forelimb on the NR and WD beams. The impaired hind limb on the GR beam also had significantly shorter strides. PNL animals have a reduced ability to move the body forward using the impaired limb; they stay in stance for a longer period of time to allow the non-impaired limbs to move the body forward when entering the swing phase.

Quantitative analysis of postural instability during over-ground locomotion of healthy and hemi-parkinsonian rats is also presented. Differences in posture and increased postural instability were measured in a rodent model of PD by means of 3D MA. The current study introduces a sensitive quantitative assessment of angular changes of body rotations during walking on three different beams. Walking patterns were recorded by means of marker-based motion capture; posture was analysed using rotational data of the Cartesian x, y and z axes known as *roll*, *pitch* and *yaw*, respectively. Video data monitoring limb and tail position were also analysed. The comparison of lesion and control animals indicates that even small changes in posture can be quantified using 3D motion capture technology during gait. PNL

animals with unilateral dopamine depletion presented motor deficits on the side contra-lateral to surgery. Furthermore, postural attributes of contra-lateral gait and how this translates to balance the body on the beams, limb placement and the use of tail as a counter balance to the impaired side are also observed in PNL animals, since the PNL animals stayed in stance for a longer period of time allowing the non-impaired limbs to move the body forward when entering the swing phase. There is a reduced ability to move the body forward using the impaired limb. These impairments have an effect on the orientation of the body in space, i.e. the rats' posture.

Miklyaeva *et al.* (1995) suggested that compensatory postural adjustments observed in dopamine depleted rats are active strategies directed towards maintaining posture and not the inability to use the bad limbs for support. Hemi-parkinsonian rats show typical symptoms of PD (Adkin *et al.*, 2005, Giladi *et al.*, Woollacott and Shumway-Cook, 2002, Whishaw and Dunnett, 1985); they use a greater range of rotation, illustrated by a larger body *roll* from left (impaired) to right (healthy) and a turning effect towards the right when viewed from above (*yaw*). Previous studies have used various methods of analysing posture and body orientation. However, none have investigated body postural instability of hemi-parkinsonian rats by quantifying angular measurements (i.e. *roll*, *pitch* and *yaw*) of the trunk during gait.

During forward motion on the WD beam, which has a larger base of support, a significantly higher ROM in the parameter *roll* was recorded for the PNL cohort; this was coupled with a positively biased *roll* rotation (leaning towards the impaired side) during the course of a gait cycle. DA-depleted rats display compensatory postural adjustments used to maintain postural control following an impaired contra-lateral gait caused by the rats' inability to shift body posture with the impaired limbs

[Miklyaeva *et al.*, 1995; Martens *et al.*, 1996]. Thus, instability is expressed as a (negative) body *roll* towards the healthy hemisphere side of the body. The *pitch* and *yaw* values did not show any significant differences.

2D video analysis revealed the effects of increasing the difficulty of the beam walking task by introducing a narrower beam. While walking along the NR beam, both the CNL and PNL cohorts had either their right or left limbs on the ledge 50% of the length of the beam, compared to a lower incidence on the WD beam (CNL: 0 % and PNL 15 %).

The NR beam caused both animal cohorts to walk with foot-slips which were unintentional rather than being related to compensatory strategies adopted to maintain balance. In addition, tail position for support by the PNL cohort was predominantly towards the right (healthy) side on the NR beam. Decreasing the width of the beam did not show a difference between the two groups in terms of rotation ROM and the kinematic waveforms. The current study also evaluates the effect of dual tasking (gradually changing the beam width whilst walking along the beam) on both cohorts.

Zonal Speed was calculated for three different zones of the beams to investigate the effect of a graduating walkway on locomotion ability. The results disclose that the lesioned animals accelerated on the GR and the NR beam, possibly dealing with the decreasing path width and trying to reach the other end of the beam and the safe resting box more quickly. The CNL cohort was able to adapt their gait and to cope with the varying beam widths at all times. Comparison of zonal speed between the two cohorts displays a significant slower speed in zone 2 for the PNL animals on the GR beam (the GR beam is supposed to be the most difficult one as a constant

adaptation of gait is required); zone 2 is the area of the beam where the “graduating” of the path width begins indicating that the PNL group took longer to adjust their speed as the beam narrowed. However, on the NR beam the significant difference occurs in zone 3; where the PNL animals decelerated more than the CNL animals to allow for adjustments of their walking pattern.

Hemi-parkinsonian rats show typical symptoms of Parkinson’s disease (Metz and Whishaw, 2002, Miklyaeva et al., 1994, Klein et al., 2009): not only the rats’ gait is severely impaired, but also other motor deficits are obvious such as cataleptic behaviour (Klein et al., 2009) and motor coordination deficits (Metz and Whishaw, 2009).

Although the PNL rats walk more slowly over the beam than their healthy counterparts, their speed varies between the zones. This might be part of compensatory mechanisms to overcome some of the motor deficits. Similar behaviour can be observed in patients with shuffling gait but high cadence (Brown et al., 2006). After a period of slow initiation of motion, a higher cadence/speed is needed to overcome freezing and brady-kinesia.

This study enables the quantification of animal motion in terms of the ability to adjust their gait to cope with the different beam widths, thus introducing an element of dual tasking. For example, the zonal speed varied as the animals adjusted their speed to compensate the change in beam width. Therefore, the present protocol can successfully quantify compensatory behaviour, gait variability and deficits in executive function in a group of hemi-parkinsonian rats allowing future correlation of motor performance with patients’ data.

The present analysis enabled quantification of compensatory behaviour of hemiparkinsonian rats in terms of body orientation while trying to cope with different beam widths. For example on the GR beam, zonal range of rotation (*roll*) varied as the animals adjusted their position to compensate the change in beam width. The results on the GR beam disclose that the CNL cohort was able to adapt their gait to cope with the varying beam widths at all times. There was a consistently lower ROM as the beam became narrower; in contrast, the PNL cohort showed increased instability as the ROM of the *roll* and *pitch* increased between each zone.

The results demonstrate PNL rats' reduced ability to adjust their posture to maintain balance when the beam starts to narrow. Similar to the WD beam, a gait pattern with a bias toward the ipsi-lateral (healthy) side is observed as part of a compensatory strategy. These mechanisms allow the rat to overcome weight bearing issues on the more affected (contra-lateral) limbs to maintain balance and support, hence avoiding falling from the beam. Similar behaviour is observed in patients with decreased ability to internally control changes in the centre of mass during self directed activities that involve maintenance and control of the centre of mass (Bishop et al., 2006, Adkin et al., 2005).

CHAPTER 4

4. Quantifying locomotion of stroke rats

This chapter explores the application of the motion analysis (MA) data collection and processing protocols developed in Chapter 2 and Chapter 3 to a rat model of stroke. In brief, three dimensional (3D) Cartesian data of markers attached to the rat were used to record and analyse gait whilst they walked along a wide (WD) beam using an optoelectronic camera system. The narrow and graduated beams were not used in the stroke model due to the time constraints and the type of model but will be part of the protocol in any future studies. The data acquired aimed to investigate behavioural and functional attributes of Middle Cerebral Artery Occlusion (MCAO) lesion surgery and the outcomes of embryonic grafting. The chapter begins with a brief background to the study and an outline of the main hypotheses. Thereafter the results of the study acquired from 30 rats are presented and discussed followed by an overall discussion of the findings.

4.1. Introduction

MCAO in the rat is used to mimic large vessel occlusion in humans. As is the case with humans, the territory of the middle cerebral artery is the largest of all the cerebral arteries, and the proximal branches supply the posterior striatum and internal capsule (Paxinos, 1995). The MCAO technique should, theoretically, produce restriction in blood supply both in the cortex and in striatum. However, blood

flow from parallel (collateral) blood vessels can contribute to maintenance of cerebral blood flow that sustains tissue viability in the cortex. This means that the behaviour exhibited by the rat is dependent on the location and size of the lesion.

Embryonic grafting is a technique that is used to replace neuronal populations within the lesioned brain. Grafting embryonic tissue into the damaged areas of rat's brain has been shown to restructure synaptic, neuro-chemical and behavioural deficits in rat models of neurological dysfunction such as Parkinson's disease (PD) and Huntington's disease HD (Dunnett, 1992). Striatal tissue grafted within the damaged striatum partially restores an appropriate anatomical distribution of neuro-chemicals decreases lesion induced hyperactivity and reintegrates into the striatal circuitry (Dunnett et al., 1988, Björklund, 1992). Therefore the use of embryonic tissue for grafting can provide a functional recovery to the damaged brain.

The most common symptom of human MCAO is total or partial inability to move one side of the body and the loss of sensation on one side of the body. The most common behavioural tests for rodents with stroke were designed to examine the differences in function between the intact (ipsi-lateral) and impaired (contra-lateral) side of the body using asymmetry tests (Schallert et al., 2003, Ungerstedt et al., 1968). Many of these tests were originally developed for other unilateral models of basal ganglia disorders, such as PD and HD disease. However, these tests also reveal deficits in rats with MCAO (Modo et al., 2000). This chapter applies a 3D marker based motion analysis (3DMA) technique which has been shown to work for a cohort of PD models (Chapter 3) where temporal and postural gait parameters were successfully processed and discussed.

The results presented in Chapter 3 prove that the developed protocol is objective and practical in investigating and assessing motor deficits during gait of rodent models. The method is quantitative, sensitive and furthermore it allows important and subtle differences to be determined that can be missed when using traditional studies. The effect of MCAO lesion and embryonic grafting on gait was investigated, and a group of naive controls were also tested for age matched comparisons.

4.2. Methods

4.2.1. Data collection

All procedures were carried out in accordance with the United Kingdom Animals (Scientific Procedures) Act, 1986. 50 adult male Wistar rats were used in this experiment (Harlan, UK). The analysis would form part of a larger study to assess the behavioural characterisation of the MCAO rat Model. The rats were investigated using several behavioral tests including some of the ones introduced in Chapter 1, i.e., including staircase paw reaching and the balance cylinder and the elevated beam. The results presented in this chapter will only focus on gait analysis on an 'elevated beam'.

Initially, all rats were habituated to walk along the beam following which marker based 3D digital video recordings, using a seven Qualisys PRO-reflex optoelectronic camera system (Qualisys, Sweden), were captured as described in detail in Chapter 2. This was the first MA session (MA1). After MA1, 40 of the rats underwent MCAO surgery and the remaining 10 rats were used as naive control rats. The surgeries were carried out by a licensed member of staff at the Cardiff Brain Repair Group. 24 hours later they had MRI scans that excluded those rats that did not exhibit a lesion,

or showed signs of haemorrhage. 23 rats had suitable lesions and were included in the further study. Seven to 12 days after the MCAO surgery 10 of the 23 lesioned rats received embryonic grafts Six weeks after the MCAO surgery the rats were re-trained on the beam and a second MA beam walking trial was performed (MA2). The data collection points were pre determined by the surgery and training schedule. A summary of the timeline for the two MA trials and performed surgeries is presented in Figure 4-1.

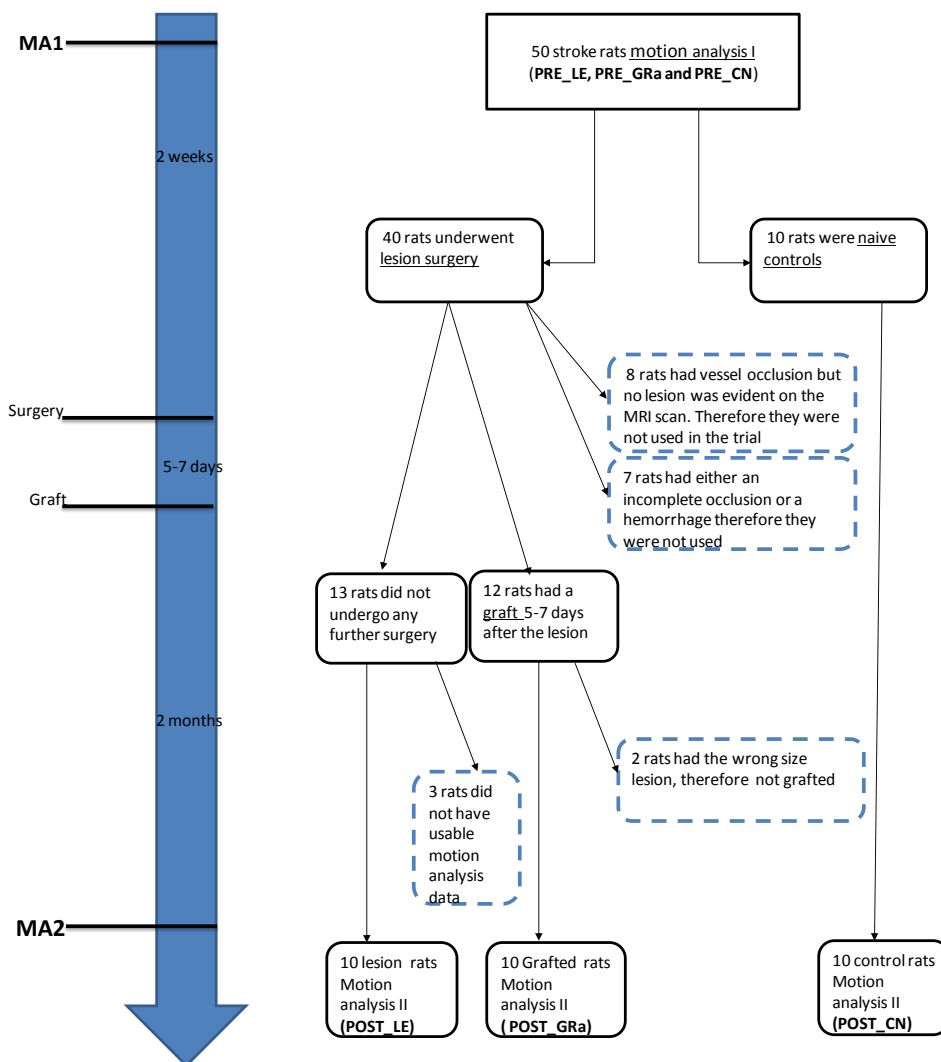


Figure 4-1: Experimental design and timeline of the stroke MA study

4.2.1.1. Middle cerebral artery occlusion surgery

Rats were anaesthetised and the rat's core body temperature was kept at $36.7 \pm 1^\circ\text{C}$ using automated heat blankets with temperature feedback (Harvard, UK). Laser Doppler probe was used to assess changes in cerebral blood flow (CBF) to the middle cerebral artery (MCA) territory and was monitored using a Laser Doppler Perfusion Monitor (Moor Instruments, UK).

An incision was then made in the neck, the mandibular glands, pretracheal strap, and sternomastoid muscles were retracted to expose the right carotid artery (CA) and the vagus nerve was gently dissected and retracted away. Subsequently, silk sutures were tied on the external carotid artery (ECA) and CA and a microclip was placed on the internal carotid artery (ICA). A second loose suture was placed on the CA above the initial suture, and a small incision was made in the CA for filament insertion. The filament (390 or 410 μm , Docol Company, USA) was inserted and the loose suture was tightened around the filament to allow release of the microclip. The filament was then advanced up the ICA (approximately 20mm) to the MCA branch and decrease in blood flow was monitored by the Laser Doppler Perfusion Monitor (Moor Instruments, UK).

The filament was removed after 30 minutes, the microclip was replaced. The incision in the CA was sealed with electrocoagulation using bipolar diathermy probes (Aesculap, Germany) attached to a cautery unit (Diathermo MB122, Veterinary Instrumentation, UK), prior to release of all sutures so that complete reperfusion of all vessels was achieved.

The muscles and glands were guided back into place and the incisions sutured. Rats received 2.5mL of physiological saline and 5% glucose (Rat Care Limited, UK)

subcutaneously prior to recovery, and those with severe weight loss were re-hydrated daily in a similar fashion until weight stabilized. No rat's weight fell below 80% of their pre surgery weight. All cages were provided with moistened rat chow and cereal to facilitate eating during the first postoperative week and 1mg/mL of Paracetamol (Boots, UK) was provided in the drinking water one day prior to surgery and for 3 days after to assist with pain relief.

4.2.1.2. Grafting

7-12 days following MCAO surgery, 10 of the 23 rats received grafts of E14 whole ganglionic eminence tissue. Pregnant Wistar dams were sacrificed at E14 days of embryonic age. The embryos were removed and the whole ganglionic eminence was carefully dissected out, as done previously (Björklund, 1992 S.B., 1992) The tissue pieces were then dissociated into a cell suspensions as described in (Björklund, 1992 S.B., 1992). 500, 000 cells, in a 2 μ l solution were injected into the lesioned hemisphere, using a 10 μ l Hamilton microsyringe connected to a thin-walled widebore needle (dia = 0.25mm). The rats were anesthetized with isoflurane (Abbott, Queensborough, UK) and were stereotactically injected unilaterally with the cells. The coordinates were set according to bregma and dura: tooth bar -2.3, anterior / posterior +1.4, lateral -3, dorso-ventral -4 and -4.5. Injection volume was 2 μ l and the injection rate was 1 μ l over 90 seconds, with 1 μ l deposited at each depth. The needle was left in place for 3 min before withdrawal, cleaning and suturing of the wound. Paracetamol (Boots, UK) was provided in the drinking for 3 days after surgery to assist with pain relief.

4.2.2. Data processing

Temporal and postural gait parameters were obtained and subsequent classification analysis was performed for 30 Wister rats. The rats were divided into three different cohorts as illustrated in Figure 4-2; 10 naive controls, 10 that had undergone MCAO lesion and 10 that received an embryonic graft following lesion. This chapter presents outputs from data following two beam walking trials; MA1, was carried out on all the rats before any surgery and MA2 was carried out six weeks later following the MCAO lesion surgery and grafting. All variables were compared statistically between the three groups using a ANOVA, ($p < 0.05$).

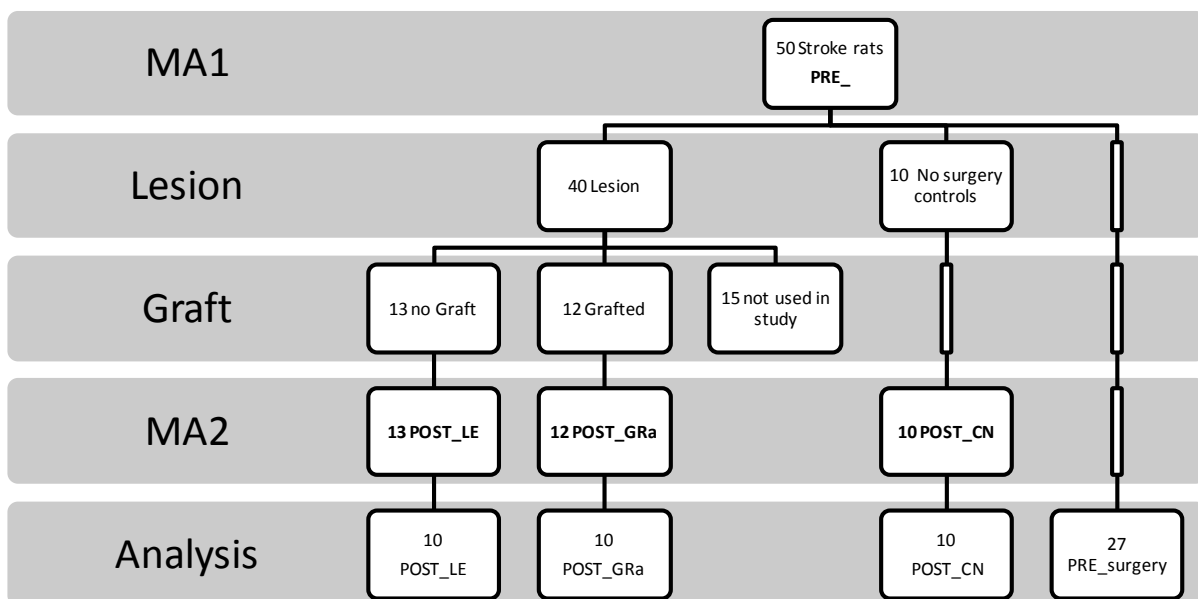


Figure 4-2: Post analysis division of the three cohorts

4.2.2.1. Temporal gait parameters

Temporal gait parameters were quantified by calculating the position vectors of the markers attached to the four limbs of the rat as described in Chapter 2. The data was input into in house software that calculated the stance time, swing time, stride length, speed and cadence for comparisons between the control, lesioned and grafted cohorts while walking along a WD elevated beam

4.2.2.2. Postural parameters (ROM)

Postural gait was quantified by calculating the rat's body displacement and orientation using Euler angles from markers placed on appendicular parts of the rat's skeletal structure as described in Chapter 2. These markers effectively define a "rigid body" attached to the trunk and enable six degrees of freedom (6DOF) calculation as displacement angles defined as the *roll*, *pitch* and *yaw*.

4.2.2.3. Kinematic waveforms

The 6DOF displacement was also illustrated as kinematic waveforms that represent one gait cycle (left forelimb taken as reference) calculated as the average of three gait cycles taken along the central section of the beams. The mean waveform of the three cycles were resample to 100 data points and the average of each cohort was used to compare the differences presented on the beam.

4.2.3. Statistical and error analysis

An ANOVA, a SIDAK post-hoc test and an ICC were used to compare the mean kinematic data between the three groups of rats. Subgroups were categorized based on side of lesion (left versus right), time point (before or after stroke), surgery (lesion, graft and control).

4.2.3.1. Classification simplex plots

A classification method was used to further asses the outcome of the data collected. The *roll* range of motion (ROM) and swing time variables were used to train the Dempster-Shafer theory (DST) Cardiff classifier. The classification tool helps to deal with conflicting data produced from MA by assigning levels of support to each measurement variable; taking each piece of evidence to classify the data presented.

The classifier was trained using two variables that were found to be significantly different for most of the cohorts, i.e., swing time for all four limbs and *roll* ROM were used. These variables showed significant differences ($p < 0.05$), before and after surgery for the control (*roll*) and lesion (*swing time*) cohorts. The classifier will enable direct comparison between three cohorts and establish the level of benefit achieved by the MCAO and grafting procedures. A series of six classifications were used to investigate differences in walking patterns of all the rat data for MA1 and MA2 to test the hypotheses that:

1. **Classification 1:** There is no difference in gait variables in the control group between for MA1 and MA2; (PRE_CN and POST_CN)
2. **Classification 2:** MCAO rats show gait function deficits when comparing the data between MA1 and MA2. (PRE_LE and POST_LE)
3. **Classification 3:** Grafted rats do not show gait function deficits when comparing the data between MA1 and MA2. (PRE_GRa and POST_GRa)
4. **Classification 4:** MCAO rats show gait function deficits when comparing data for MA2 with their age matched controls. (POST_LE and POST_CN)
5. **Classification 5:** Grafted rats do not show gait function deficits when comparing data for MA2 with their age matched controls (POST_GRa and POST_CN)
6. **Classification 6:** Grafted rats show improved gait function when compared with MCAO rats from MA2. (POST_LE and POST_GRa).

4.3. Results

The results were presented in three sections;

1. Temporal gait parameters (cadence, speed, swing time, stance time and stride length).
2. Postural parameters in terms of *roll, pitch and yaw* angles
3. Postural Kinematic waveforms and functional classification.

4.3.1. Temporal Gait Parameters

The data was recorded as the average values of two walking trials for each rat, and the average taken for all the rats from each cohort to test the hypotheses that:

1. There is no difference in gait variables between the two test points (MA1 and MA2)
2. There are no differences in gait between the three cohorts (controls, lesioned and grafted) and between the right and left limbs.

4.3.1.1. Comparing two test points

This section compares the data from MA1 and MA2. The mean and standard mean errors (SME) for the temporal gait parameters of the rat models and their controls were recorded in Table 4-1. The data illustrates the impact of age, MCAO lesion surgery and embryonic grafting on gait.

The main observations comparing the data from MA1 and MA2 were as follows:

1. POST_CN cohort walked with fewer steps per minute, a longer stance time, a longer swing time and shorter stride length on each limb compared to the PRE_CN cohort.
2. POST_LE cohort walked with slower gait, fewer steps per minute, a longer stance time and a longer swing time for each limb with the exception of RBL compared to the PRE_LE cohort.
3. POST_GRa cohort walked slower, fewer steps per minute, a significantly longer stance time, a significantly longer swing time on the RBL and the LFL and a significantly shorter stride length was recorded for the RBL as compared to the PRE_GRa cohort.

To observe the interactions related to age, lesion and graft, all the data was analysed together using an ANOVA. This also allowed to comparisons of each rat back to its own baseline performance in MA1. Following a ANOVA, grafted data from MA1 and MA2 was eliminated from the overall statistical analysis because initial results revealed that there was insufficient data for accurate evaluation of interactions between the three groups. The ANOVA therefore was carried to compare the control and lesioned rats for the two test points (MA1 and MA2). The performance was stable across test points for all the variables, with the exception of the fore and hind limb swing times, the difference was significantly lower for MA1 data for both the control and lesioned groups ($p < 0.05$).

Table 4-1: Kinematic parameters of the rats for MA1 (PRE_prefix) and MA2 (POST_prefix) showing temporal and postural gait parameters for the CN; LE and GRa cohorts while walking along the beam. Where LFL= left fore limb, LHL= left hind limb, RFL= Right fore limb, RHL=right hind limb. The results are expressed as mean \pm *SME* of each cohort.

Variable	Limb	PRE_CN (n=10)	PRE_LE (n=10)	PRE_GRa (n=7)	POST_CN (n=10)	POST_LE (n=10)	POST_Gra (n=10)
Cadence (steps per minute)	Average	251.50 \pm 21.66	242.50 \pm 17.70	267.20 \pm 15.24	258.20 \pm 32.29	261 \pm 12.89	315.20 \pm 30.62
	Average	28.72 \pm 0.38	26.21 \pm 0.17	35.33 \pm 0.47	26.91 \pm 0.30	26.41 \pm 0.26	26.23 \pm 0.29
Speed/cm/s	LHL	218.50 \pm 30.65	255.83 \pm 37.23	181.00 \pm 12.98	259.67 \pm 48.20	242.50 \pm 27.33	255.67 \pm 30.18
	RHL	217 \pm 22.25	266.17 \pm 41.22	185.17 \pm 16.77	258 \pm 41.72	263.67 \pm 23.63	188.50 \pm 25.45
stance time/ ms	LFL	231.83 \pm 30.32	258.33 \pm 28.88	147.67 \pm 8.70	273.67 \pm 43.27	250.83 \pm 15.20	253.83 \pm 21.78
	RFL	257.50 \pm 34.77	248.33 \pm 27.55	162.17 \pm 14.78	296 \pm 40.10	265.00 \pm 22.20	271.50 \pm 15.67
Swing time/ms	LFL	185.17 \pm 11.60	182 \pm 14.64	162.00 \pm 13.01	210.67 \pm 17.83	215.83 \pm 12.47	208.50 \pm 11.77
	RFL	168 \pm 17.14	185.83 \pm 13.64	146.33 \pm 19.37	207.33 \pm 21.23	217 \pm 9.67	207.17 \pm 9.77
stride length/mm	LHL	199.83 \pm 17.98	156.33 \pm 11.42	127.33 \pm 11.28	209 \pm 30.55	220.50 \pm 20.62	301.50 \pm 30.68
	RHL	196 \pm 25.67	177.50 \pm 18.25	165.33 \pm 20.55	234 \pm 21.48	209.50 \pm 17.58	287.67 \pm 21.88
stride length/mm	LFL	164.80 \pm 10.74	156.30 \pm 4.57	148.20 \pm 2.43	157.80 \pm 6.86	155.30 \pm 12.25	151 \pm 6.17
	RFL	159.60 \pm 12.03	148.40 \pm 4.21	146.50 \pm 3.40	151 \pm 8.70	157.20 \pm 7.01	149.10 \pm 7.65
stride length/mm	LHL	162.70 \pm 11.09	144.20 \pm 3.92	123.20 \pm 14.95	148 \pm 9.60	148.40 \pm 7.96	157.90 \pm 8.55
	RHL	161.20 \pm 13.43	145.10 \pm 6.07	160.90 \pm 7.79	159.80 \pm 7.08	143.60 \pm 10.12	147.90 \pm 9

4.3.1.2. Comparing the three cohorts

This section investigates the impact of MCAO lesion surgery and graft on gait compared with an age-matched control cohort (POST_CN); and the impact of grafting compared to lesion on gait. The mean and SME for the temporal gait parameters of the rat models and their controls were recorded in Table 4-1. The main observations were as follows:

1. The POST_LE walked slower, fewer steps per minute; longer stance , longer swing times ; and a shorter stride length compared with POST_CN cohort
2. The POST_GRa walked slower, fewer steps per minute, a shorter stance time, a longer swing time as well as a shorter stride length compared with POST_CN cohort.
3. The POST_LE walked slower, fewer steps per minute, a longer stance time, shorter swing time and a shorter stride length compared with POST_GRa cohort.

Similarly a MANOVA was carried out to compare the POST_CN and POST_LE data. There was no interactions that suggested effect of lesion on temporal gait parameters gait following a MANOVA: (*cadence*, $F_{1,17} = 0$, $P=n.s.$; *speed*, $F_{1,17} = 0.29$, $P=n.s.$; *fore limb stance time*, $F_{1,17} = 0.14$, $P=n.s.$; *hind limb stance time*, $F_{1,17} = 0.09$, $P=n.s.$; *fore limb swing time*, $F_{1,17} = 0.31$, $P=n.s.$; *hind limb swing time*, $F_{1,17} = 1.24$, $P=n.s.$; *fore limb stride length*, $F_{1,17} = 0.22$, $P=n.s.$; *hind limb stride length*, $F_{1,17} = 1.74$, $P=n.s.$)

4.3.1.3. Comparing the two sides; Left and right

A MANOVA revealed that there was no effect of lesion on the right and left side therefore, no asymmetry was observed for the temporal gait parameters following lesion. (*Fore limb stance time*, $F_{1,17} = 1.70$, $P=n.s$; *hind limb stance*, $F_{1,17} = 0.38$, $P=n.s$; *fore limb stride length*, $F_{1,17} = 1.24$, $P=n.s$; *hind limb stride length*, $F_{1,17} = 0.59$, $P=n.s$; *fore limb swing time*, $F_{1,17} = 0.14$ $P=n.s$; and *hind limb swing time* = $F_{1,17} = 0.963$, $P=n.s$)

4.3.2. Postural parameters (ROM)

The displacements were recorded as average ROM of the *roll*, *pitch* and *yaw* angles. A MANOVA (without the GRa group) was carried out to compare the ROM values in Table 4-2 for the *roll*, *pitch* and *yaw* rotations. There was no effect of lesion on *pitch*, $F_{1,17} = 0.05$, $P=n.s$. and *yaw*, $F_{1,17} = 2.36$, $P=n.s$ and the ROM performance was stable across MA1 and MA2 (*Pitch*= $F_{1,14} = 3.56$, $P=n.s$ and *Yaw*= $F_{1,14} = 3.77$, $P=n.s$).

There was a significant difference between the CN and LE cohorts. The POST_LE cohort exhibited more *roll*, $F_{1,17} = 15.18$, $P < 0.01$ than the POST_CN cohort. There was also a significant difference in performance across MA1 and MA2 time points for the two cohorts independently ($F_{1,13} = 5.14$) and after POST hoc SIDAK analysis, this effect showed interactions within the LE and CN cohorts $F_{1,13} = 5.14$, $P < 0.05$, with the control animals improving over the two test points, MA1 and MA2 ($T_{29.37} = 3.12$). The LE animals did not improve between MA1 and MA2 ($T_{29.37} = 0.20$, $p = n.s.$)

4.3.3. Postural parameters (ROM)

Body displacements were recorded as average ROM of the *roll*, *pitch* and *yaw* angles. An ANOVA was carried out to compare the ROM values in Table 4-2 for the *roll*, *pitch* and *yaw* rotations. There was no effect of lesion on *pitch*, $F_{1,17} = 0.05$, and *yaw*, $F_{1,17} = 2.36$, and the ROM performance was stable across MA1 and MA2 ($Pitch=F_{1,14}=3.56$, and $Yaw=F_{1,14}=3.77$).

There was a significant difference between the control and lesion cohorts. The lesion cohort exhibited more *roll*, $F_{1,17}=15.18$, than the control cohort in MA2.

There was also a significant difference in performance across MA1 and MA2 time points for the two cohorts independently ($F_{1,13}=5.14$) and after Posthoc SIDAK analysis, this effect showed interactions within the LE and CN cohorts $F_{1,13}=5.14$, with the control rats improving over the two test points, MA1 and MA2 ($T_{29,37}=3.12$). The LE rats did not improve between MA1 and MA2 ($T_{29,37}=0.20, p = n.s.$)

Table 4-2: Range of motion of the rats for MA1 (PRE_prefix) and MA2 (POST_prefix) showing postural gait parameters in terms of roll, pitch and yaw angles for the control (CN); Lesion (LE) and graft (GRa) cohorts while walking along the beam. The results are expressed as mean \pm SEEM of each cohort)

Variable	PRE_CN (n=10)	PRE_LE (n=10)	PRE_GRa (n=7)	POST_CN (n=10)	POST_LE (n=10)	POST_Gra (n=10)
Roll/o	41.09 \pm 3.21	46.52 \pm 2.39	26.09 \pm 4.63	27.45 \pm 3.57	48.90 \pm 3.27	21.38 \pm 2.16
Pitch/o	4.33 \pm 0.40	5.09 \pm 0.98	9.35 \pm 1.68	6.53 \pm 1.12	5.99 \pm 0.87	9.71 \pm 0.93
Yaw/o	6.58 \pm 0.58	5.93 \pm 0.66	9.41 \pm 1.30	9.38 \pm 1.52	7.43 \pm 1.07	6.02 \pm 1.16

4.3.4. Kinematic waveforms and classification simplex plots

To compare the patterns of *Roll*, *Pitch* and *Yaw* for the rats, the mean and SD of three gait cycles (left forelimb as the reference limb) along the central section of the beam was calculated. for the WD and NR beams. The 6DOF waveforms and simplex plot from the DST classifier were used to visually represent the differences in gait data between the following pairs:

1. Control rats when first tested *versus* six weeks later, (PRE_CN and POST_CN) ;
2. Lesioned rats before *versus* after surgery(PRE_LE and POST_LE);
3. Grafted rats before *versus* after grafting (PRE_GRa and POST_GRa) ;
4. Lesioned rats after surgery *versus* control rats 6 weeks after initial testing. (POST_LE and POST_CN);
5. Grafted rats after surgery *versus* control rats 6 weeks after initial testing. (POST_GRa and POST_CN).
6. Grafted rats after surgery *versus* Lesioned rats after surgery (POST_GRa and POST_LE)

4.3.4.1. Control rats when first tested versus six weeks later

The mean rotations in the kinematic waveforms along the WD beam were illustrated in Figure 4-3. Control cohort produced a negatively biased *roll and yaw* six weeks after initial testing.

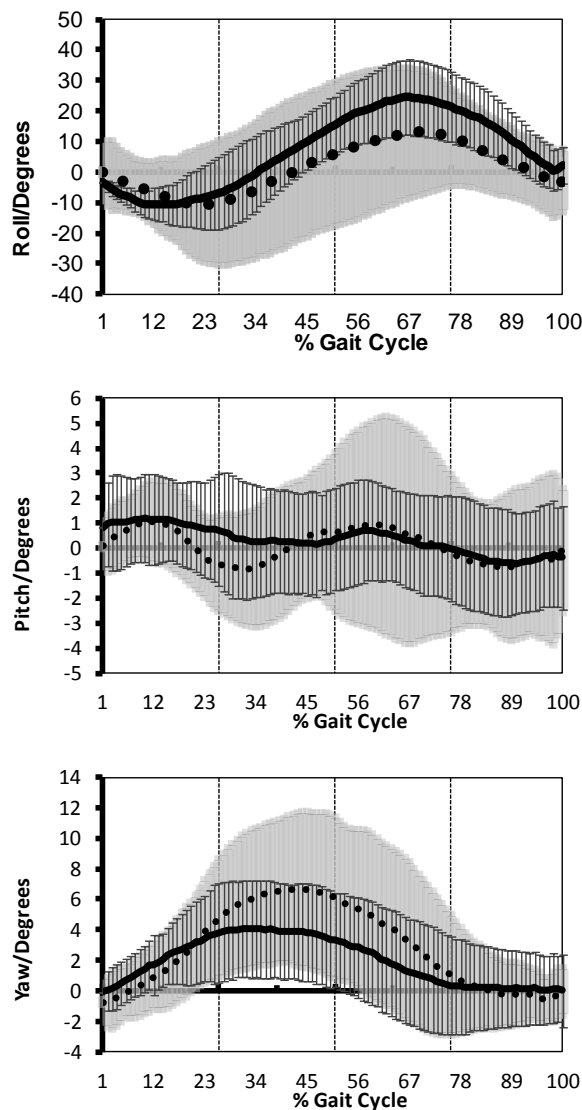


Figure 4-3: Kinematic waveforms for the average walking performance and its SD for one gait cycle on the beam. The bold black lines represent the average performances of the PRE_CN cohort (the SD is plotted in thin black lines); the dotted lines represent the average performance of the POST_CN cohort (the SD is plotted in grey).

The control cohort achieved 6 out of 10 dominant classifications six weeks apart, where $m_c(\{POST_CN\}) > m_c(\{PRE_CN\}) + m_c(\{\Theta\})$ see Figure 4-4. Three months between the walking trials show that the rats are better classified as having different gait patterns to normal with an out of sample accuracy 85%. Most of the $\{PRE_CN\}$ cohort, except for 2, were accurately classified with positioning of their simplex coordinates within their dominant classification region of the simplex plot.

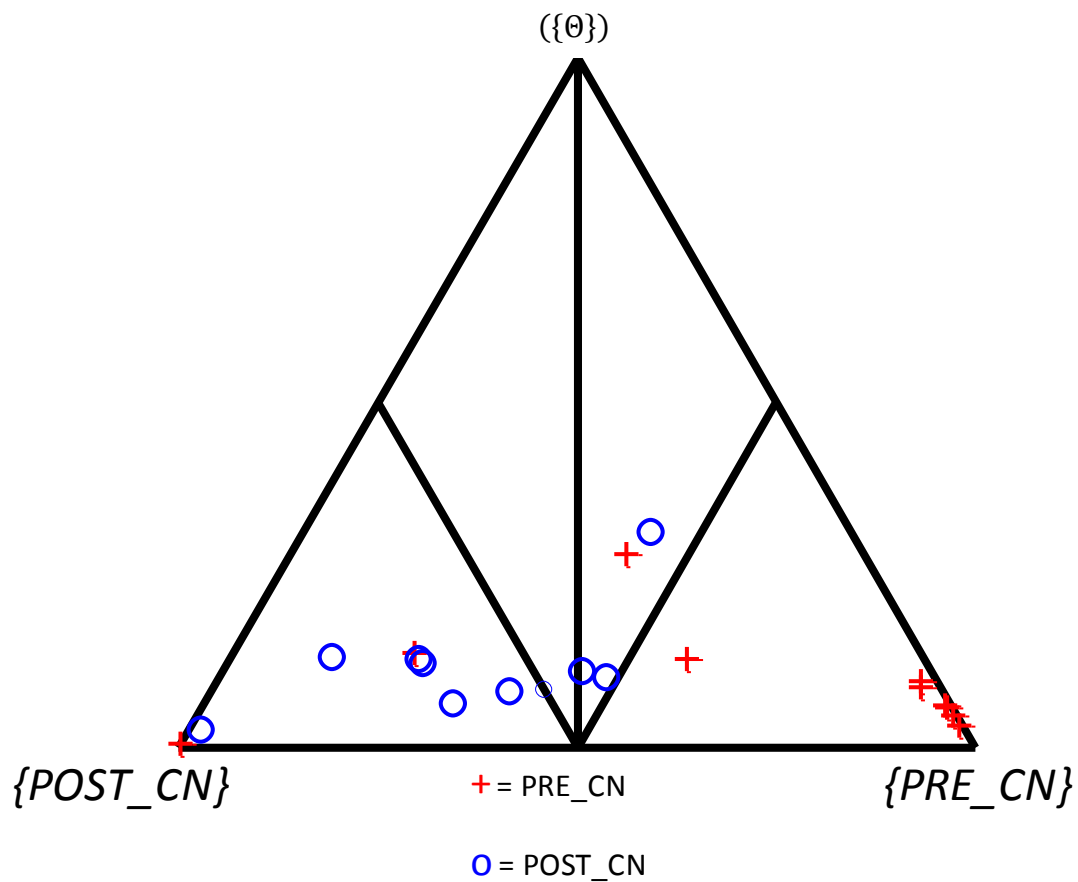


Figure 4-4 Simplex co-ordinate representations of the BOEc for the PRE_CN classified with the $POST_CN$ cohorts

4.3.4.2. Lesioned rats before versus after surgery

The kinematic waveforms (Figure 4-5) also reveal during the swing phase, Lesioned rats after the surgery have a positively biased *Roll* on the LF swing phase of the gait cycle compared to the rats before the surgery.

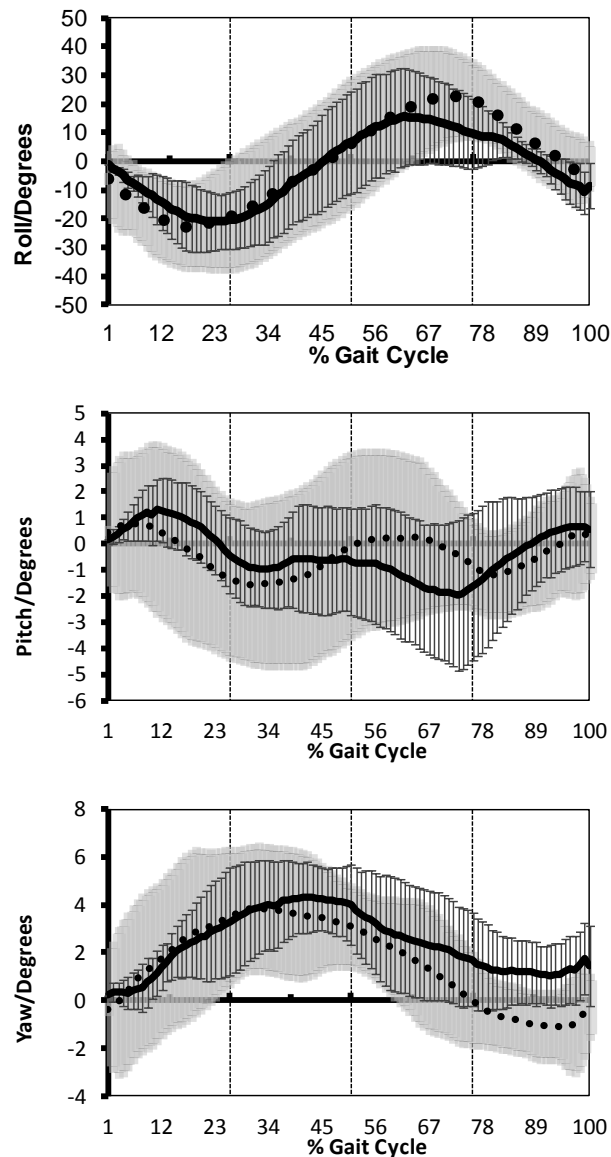


Figure 4-5: Kinematic waveforms for the average walking performance and its SD for one gait cycle on the WD beam. The bold black lines represent the average performances of the PRE_LE cohort (the SD is plotted in thin black lines); the dotted lines represent the average performance of the POST_LE cohort (the SD is plotted in grey).

The lesioned cohort after surgery achieved 7 out of 10 dominant classifications where $m_c(\{POST_LE\}) > m_c(\{PRE_LE\}) + m_c(\{\emptyset\})$ see Figure 4-6. MCAO Lesion surgery reduced normal gait function allowing for a classification with an out of sample accuracy 86.31%. Most of the $\{PRE_LE\}$ cohort, had 6 out of 9 subjects accurately classified with positioning of their simplex coordinates within their dominant classification region of the simplex plot

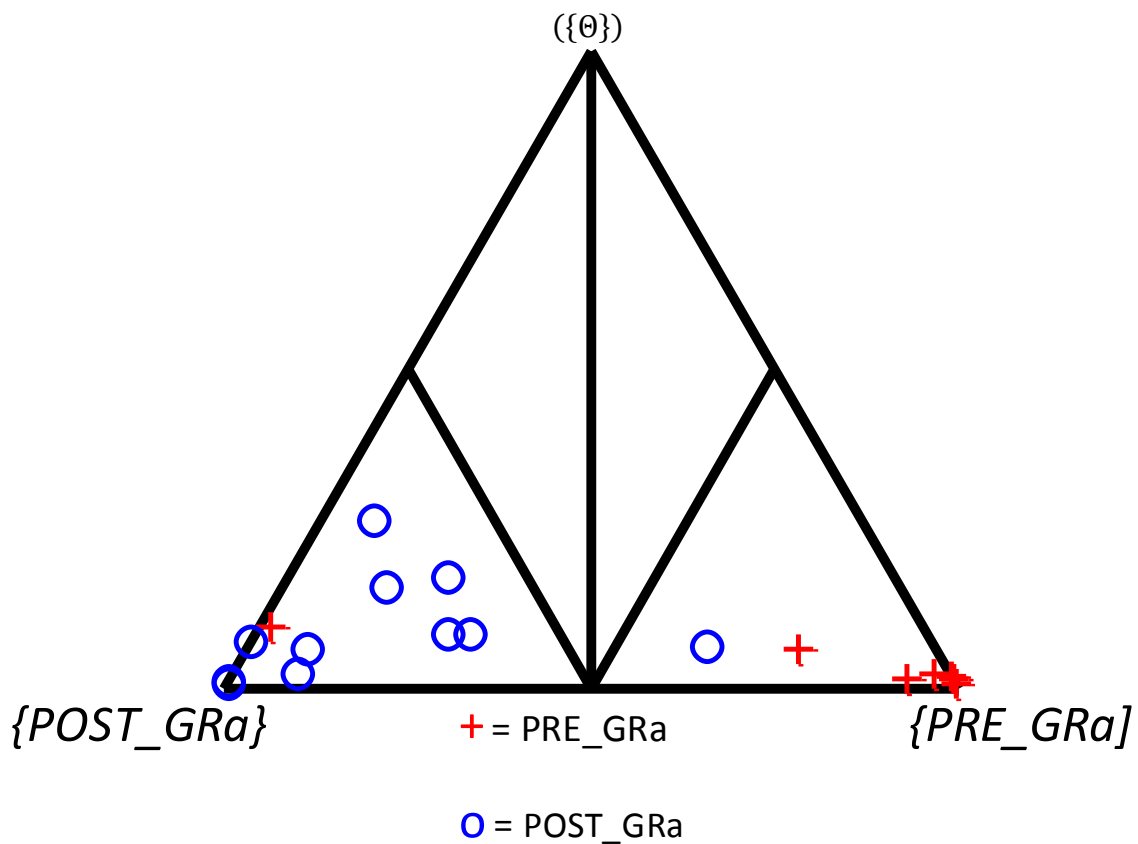


Figure 4-6 Simplex co-ordinate representations of the BOEc for the PRE_LE classified with the $POST_LE$ cohorts

4.3.4.3. Grafted rats before versus after grafting

The mean kinematic rotations along the WD beam are illustrated in Figure 4-7.

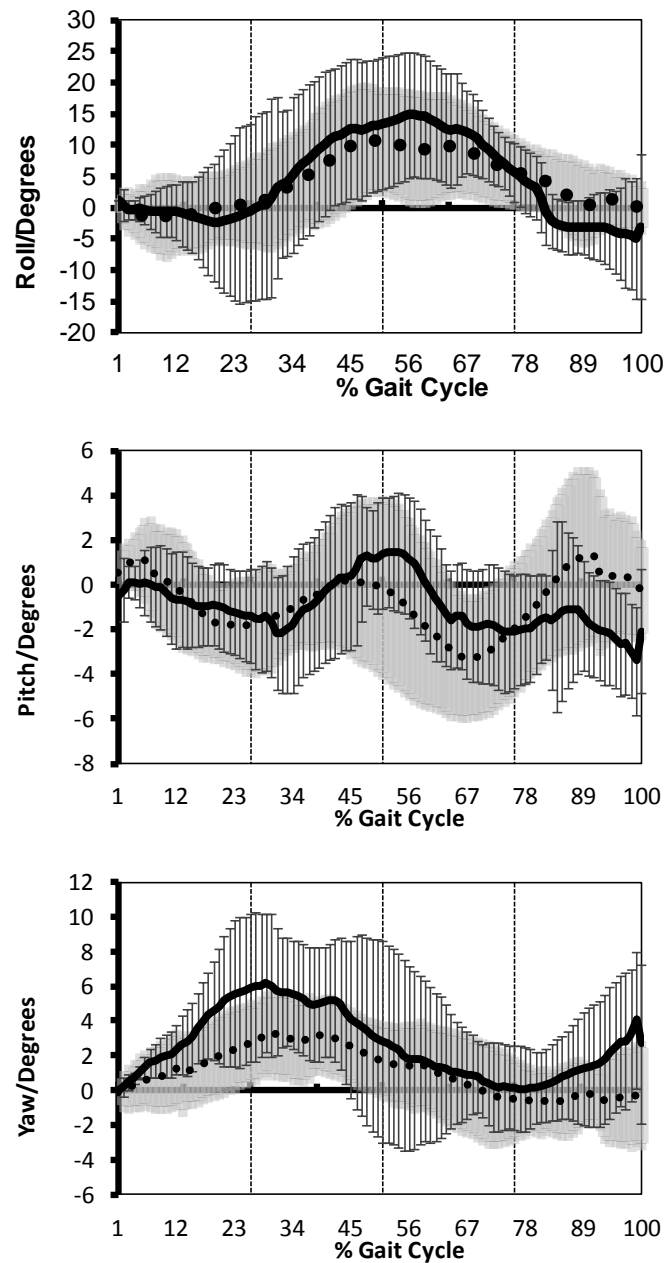


Figure 4-7 : Kinematic waveforms for the average walking performance and its SD for one gait cycle on the WD beam. The bold black lines represent the average performances of the PRE_GRa cohort (the SD is plotted in thin black lines); the dotted lines represent the average performance of the POST_GRa cohort (the SD is plotted in grey).

After classification the data revealed that the grafted cohort achieved 9 out of 10 dominant classifications after surgery where $m_c(\{POST_GRa\}) > m_c(\{PRE_GRa\}) + m_c(\{\emptyset\})$ see Figure 4-8. Grafting affected gait function allowing for a classification with an out of sample accuracy of 88%. Most of the $\{PRE_GRa\}$ cohort, except for 1, was accurately classified with positioning of their simplex coordinates within their dominant classification region of the simplex plot.

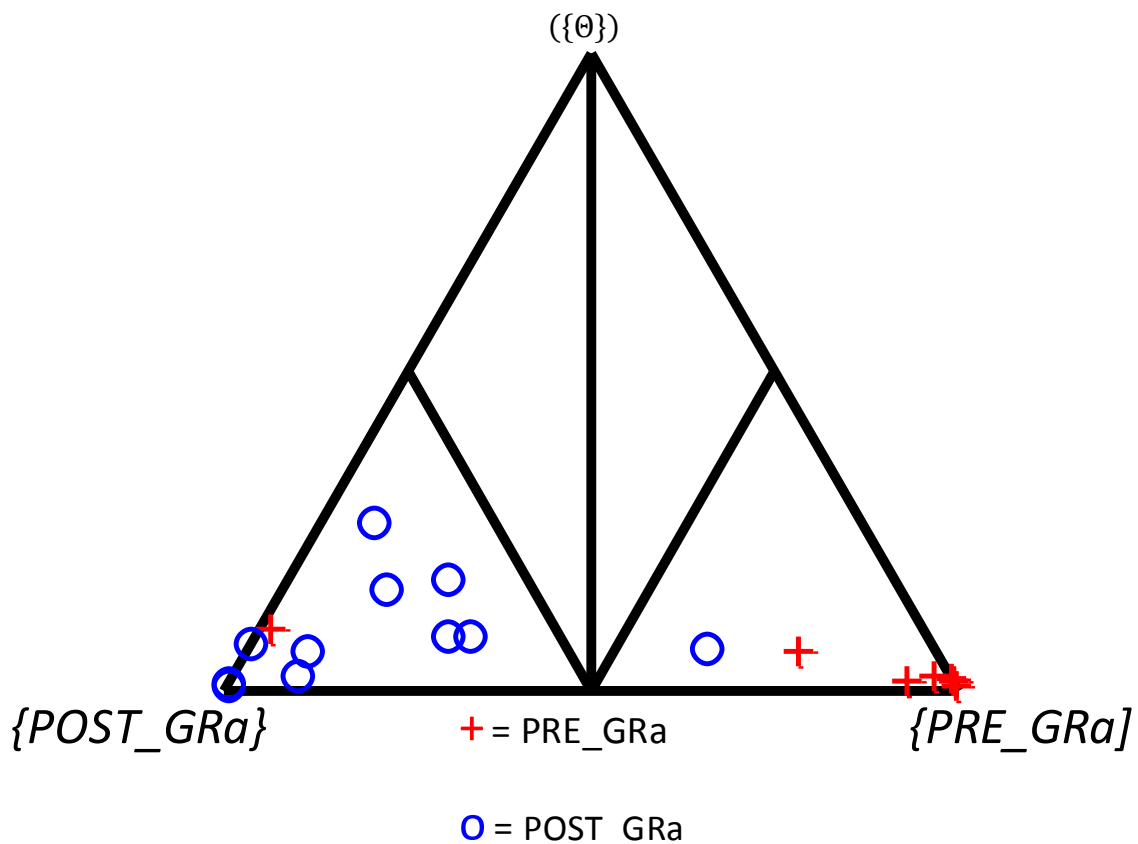


Figure 4-8 Simplex co-ordinate representations of the BOEc for the PRE_GRa classified with the POST_GRa cohorts

4.3.4.4. Lesioned rats after surgery versus control rats 6 weeks after initial testing

The mean kinematic rotations along the WD beam were illustrated in Figure 4-7. The lesioned cohort had a negatively biased *roll* during stance phase and a negatively biased *roll* during swing phase

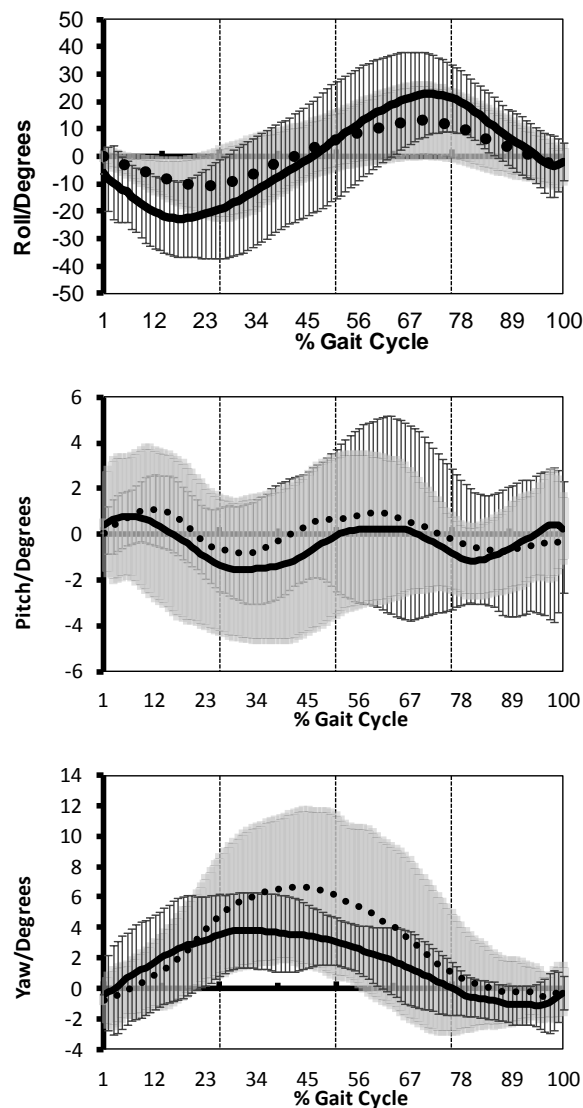


Figure 4-9 : Kinematic waveforms for the average walking performance and SD for one gait cycle on the WD beam. The bold black lines represent the average performances of the POST_LE cohort (the SD is plotted in thin black lines); the dotted lines represent the average performance of the POST_CN cohort (the SD is plotted in grey).

8 of the 10 rats in the lesioned cohort were accurately classified after surgery with an out of sample accuracy of 83.15% where $m_c(\{POST_LE\}) > m_c(\{POST_CN\}) + m_c(\{\Theta\})$ see Figure 4-10. MCAO affected gait function when compared to an age matched control. 6 of the $\{POST_CN\}$ cohort were accurately classified with positioning of their simplex coordinates within their dominant classification region of the simplex plot

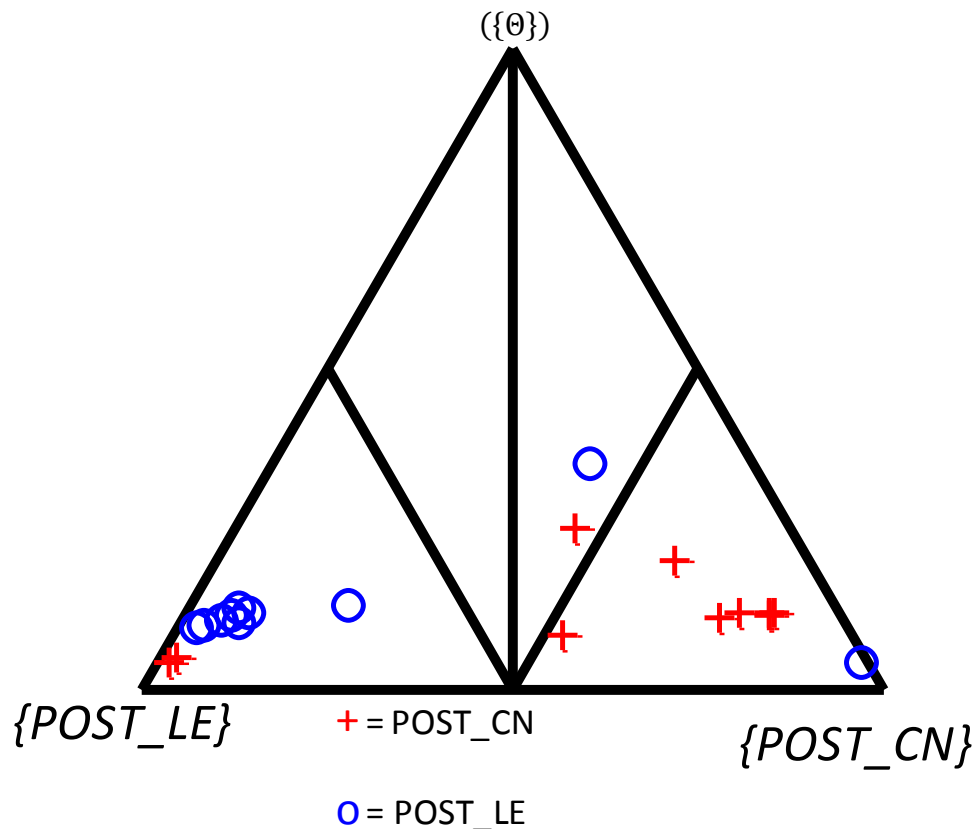


Figure 4-10: Simplex co-ordinate representations of the BOEc for the $\{POST_CN\}$ classified with the $\{POST_LE\}$ cohorts

4.3.4.5. Grafted rats after surgery versus control rats 6 weeks after initial testing.

The mean kinematic rotations along the WD beam are illustrated in Figure 4-11. Although no significant difference was recorded, it was interesting to note that the grafted cohort approached the control dominant region function better than the lesioned cohort after surgery.

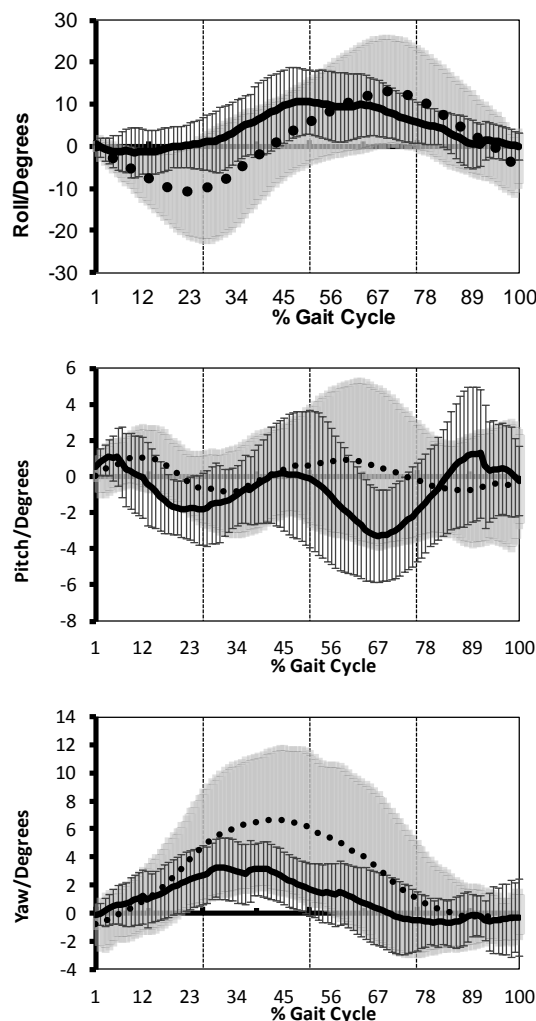


Figure 4-11 : Kinematic waveforms for the average walking performance and its SD for one gait cycle on the WD beam. The bold black lines represent the average performances of the POST_GRa cohort (the SD is plotted in thin black lines); the dotted lines represent the average performance of the POST_CN cohort (the SD is plotted in grey).

5 out of the 10 grafted rats were accurately classified with an out of sample accuracy of 81% where $m_c(\{POST_GRa\}) > m_c(\{POST_CN\}) + m_c(\{\Theta\})$ see Figure 4-12. Similarly, only 5 out of 10 $\{POST_CN\}$ rats were accurately classified with positioning of their simplex coordinates within their dominant classification region of the simplex plot.

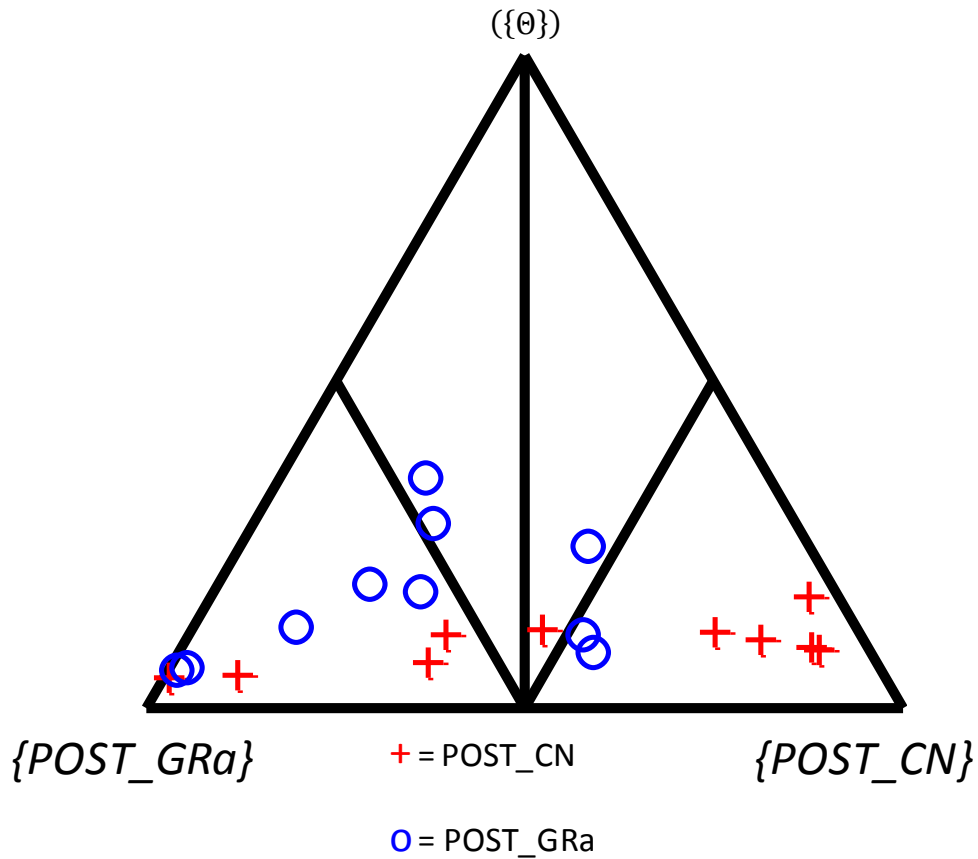


Figure 4-12: Simplex co-ordinate representations of the BOEc for the $POST_CN$ classified with the $POST_GRa$ cohorts

4.3.4.6. Grafted rats after surgery versus Lesioned rats after surgery

The mean kinematic rotations along the WD beam were illustrated in Figure 4-13 .

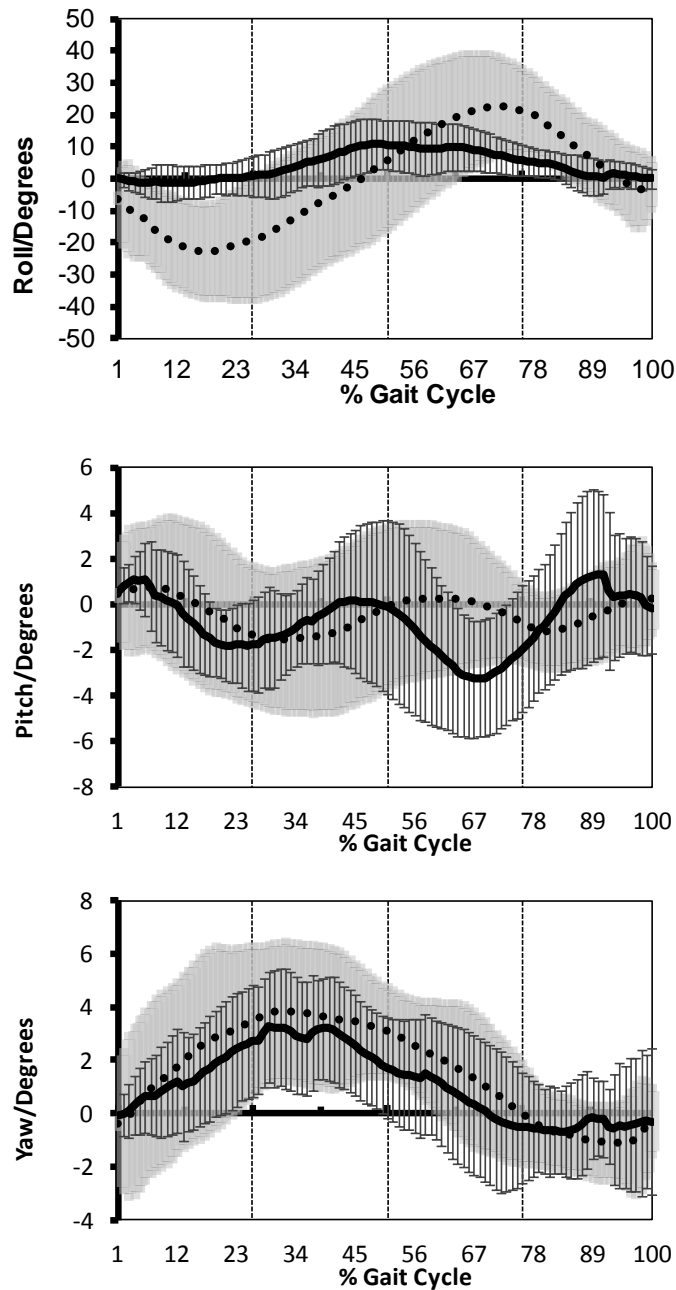


Figure 4-13 : Kinematic waveforms for the average walking performance and its SD for one gait cycle on the WD beam. The bold black lines represent the average performances of the POST_GRa cohort (the SD is plotted in thin black lines); the dotted lines represent the average performance of the POST_CN cohort (the SD is plotted in grey).

Grafted cohort achieves 9 out of 10 dominant classifications with an out of sample accuracy of 91.84% where $m_c(\{POST_GRa\}) > m_c(\{POST_LE\}) + m_c(\{\Theta\})$ see Figure 4-14. Similarly, 9 out of 10 $\{POST_LE\}$ rats were accurately classified with positioning of their simplex coordinates within their dominant classification region of the simplex plot. Gait function changed after grafting when compared to lesion rats.

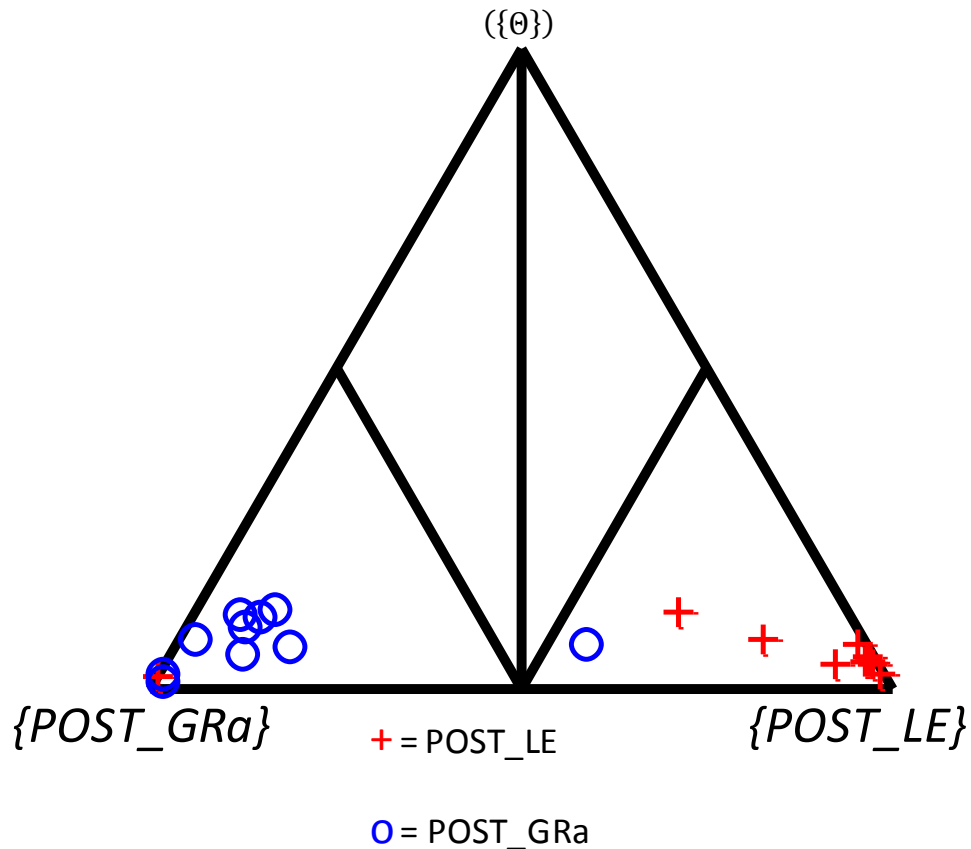


Figure 4-14: Simplex co-ordinate representations of the BOEc for the $POST_LE$ classified with the $POST_GRa$ cohorts

A seventh classification was performed to investigate the effect of the MCAO and grafting. After classification the data revealed that the grafted cohort achieved a 9 out of 10 accurately classified rats with positioning of their simplex coordinates within their dominant classification region of the simplex plot. The Lesioned rats achieved 10 out of 10 rats classification with most of the control rats having 5 out of the 10 classified in the dominant grafted region the five in the dominant lesioned region.

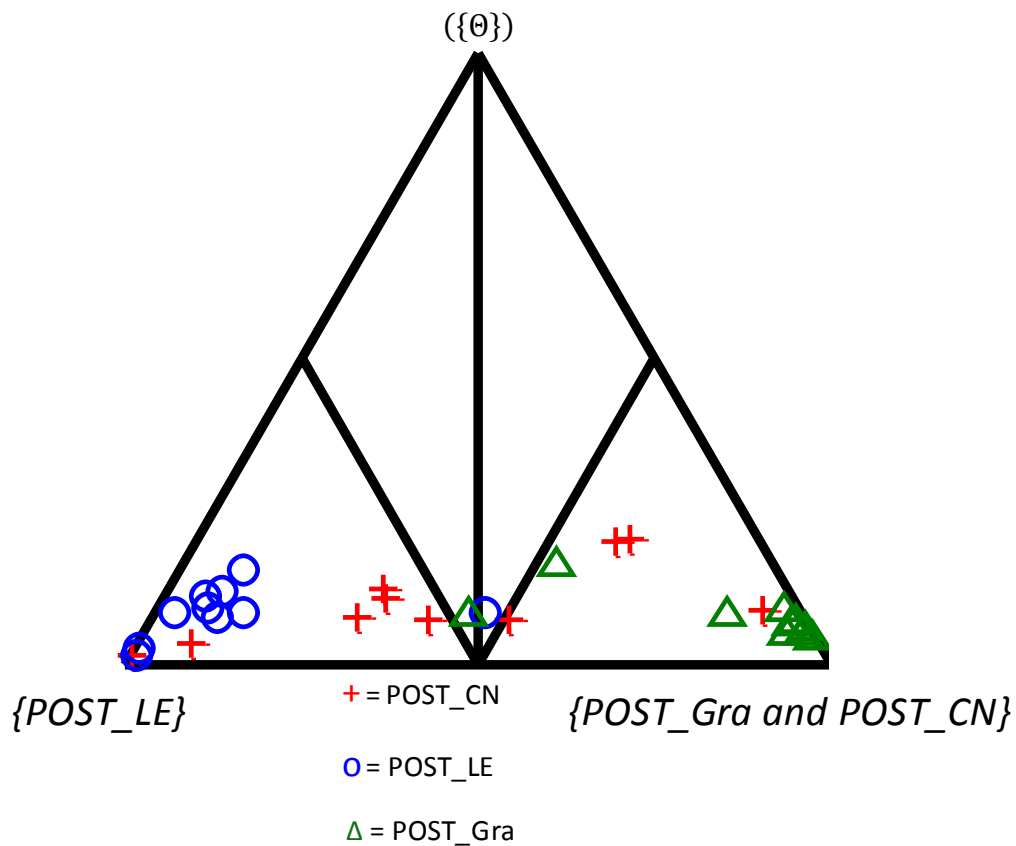


Figure 4-15: Simplex co-ordinate representations of the BOEc for the POST_LE classified with the POST_GRa and POST_CN cohorts.

4.4. Discussion

This chapter applies a 3D marker based motion analysis (3DMA) technique which has been shown to work for a cohort of PD models (Chapter 3) where temporal and postural gait parameters were successfully processed and discussed. Gait parameters during over-ground locomotion of MCAO, grafted Wister rats and their controls before and after surgery were quantified to further validate the developed protocol. The rats were part of a larger study that was aimed at looking at various behavioural characteristics of MCAO.

Gait parameter data was obtained for 27 rats before surgery (MA1) and 30 rats after surgery (MA2) to provide a measure of different behaviour and functional characteristics of all four limbs. Eight different variables, (cadence, speed, swing time, stance time, stride length, *roll* ROM, *pitch* ROM and *yaw* ROM) were tested for significant differences between the three cohorts to quantify the effects of training and age on gait; the effect of MCAO lesion surgery and graft on gait between the two testing time-points and; body asymmetry between the impaired and the healthy side within the lesion cohort.

Data was further classified using the DST classification method developed by Jones et. al., (2004) to assess the outcome of the data collected. The DST uses mathematical probability to quantify objective data and provides a means of interpreting several data sets simultaneously. More importantly the DST helps to deal with conflicting data produced from MA by assigning levels of support to each measurement variable; taking each piece of evidence to classify the data presented.

The *roll* ROM and swing time variables were used to train classifier as they were variables that were found to be significantly different within the cohorts.

4.4.1. Temporal and postural gait parameters

The most common behavioural tests for rodents with stroke were designed to examine the differences in function between the intact (ipsi-lateral) and impaired (contra-lateral) side of the body using asymmetry tests (Schallert et al., 2003) (Ungerstedt et al., 1968). Many of these tests were originally developed for other unilateral models of basal ganglia disorders, such as PD and HD disease. However, these tests also reveal deficits in rats with ischemia confined to subcortical areas, predominantly the striatum (Modo et al., 2000).

The characteristics of human Ischemic stroke are very diverse since the location of the damage plays an important part in determining the observed symptoms (van der Staay et al., 1996, Corbett and Nurse, 1998). Similar to PD patients, spatio-temporal gait and posture are affected in patients with stroke. Patients walk slower than the average healthy subjects; their gait cycle is characterised by a low stride length, lower cadence, longer stance phase, toe-drag during the swing phase and exhibit increased double support times (De Bujanda et al., 2004, Olney et al., 1994, Shumway-cook and Woollacott, 1995). MCAO in the rat is used to mimic large vessel occlusion in humans however the behaviour exhibited by the rat is dependent on the location and size of the lesion.

MCAO rat models are used to understand stroke in humans and results vary from study to study, depending on the strain of rat used and the nature of the behaviour analysis carried out (Whishaw and Kolb, DeVries et al., 2001). Locomotor activity has been reported in previous studies to either increase or decrease in experimental

stroke rats depending on the model of stroke used. (Shen and Wang, 2010, Tomac et al., 2002, Ji et al., 2007). In the current study, POST_LE rats walked slower than POST_CN. Subsequently, stance times were longer and swing times were shorter, suggesting that although POST_LE stayed in stance for longer, thus affecting their speed, the increase in swing times meant that the speed difference was not significant.

The rat data between time-points, MA1 and MA2, show that the rats are older and are accustomed to the beam thus an overall improved orientation on the beam is observed for the control cohort. The control group also showed improvements in the *roll* ROM and in the swing times between trials MA1 and MA2. The control cohort learnt how to navigate the beam after training where as the lesion rats did not show differences in gait function, therefore the control group were better at learning the beam after training than the lesioned rats.

A 30 minute MCAO surgery has been shown to increase swing time, but does not affect the other temporal gait parameters. The lesion cohort data between the two time points was to illustrate the impact of MCAO lesion surgery on gait. Quantitative analysis of postural instability during over-ground locomotion revealed a greater difference between healthy and MCAO rats. The sensitivity of the protocol allowed for quantitative assessment of angular changes of body rotations during gait. Lesioned rats did not show any asymmetry toward the contra-lateral side as expected, but revealed a high (not significant $p < 0.05$) *roll* ROM when compared to the control cohort. It is useful to note that impairments are mainly manifested in the first few days after MCA occlusion; studies have shown that there is complete recovery after 3-4 weeks of testing (Corbett and Nurse, 1998). Classification

demonstrated deficits that are not evident using other behavioural studies such as those used by (Shen and Wang, 2010).

Embryonic grafting is a technique that is used to replace neuronal populations within the lesioned brain. Grafting embryonic tissue into the damaged areas of rat's brain has been shown to restructure synaptic, neuro-chemical and behavioural deficits in rat models of neurological dysfunction such as PD and HD (Dunnett, 1992). Therefore the use of embryonic tissue for grafting can provide a functional recovery to the damaged brain. The grafted rats should approach normal values compared to the lesion cohort. Although the results show improvements in gait following grafting (the grafted rats walk faster than the lesioned rats which is reflected with shorter swing, shorter stance time, increased cadence and increased stride length), these differences were not found to be significant. The graft cohort compared to the controls had significantly longer stance and swing phase times thus they walked with a slower gait and less steps per minute compared with gait before surgery. Therefore grafting affected normal gait function.

4.4.2. Classification

Classification of data sets between the two test points (MA1 and MA2 data) for the three cohorts showed accurate classification of the rats using swing times and *roll* ROM. This suggested that there are differences in gait due to training (accurate classification between the PRE_CN and POST_CN); there are differences in gait after MCAO lesion (accurate classification between the PRE_LE and POST_LE) and there are differences in gait after grafting (accurate classification between the PRE_GRa and POST_GRa). With all classifications having an accuracy of above

80% with more than seven out of 10 rats accurately classified on the dominant region of the simplex plot.

Classification between the three cohorts also revealed greater than 80% accuracy. A better classification is observed when comparing the POST_LE cohort with the POST_CN cohort than when comparing it with the POST_GRa data, with 9 out of 10 rats achieving a dominant classification in the POST_LE group and only 5 in the POST_GRa cohort. More rats from the POST_GRa cohort approached normal gait than the POST_LE cohort.

The results strongly validate the novel marker-based optoelectronic MA protocol developed in Chapter 2 by demonstrating that it can provide an effective and simple approach to quantifying temporal gait parameters for rat models of stroke and the effect of grafting. Swing time and *roll* ROM indicative of postural adaptation strategies, were found to be stronger variables for the classification of stroke rats.

The data can be used as a basis for correlation with healthy human data based on a similar 3D MA in human subjects in Chapter 5. The results of this study demonstrate the sensitivity of the MA protocol to quantify functional characteristics of the stroke model. They also reveal the use of a powerful classification tool that has allowed data analysis in terms of comparison between the three surgical interventions and their controls. It has also allowed the relationship between outcomes of the rats' pre and post surgery and the use of important variable that distinguish between MCAO function.

CHAPTER 5

5. Quantifying locomotion of Healthy Humans

5.1. Introduction

Gait disorders are a fundamental symptom in patients suffering from neurodegenerative disorders that affect the motor cortex such as Parkinson's disease (PD) and stroke. These disorders leave the patients unable to adjust their walking patterns with ease according to the demands of the situation (Moreau and Hill, 2008). For example, patients with PD have reduced arm swing, shuffling of gait, reduced walking speed, shorter stride length and an abnormal cadence (Moreau and Hill, 2008, Schaafsma et al., 2003). This leads to increased gait variability and decreased executive function which eventually leads to falls and the condition known as "freezing of gait" (Plotnik et al., 2008, Woollacott and Shumway-Cook, 2002).

As a result, PD patients walk with a more cautious gait, exhibiting compensatory behaviour in an attempt to improve their stability (Latt et al., 2009). To fully appreciate the different pathological gait parameters, it is paramount to understand healthy gait. A protocol was developed to assess gait in healthy human subjects. It was designed specifically for comparisons with the previously described rat model analyses.

According to Duhamel et al., (2004), motion Analysis (MA) protocols should include a minimum of four gait cycles in order to reduce single cycle abnormalities. The current study introduces a MA protocol that guaranteed that at least four gait cycles were

measured, with the possibility of more at the laboratory. The number of gait cycles measured is limited only by the room dimensions and the number of cameras available.

The aim of this chapter was to present and discuss the results obtained from the human data collection and processing protocols, described in Chapter 2. To achieve this aim, the various sections in this chapter explored the following objectives:

1. Identify the effects of dual tasking on healthy gait by introducing walkways of different widths.
2. Demonstrate the protocol's sensitivity in identifying gait differences between two cohorts.
3. Validate the protocol by comparing the results to the work of others.

The chapter begins by providing a brief introduction to the study, followed by the results for healthy subjects as they walked along three different 8m walkways.

5.2. Methods

5.2.1. Data collection

Human gait was assessed by taking three dimensional (3D) Cartesian data of markers attached on specific points of the subject while walking along a WDw, NRw and GRw. Ten healthy volunteers, five male (mean age : 23.3 ± 2.1 years; height 1.77 ± 0.09 m; weight 74.5 ± 17.1 kg BMI 23.4 ± 3.5 kg/m²) and five female (mean age (24.2 ± 2.3 years, height 1.68 ± 0.08 m, weight 63.9 ± 9 kg, BMI 22.4 ± 1.6 kg/m²) were recruited to the study. Their gait cycle was collected and processed as they walked on an 8m walkway following the methods described in Chapter 2.

5.2.2. Data processing

The temporal gait parameters, stance time, swing time, stride length, speed and cadence were calculated from the calcaneus marker trajectory data. Postural asymmetry in terms of body rotational angles, *roll*, *pitch* and *yaw* range of motion (ROM) body orientations of the three rigid bodies; upper body, trunk and pelvis, were recorded. The temporal gait parameters were processed for four gait cycles, however the postural gait parameters were processed for three gait cycles due to marker drop out during data collection.

5.2.2.1. Temporal gait

Comparisons of the temporal gait parameters were calculated from three gait cycles taken along the central section of the WDw and NRw. Data for the GRw was divided into two zones, two gait cycles at the wide end of the walkway (GRw-wide) and also two gait cycles from the narrow end of the walkway (GRw-narrow).

The differences in the kinematic waveforms for *roll*, *pitch* and *yaw* for the trunk, pelvis and upper body rigid bodies were also examined. The data enabled the understanding of postural strategies in healthy human subjects when dealing with different walking situations along the central section of the walkways. The GRw was not divided into two sections for postural analysis due to insufficient data at the beginning and at the end of the walkways.

5.2.2.2. Postural parameters

Postural data was acquired for the trunk, pelvis and the upper body. The trunk and the pelvis have different functional obligations leading to dissimilar motion patterns during gait (Perry, 1992). Three rigid bodies were defined according to the methods described in Chapter 2, and are illustrated in Figure 5-1. The figure shows markers in Qualisys Track Manager (QTM) that define the three rigid bodies used to illustrate healthy human posture as follows:

1. The trunk rigid body was defined using four appendicular markers of the upper body, i.e., the two hips, and the two shoulders.
2. The pelvis rigid body was identified by the two hip markers and one spine marker.
3. The upper body rigid body was defined using the two shoulder marker and the mid-spine marker.

Kinematic waveforms were illustrated in Figure 5-2 for the postural data. The waveforms displayed human body orientation and brought insight into the vertical, lateral and anterior-posterior displacements of the three rigid bodies during gait.

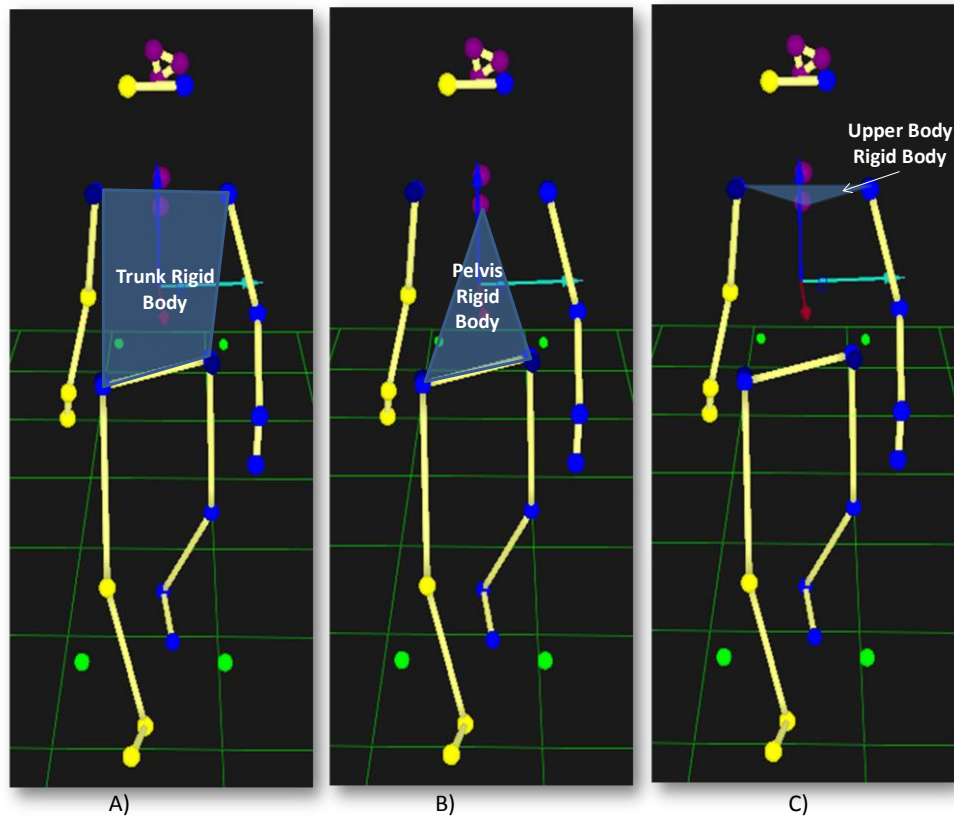


Figure 5-1: QTM screen shots of the three defined rigid bodies, A) Trunk, B) Pelvis and C) Upper Body; used to investigate human posture during gait.

5.2.3. Statistical and error analysis

Differences of temporal and postural gait parameters were assessed by ANOVA ($p < 0.05$) where ($F_{1, \text{degrees of freedom}}$) followed by a SIDAK post hoc test. Subgroups were categorized based on gender (men versus women), and side (right or left). The inter-trial repeatability of gait parameters was calculated by the one-way random intra-class correlation coefficient (ICC) and the 95% confidence interval (CI) of the ICC, using one-way ANOVA (Oken et al., 2008;). The evaluation criteria and standards for ICC values are accepted as follows: values ≥ 0.75 represent excellent repeatability, 0.4-0.74 represents adequate repeatability, and values ≤ 0.40 represent poor repeatability.

5.3. Results

The results of the study are presented and discussed in two sections:

1. Comparison between the three walkways,
2. Comparison between the male and female cohorts.

5.3.1. Comparisons between the three Walkways

5.3.1.1. Temporal parameters

The mean and standard deviations (SD) of the temporal parameters were recorded in Table 5-1. The differences observed between the three walkways were as follows;

1. Slower speed, longer stance time, longer swing time, smaller stride length and more steps per minute on the **NRw** compared to the **WDw** (differences were not significant).
2. Slower speed, longer stance time, longer swing time, smaller stride length and fewer steps per minute on the **GRw-Wide** compared to the **WDw** (differences were not significant).
3. Fast speed, longer stance time, shorter swing time, smaller stride length and more steps per minute on the **GRw-Narrow** compared to the **WDw** (differences were not significant, except for the cadence).
4. Slower speed, longer stance time, longer swing time, larger stride length and fewer steps per minute on the **GRw-Wide** compared to the **NRw** (differences were not significant).
5. Faster speed, shorter stance time, shorter swing time, larger stride length and more steps per minute on the **GRw-Narrow** compared to the **NRw** (differences were not significant).

6. Faster speed, shorter stance time, shorter swing time, larger stride length and more steps per minute on the **GRw -Narrow** compared to the **GRw Wide** (differences were not significant, except for the speed and cadence.)

Table 5-1: Temporal parameters comparing the WDw, NRw and GRw. The results are expressed as mean \pm SD of both the right and left limbs.

	Limb	WDw	NRw	GRw narrow	GRw wide
Stance time/ms	Right	0.37 \pm 0.09	0.43 \pm 0.06	0.44 \pm 0.08	0.40 \pm 0.09
	Left	0.39 \pm 0.10	0.44 \pm 0.07	0.49 \pm 0.11	0.39 \pm 0.07
Swing time/ms	Right	0.62 \pm 0.06	0.63 \pm 0.11	0.63 \pm 0.09	0.59 \pm 0.04
	left	0.63 \pm 0.06	0.60 \pm 0.06	0.61 \pm 0.05	0.60 \pm 0.08
Stride length/m	Right	1.28 \pm 0.08	1.25 \pm 0.24	1.26 \pm 0.20	1.35 \pm 0.08
	left	1.28 \pm 0.07	1.25 \pm 0.15	1.22 \pm 0.14	1.33 \pm 0.10
Cadence/ steps/minute	Right	109.85 \pm 10.09	109.72 \pm 23.53	128.00 \pm 13.86	121.22 \pm 18.70
	left	113.24 \pm 15.70	116.17 \pm 5.49	127.69 \pm 8.46	117.26 \pm 8.72
Speed/ m/s	Average	1.25 \pm 0.34	1.19 \pm 0.15	1.12 \pm 0.15	1.31 \pm 0.13

5.3.1.2. Postural parameters

The mean \pm SD ROM *roll*, *pitch* and *yaw* angles along the GRw, NRW and WDw are recorded in Table 5-2. Although there were no significant difference between the three walkways following an ANOVA ($p < 0.05$), the results from the central section of the walkway to test dual tasking on posture was tested for the trunk, pelvis and upper body ROM's.

Trunk ROM was;

1. Less for *roll*, *pitch* and *yaw*, on the **NRw** compared to the **WDw**
2. Less for *roll*, and greater for *pitch* and larger *yaw* on the **GRw** compared to the **WDw**.
3. Greater for *roll* and *yaw*, as well as smaller *pitch* on the **GRw** compared to the **NRw**.

Pelvis ROM was:

1. Greater for *roll* and *yaw* as well as less for *pitch* on the **NRw** compared to the **WDw**.
2. Less *roll*, *pitch* and *yaw* on the **GRw** compared to the **WDw**.
3. Less *roll*, *pitch* and *yaw* on the **GRw** compared to the **NRw**.

Upper body ROM was:

1. Greater for *roll*, as well as less for *pitch* and *yaw* ROM's, on the **NRw** compared to the **WDw**.
2. Less for *roll* as well as greater for *pitch* and *yaw* on the **GRw** compared to the **WDw**.
3. Less for *roll*, as well as greater for *pitch* and *yaw* on the **GRw** compared to the **NRw**.

Table 5-2: Postural parameters comparing the WDw, NRw and GRw. The results are expressed as mean \pm SD for the *roll*, *pitch* and *yaw* ROM angles.

	Trunk			Pelvis			Upper Body		
	WDw	NRw	GRw	WDw	NRw	GRw	WDw	NRw	GRw
Roll /°	3.82 \pm 1.51	3.68 \pm 1.94	4.26 \pm 2.26	5.50 \pm 3.29	5.83 \pm 3.30 \pm	4.76 \pm 3.59	4.10 \pm 2.32	4.29 \pm 3.53	3.67 \pm 2.11
Pitch /°	3.85 \pm 2.24	3.76 \pm 2.18	3.25 \pm 1.19	5.10 \pm 5.65	4.79 \pm 3.59 \pm	3.73 \pm 3.03	4.99 \pm 2.62	3.93 \pm 2.27	6.02 \pm 3.06
Yaw /°	7.16 \pm 2.80	6.50 \pm 3.67	7.19 \pm 3.94	11.30 \pm 5.40	13.11 \pm 6.74 \pm	10.93 \pm 6.02	9.20 \pm 5.36	8.32 \pm 5.22	10.70 \pm 4.63

5.3.1.3. Kinematic waveforms

The waveforms were representative of the *roll*, *pitch* and *yaw* rotation waveforms, i.e.:

1. Two oscillations for the anterior -posterior *roll* movement (mean amplitude for trunk = $3.92 \pm 0.30^\circ$; pelvis = $5.36 \pm 0.54^\circ$ and upper-body = $4.20 \pm 0.3^\circ$) representative of the shift from left to right limb.
2. Two oscillations for the vertical up and down *pitch* (mean amplitude for trunk = $3.62 \pm 0.32^\circ$; pelvis = $4.54 \pm 0.72^\circ$ and upper-body = $4.98 \pm 1.04^\circ$) representative and the dropping of the body weight as the subject moved from terminal stance to make contact with the ground ready for heel strike.
3. One oscillation for the lateral left to right *yaw rotation* (mean amplitude for trunk = $6.95 \pm 0.39^\circ$; pelvis = $11.78 \pm 1.17^\circ$ and upper-body = $9.41 \pm 1.20^\circ$) representative of the body motion from the left to the right side.

Rigid body movement was related to the change in limb support from one limb to the next as the subjects walked along the walkways.

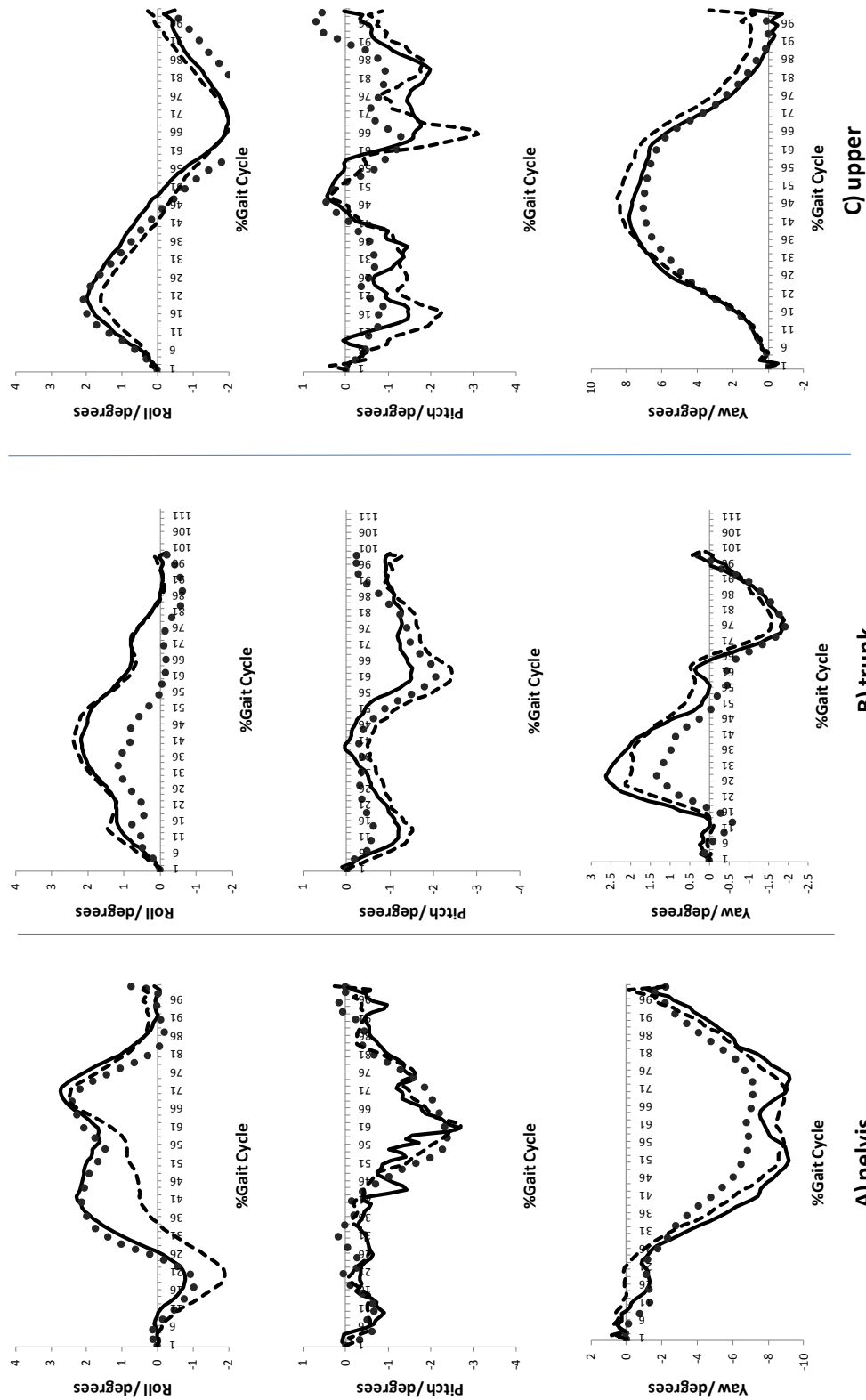


Figure 5-2: Kinematics waveforms representative of roll, pitch and yaw rotations of the three rigid bodies (A) Pelvis; (B) Trunk and (C) upper-body. On the three walkways: WDw =solid line; NRw =dotted lines and GRw = dashed lines.

5.3.2. Comparisons between the male and female cohorts

5.3.2.1. Temporal parameters

The temporal parameters were determined for comparison of the male and female cohorts and are summarised in Table 5-3. This specific comparison was made in order to determine the efficiency of the developed protocol, by determining how well the results compared to published literature (Perry). The main observations comparing the male and female cohorts during walking are as follows:

In comparison to the male cohort, the female cohort walked with:

1. Slower speed, shorter stance time, shorter swing time, smaller stride length and more steps per minute on the **WDw** (differences were not significant, except for the stride length).
2. Slower speed, shorter stance time, longer swing time, longer stride length and fewer steps per minute on the **NRw** (differences were not significant,).
3. Slower speed, shorter stance time, shorter swing time, smaller stride length and more steps per minute on the **GRw-Wide** (differences were not significant)
4. Slower speed, longer stance time, longer swing time, smaller stride length and more steps per minute on the **GRw-Narrow** (differences were not significant, except for cadence)
5. Longer left stride length on the **GR-Narrow** than on the **GRw-Wide**.

Both cohorts had faster speeds, shorter stance times, shorter swing times as well as longer stride lengths on the left limbs in comparison to the right and more steps per minute on the **GRw-Narrow** than on the **GRw-Wide**.

Table 5-3: Temporal parameters comparing the male and female cohort along the WDw, NRw and GRw. The results are expressed as mean ± SD of both the right and left limbs.

Variables	Limb	WDw		NR w		GRw-Wide		GRw-Narrow	
		Male	Female	Male	Female	Male	Female	Male	Female
SPEED/m/s	Average	1.42±0.42	1.07±0.08	1.22±0.14	1.16±0.17	1.20±0.12	1.04±0.13	1.33±0.13	1.28±0.13
	Right Left	0.40±0.10 0.40±0.12	0.35±0.07 0.38±0.08	0.44±0.06 0.43±0.07	0.42±0.06 0.43±0.09	0.45±0.08 0.48±0.08	0.43±0.09 0.50±0.15	0.39±0.03 0.40±0.06	0.42±0.13 0.42±0.12
SWING TIME/s	Right left	0.62±0.07 0.61±0.08	0.61±0.05 0.65±0.05	0.60±0.14 0.60±0.06	0.67±0.06 0.61±0.07	0.67±0.08 0.61±0.06	0.60±0.09 0.61±0.04	0.60±0.02 0.61±0.11	0.58±0.05 0.59±0.04
	STRIDE LENGTH/m	Right left	1.33±0.09 1.32±0.09	(1.24±0.03)* 1.25±0.01	1.20±0.33 1.31±0.10	1.29±0.13 1.24±0.20	1.33±0.11 1.27±0.16	1.18±0.25 1.18±0.12	1.37±0.09 1.08±0.61
CADENCE/steps/minute	Right Left	109.78±10.70 114.70±21.34	109.92±10.70 111.78±9.70	127.43±20.53 116.41±3.77	115.00±16.39 118.10±12.46	103.64±33.49 115.60±5.60	115.80±5.65 116.75±5.97	119.46±10.13 126.13±6.27	(136.53±12.15)* 129.26±10.75

*Significant differences (p<0.05)

5.3.2.2. Postural parameters

The mean *roll*, *pitch* and *yaw* ROM's were calculated comparing the male and female cohorts for the three rigid bodies (trunk, Pelvis and upper body). The differences were not significant when the male and female data was compared for the Trunk rigid body, (Table 5-4), the Pelvis rigid body (Table 5-5) and the Upper body rigid body (Table 5-6).

Table 5-4: Mean \pm SD postural parameters comparing the male and female cohorts during gait along the WDw, NRw and GRw for the *roll*, *pitch* and *yaw* ROM values of the trunk rigid body.

	Trunk					
	WDw		NRw		GRw	
	Male	Female	Male	Female	Male	Female
Roll /°	4.56 \pm 1.55	3.07 \pm 1.15	2.59 \pm 0.9	3.15 \pm 1.56	4.06 \pm 2.05	4.47 \pm 2.68
Pitch /°	5.15 \pm 2.42	2.56 \pm 1.15	1.29 \pm 1.04	3.61 \pm 2.60	2.79 \pm 1.28	3.72 \pm 1.01
Yaw /°	7.46 \pm 1.50	6.86 \pm 3.89	4.40 \pm 3.67	3.19 \pm 5.50	6.28 \pm 2.94	8.09 \pm 4.92

Table 5-5: Mean \pm SD postural parameters comparing the male and female cohorts during gait along the WDw, NRw and GRw for the *roll*, *pitch* and *yaw* ROM values of the Pelvis rigid body.

	Pelvis					
	WDw		NRw		GRw	
	Male	Female	Male	Female	Male	Female
Roll /°	4.79 \pm 0.76	7.17 \pm 3.52	5.19 \pm 1.70	7.51 \pm 3.14	4.73 \pm 1.28	7.17 \pm 3.76
Pitch /°	3.88 \pm 1.44	7.09 \pm 7.57	3.65 \pm 2.05	6.65 \pm 3.80	3.76 \pm 2.33	5.57 \pm 2.88
Yaw /°	13.79 \pm 3.32	11.56 \pm 4.37	15.65 \pm 6.64	13.70 \pm 4.40	14.43 \pm 1.32	12.90 \pm 2.44

Table 5-6: Mean \pm SD postural parameters comparing the male and female cohorts during gait along the WDw, NRw and GRw for the *roll*, *pitch* and *yaw* ROM values of the upper body rigid body.

Upper Body						
	WDw		NRw		GRw	
	Male	Female	Male	Female	Male	Female
Roll /°	5.25 \pm 1.28	3.99 \pm 2.32	4.63 \pm 0.91	6.10 \pm 4.46	4.29 \pm 1.44	3.91 \pm 2.15
Pitch /°	5.57 \pm 2.43	5.53 \pm 2.03	4.28 \pm 0.78	5.55 \pm 0.93	6.56 \pm 1.77	6.80 \pm 2.93
Yaw (/°	9.43 \pm 3.31	10.85 \pm 5.65	7.61 \pm 4.45	10.55 \pm 4.73	8.29 \pm 2.66	13.07 \pm 5.38

5.3.2.3. Kinematic waveforms

The **trunk** rigid body kinematic waveforms shown in Figure 5-3 show that the female cohort had a negatively biased *roll* rotation especially during the swing phase of the gait cycle on all three walkways.

The **pelvis** rigid body kinematic waveforms shown in Figure 5-4 show that the *pitch* and *roll* patterns are similar for the two cohorts, with the female cohort displaying a slightly negatively biased *roll* during stance phase of the gait cycle, which changes to a positively biased *roll* during the swing phase (after 50% cycle) on all walkways.

The **upper body** rigid body kinematic waveforms shown in Figure 5-5 show that the female cohort show a slightly positively biased *roll* on the WDw, whereas along the NRw and GRW none of the cohorts showed any bias.

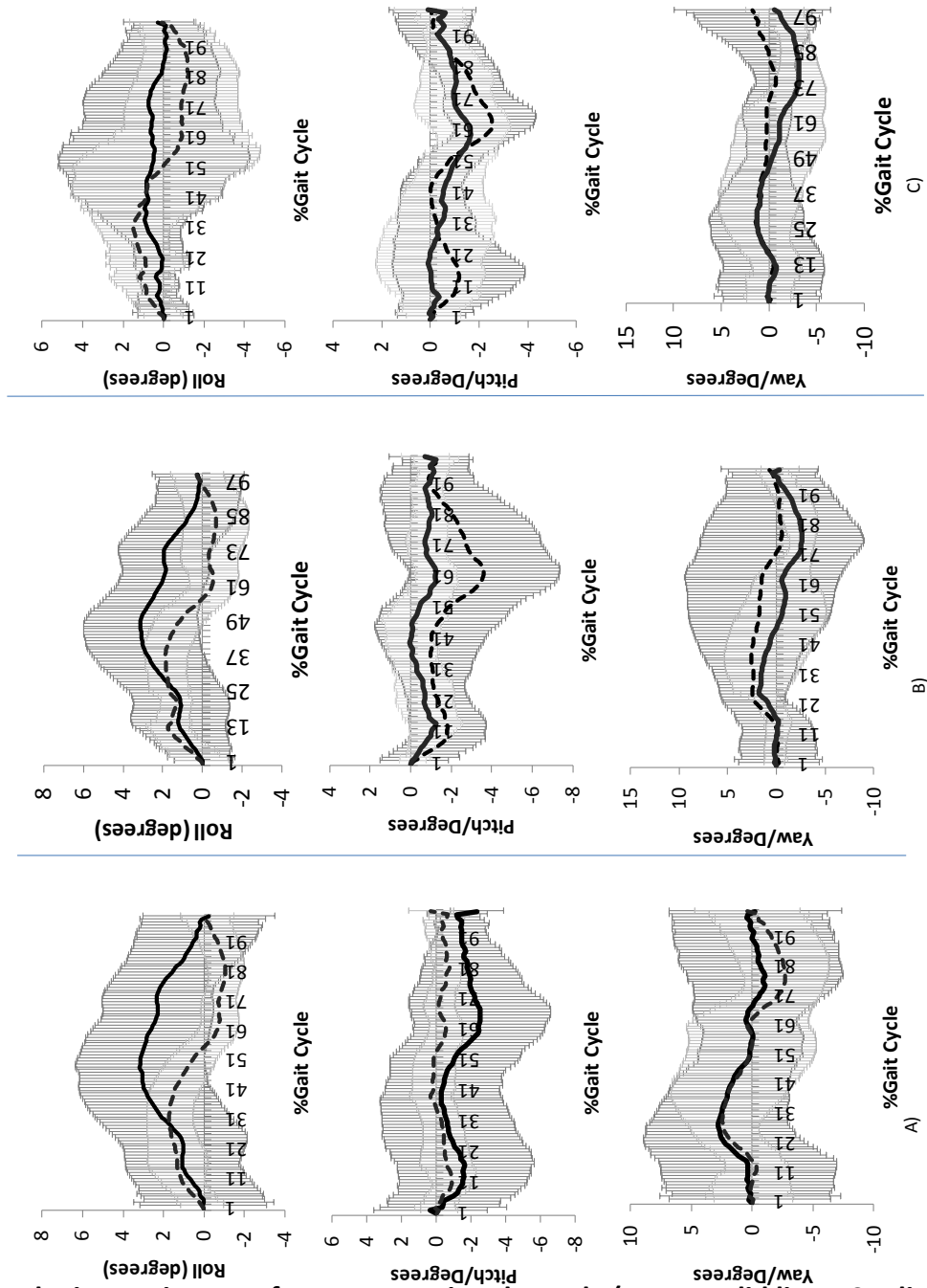


Figure 5-3: Trunk Kinematics waveforms comparing the male (mean=solid lines, SD=light grey lines) and female (mean=dashed lines; SD=dark grey lines) roll, pitch and yaw rotations on the A) WDw, B) NRw and C) GRw

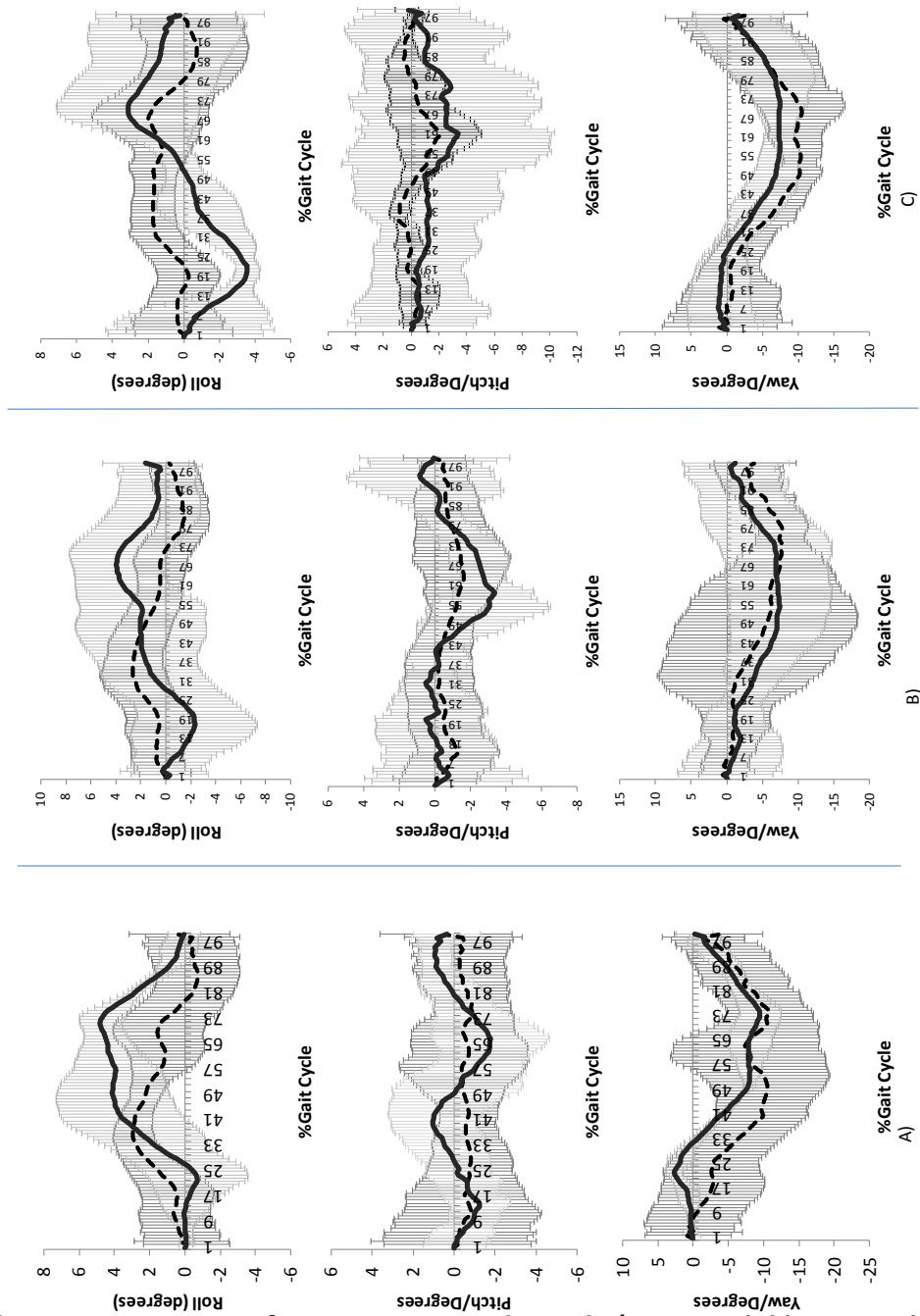


Figure 5-4: Pelvis Kinematics waveforms comparing the male (mean=solid lines, SD=light grey lines) and female (mean=dashed lines; SD=dark grey lines) *roll, pitch and yaw* rotations on the A) WDw, B) NRw and C) GRw.

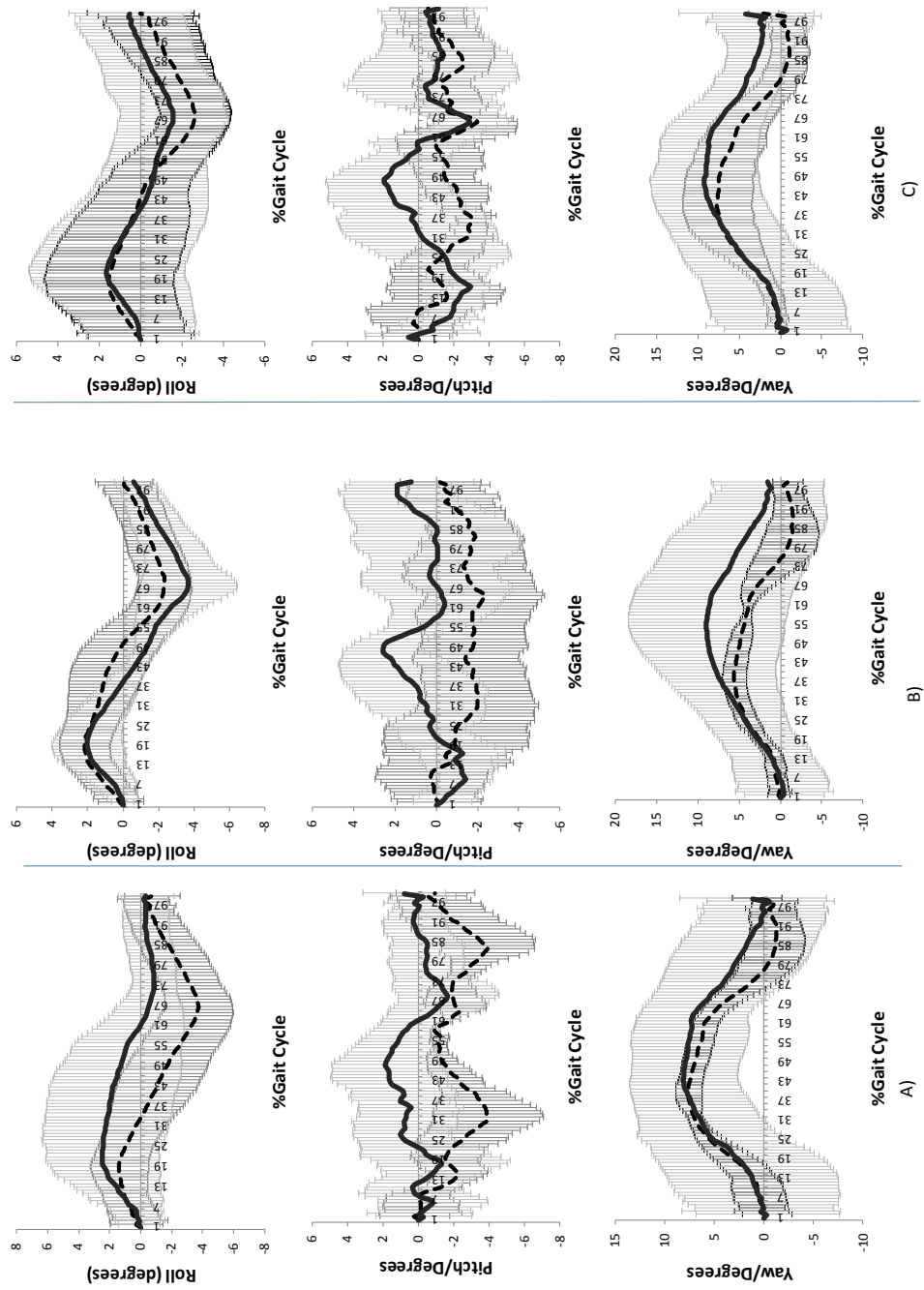


Figure 5-5: Upper body kinematics waveforms comparing the male (mean=solid lines, SD=light grey lines) and female (mean=dashed lines; SD=dark grey lines) *roll, pitch and yaw* rotations on the A) WDw, B) NRw and C) GRw

5.4. Discussion

The adapted data collection and data processing protocol investigated the same temporal and postural parameters as those observed for the rats reported in Chapters 3 and 4. The study presented a practical, simple, repeatable (ICC >0.75) and translatable method for assessing gait function in healthy humans and furthermore allowed for the correlation of data between the two species.

A discussion of the overall results from this study is now given in reference to these objectives.

1. Identify the effects of dual tasking on healthy gait by introducing walkways of different widths.

Subjects walked faster on the **WDw** in comparison to the **NRw** and **GRw-Wide** (1.25 ± 0.34 m/s for the **WDw**, 1.19 ± 0.15 m/s for the **NRw**, 1.12 ± 0.15 m/s for the **GRw - Wide**). On the **WDw**, although still confined, the walkway was wide enough (stride width) for the subjects to walk freely without fear of stepping over the predestined width of the walkway. Their gait phases, i.e., swing time and stance time, were shorter and they walked on the **WDw** with longer strides and faster cadence. However, no significant differences were found between the **WDw**, **NRw** and **GRw**.

Furthermore, a comparison between the **WDw** and **NRw** with the **GRw-narrow** kinematic waveforms revealed that subjects walked with a different pattern on the **NRw** in comparison to the **WDw** and the **GRw-Narrow**. They were faster in **GRw-narrow** compared to **NRw** and **WDw**. This shows that the subjects slowed down as they approached the narrow end of the **GRw** and increased their walking speed to

complete the walkway towards the end. A similar pattern was also observed for the study on the PD rats (Chapter 3) as an effect of the gradually narrowing the walkway.

2. Demonstrate the protocol's sensitivity in identifying gait differences between two cohorts.

The female cohort showed that as they walked with a slower speed, they took smaller strides and walked with more steps per minute on average along the walkways. They also had a greater anterior-posterior *roll* ROM as representative of the shift from left to right limb. Conversely, they also showed less *yaw* ROM on the NRw compared to the male cohort.

3. Validate the protocol by comparing the results to the work of others.

Comparisons between male and female gait has been published and clearly summarised by Perry, (1992). General level of walking speed for adults was found to be about 1.36m/s. Perry found Male subjects walked 5% faster and female subjects walked 6% slower. The results presented in the current study show that compared to the average population speed of 1.36 m/s:

1. The male subjects walked 4% faster and the female subjects were 20% slower in general.
2. The male subjects walked 12% slower and the female subjects 23% slower on the NRw
3. On the GRw-wide, the male subjects walked 2% slower where as the female cohort walked 6% slower.
4. In GRw-narrow, the male subjects were 10% slower where as female subjects were 14% slower.

The results for stride length and cadence in the current study are in agreement with Perry (1992) as the primary determinants of speed are the stride length and the cadence. The average stride length was 1.42 m with men having a 14% longer stride than the women. The recorded average cadence of women was 117 steps per minute which is faster than that of men (111 steps per minute) therefore compensates for their shorter stride. The results obtained for stride lengths and cadence is consistent with the findings obtained by Perry (1992). The trends show that the protocol produced results that are similar to published data and further validates the method for gait analysis.

The number of gait cycles recorded could be increased by adding extra cameras or increasing marker size as the majority of marker drop out was due to the large distance from each camera to final end position of the walking task. However, the size limitation only affected camera placement. The protocol did offer advantages such as: the task pathway was sufficiently long to capture over six cycles for all subjects. Secondly the developed protocol was shown to provide data that was comparable and suitable for both genders and can be used on multiple subjects.

In conclusion, the data demonstrated a successful execution of a human gait protocol that was developed from an already established rat MA protocol. The protocol will aim to strengthen the generalization that can be made in experimental neuroscience studies, that use of the information based on rat models are accurately transferable to human data in terms of Gait. As a pilot study on a healthy human cohort, the results show that both the temporal and postural patterns can provide data that could be compared with that rat data. However, data from subjects with either PD or stroke would help with correlative analysis between the two species.

CHAPTER 6

6. Discussion

Developments in motion analysis (MA) technology over the last two decades have enhanced our understanding of rat locomotion (Brown et al., 2005, Fan et al., 2008, Klein et al., 2009, Fan et al., 2008 Coulthard et al., 2002, Canu et al., 2005, Metz et al., 1998, Couto et al., 2008b). However, such advances in knowledge are futile if no practical use is made of them. Scientists and engineers should make the most of these developments by forging stronger links with bio-scientist that use these rat models. Further advances in MA knowledge should be applied to clinical problems involving rat models for the long-term benefit to patients with neurodegenerative diseases that affect gait.

Over the last decade, the need to cross validate rat models with human data following direct comparisons have been identified to show that there are similarities in the behaviour of the two species and thus rat models studies could be more convincingly generalized to human studies (Whishaw et al., 2002, Whishaw et al., 1992, Sacrey et al., 2009). For this reason, the main purpose of this study was to determine if three dimensional marker based MA (3DMA) techniques are practical and sensitive enough to investigate the gait of both rats and humans in terms on temporal and postural parameters.

This research project was conducted to design, develop and examine the ability of a developed protocol that identifies the differences in gait for rat models of Parkinson's disease (PD) (*Experiment 1* described in Chapter 3) and stroke (*Experiment 2*

described in Chapter 4) and to replicate the designed protocol to investigate human gait allowing for correlation and cross validation with the rat gait data (*Experiment 3* described in Chapter 5).

The three experiments were carried out using 3DMA as described in Chapter 2. *Experiment 1* was a pilot study involving a cohort of 10 rat models of PD. This pilot study was the foundation of the project and allowed exploration of measurement and analysis techniques applied to the rats as they walked across an elevated beam. Temporal gait, spatial and distance parameters were investigated using MA techniques to acquire 3D kinematic measurements while rats walked continuously along a straight walkway.

The rats showed differences in the way they adapted their gait on a narrow path and a gradually narrowing path (Madete 2011, 2010). The results were compared to walking along a wide (control) beam which only directs their forward motion and allows them to walk freely otherwise. The results also provided data that matches those found in literature, i.e., PD rat models presented a motor deficit on the side contralateral to surgery, (Metz et al., 2005) and that speed was slower following surgery (Lundblad et al., 2002). Postural adaptation strategies of PD and healthy rats during gait were presented for the first time in terms of *roll*, *pitch* and *roll* of the rats' body. The results revealed increased levels of complexity of the beam elicit compensatory movements used by the rats to maintain balance on the beam (Miklyeva et al., 1995). Furthermore, the findings allow a detailed and effective analysis of angular displacements of the rat, thus postural instability.

The study concluded that 3DMA techniques can be used in a non-invasive and practical way to record rat locomotion. Compensatory movement patterns as

suggested by Miklyaeva et al., (1995), presented as postural adjustment's. The data was written into two separate journal papers that have been published in peer review journals

Following the success of *Experiment 1* (excellent reliability ICC parameters (>0.75), the rat 3DMA protocol was applied to measure temporal gait and posture of a cohort of stroke rat models as part of a larger study involving 50 rats in *Experiment 2*. Additionally, classification of stroke gait and the utilisation of the Dempster-Shafer Theory (DST) (Jones et al., 2002) classifier in data processing were introduced.

This second experiment allowed for the protocol to be fully tested. A group of middle cerebral arterial occlusion (MCAO) rats were investigated. Occlusion time is typically 30, 60, 90, or 200, generally. For this cohort, the experimenter occludes the MCA for 30 minutes, 30 minutes of MCAO produces striatal insults where as longer occlusion times (60 minutes or more) produce larger strokes (Shen et al., 2010, Wang et al., 2009). In the literature there is disputing evidence as to whether any behavioural conditions can be quantified post-stroke from a 30 minute MCAO (Shen et al., 2010, Corbett and nurse). Therefore there is a need for a sensitive approach that can pick up and analyse slight differences in behaviour and function following a 30 minute MCAO.

The 3DMA protocol was applied to investigate behavioural characteristics of the stroke cohort due to its proven sensitivity in picking up small changes in rat temporal and postural gait. The results from the stroke walking trial were interpreted using the Cardiff DST objective classifier tool, developed by Jones et al., (2004). The tool enables distinct classification of cohorts that otherwise would present uncertain, inadequate and conflicting evidence. From statistical results of the walking trial of the

PD rat data the input variables that were found to be the most influential for the final DST classification were swing time and range of rotation around the x axes (*roll*). These variables may provide useful information as to which are the most significant variables involved in the analysis of temporal and postural gait of stroke rats. **Experiment 2** helps further validate the developed protocol and demonstrates that the developed techniques are reproducible and can be replicated to successfully record and measure rat gait.

Whishaw et al., (1992), states that it is important to demonstrate any similarities between rats and humans because it strengthens the generalizations made when interpreting rat model experiments on behaviour and function following brain damage. Therefore the developed rat data collection protocol was modified to accommodate measurements for human gait in **Experiment 3**. The conversion of the small scale gait protocol into a larger one took into account average values of stride length and base of support of both species and determined a ratio of 1:9. This ratio was used to determine the length and width of the human walkway in order to maintain the generic nature of the study. The outcome would aim to provide validation and further understanding of the rat model of disease

Experiment 3 involved applying 3DMA techniques were used to acquire data from several cycles during continuous human walking along a straight line on a defined walkway. Temporal and postural gait parameters were analysed. Dual tasking introduced by including three different beam widths was repeated in the human study with walkways of varying widths in order to compare gait data on a narrow path and a gradually narrowing path with a wide path. The study concluded that the protocol was successful in collecting and processing data that produced similar outputs as that of

the rat cohort. Data allowed comparisons of male and female cohorts which compared well to published temporal data (Perry, 1992, Whittle et al.). Results from the three beams were also compared and no significant differences from data for the three beams were found.

Experiment 1, 2 and 3 allowed comparative temporal and postural data of the rat models of PD and stroke and humans from the developed protocols to be produced.

There are not many studies that investigate the comparison between rats and humans. Several studies have done this; Whishaw et al., (1992) aimed to compare healthy rat to healthy human reaching. They compared reaching movements made by rats with those made by humans tested in similar circumstances. They combined the use of video analysis, Cartesian reconstructions of movement trajectories and velocity profiles. They varied the size of the target to determine whether the movements that both species used were subject to the same constraints. Furthermore, Whishaw et al (2002) looked at data from a group of PD patient's compared to rat model of the disease. They investigated whether the reaching movements of rats that were affected by DA-depletion had related deficits studied in PD patients. They concluded that the use of a similar task across a number of species proves helpful in understanding the motoric consequences of the disorder as well as the potential of treatments to improve motor performance.

Sacrey et al 2009 investigated hand shaping during skilled reaching and compared the results for rats and humans using high-speed video recording to capture representative reaches for both species at 1000 frames per second. Rats were examined in a single-pellet reaching task box in which they were required to reach through a slot for a food pellet placed on a shelf, grasp the pellet and withdrawal their

hand to place the pellet in the mouth for eating. Humans reached for a Cheerio™ while seated. The ‘complexity and degree of correspondence’ of hand shaping between rats and humans was measured by digitizing the tips of the digits offline to compare the spatial and temporal aspects of digit movements during frame-by-frame analysis. They also found similarities across the two species.

For this thesis, the most relevant rat measurements that the study achieved a direct comparison with humans were temporal and postural parameters during gait. Rats have a quadrupedal gait cycle (Hamers et al., 2006) that can be categorised either by how many feet are on the ground at any one time (Hildebrand et al., 1976) or which limbs are on the ground together (Muybridge 1899) while humans are bipedal. Temporal gait similarities in the movements made by rats and humans during over ground locomotion show a consistent and cyclic gait movement pattern with the stance and swing phases clearly observed for each limb.

Postural control during gait was defined in rats and humans described using body rotations of a rigid body on the subject’s anatomy during gait. For both species, the body orientation observed from kinematic waveforms was cyclic and affected by the swing and stance phases of the limbs. Three rigid bodies, upper body, trunk, and the pelvis, were investigated in the human trials, where in the rats trial, only one rigid body was defined representative of the entire body. This was due to the small nature and the skin covering of the rats.

Kinematic waveforms revealed that during one gait cycle, body orientation is towards the weight bearing limbs for both species (Miklyaeva et al., 1995). The upper body rigid body matched patterns produced from the rat rigid body. The *roll* of the body from left to right during one gait cycle which involves rotations towards the side of the

weight bearing limb during gait. The *Pitch* rotation, representative of the vertical axial displacements with the human upper body rotations, matches the pattern of the rat motion of a double sinusoidal path. This represents two cycle of downward and upward displacement in each stride of the right and left steps. The two dips occur during periods of double limb support each followed by a progressive rise above zero degrees due to the two single support intervals during terminal stance and late mid swing. The *yaw* Displacements occur during single stance as the limb support shifts from the left to right limbs. Maximum displacement is at 50% gait cycle representative of double limb support in humans and three limbs are in contact with the ground in rats (Miklyeva et al., 1995).

The developed protocols were able to analyse over-ground locomotion of rat and human subjects using 3DMA techniques. The thesis demonstrates how the results can be translated to compare results from the two species successfully and have moved one step closer in the validation of rat models of disease for disease testing. In addition, the measurement protocol can be applied to subjects that have the modelled disease to compare function and behaviour of the disease.

3DMA can provide an effective and practical approach to quantifying temporal gait parameters for rat models of PD and stroke. The results of this exploratory study demonstrate functional characteristics of models in terms of the disability to maintain posture during locomotion. They also reveal how increased levels of complexity of the walkway elicit compensatory strategies used by the PD rats to maintain balance on the beam. Furthermore, the findings allow a detailed and effective analysis of angular displacements of the body, thus postural instability.

Rat 3DMA can thus provide a practical and powerful tool for validating these models. The new protocol identified gait deficits and thus classified the rats' function objectively. Furthermore, rat measurements were directly compared with human measurements to explore correlations between patients and rat behaviour..

The results demonstrate that marker-based MA techniques provide an effective and practical approach to quantifying temporal gait parameters. A method that allowed detailed and effective analysis of angular displacements of the human and rat body was developed. This was further validated by a second study carried out on a larger cohort of rat models of stroke. The protocol allowed direct correlations of human and rat gait data. The clinical relevance and appeal of the protocol is that it is practical, non-invasive and the visualisation nature of the body rotation data for direct comparison.

This research was in collaboration with a bio-scientist that was involved with patients who had neurodegenerative condition discussed in this thesis. These interactions enabled understanding of the limitations and constraints of performing the trial in a clinical setting. This partnership has provided an invaluable insight in understanding the clinical application of the protocol in correlating rat findings with those of patients. The protocol was designed with a clinical application in mind, therefore given more time in conjunction with doctors and patients in clinics, the protocol application could be carried out on patients in a clinical setting.

The results demonstrate that marker-based optoelectronic motion analysis (MA) is an effective and practical approach to quantifying in vivo, non invasive, temporal and postural gait parameters on both rats and human. The rat protocol further validated by a second study carried out on a larger cohort of models of stroke. The results

showed that rat three dimensional (3D) marker based MA (3DMA) can thus provide a practical and powerful tool for validating rat models as well as to identify gait deficits and classify healthy and pathological function objectively. These measures can be used to explore correlations between patients and rat behaviour highlighting the findings and scientific achievements of the study.

CHAPTER 7

7. Conclusions and further work

7.1. Conclusions

Three experiments were carried out using three dimensional (3D) marker based motion analysis (3DMA) to measure gait of animal models of Parkinson's disease (PD) and stroke and on a healthy human cohort. Conclusions specific to each of the key objectives outlined in Chapter 1 will be discussed.

Objective 1: Development of a novel technique for the measurement of temporal and postural parameters of animal model of Parkinson's disease.

A novel protocol was developed (described in Chapter 2) and data produced that described for temporal and postural gait data of a cohort of ten animal models of PD (Chapter 3). This pilot study was the basis of the thesis and allowed for the exploration of measurement and analysis techniques that were applied to a cohort of rats as they walked across an elevated beam temporal gait, spatial and distance parameters were investigated MA techniques to acquire 3D kinematic measurements while rats walked continuously along a straight line.

The animals showed differences in the way they adapted their gait on a narrow path and a gradually narrowing path. The results were compared to walking along a wide (control) beam which only directs their forward motion and allows them to walk freely otherwise. The study concluded that 3DMA techniques can be used in a practical,

non-invasive and simple way to record animal locomotion. The data was written into two separate journal papers that have been published in peer review journals.

Postural adaptation strategies of hemi-parkinsonian and healthy rats during gait were presented for the first time. The results revealed increased levels of complexity of the beam elicit compensatory movements used by the rats to maintain balance on the beam. Furthermore, the findings allow a detailed and effective analysis of angular displacements of the body, thus postural instability. Compensatory movement patterns presented as postural adjustments have successfully been quantified and could be used for correlation with patient data based on a similar 3DMA in human subjects.

Objective 2: Application of the developed animal motion analysis protocol to measure temporal gait and posture of animal model of stroke and their classification of stroke gait and the utilisation of the Demster-Shafer Theory classifier in data processing.

This second experiment allowed for the protocol to be fully tested. A set of middle cerebral arterial occlusion rats were used. The occlusion only lasts 30 minutes and there is disputing evidence as to whether any behavioural conditions can be quantified post-stroke. 3DMA was used to analyse this cohort due to its proven sensitivity in picking up small changes in behaviour. Furthermore, data collection further validate the developed protocol.

The protocol was successfully applied to a cohort of 50 stroke rats as they walked along a wide beam. Recordings described temporal and postural gait parameters for 27 of the 50 animals before and after surgical intervention. The animals were divided

into three groups, before and after lesion surgery; before and after grafting and their controls before and after surgery.

The results from the stroke walking trial were interpreted with the Cardiff Dempster-Shafer (DS) objective classifier tool, developed by Jones et al., (2004). The tool enables distinct classification of cohorts that otherwise would present uncertain, inadequate and conflicting evidence. The DS classifier incorporates an optimisation technique and simplex plots to classify normal and stroke behaviour and function of the rats. Simplex plots allowed the classification of the rats and each associated characteristic to be represented visually.

The input variables that were found to be the most influential for the final classification were swing time and range of rotation around the x axes (*roll*). These variables may provide useful information as to which are the most significant variables involved in the analysis of temporal and postural gait of stroke rats.

This study was carried out to validate the developed protocol and demonstrate that the technique and experiences gained from the first study may be replicated on group of different rats to successfully record and measure their gait.

Introducing an element of dual tasking was not applied to this walking trial as the animals were too small and walked on the narrowest beam without adjusting their gait. The study concluded that the protocol developed could be applied to a different set of rats. In addition, the uses of previously developed objective classification techniques to further understand and interpret the data.

Objective 3: Development of a novel technique for the measurement of temporal and postural parameters of human subjects adapted from the animal model of Parkinson's disease protocol.

The animal data collection protocol was modified to accommodate measurements for human gait. The conversion from smaller scale to larger scale took into account average values of stride length and stride width of both species to determine what proportions to scale the set up. The procedure would provide validation and further understanding of the animal model of disease

Temporal gait, spatial and distance parameters were recorded and analysed using Motion analysis (MA) techniques to acquire data during continuous human walking from several cycles along a straight line. The element of dual tasking was repeated in the human study with paths of varying widths to compare gait data on a narrow path and a gradually narrowing path. The results were also compared to walking along a wide path.

The study concluded that the protocol was successful in achieving similar outputs as of that animal cohort. Data allowed comparisons of male and female cohorts which compared well to published temporal data (Perry, 1992). Results from the three beams were also compared and no significant differences from data for the three beams were found.

Objective 4: Correlating temporal and postural parameters of the animal models and humans from the developed protocols.

There are not many studies that have investigated the correlation of both animals and humans. Whishaw et al.,(1992) compared human and rat skilled reaching. They

reasoned that if it could be shown that there are similarities in the behaviour of the two species then the results of behavioural studies on the rat could be more convincingly generalised to humans. The author compared temporal gait and postural gait parameters of control rats with those made by healthy humans tested in similar circumstances.

The results demonstrate that marker-based MA techniques provide an effective and simple approach to quantifying temporal gait parameters. A method that allowed detailed and effective analysis of angular displacements of the human and rat body was developed. This was further validated by a second study carried out on a larger cohort of animal models of stroke. The protocol allowed direct correlations of human and animal gait data. The clinical relevance and appeal of the protocol is that it is practical, non-invasive and the visualisation nature of the body rotation data for direct comparison.

This research was in collaboration with bio-scientist that was involved with patients who had neurodegenerative condition discussed in this thesis. These interactions enabled understanding of the limitations and constraints of performing the trial in a clinical setting. This partnership has provided an invaluable insight in understanding the clinical application of the protocol in correlating animal findings with those of patients. The protocol was designed with a clinical application in mind, therefore given more time in conjunction with doctors and patients in clinics, the protocol application could be carried out on patients in a clinical setting.

7.2. Further work

To meet the overall aims of this project, the novel protocol needs further development in a number of ways.

Data from the walking trials was not always correctly tracked therefore leading to a number of rat and human subjects to be eliminated. The errors may lie in imprecision, errors due to skin movement artefacts and the overall camera set up before calibration.

In addition, the method used for rat marker placement needs to be reviewed further due to the slight discomfort to the rats. Couto et al., (2008), Canu et al., (2009) and Metz et al., (2005) used self-sticking infrared reflective markers of varying sizes, and the need to shave the rats was essential to ensure marker fixation. Therefore this route should be considered. Marker clusters (three markers in one position) should also be explored to calculate entire six degrees of freedom (6DOF) of the representative bodies.

Further biomechanical and clinical problems should be investigated, e.g., identification of upper body and pelvis 6DOF, introducing an elevated beam to the human protocol and data collection of patients with gait disorders. A healthy human data base should be established with a larger cohort of subjects from all age groups. Additionally, it is suggested that the classification method be used for the assessment of the human gait patterns comparing different walkway scenarios e.g., identification of the differences in gait along the wide and narrow walkways.

8. REFERENCES

- ACKLAND, G. L., GUTIERREZ DEL ARROYO, A., YAO, S. T., STEPHENS, R. C., DYSON, A., KLEIN, N. J., SINGER, M. & GOURINE, A. V. 2010. Low-molecular-weight polyethylene glycol improves survival in experimental sepsis. *Critical care medicine*, 38, 629-36.
- ADAMSON, J., BESWICK, A. & EBRAHIM, S. 2004. Is stroke the most common cause of disability? *Journal of stroke and cerebrovascular diseases : the official journal of National Stroke Association*, 13, 171-7.
- ADKIN, A. L., BLOEM, B. R. & ALLUM, J. H. 2005. Trunk sway measurements during stance and gait tasks in Parkinson's disease. *Gait & posture*, 22, 240-9.
- AUER, R. N. & SUTHERLAND, G. R. 2005. Primary intracerebral hemorrhage: pathophysiology. *The Canadian journal of neurological sciences. Le journal canadien des sciences neurologiques*, 32 Suppl 2, S3-12.
- BEAUCHET, O., ALLALI, G., ANNWEILER, C., BRIDENBAUGH, S., ASSAL, F., KRESSIG, R. W. & HERRMANN, F. R. 2009. Gait variability among healthy adults: low and high stride-to-stride variability are both a reflection of gait stability. *Gerontology*, 55, 702-6.
- BISHOP, M., BRUNT, D. & MARJAMA-LYONS, J. 2006. Do people with Parkinson's disease change strategy during unplanned gait termination? *Neuroscience letters*, 397, 240-4.
- BJÖRKLUND, A., DUNNETT, S.B., 1992. *Neural transplantation in adult rats* In: Dunnett, S.B., Björklund, A. (Eds.), *Neural Transplantation: A Practical Approach*, Oxford, , IRL Press.
- BLIN, O., PAILHOUS, J., LAFFORGUE, P. & SERRATRICE, G. 1990. Quantitative analysis of walking in patients with knee osteoarthritis: a method of assessing the effectiveness of non-steroidal anti-inflammatory treatment. *Annals of the rheumatic diseases*, 49, 990-3.
- BOND, J. M. & MORRIS, M. 2000. Goal-directed secondary motor tasks: their effects on gait in subjects with Parkinson disease. *Archives of physical medicine and rehabilitation*, 81, 110-6.
- BOYD, L. A., QUANEY, B. M., POHL, P. S. & WINSTEIN, C. J. 2007. Learning implicitly: effects of task and severity after stroke. *Neurorehabilitation and neural repair*, 21, 444-54.
- BROWN, D. A., NAGPAL, S. & CHI, S. 2005. Limb-loaded cycling program for locomotor intervention following stroke. *Physical therapy*, 85, 159-68.
- BROWN, L. A., COOPER, S. A., DOAN, J. B., DICKIN, D. C., WHISHAW, I. Q., PELLIS, S. M. & SUCHOWERSKY, O. 2006. Parkinsonian deficits in sensory integration for postural

-
- control: temporal response to changes in visual input. *Parkinsonism & related disorders*, 12, 376-81.
- BROWN, M. & TAYLOR, J. 2005. Prehabilitation and rehabilitation for attenuating hindlimb unweighting effects on skeletal muscle and gait in adult and old rats. *Archives of physical medicine and rehabilitation*, 86, 2261-9.
- CANU, M. H. & GARNIER, C. 2009. A 3D analysis of fore- and hindlimb motion during overground and ladder walking: comparison of control and unloaded rats. *Experimental neurology*, 218, 98-108.
- CANU, M. H., GARNIER, C., LEPOUTRE, F. X. & FALEMPIN, M. 2005. A 3D analysis of hindlimb motion during treadmill locomotion in rats after a 14-day episode of simulated microgravity. *Behavioural brain research*, 157, 309-21.
- CENCI, M. A., WHISHAW, I. Q. & SCHALLERT, T. 2002. Animal models of neurological deficits: how relevant is the rat? *Nat Rev Neurosci*, 3, 574-9.
- CHASTAN, N., DO, M. C., BONNEVILLE, F., TORNAY, F., BLOCH, F., WESTBY, G. W., DORMONT, D., AGID, Y. & WELTER, M. L. 2009. Gait and balance disorders in Parkinson's disease: impaired active braking of the fall of centre of gravity. *Movement disorders : official journal of the Movement Disorder Society*, 24, 188-95.
- CORBETT, D. & NURSE, S. 1998. The problem of assessing effective neuroprotection in experimental cerebral ischemia. *Progress in neurobiology*, 54, 531-48.
- COULTHARD, P., PLEUVRY, B. J., BREWSTER, M., WILSON, K. L. & MACFARLANE, T. V. 2002. Gait analysis as an objective measure in a chronic pain model. *Journal of neuroscience methods*, 116, 197-213.
- COUTO, P. A., FILIPE, V. M., MAGALHAES, L. G., PEREIRA, J. E., COSTA, L. M., MELO-PINTO, P., BULAS-CRUZ, J., MAURICIO, A. C., GEUNA, S. & VAREJAO, A. S. 2008a. A comparison of two-dimensional and three-dimensional techniques for the determination of hindlimb kinematics during treadmill locomotion in rats following spinal cord injury. *Journal of neuroscience methods*, 173, 193-200.
- COUTO, P. A., FILIPE, V. M., MAGALHAES, L. G., PEREIRA, J. E., COSTA, L. M., MELO-PINTO, P., BULAS-CRUZ, J., MAURICIO, A. C., GEUNA, S. & VAREJAO, A. S. 2008b. A comparison of two-dimensional and three-dimensional techniques for the determination of hindlimb kinematics during treadmill locomotion in rats following spinal cord injury. *J Neurosci Methods*, 173, 193-200.
- DAVIES, A. M., CHANSKY, K., LAU, D. H., LEIGH, B. R., GASPAR, L. E., WEISS, G. R., WOZNIAK, A. J., CROWLEY, J. J. & GANDARA, D. R. 2006. Phase II study of consolidation paclitaxel after concurrent chemoradiation in poor-risk stage III non-small-cell lung cancer: SWOG S9712. *Journal of clinical oncology : official journal of the American Society of Clinical Oncology*, 24, 5242-6.
-

-
- DE BUJANDA, E., NADEAU, S. & BOURBONNAIS, D. 2004. Pelvic and shoulder movements in the frontal plane during treadmill walking in adults with stroke. *Journal of stroke and cerebrovascular diseases : the official journal of National Stroke Association*, 13, 58-69.
- DE LAU, L. M. & BRETELER, M. M. 2006. Epidemiology of Parkinson's disease. *Lancet neurology*, 5, 525-35.
- DEVRIES, A. C., NELSON, R. J., TRAYSTMAN, R. J. & HURN, P. D. 2001. Cognitive and behavioral assessment in experimental stroke research: will it prove useful? *Neuroscience and biobehavioral reviews*, 25, 325-42.
- DONNAN, G. A., FISHER, M., MACLEOD, M. & DAVIS, S. M. 2008. Stroke. *Lancet*, 371, 1612-23.
- DUBUC, B. 2002. Body Movement and the Brain. In: BOTTOM, T. B. F. T. T. (ed.) *Denis Paquet* Quebec: webdrifters
- DUHAMEL, A., BOURRIEZ, J. L., DEVOS, P., KRYSKOWIAK, P., DESTEE, A., DERAMBURE, P. & DEFEBVRE, L. 2004. Statistical tools for clinical gait analysis. *Gait & posture*, 20, 204-12.
- DUNNETT, S. B., BJÖRKLUND, A., 1992. *Staging and dissection of rat embryos*. In: *Dunnett, S.B., Björklund, A. (Eds.), Neural Transplantation: A Practical Approach.*, Oxford, IRL Press.
- DUNNETT, S. B., ISACSON, O., SIRINATHSINGHI, D. J., CLARKE, D. J. & BJÖRKLUND, A. 1988. Striatal grafts in rats with unilateral neostriatal lesions--III. Recovery from dopamine-dependent motor asymmetry and deficits in skilled paw reaching. *Neuroscience*, 24, 813-20.
- FAN, L. W., CHEN, R. F., MITCHELL, H. J., LIN, R. C., SIMPSON, K. L., RHODES, P. G. & CAI, Z. 2008. alpha-Phenyl-n-tert-butyl-nitron attenuates lipopolysaccharide-induced brain injury and improves neurological reflexes and early sensorimotor behavioral performance in juvenile rats. *Journal of neuroscience research*, 86, 3536-47.
- FERRARI, S. 2008. Secondary prevention of osteoporotic fractures: why not apply the evidence? *Swiss medical weekly*, 138, 656-7.
- FERRARIN, M., CARPINELLA, I., RABUFFETTI, M., CALABRESE, E., MAZZOLENI, P. & NEMNI, R. 2006. Locomotor disorders in patients at early stages of Parkinson's disease: a quantitative analysis. *Conference proceedings : ... Annual International Conference of the IEEE Engineering in Medicine and Biology Society. IEEE Engineering in Medicine and Biology Society. Conference*, 1, 1224-7.

-
- FIELD, E. F., METZ, G. A., PELLIS, S. M. & WHISHAW, I. Q. 2006. Sexually dimorphic postural adjustments during vertical behaviour are altered in a unilateral 6-OHDA rat model of Parkinson's disease. *Behavioural brain research*, 174, 39-48.
- FILIFE, V. M., PEREIRA, J. E., COSTA, L. M., MAURICIO, A. C., COUTO, P. A., MELO-PINTO, P. & VAREJAO, A. S. 2006. Effect of skin movement on the analysis of hindlimb kinematics during treadmill locomotion in rats. *Journal of neuroscience methods*, 153, 55-61.
- GARNIER, C., FALEMPIN, M. & CANU, M. H. 2008. A 3D analysis of fore- and hindlimb motion during locomotion: comparison of overground and ladder walking in rats. *Behav Brain Res*, 186, 57-65.
- GILADI, N., SHABTAI, H., ROZENBERG, E. & SHABTAI, E. Gait festination in Parkinson's disease.
- GILLIS, G. B. & BIEWENER, A. A. 2001. Hindlimb muscle function in relation to speed and gait: in vivo patterns of strain and activation in a hip and knee extensor of the rat (*Rattus norvegicus*). *The Journal of experimental biology*, 204, 2717-31.
- GOTZ, J. & ITTNER, L. M. 2008. Animal models of Alzheimer's disease and frontotemporal dementia. *Nature reviews. Neuroscience*, 9, 532-44.
- HAMERS, F. P., LANKHORST, A. J., VAN LAAR, T. J., VELDHUIS, W. B. & GISPEN, W. H. 2001. Automated quantitative gait analysis during overground locomotion in the rat: its application to spinal cord contusion and transection injuries. *Journal of neurotrauma*, 18, 187-201.
- HAUSDORFF, J. M., CUDKOWICZ, M. E., FIRTION, R., WEI, J. Y. & GOLDBERGER, A. L. 1998. Gait variability and basal ganglia disorders: stride-to-stride variations of gait cycle timing in Parkinson's disease and Huntington's disease. *Movement disorders : official journal of the Movement Disorder Society*, 13, 428-37.
- HENDERSON, J. M., WATSON, S., HALLIDAY, G. M., HEINEMANN, T. & GERLACH, M. 2003. Relationships between various behavioural abnormalities and nigrostriatal dopamine depletion in the unilateral 6-OHDA-lesioned rat. *Behavioural brain research*, 139, 105-13.
- HENDERSON, J. M. & WATSON, S. H. 2003. Convulsive and postural effects of lesioning the mid-substantia nigra pars reticulata in naive and 6-hydroxydopamine lesioned rats. *Brain research bulletin*, 60, 179-85.
- IWANIUK, A. N. & WHISHAW, I. Q. 2000. On the origin of skilled forelimb movements. *Trends Neurosci*, 23, 372-6.
- JANSSON, Y., ERIKSSON, B. & JOHNELS, B. 1998. Dispersible levodopa has a fast and more reproducible onset of action than the conventional preparation in Parkinson's

-
- disease. A study with optoelectronic movement analysis. *Parkinsonism & related disorders*, 4, 201-6.
- JI, H. J., CHAI, H. Y., NAHM, S. S., LEE, J., BAE, G. W., NHO, K., KIM, Y. B. & KANG, J. K. 2007. Neuroprotective effects of the novel polyethylene glycol-hemoglobin conjugate SB1 on experimental cerebral thromboembolism in rats. *European journal of pharmacology*, 566, 83-7.
- JONES, L. 2004. *The development of a novel method for the classification of osteoarthritic and normal knee function* PhD, Cardiff University.
- JONES, L., BEYNON, M. J., HOLT, C. A. & ROY, S. 2006. An application of the Dempster-Shafer theory of evidence to the classification of knee function and detection of improvement due to total knee replacement surgery. *Journal of biomechanics*, 39, 2512-20.
- JONES, L. & HOLT, C. A. 2008. An objective tool for assessing the outcome of total knee replacement surgery. *Proceedings of the Institution of Mechanical Engineers. Part H, Journal of engineering in medicine*, 222, 647-55.
- JONSDOTTIR, J., RECALCATI, M., RABUFFETTI, M., CASIRAGHI, A., BOCCARDI, S. & FERRARIN, M. 2009. Functional resources to increase gait speed in people with stroke: strategies adopted compared to healthy controls. *Gait & posture*, 29, 355-9.
- KLEIN, A., WESSOLLECK, J., PAPAZOGLU, A., METZ, G. A. & NIKKHAH, G. 2009. Walking pattern analysis after unilateral 6-OHDA lesion and transplantation of foetal dopaminergic progenitor cells in rats. *Behavioural brain research*, 199, 317-25.
- KOLB, B. & CIOE, J. 2000. Recovery from early cortical damage in rats, VIII. Earlier may be worse: behavioural dysfunction and abnormal cerebral morphogenesis following perinatal frontal cortical lesions in the rat. *Neuropharmacology*, 39, 756-64.
- KOOPMANS, G. C., DEUMENS, R., BROOK, G., GERVER, J., HONIG, W. M., HAMERS, F. P. & JOOSTEN, E. A. 2007. Strain and locomotor speed affect over-ground locomotion in intact rats. *Physiology & behavior*, 92, 993-1001.
- LATT, M. D., LORD, S. R., MORRIS, J. G. & FUNG, V. S. 2009. Clinical and physiological assessments for elucidating falls risk in Parkinson's disease. *Movement disorders : official journal of the Movement Disorder Society*, 24, 1280-9.
- LIM, S. H., LEE, J. S., LEE, J. I., IM, S., KO, Y. J. & KIM, H. W. 2008. The quantitative assessment of functional impairment and its correlation to infarct volume in rats with transient middle cerebral artery occlusion. *Brain Research*, 1230, 303-9.
- MADETE, J. K., KLEIN, A., DUNNETT, S. B. & HOLT, C. A. 2011. Three-dimensional motion analysis of postural adjustments during over-ground locomotion in a rat model of Parkinson's disease. *Behavioural brain research*, 220, 119-25.
-

-
- MADETE, J. K., KLEIN, A., FULLER, A., TRUEMAN, R. C., ROSSER, A. E., DUNNETT, S. B. & HOLT, C. A. 2010. Challenges facing quantification of rat locomotion along beams of varying widths. *Proceedings of the Institution of Mechanical Engineers. Part H, Journal of engineering in medicine*, 224, 1257-65.
- MAHMUD, J., HOLT, C. A. & EVANS, S. L. 2010. An innovative application of a small-scale motion analysis technique to quantify human skin deformation in vivo. *Journal of biomechanics*, 43, 1002-6.
- MCCAIN, K. J., POLLO, F. E., BAUM, B. S., COLEMAN, S. C., BAKER, S. & SMITH, P. S. 2008. Locomotor treadmill training with partial body-weight support before overground gait in adults with acute stroke: a pilot study. *Archives of physical medicine and rehabilitation*, 89, 684-91.
- MCCAIN, K. J. & SMITH, P. S. 2007. Locomotor treadmill training with body-weight support prior to over-ground gait: promoting symmetrical gait in a subject with acute stroke. *Topics in stroke rehabilitation*, 14, 18-27.
- METZ, G. A., DIETZ, V., SCHWAB, M. E. & VAN DE MEENT, H. 1998. The effects of unilateral pyramidal tract section on hindlimb motor performance in the rat. *Behavioural brain research*, 96, 37-46.
- METZ, G. A., TSE, A., BALLERMANN, M., SMITH, L. K. & FOUAD, K. 2005. The unilateral 6-OHDA rat model of Parkinson's disease revisited: an electromyographic and behavioural analysis. *The European journal of neuroscience*, 22, 735-44.
- METZ, G. A. & WHISHAW, I. Q. 2002. Drug-induced rotation intensity in unilateral dopamine-depleted rats is not correlated with end point or qualitative measures of forelimb or hindlimb motor performance. *Neuroscience*, 111, 325-36.
- METZ, G. A. & WHISHAW, I. Q. 2009. The ladder rung walking task: a scoring system and its practical application. *J Vis Exp*.
- MIKLYAEVA, E. I., CASTANEDA, E. & WHISHAW, I. Q. 1994. Skilled reaching deficits in unilateral dopamine-depleted rats: impairments in movement and posture and compensatory adjustments. *The Journal of neuroscience : the official journal of the Society for Neuroscience*, 14, 7148-58.
- MIKLYAEVA, E. I., MARTENS, D. J. & WHISHAW, I. Q. 1995. Impairments and compensatory adjustments in spontaneous movement after unilateral dopamine depletion in rats. *Brain research*, 681, 23-40.
- MOREAU, F. & HILL, M. D. 2008. Transient ischaemic attack is an emergency: think about best current stroke prevention options. *International journal of stroke : official journal of the International Stroke Society*, 3, 251-3.

-
- MULROY, S., GRONLEY, J., WEISS, W., NEWSAM, C. & PERRY, J. 2003. Use of cluster analysis for gait pattern classification of patients in the early and late recovery phases following stroke. *Gait & posture*, 18, 114-25.
- MUYBRIDGE, E. 1899. *Animals in Motion*, London, Chapman and Hall
- NADEAU, S., GRAVEL, D., ARSENAULT, A. B. & BOURBONNAIS, D. 1999. Plantarflexor weakness as a limiting factor of gait speed in stroke subjects and the compensating role of hip flexors. *Clinical biomechanics*, 14, 125-35.
- NADEAU, S., GRAVEL, D., ARSENAULT, A. B., BOURBONNAIS, D. & GOYETTE, M. 1997. Dynamometric assessment of the plantarflexors in hemiparetic subjects: relations between muscular, gait and clinical parameters. *Scandinavian journal of rehabilitation medicine*, 29, 137-46.
- OZNUR OKEN A, GUNES YAVUZER, SALIH ERGOCEN, Z. REZAN YORGANCIOGLU A, HENK J. STAMD. 2008. Repeatability and variation of quantitative gait data in subgroups of patients with stroke. *Gait & Posture* 27 ,506–511
- OLNEY, S. J., GRIFFIN, M. P. & MCBRIDE, I. D. 1994. Temporal, kinematic, and kinetic variables related to gait speed in subjects with hemiplegia: a regression approach. *Physical therapy*, 74, 872-85.
- PAXINOS, G. 1995. *The rat nervous system*, Academic Press.
- PEIRIS, M. R., JONES, R. D., DAVIDSON, P. R. & BONES, P. J. 2006. Detecting behavioral microsleeps from EEG power spectra. *Conference proceedings : ... Annual International Conference of the IEEE Engineering in Medicine and Biology Society. IEEE Engineering in Medicine and Biology Society. Conference*, 1, 5723-6.
- PENNEY, J. B., JR. & YOUNG, A. B. 1983. Speculations on the functional anatomy of basal ganglia disorders. *Annual review of neuroscience*, 6, 73-94.
- PEPPE, A., CHIAVALON, C., PASQUALETTI, P., CROVATO, D. & CALTAGIRONE, C. 2007. Does gait analysis quantify motor rehabilitation efficacy in Parkinson's disease patients? *Gait Posture*, 26, 452-62.
- PERRY, J. 1992. *Gait Analysis Normal and pathological function*, Canada, Harry C. Benson.
- PINNA, A., PONTIS, S., BORSINI, F. & MORELLI, M. 2007. Adenosine A2A receptor antagonists improve deficits in initiation of movement and sensory motor integration in the unilateral 6-hydroxydopamine rat model of Parkinson's disease. *Synapse*, 61, 606-14.
- PLOTNIK, M., GILADI, N. & HAUSDORFF, J. M. 2008. Bilateral coordination of walking and freezing of gait in Parkinson's disease. *The European journal of neuroscience*, 27, 1999-2006.

-
- PLOTNIK, M. & HAUSDORFF, J. M. 2008. The role of gait rhythmicity and bilateral coordination of stepping in the pathophysiology of freezing of gait in Parkinson's disease. *Movement disorders : official journal of the Movement Disorder Society*, 23 Suppl 2, S444-50.
- ROCHESTER L FAU - HETHERINGTON, V., HETHERINGTON V FAU - JONES, D., JONES D FAU - NIEUWBOER, A., NIEUWBOER A FAU - WILLEMS, A.-M., WILLEMS AM FAU - KWAKKEL, G., KWAKKEL G FAU - VAN WEGEN, E. & VAN WEGEN, E. 2004. Attending to the task: interference effects of functional tasks on walking in Parkinson's disease and the roles of cognition, depression, fatigue, and balance.
- ROERDINK, M. & BEEK, P. J. 2011. Understanding inconsistent step-length asymmetries across hemiplegic stroke patients: impairments and compensatory gait. *Neurorehabilitation and neural repair*, 25, 253-8.
- SCHAAFSMA, J. D., GILADI, N., BALASH, Y., BARTELS, A. L., GUREVICH, T. & HAUSDORFF, J. M. 2003. Gait dynamics in Parkinson's disease: relationship to Parkinsonian features, falls and response to levodopa. *Journal of the neurological sciences*, 212, 47-53.
- SCHALLERT, T. 2006. Behavioral tests for preclinical intervention assessment. *NeuroRx : the journal of the American Society for Experimental NeuroTherapeutics*, 3, 497-504.
- SCHALLERT, T., FLEMING, S. M. & WOODLEE, M. T. 2003. Should the injured and intact hemispheres be treated differently during the early phases of physical restorative therapy in experimental stroke or parkinsonism? *Physical medicine and rehabilitation clinics of North America*, 14, S27-46.
- SCHALLERT, T. & HALL, S. 1988. 'Disengage' sensorimotor deficit following apparent recovery from unilateral dopamine depletion. *Behavioural brain research*, 30, 15-24.
- SEIDEL, H., BLUTHNER, R. & HINZ, B. 2001. Application of finite-element models to predict forces acting on the lumbar spine during whole-body vibration. *Clinical biomechanics*, 16 Suppl 1, S57-63.
- SHEN, H. & WANG, Y. 2010. Correlation of locomotor activity and brain infarction in rats with transient focal ischemia. *Journal of neuroscience methods*, 186, 150-4.
- SHUMWAY-COOK, A. & WOOLLACOTT, M. 1995. *Motor Control-Theory an practical applications*, Maryland, Williams and Wilkins.
- SIMJEE, S. U., JAWED, H., QUADRI, J. & SAEED, S. A. 2007. Quantitative gait analysis as a method to assess mechanical hyperalgesia modulated by disease-modifying antirheumatoid drugs in the adjuvant-induced arthritic rat. *Arthritis research & therapy*, 9, R91.

-
- SOFUWA, O., NIEUWBOER, A., DESLOOVERE, K., WILLEMS, A. M., CHAVRET, F. & JONKERS, I. 2005. Quantitative gait analysis in Parkinson's disease: comparison with a healthy control group. *Archives of physical medicine and rehabilitation*, 86, 1007-13.
- TAKEDA, R., TADANO, S., NATORIGAWA, A., TODOH, M. & YOSHINARI, S. 2009. Gait posture estimation using wearable acceleration and gyro sensors. *Journal of biomechanics*, 42, 2486-94.
- TOMAC, A. C., AGULNICK, A. D., HAUGHEY, N., CHANG, C. F., ZHANG, Y., BACKMAN, C., MORALES, M., MATTSON, M. P., WANG, Y., WESTPHAL, H. & HOFFER, B. J. 2002. Effects of cerebral ischemia in mice deficient in Persephin. *Proceedings of the National Academy of Sciences of the United States of America*, 99, 9521-6.
- UNGERSTEDT, U. 1968. 6-Hydroxy-dopamine induced degeneration of central monoamine neurons. *European journal of pharmacology*, 5, 107-10.
- UNGERSTEDT U FAU - ARBUTHNOTT, G. W. & ARBUTHNOTT, G. W. Quantitative recording of rotational behavior in rats after 6-hydroxy-dopamine lesions of the nigrostriatal dopamine system.database, 1968.
- VAN DER BURG, J. C., VAN WEGEN, E. E., RIETBERG, M. B., KWAKKEL, G. & VAN DIEEN, J. H. 2006. Postural control of the trunk during unstable sitting in Parkinson's disease. *Parkinsonism & related disorders*, 12, 492-8.
- VAN DER STAAY, F. J., AUGSTEIN, K. H. & HORVATH, E. 1996. Sensorimotor impairments in Wistar Kyoto rats with cerebral infarction, induced by unilateral occlusion of the middle cerebral artery: recovery of function. *Brain research*, 715, 180-8.
- VRINTEN, D. H. & HAMERS, F. F. 2003. 'CatWalk' automated quantitative gait analysis as a novel method to assess mechanical allodynia in the rat; a comparison with von Frey testing. *Pain*, 102, 203-9.
- WANG, Y., BONTEMPI, B., HONG, S. M., MEHTA, K., WEINSTEIN, P. R., ABRAMS, G. M. & LIU, J. 2008a. A comprehensive analysis of gait impairment after experimental stroke and the therapeutic effect of environmental enrichment in rats. *Journal of cerebral blood flow and metabolism : official journal of the International Society of Cerebral Blood Flow and Metabolism*, 28, 1936-50.
- WANG, Y., BONTEMPI, B., HONG, S. M., MEHTA, K., WEINSTEIN, P. R., ABRAMS, G. M. & LIU, J. 2008b. A comprehensive analysis of gait impairment after experimental stroke and the therapeutic effect of environmental enrichment in rats. *J Cereb Blood Flow Metab*, 28, 1936-50.
- WEGENER, S., WEBER, R., RAMOS-CABRER, P., UHLENKUEKEN, U., WIEDERMANN, D., KANDAL, K., VILLRINGER, A. & HOEHN, M. 2005. Subcortical lesions after transient thread occlusion in the rat: T2-weighted magnetic resonance imaging findings

-
- without corresponding sensorimotor deficits. *Journal of magnetic resonance imaging : JMRI*, 21, 340-6.
- WHATLING, G. 2009. *A contribution to the clinical validation of a generic method for the classification of osteoarthritic and non-pathological knee function / Gemma Marie Whatling*. PhD, Cardiff University.
- WHATLING, G. M., DABKE, H. V., HOLT, C. A., JONES, L., MADETE, J., ALDERMAN, P. M. & ROBERTS, P. 2008. Objective functional assessment of total hip arthroplasty following two common surgical approaches: the posterior and direct lateral approaches. *Proceedings of the Institution of Mechanical Engineers. Part H, Journal of engineering in medicine*, 222, 897-905.
- WHATLING, G. M. & HOLT, C. A. 2010. Does the choice of stair gait cycle affect resulting knee joint kinematics and moments? *Proceedings of the Institution of Mechanical Engineers. Part H, Journal of engineering in medicine*, 224, 1085-93.
- WHISHAW, I. Q. & DUNNETT, S. B. 1985. Dopamine depletion, stimulation or blockade in the rat disrupts spatial navigation and locomotion dependent upon beacon or distal cues. *Behav Brain Res*, 18, 11-29.
- WHISHAW, I. Q. & KOLB, B. 2005. *The Behavior of the laboratory rat - a handbook with tests*, Oxford university press.
- WHISHAW, I. Q., LI, K., WHISHAW, P. A., GORNY, B. & METZ, G. A. 2003a. Distinct forelimb and hind limb stepping impairments in unilateral dopamine-depleted rats: use of the rotorod as a method for the qualitative analysis of skilled walking. *J Neurosci Methods*, 126, 13-23.
- WHISHAW, I. Q., PELLIS, S. M. & GORNY, B. P. 1992. Skilled reaching in rats and humans: evidence for parallel development or homology. *Behav Brain Res*, 47, 59-70.
- WHISHAW, I. Q., PIECHARKA, D. M. & DREVER, F. R. 2003b. Complete and partial lesions of the pyramidal tract in the rat affect qualitative measures of skilled movements: impairment in fixations as a model for clumsy behavior. *Neural plasticity*, 10, 77-92.
- WHISHAW, I. Q., SUCHOWERSKY, O., DAVIS, L., SARNA, J., METZ, G. A. & PELLIS, S. M. 2002. Impairment of pronation, supination, and body co-ordination in reach-to-grasp tasks in human Parkinson's disease (PD) reveals homology to deficits in animal models. *Behavioural brain research*, 133, 165-76.
- WINTER, D. A. 1995. Balance control: an overriding challenge in standing and walking. *Gait & Posture*, 3, 170-170.
- WOLFE, C. 1996. *The Burden of Stroke In Stroke Services and Research* The Stroke Association.

WOOLLACOTT, M. & SHUMWAY-COOK, A. 2002. Attention and the control of posture and gait: a review of an emerging area of research. *Gait Posture*, 16, 1-14.

YAVUZER, G., OKEN, O., ELHAN, A. & STAM, H. J. 2008. Repeatability of lower limb three-dimensional kinematics in patients with stroke. *Gait & posture*, 27, 31-5.

A. APPENDICES

A. List of publications and conferences

Journals

Madete JK, Klein A, Fuller A, Trueman RC, Rosser AE, Dunnett SB, Holt CA, Challenges facing quantification of rat locomotion along beams of varying widths. *Proc Inst Mech Eng H*. 2010 Nov;224(11):1257-65

Madete JK, Klein A, Dunnett SB, Holt CA.; Three-dimensional motion analysis of postural adjustments during over-ground locomotion in a rat model of Parkinson's disease; **Behav Brain Res**. 2011 Jun 20;220(1):119-25. Epub 2011 Feb 3

Whatling GM, Dabke HV, Holt CA, Jones L, **Madete J**, Alderman PM, Roberts P Objective functional assessment of total hip arthroplasty following two common surgical approaches: the posterior and direct lateral approaches.

Conferences

Madete J.K. , Holt C.A., Ben Hammada A, Dunnett S. B. And Rosser A.E. **Quantifying voluntary motion of facial expressions**; Cardiff institute of tissue engineering and repair, 7th annual meeting, The hill education and conference centre, abergavenny, Wednesday 3rd september & thursday 4th september 2008.

Madete J.K. ,Holt C.A., White A., Sprinz P., Dunnett S. B. And Rosser A.E. , **Animal Model Motion Capture During Locomotion**; Cardiff institute of tissue engineering and repair, 8th annual meeting, The lecture theatre, optometry building, maindy road, Wednesday 2nd september 2009.

Madete J.K. , Klein A. , Dunnett S. B., Holt C.A; **Quantifying Locomotion of an Animal Model of Parkinson's disease Along a Graduated, Narrow and Wide Beam**,. Cardiff institute of tissue engineering and repair, 9th annual meeting, And Arthritis research UK biomechanics and bioengineering centre, 1st annual meeting, Eastwood Park, falfield, Gloucestershire,

Thursday 16th September & Friday 17th September 2010.

GM Whatling, CA Holt, L Jones, JK Madete, H Dabke, PM Alderman, P Roberts; **Investigating the effects of surgical approach on total hip arthroplasty recovery using 3D gait analysis;** 8th International Symposium on Computer Methods in Biomechanics and Biomedical Engineering CMBBE 2008 Sheraton Hotel and SPA, Porto, Portugal, 27th February-1st March 2008.

Madete JK, A. Klein, S.B. Dunnett and C. A. Holt; **Postural adjustments of an animal model of Parkinson's disease during over-ground locomotion;** 9th International Symposium on Computer Methods in Biomechanics and Biomedical Engineering CMBBE 2010; The Westin hotel, Valencia.








Madete J.K. , Fuller A., Klein A. , Dunnett S. B., Holt C.A.: **Quantifying Rat Temporal Parameters and Body Posture While they Walk Along Wide, Narrow and Graduated Beams;** European society of Biomechanics 2010: 5 - 8 July 2010, Edinburgh UK.











Madete J.K.¹, Holt C.A. , White A. , Sprinz P. , Dunnett S . and Rosser A.: **3D Motion Capture of Parkinson's and Huntington's Disease Rat Models ;** 10th International Symposium; 3D analysis of human movement, Santpoort/Amsterdam. 29th – 31st October 2008.

June Madete, Cathy Holt., Andrew Lawrence, Assia Ben- Hammada , Steve Dunnett. And Anne Rosser; **Facial mimicking using 3d motion analysis capture compared to qualitative data:** congress of the international society of biomechanics, cape town, south africa from 5th to 9th July 2009.

B. Data collection protocol

Equipment check list

Item		Check
Calibration kit (110) and (300)		
Makers		
Double sided tape		
Scissors		
Laptop		
Mouse		
Laptop Power cable		

<p>PCI card</p>					
<p>Qualisys MCU and tripods</p>					
<p>Qualisys Power cable</p>					
<p>Data Cable - Blue Data cable -yellow</p>					
<p>Video Camera</p>					
<p>Video Power cable</p>					
<p>Video - power adapter,</p>					
<p>Video - USB connectors</p>					
<p>Tape measure for mapping</p>					
<p>Protractor for mapping</p>					

Animal protocol

Apparatus

- ❖ 7 Qualisys cameras,
- ❖ Camera power cables
- ❖ Camera data connecting cables,
- ❖ Camera tripods
- ❖ Two video cameras and power cables
- ❖ USB cables for video cameras
- ❖ video camera tripods
- ❖ At least twenty 5mm makers which include - four makers placed on a cable tie
- ❖ Cable tie clippers
- ❖ 300 mm calibration frame and wand
- ❖ Wig tape (at least half a *roll*)
- ❖ Scissors
- ❖ Tape-measure to set up the cameras
- ❖ Three elevated beams, narrow (NR), graduated (GR) and wide (WD). (the NR and GR beams were not used for the stroke motion capture).

Procedure

1. Set up the seven cameras as shown in Figure 8-1.
2. Check that the cable connection is correct, that is the blue data cables are connected from previous camera to next camera and the computer yellow data cable is in the data port of the master cameras (camera 1).
3. Turn on the computer and check that all the cameras are accurately identified.
4. Ensure that all the cables are tied up and stuck with masking tape to reduce trip hazards
5. Using the calibration frame as a guide, check that all the cameras are in the correct height and angle for filming the volume surrounding the beam.
6. Calibrate the system using the 300 mm calibration kit (placement shown in Figure 8-1) checking that the workspace tools are as follows:
 - The camera linearization files are present and accurate.
 - Videos are connected and checked on the *video devices* page
 - Maximum maker size is accurate
 - Maker number is set at 1 plus the actual number of markers present (20)
 - Calibration frame type and size are accurate. (300.1mm)
 - Bounding parameters are within the required limit
 - Tracking parameters are set at the required limit (maximum residual between 2 and 5 and the prediction error is less than 25mm)
 - Frequency is set at 60HZ
7. After calibration, place 8 makers 5 mm on the underside of the beam as shown in Figure 8-2 using the wig tape.

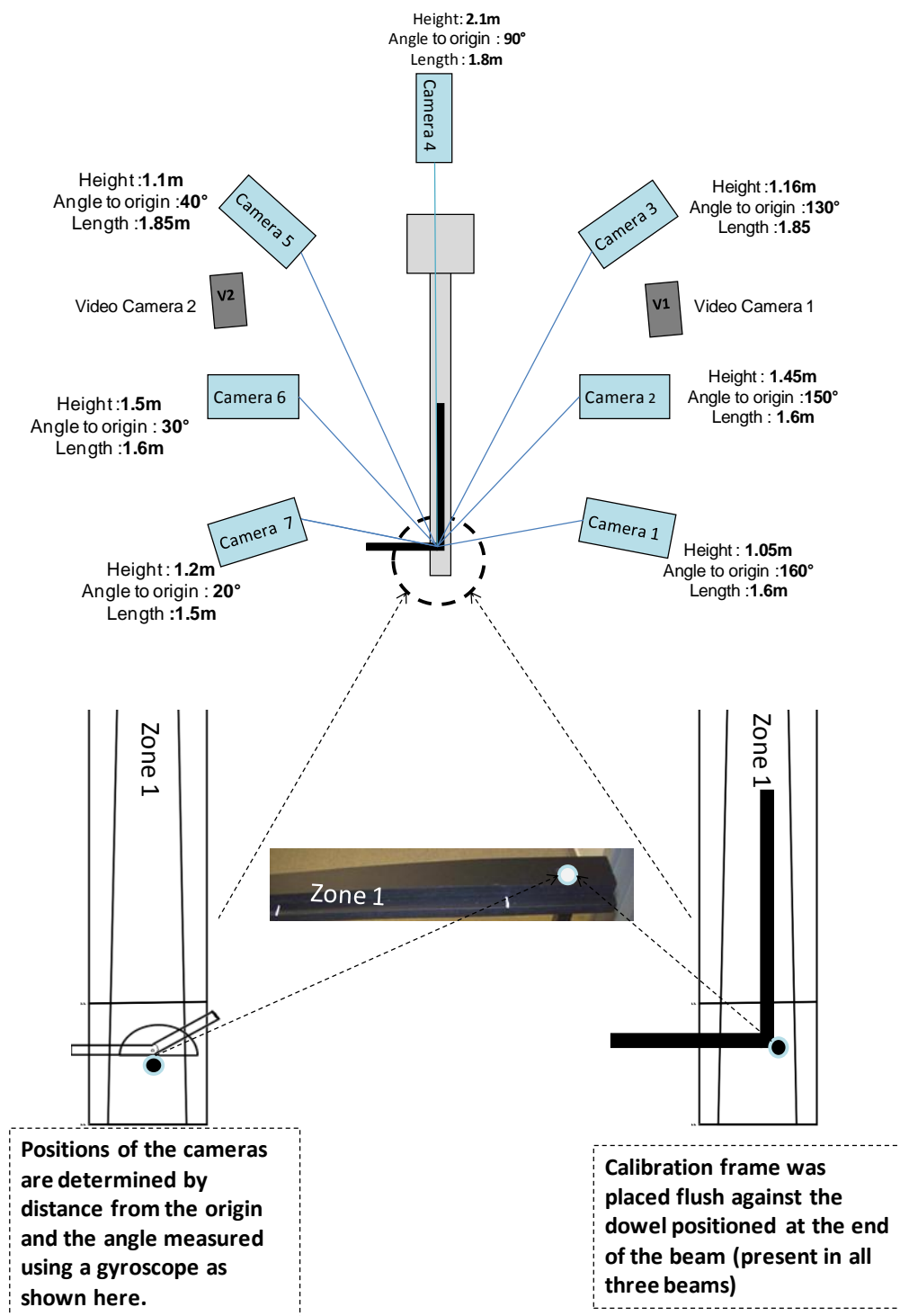


Figure 8-1: Camera map and calibration frame position



Figure 8-2: maker placement on the beam

8. Make sure you have the *data collection form* illustrated below for recording the trial and adding comments during the trial printed and in-front of you. Record the rats details i.e., condition e.g., stroke or PD; number e.g., ASUB1; weight and age.
9. A licensed member of staff from the brain repair group then brings in the rats and they are acclimatised on the beam and are then ready for maker placement.
10. The makers are placed as shown in figure Figure 8-3 on head, mid spine and rear spine, four points of the appendicular aspects of the rat skeletal, On the 4 paws using cable ties (Figure 8-4).

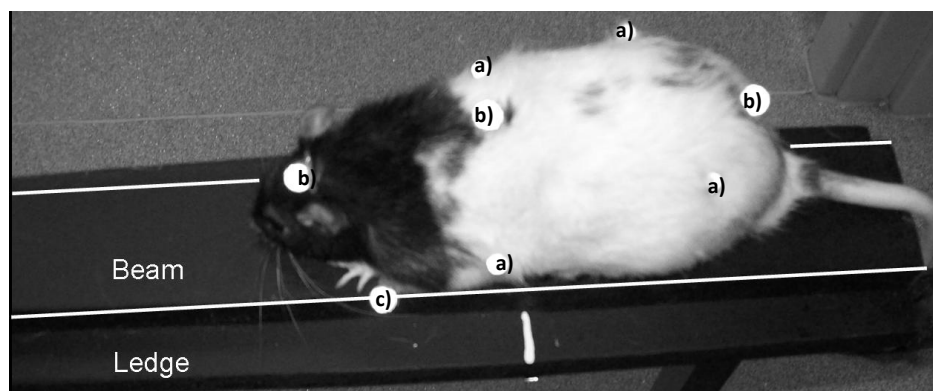


Figure 8-3 markers attached to the rats body a) appendicular aspects of the rats skeletal , b) Head, mid-spine and back- spine and c) on the 4 paws using cable ties



Figure 8-4 Cable-tie and maker configuration

11. Data collection motion capture begins by placing the rat on the end of the beam without a box and engaging the record button on the QTM software.
12. Motion capture is complete when data from three good walks from each animal on each of the three beams, NR, WD and GR is acquired. A good walk is classified as a walk along the beam from beginning to the end of the beam without stopping and where all the markers are visible.
13. Trial ends and the files are saved and checked that they are in the correct files for post-analysis

Human protocol

Apparatus

- ❖ 12 Qualisys cameras,
- ❖ Camera power cables
- ❖ Camera data connecting cables,
- ❖ Qualisys camera tripods
- ❖ Two video cameras and power cables
- ❖ USB cables for video cameras
- ❖ video camera tripods
- ❖ markers
 - At least twenty eight, 25mm makers
 - One marker cluster consisting of three 5mm markers attached to a head band.
- ❖ 710 mm calibration frame and wand
- ❖ Wig tape (at least half a *roll*)
- ❖ Scissors
- ❖ Tape-measure to set up the cameras
- ❖ 2 Path outlining ropes 8m long (this ropes are used to define the three walkways as wide(WDw), narrow NRw and graduated (GRw)).
 - The width of the walkway was specified as three times the base of support of an averaged human subject therefore the walkway approximate width of 54cm.
 - The length of the walkway was based on acquiring five complete gait cycles during testing. The average stride length of a human subject is approximately 1.5m in healthy humans; the chosen length of the walkway was 8m.
 - The WDw had the same width as the wide section of the GRw; and the NRw as the narrow end of the GR walkway.

Procedure

1. Set up the 12 cameras as shown in Figure 2-6.
2. Check that the cable connection is correct, that is the blue data cables are connected from previous camera to next camera and the computer yellow data cable is in the data port of the master cameras (camera 1).
3. Turn on the computer and check that all the cameras are accurately identified.
4. Ensure that all the cables are tied up and stuck with masking tape to reduce trip hazards
5. Using the calibration frame as a guide, check that all the cameras are in the correct height and angle for filming the volume surrounding the beam.

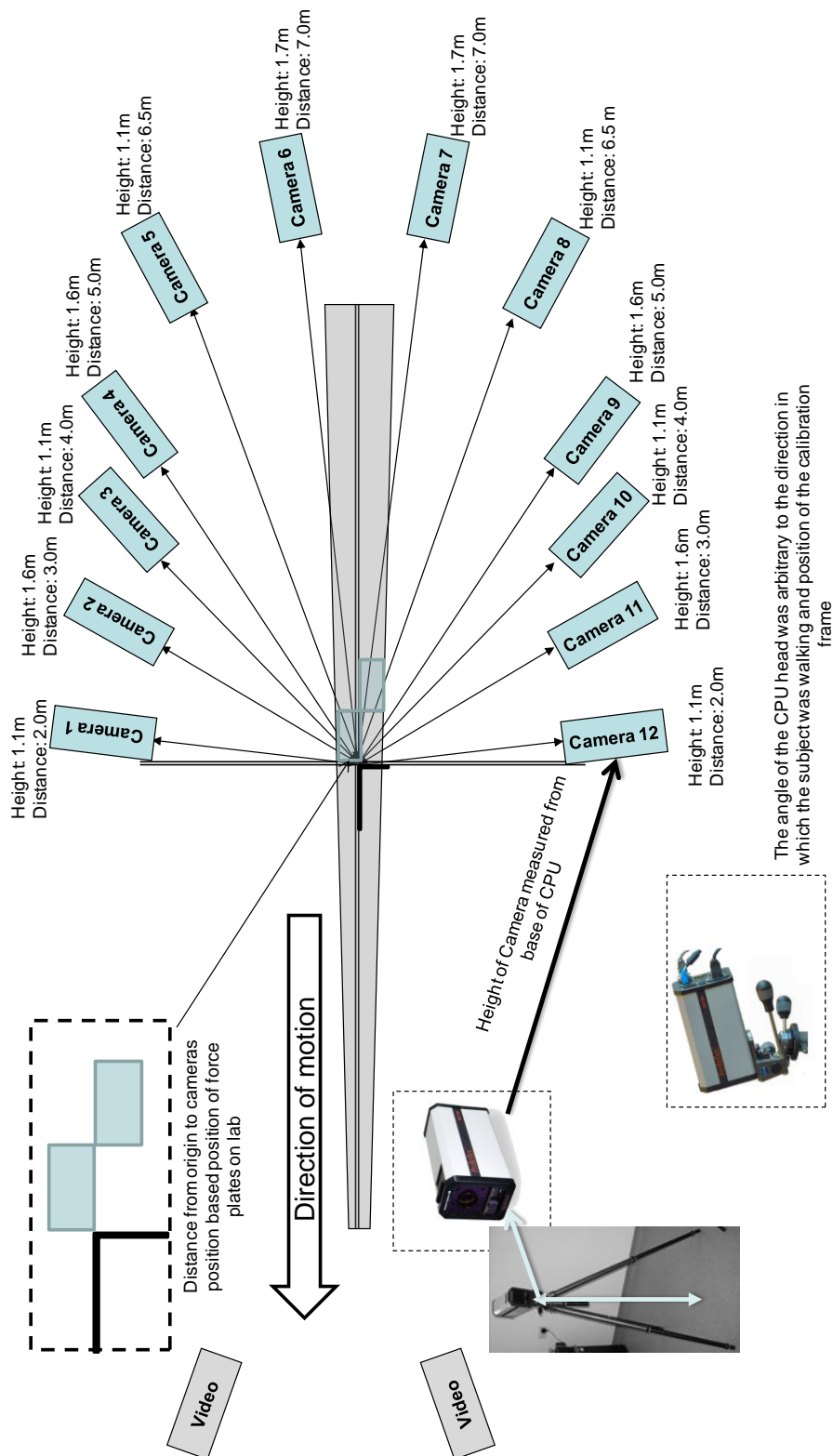


Figure 8-5: Camera map and calibration frame position

6. Calibrate the system using the 700 mm calibration kit (placement shown is Figure 8-5) checking that the workspace tools are as follows:
 - The camera linearization files are present and accurate.
 - Videos are connected and checked on the *video devices* page
 - Maximum marker size is accurate
 - Marker number is set at 1 plus the actual number of markers present
 - Calibration frame type and size are accurate. (700 mm)
 - Bounding parameters are within the required limit
 - Tracking parameters are set at the required limit (maximum residual between 2 and 5 and the prediction error is less than 1000mm).
 - Frequency is set at 60HZ
7. After calibration, the walkways are defined and 8 markers placed on the outline of the walkway using the wig tape.
8. Make sure you have the data collection form for recording the trial and adding comments during the trial printed and in-front of you.
9. Record the subjects details taking the current weight and height
10. The makers are placed as shown in Figure 8-6

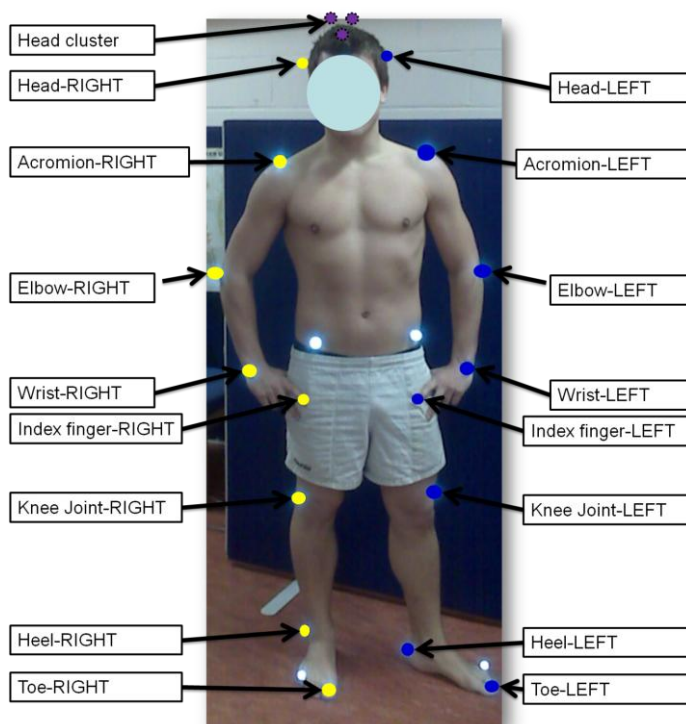


Figure 8-6: Anterior maker placements

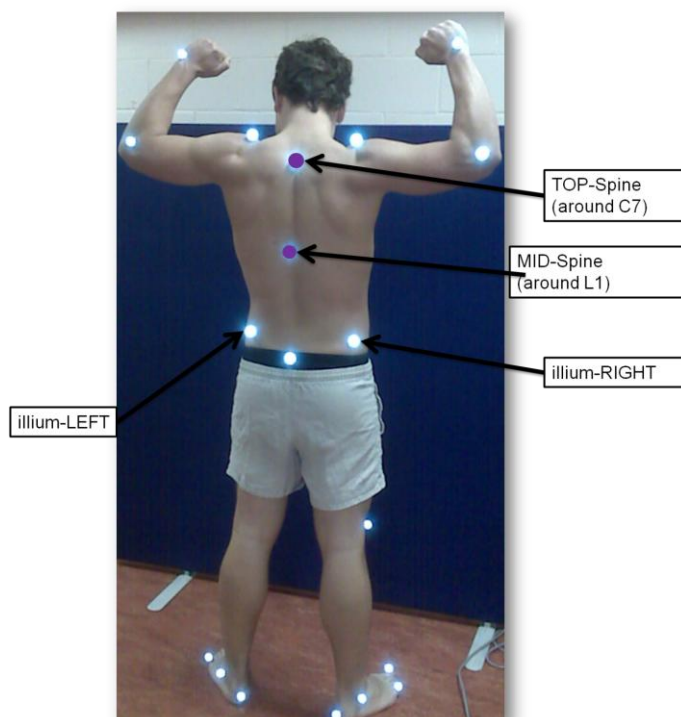


Figure 8-7 Posterior marker placement

11. Data collection motion capture begins as the subject walks from the start of the 8m walkway and engaging the record button on the QTM software .
12. Motion capture is complete when data from three good walks from each subject on each of the three walkways, NRw, WDw and GRw, are acquired. A good walk is classified as a walk:
 - a. along the walkway from beginning to the end without stopping
 - b. where the markers did not drop off.
 - c. where the tracking from 2D to 3D shows all markers for the entire length of the walkway with a minimum number of unidentified markers

Data collection form**ASUB**

Condition

Weight

Age

Comment:

Trial	Track	Comment
--------------	--------------	----------------

1

2

3

4

5

6

7

8

C. Data processing

C++ program

```
//=====
// Name      : TEP.cpp
// Author    : June Madete
//=====
#include <iostream>
#include <fstream>
#include <vector>
#include <stdlib.h>
#include <math.h>
#include "include/LEG_MOVEMENTS.h"

using namespace std;

void explode(const string& str, vector<string>& tokens, const string&
delimiters = ""){
    // Skip delimiters at beginning.
    string::size_type lastPos =
str.find_first_not_of(delimiters, 0);
        // Find first "non-delimiter".
        string::size_type pos = str.find_first_of(delimiters,
lastPos);

        while (string::npos != lastPos){
            // Found a token, add it to the vector.
            tokens.push_back(str.substr(lastPos, pos - lastPos));

                                //string::size_type temp =
lastPos ;

                //pos = lastPos ;
                // Skip delimiters. Note the "not_of"
                //lastPos = pos ;

                lastPos = str.find_first_not_of(delimiters,
pos);

                // Find next "non-delimiter"
                pos = str.find_first_of(delimiters, lastPos);
            }
        }
}
```

```

int main() {
    string file_name ;
    cout << "Please enter name of csv file to read data
from" << endl;
    cin >> file_name ; //get filename from user

    ifstream fin(file_name.c_str()); //declare input
filestream
    if(!fin){ //check if filestream is valid
        cerr << "Invalid file" << endl;
        exit(0);
    }
    vector <double> arr_1 ; //declare array to hold data for
leg movement
    vector <double> arr_2 ;
    vector <double> arr_3 ;
    vector <double> arr_4 ;

    vector <string> arr_rstr ;
    string row ;
    row.erase(row.begin(), row.end());
    while(getline(fin, row)){
        cout << "Input: " << row << "\n"; //show
input on screen

        arr_rstr.clear();
        explode(row,arr_rstr,",");

        arr_1.push_back(atof(arr_rstr.at(0).c_str()) );
        arr_2.push_back(atof(arr_rstr.at(1).c_str()) );
        arr_3.push_back(atof(arr_rstr.at(2).c_str()) );
        arr_4.push_back(atof(arr_rstr.at(3).c_str()) );

    }
    fin.close();

}

//=====
=====

```

```

    /// Write Results to File

    //Calc2 results
    //Write Title Row to file for col 2
    fout << "LFoot_a SWT" << ", "
                                                    <<
"LFoot_a SPL" << ", "
                                                    <<
"LFoot_a SRL" << endl;
    //Output Col 2
    for(unsigned int i=0; i < calc2.arr_dx().size(); ++i){
    fout << calc2.arr_dx().at(i) << ", "
        << calc2.arr_dy().at(i) << ", "
        << sqrt(pow(calc2.arr_dx().at(i),2) +
pow(calc2.arr_dy().at(i),2))
        << endl;
    }
//=====
=====
    //Calc5 results
    //Write Title Row to file for col 5
    fout << "RFoot_b SWT" << ", "
                                                    <<
"RFoot_b SPL" << ", "
                                                    <<
"RFoot_b SRL" << endl;
    //Output Col 5
    for(unsigned int i=0; i < calc5.arr_dx().size(); ++i){
    fout << calc5.arr_dx().at(i) << ", "
        << calc5.arr_dy().at(i) << ", "
        << sqrt(pow(calc5.arr_dx().at(i),2) +
pow(calc5.arr_dy().at(i),2))
        << endl;
    }

```

```
//=====
=====
//Calc6 results
//Write Title Row to file for col 6
fout << "LFoot_b SWT" << ","
<< "LFoot_b SPL" << ","
<< "LFoot_b SRL" << endl;
//Output Col 6
for(unsigned int i=0; i < calc6.arr_dx().size(); ++i){
fout << calc6.arr_dx().at(i) << ","
<< calc6.arr_dy().at(i) << ","
<< sqrt(pow(calc6.arr_dx().at(i),2) +
pow(calc6.arr_dy().at(i),2))
<< endl;
}
//=====
=====
fout.close();
return 0;
}
```

Leg Movements Function

```
* LEG_MOVEMENTS.cpp
*
* Created on: 25-Apr-2009
*   Author: fabio
*/

#include "include/LEG_MOVEMENTS.h"

LEG_MOVEMENTS::LEG_MOVEMENTS(const vector<double> &arr_data){
    _max_dx = 0; _max_dy = 0 ;
    double s, ly;
    bool chan = false ;
    unsigned int i , l ;
    l = 0 ;
    ly = arr_data.at(0);
    for(i=0; i < arr_data.size()-1; ++i){

        s = (arr_data.at(i+1) - arr_data.at(i)) ;
        if(fabs(s) > 0.9999999999 && chan == false){
            chan = true ;
            _arr_dx.push_back(i - l);
            _arr_dy.push_back(arr_data.at(i)- ly) ;
            l = i ;
            ly = arr_data.at(i);
        }else if (fabs(s) < 0.9999999999 && chan == true){
            chan = false ;
            _arr_dx.push_back(i - l);
            _arr_dy.push_back(arr_data.at(i)- ly) ;
            l = i ;
            ly = arr_data.at(i);
        }
    }
}
```

```
}
    }
    i = arr_data.size()-1;
    _arr_dx.push_back(i - l);
    _arr_dy.push_back(arr_data.at(i) - ly);

    //Find max dx
    _max_dx = _arr_dx.at(0);
    for(i=0; i < _arr_dx.size(); ++i){
        if(_max_dx < _arr_dx.at(i)) _max_dx = _arr_dx.at(i);
    }
    //Find max dy
    _max_dy = _arr_dy.at(0);
    for(i=0; i < _arr_dy.size(); ++i){
        if(_max_dy < _arr_dy.at(i)) _max_dy = _arr_dy.at(i);
    }
}

const vector <unsigned int>& LEG_MOVEMENTS::arr_dx() const{
    return _arr_dx;
}

const vector <double>& LEG_MOVEMENTS::arr_dy() const{
    return _arr_dy;
}

unsigned int LEG_MOVEMENTS::max_dx() const{
    return _max_dx;
}

double LEG_MOVEMENTS::max_dy() const{
    return _max_dy;
}
```

Matlab program for re-sampling 6-DOF data

```

%June Madete
%17th June 2010
%RESAMPLING 6DOF data from matlab for one gait cycle for three gait cycles
%NR, WD and GR
clc
clear
%%%%%%%%%%%%%%%%%%%%%%%%%%%%%%%%%%%%%%%%%%%%%%%%%%%%%%%%%%%%%%%%%%%%%%%%
%%%%%%%%
% Path where all the data is stored:
p=path;
path(p,'D:\PhD 2010\Brain repair group Studies\Animal\stroke\New 6DOF\pCN')

%%%%%%%%%%%%%%%%%%%%%%%%%%%%%%%%%%%%%%%%%%%%%%%%%%%%%%%%%%%%%%%%%%%%%%%%
%%%%%%%%

%%%%%%%%%%%%%%%%%%%%%%%%%%%%%%%%%%%%%%%%%%%%%%%%%%%%%%%%%%%%%%%%%%%%%%%%
%%%%%%%%
% Reading in the file containing the input variables in tabular form
% where the rows are observations (people) and the columns are variables:
%%%%%%%%%%%%%%%%%%%%%%%%%%%%%%%%%%%%%%%%%%%%%%%%%%%%%%%%%%%%%%%%%%%%%%%%
%%%%%%%%

%insert the filename
Filename = ('3.xlsx');

%data from (excell sheet), (file name), (sheet number )
Cycle1 = xlsread(Filename,1);
Cycle2 = xlsread(Filename,2);

[m,n]=size(Cycle1);
[o,p]=size(Cycle2);

%RESAMPLING

Cycle_100_1=RESAMPLE(Cycle1,100,m);
Cycle_100_2=RESAMPLE(Cycle2,100,o);

%change the order of the rows and columns

Cycle_1= Cycle_100_1';
Cycle_2= Cycle_100_2';

Filename1=[Filename 'hundred']

eval(['save ' Filename1 ' Cycle_1 -ascii -tabs',' Cycle_2 -ascii -tabs'])

```

Procedure for 6DOF data acquisition

The following steps were taken to acquire the 6DOF body: of the rat whilst waking along the elevated beam on QTM version 2.0..

1. The four markers on two hips, and two shoulders were selected Figure 8-8. They define the rigid body.

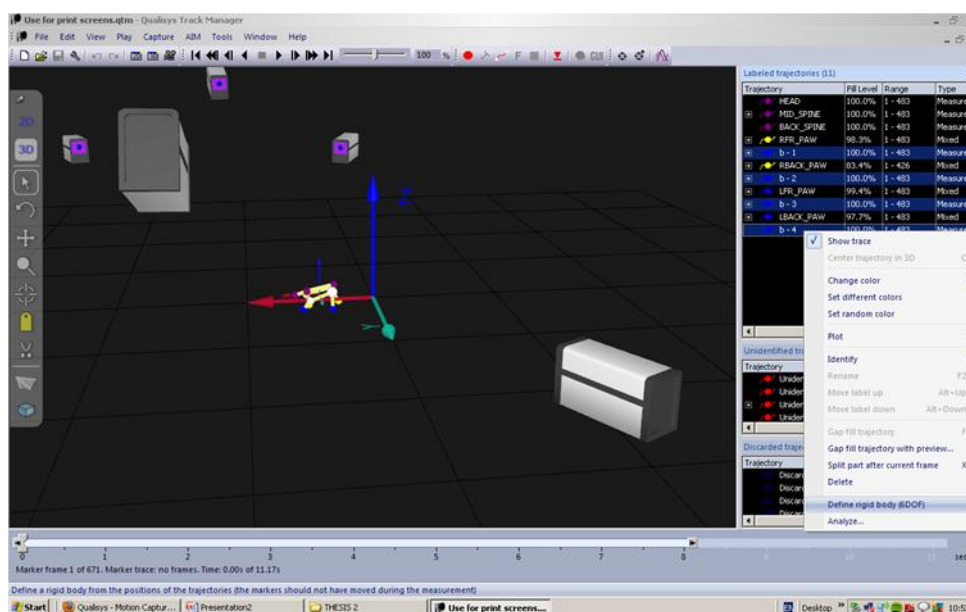


Figure 8-8: Export to 6DOF

2. A dialogue box appears (Figure 8-9) insert the new name of the rigid body A new 6DOF body is created.

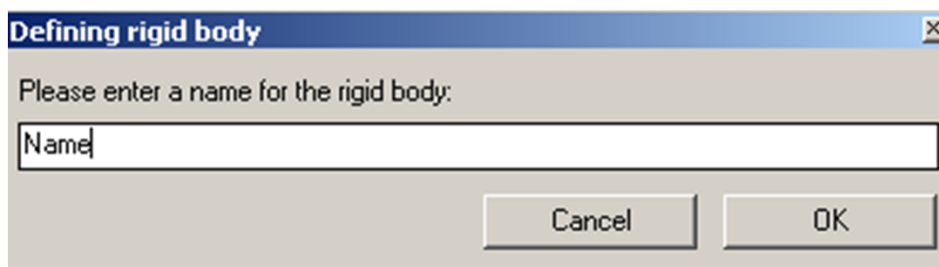


Figure 8-9: Warkspace define

3. Any previously defined rigid bodies were deleted to avoid overlap with the new one.

4. The rigid bodies' LRS was then translated to its geometric centre (Figure 8-10).

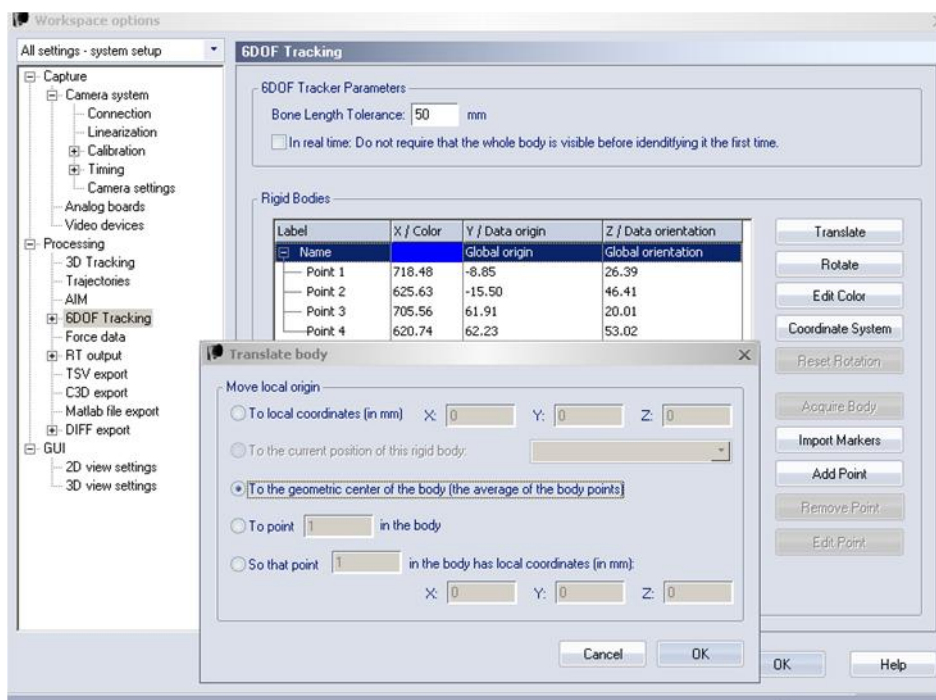


Figure 8-10: Workspace translate

5. The 6DOF data was in the form of kinematic waveforms produced of the rotation angles, *roll pitch and yaw* are shown in Figure 8-11.

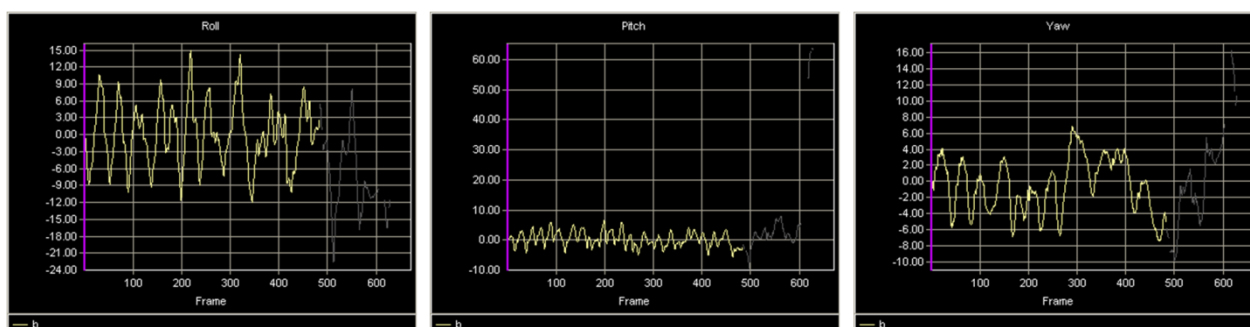


Figure 8-11: QTM export 6DOF

PD animal models limb and tail position**Table 8-1: Limb and tail Positions on the GR beam**

No.	Limb	Position of Limb (beam =1 or ledge=0)			Tail Position (Left=0 or right and straight =1)		
		Z1	Z2	Z3	Z1	Z2	Z3
1	RBL	1	1	1	L	L	L
	RFL	1	1	1			
	LBL	1	1	0			
	LFL	1	1	1/0			
2	RBL	1	1	1	S	L	R
	RFL	1	1	1			
	LBL	1	1	1			
	LFL	1	1	1			
3	RBL	1	1	0	L	L	R
	RFL	1	1	1/0			
	LBL	1	0	1			
	LFL	1	1	0			
4	RBL	1	1	1	S	L	L
	RFL	1	1	1			
	LBL	1	1	1			
	LFL	1	1	1			
5	RBL	1	1	1	L	L	L
	RFL	1	1	1			
	LBL	1	1/0	1			
	LFL	1	1	1			
6	RBL	1	1	1	S	S	R
	RFL	1	1	1			
	LBL	1	1	1			
	LFL	1	1	1			
7	RBL	1	1	1	R	R	R
	RFL	1	1	1			
	LBL	1	1	0			
	LFL	1	1	1			
8	RBL	1	1	0	SR	R	R
	RFL	1	1	0			
	LBL	1	0	0			
	LFL	1	1	1			
9	RBL	1	1	1	R	R	R
	RFL	1	1	1			
	LBL	1	1	1/0			
	LFL	1	1	0			
10	RBL	1	1	1/0	S	S	R
	RFL	1	1	1			
	LBL	1	1	1			
	LFL	1	1	1			

Table 8-2: Limb and tail position on the NR beam

No.	Limb	Position of Limb (beam =1 or ledge=0)			Tail Position (Left=0 or right and straight =1)		
		Z1	Z2	Z3	Z1	Z2	Z3
1	RBL	0	0	0	R	R	R
	RFL	0	0	1			
	LBL	1	1	0			
	LFL	-1	1	0			
2	RBL	1	1	1	L	L	L
	RFL	0	1	1			
	LBL	0	0	0			
	LFL	1	0/1	0			
3	RBL	0	0	0	R	R	R
	RFL	0	1/0	0			
	LBL	0	0	0			
	LFL	1	1	0			
4	RBL	1	1	1	L	L	L
	RFL	1	1	1			
	LBL	0	0	0			
	LFL	0	0	0			
5	RBL	0	0	0	R	R	R
	RFL	0	0/1	0/1			
	LBL	1	1	0			
	LFL	0	1	0			
6	RBL	0	0	0	R	R	R
	RFL	0	0	0			
	LBL	1	1	1			
	LFL	1	1	1			
7	RBL	1	1	1	R	R	R
	RFL	1	1	1			
	LBL	0	0	0			
	LFL	0	0	0			
8	RBL	0	0	0	-	-	R
	RFL	0	0	0			
	LBL	-1	-1	1			
	LFL	-1	-1	1			
9	RBL	-	-	1	-	-	R
	RFL	-	-	1			
	LBL	-	-	0			
	LFL	-	-	0			
10	RBL	-	-	-	-	-	-
	RFL	-	-	-			
	LBL	-	-	-			
	LFL	-	-	-			

Table 8-3: Limb and tail position on the WD beam

No.	Limb	Position of Limb (beam =1 or ledge=0)			Tail Position (Left=0 or right and straight =1)		
		Z1	Z2	Z3	Z1	Z2	Z3
1	RBL	1	1	1	S	S	S
	RFL	1	1	1			
	LBL	1	1	1			
	LFL	1	1	1			
2	RBL	1	1	0	S	L	S
	RFL	1	1	1			
	LBL	1	1	1			
	LFL	1	1	1			
3	RBL	1	1	1	S	S	S
	RFL	1	1	1			
	LBL	1	1	1			
	LFL	1	1	1			
4	RBL	1	1	1	S	S	L
	RFL	1	1	1			
	LBL	1	1	1			
	LFL	1	1	1			
5	RBL	1	1	1	S	S	S
	RFL	1	1	1			
	LBL	1	1	1			
	LFL	1	1	1			
6	RBL	1	1	1	R	R	R
	RFL	1	1	1			
	LBL	0	1	1			
	LFL	1	1	1			
7	RBL	1	1	1	R	R	R
	RFL	1	1	1			
	LBL	1	1	1			
	LFL	1	1	1			
8	RBL	0	0	1	L	L	L
	RFL	0	0	0			
	LBL	1	1	1			
	LFL	1	1	1			
9	RBL	1	1	0	R	R	R
	RFL	1	1	1			
	LBL	1	0	1			
	LFL	1	1	1			
10	RBL	1	1	1	S	L	S
	RFL	1	1	1			
	LBL	1	1	1			
	LFL	1	1	1			

D. Kinematic waveforms

Animal

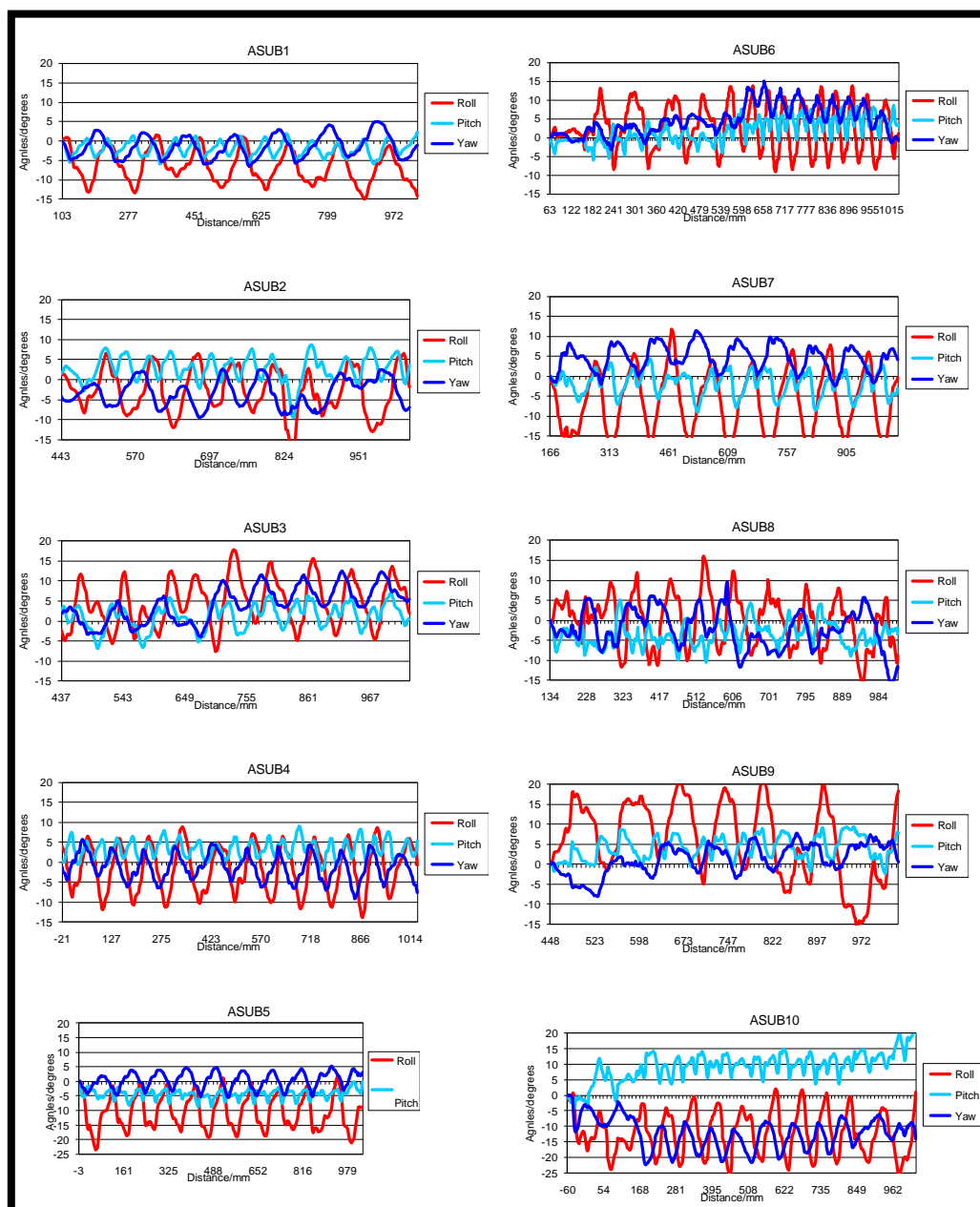


Figure 8-12:PD 6DOF kinematic waveforms along the wide beam

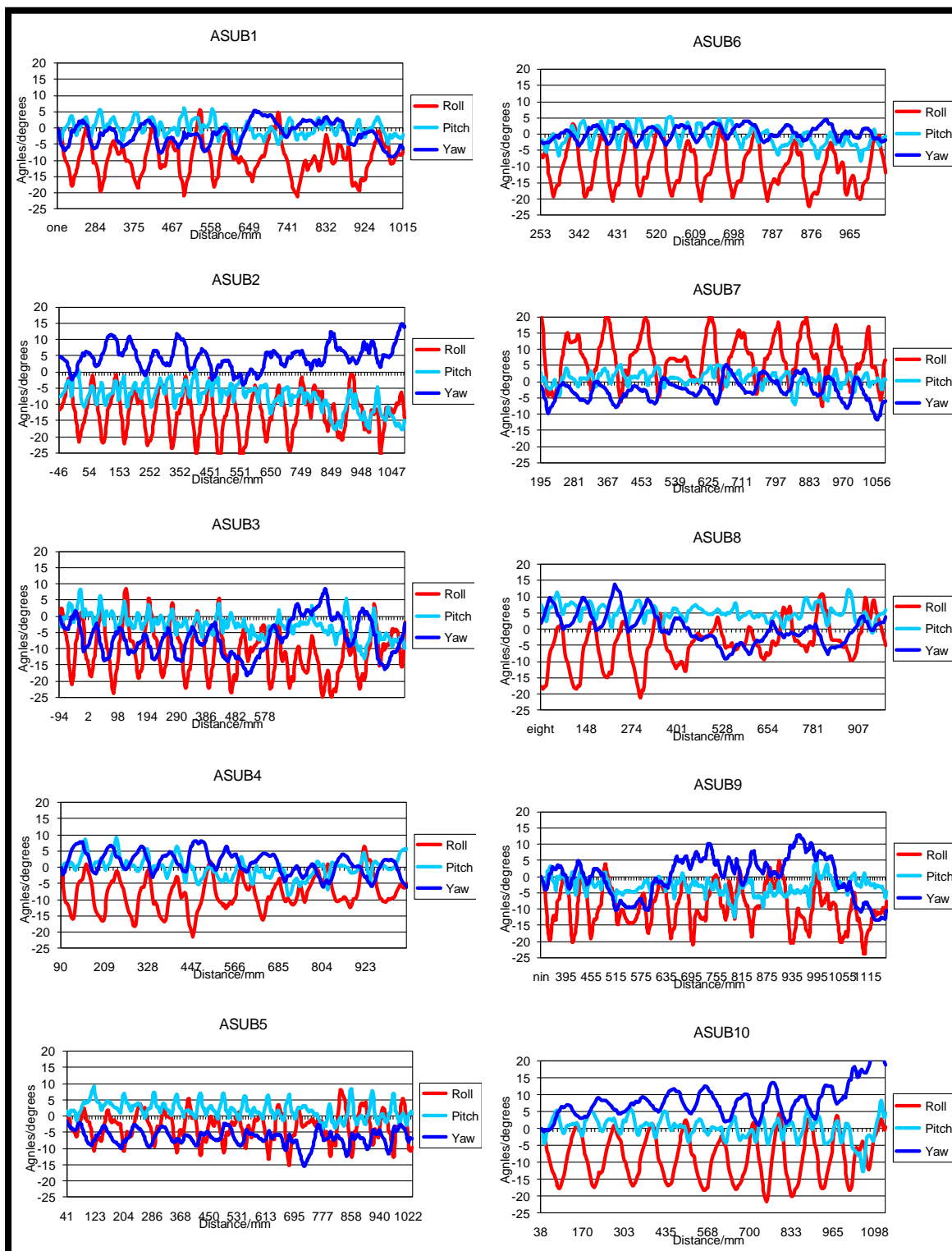


Figure 8-13: PD 6DOF kinematic waveforms along the graduated beam

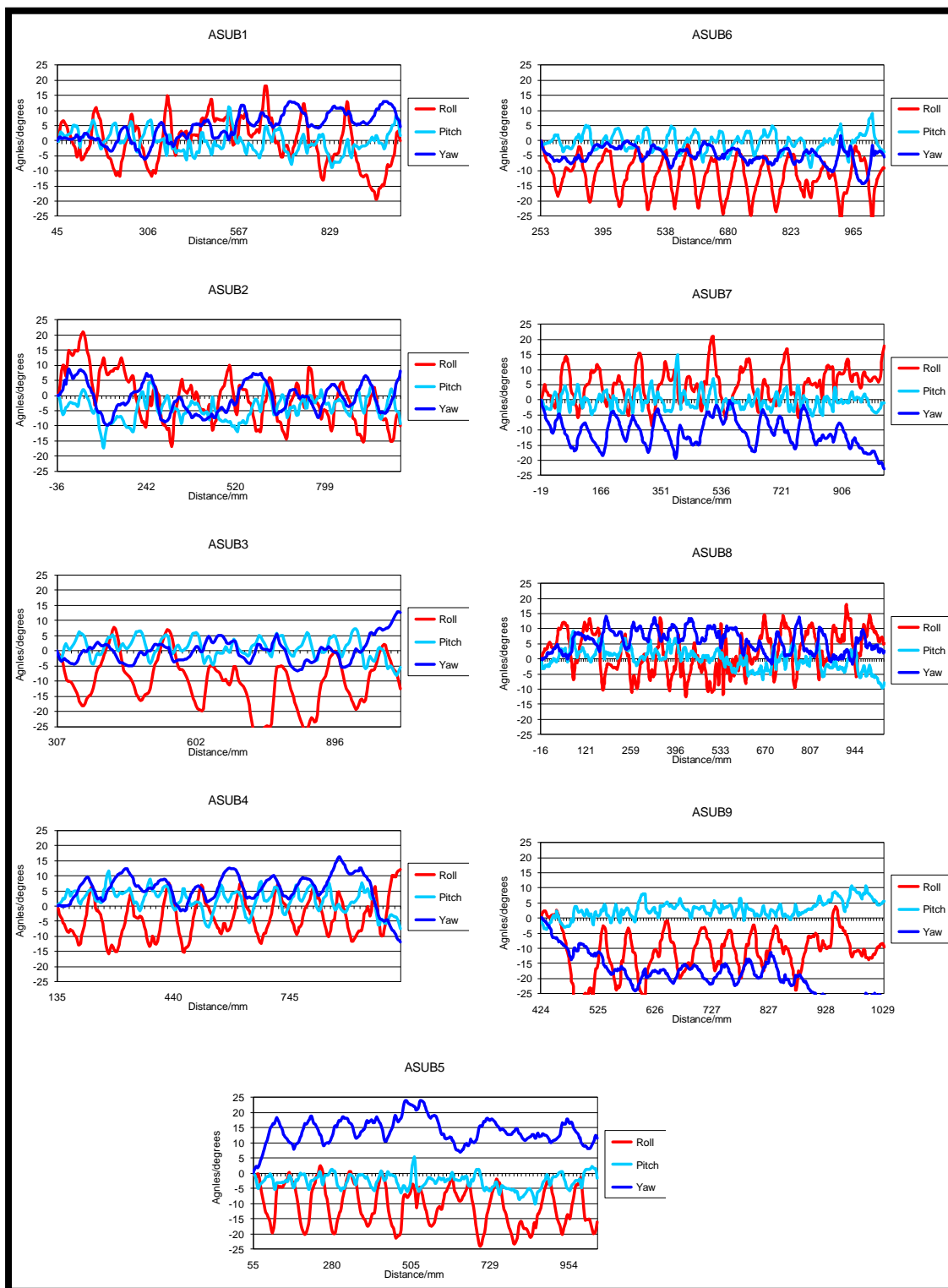


Figure 8-14: PD 6DOF kinematic waveforms along the Narrow beam

Human-Graduated walkway

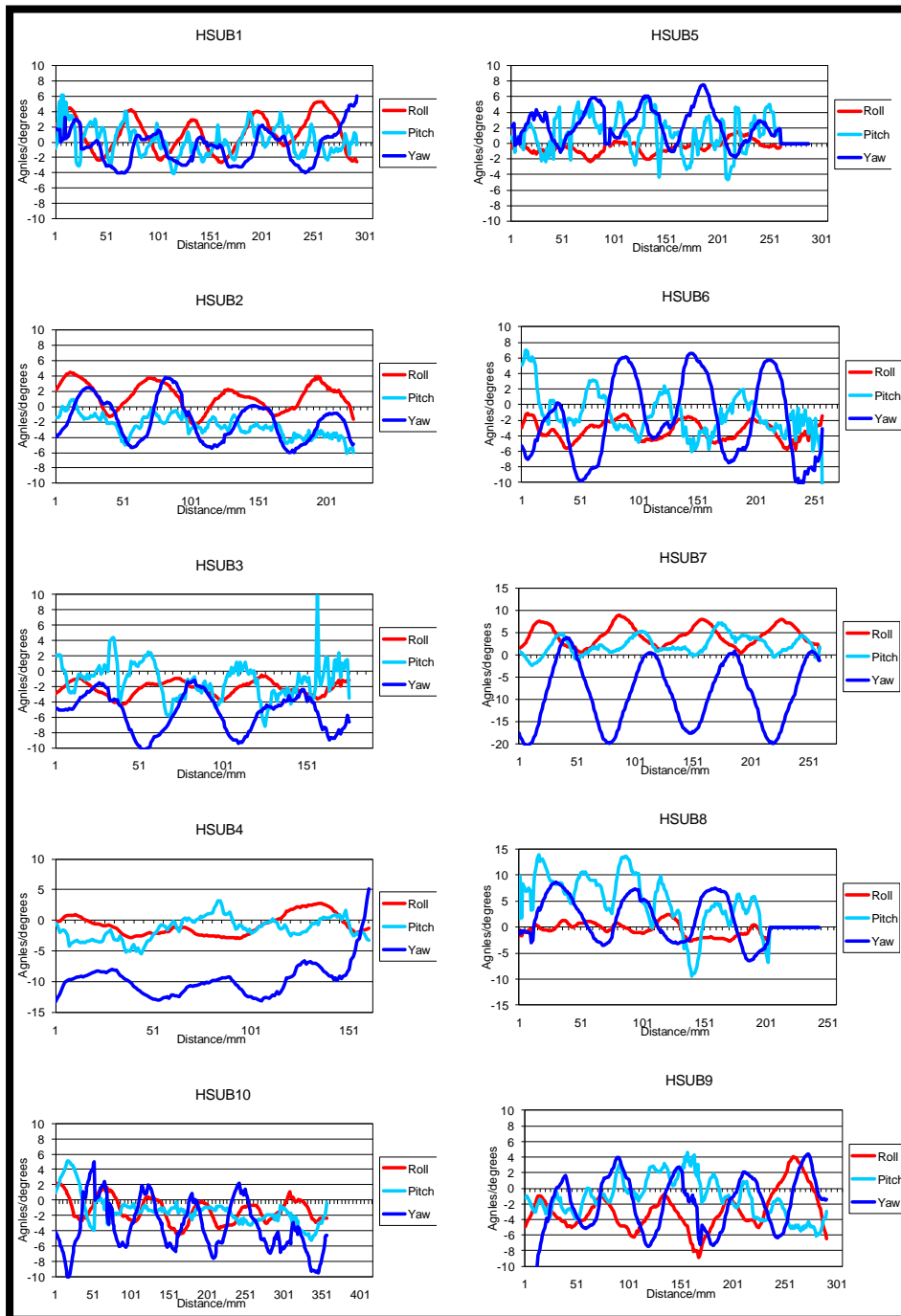


Figure 8-15: Human 6DOF Upper Body

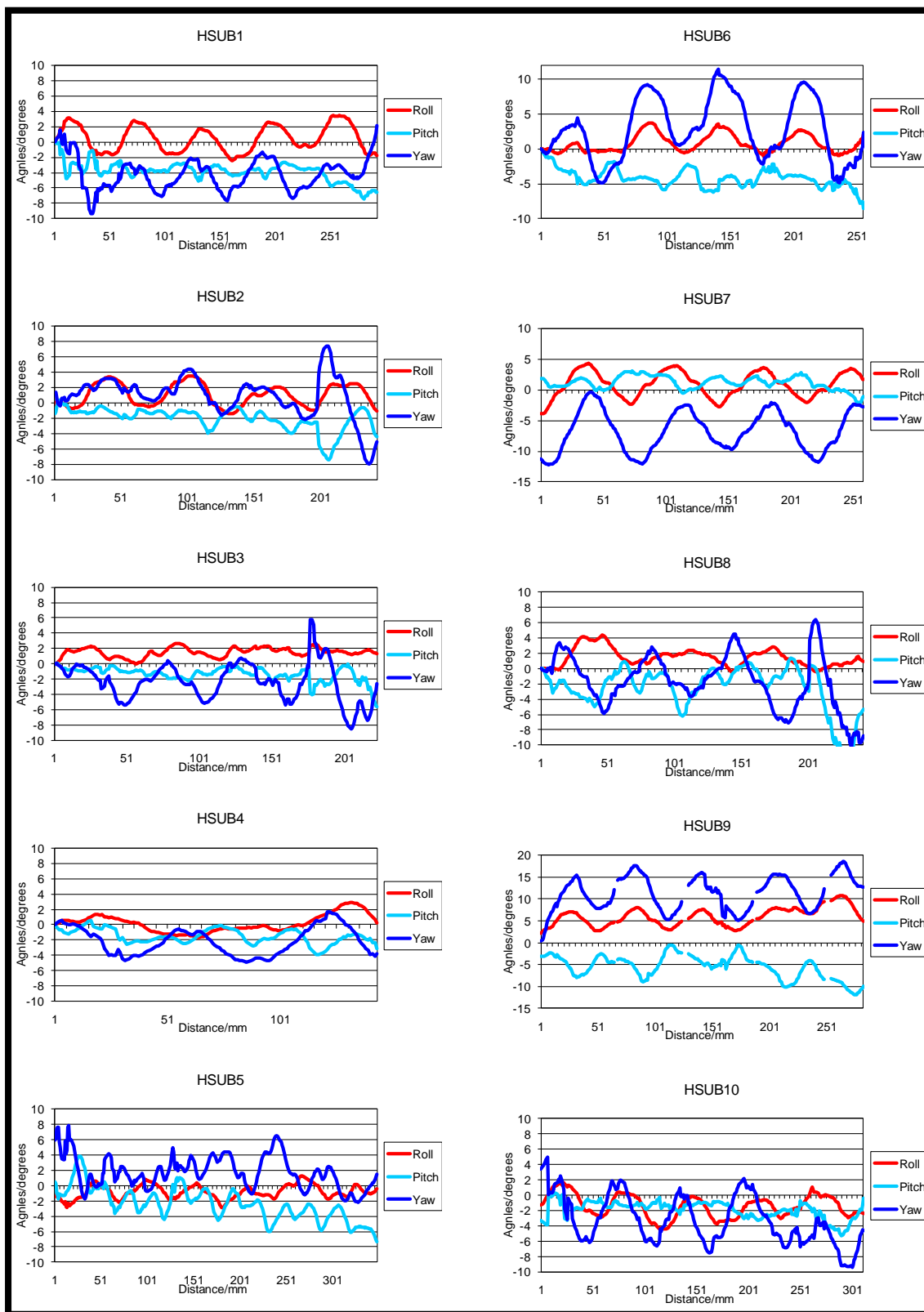


Figure 8-16: Human 6DOF Trunk

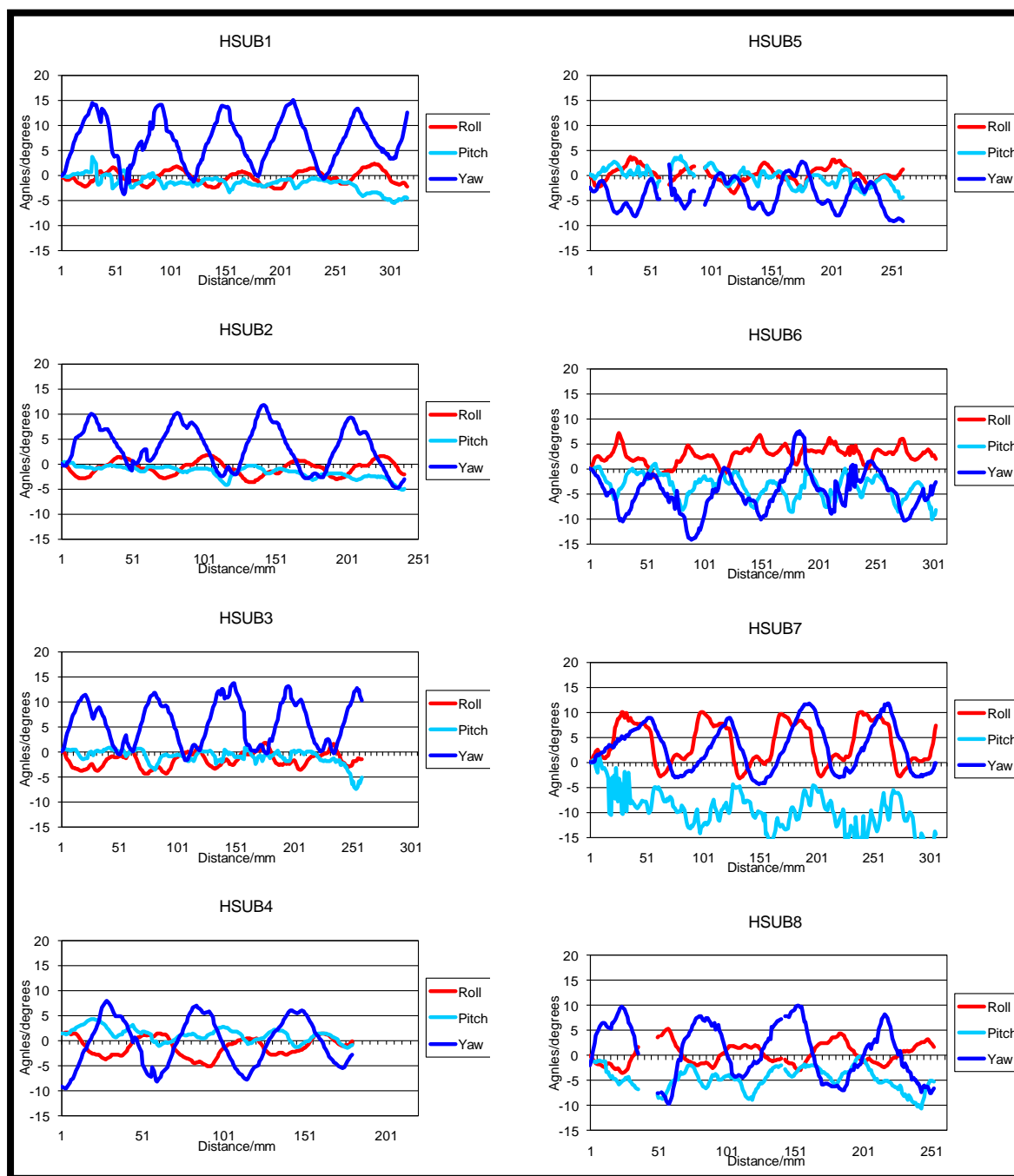


Figure 8-17: Human 6DOF Pelvis

Wide walkway

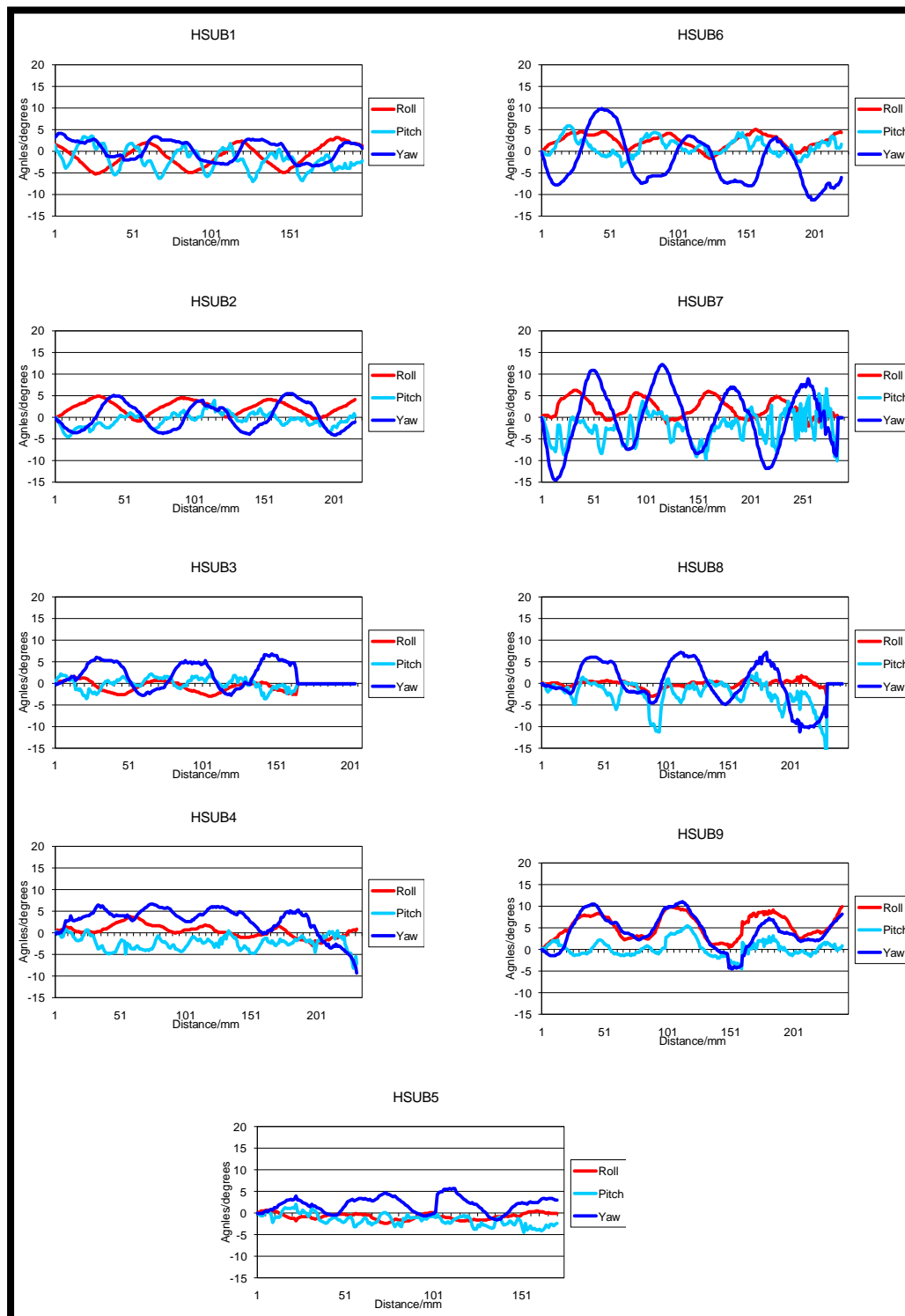


Figure 8-18: Human 6DOF upper Body

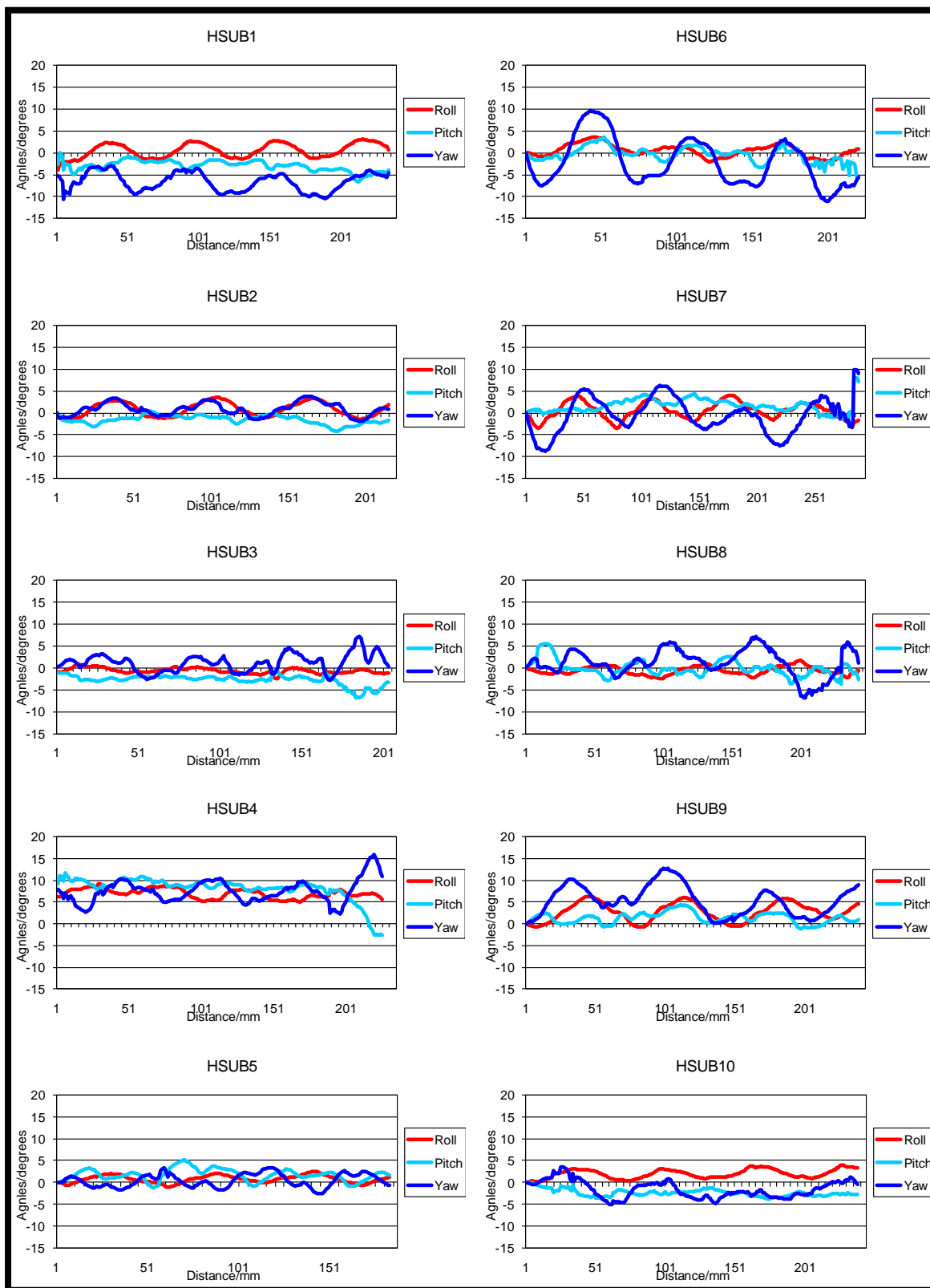


Figure 8-19: Human 6DOF Trunk

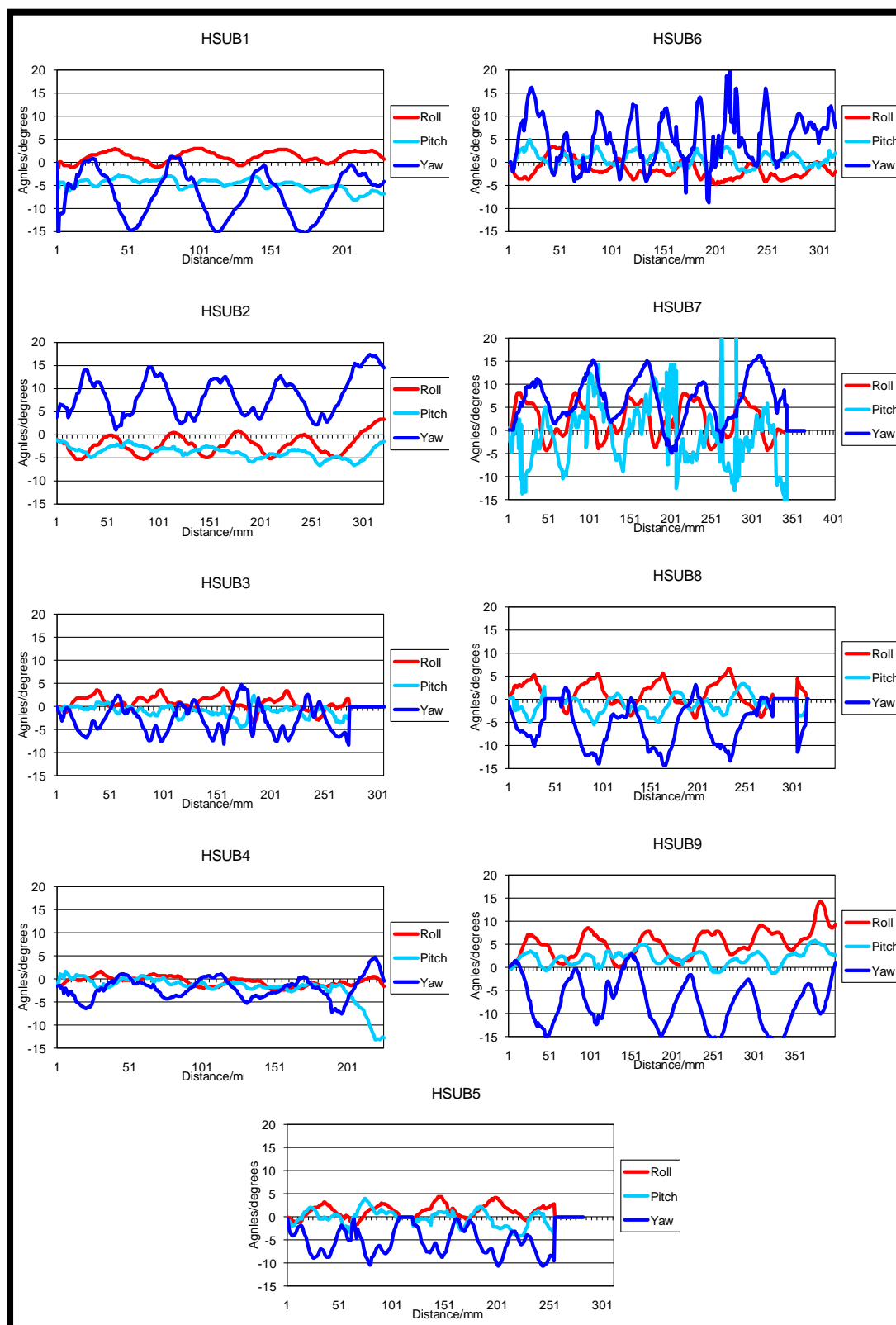


Figure 8-20: Human 6DOF Pelvis

Narrow walkway

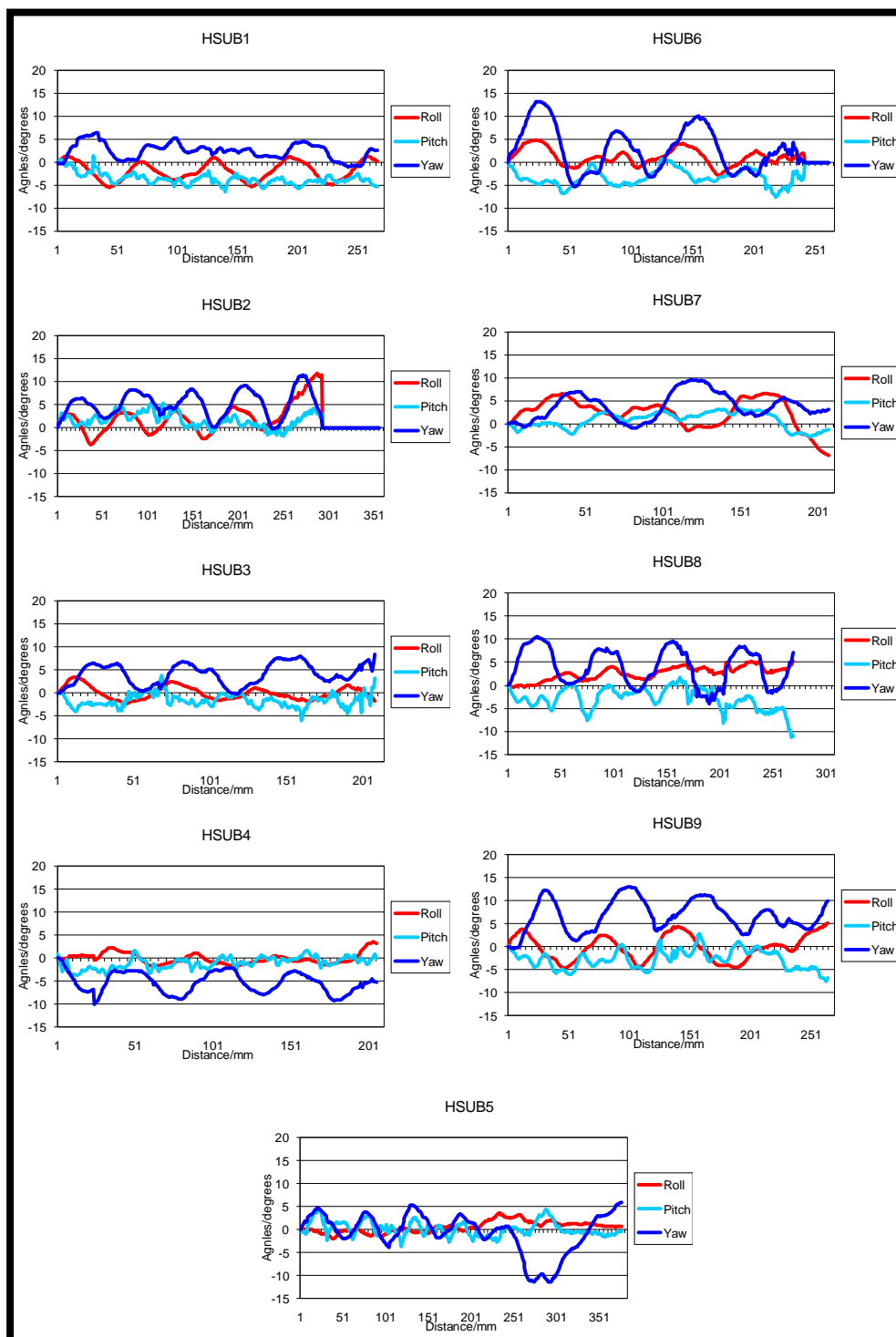


Figure 8-21: Human 6DOF upper Body

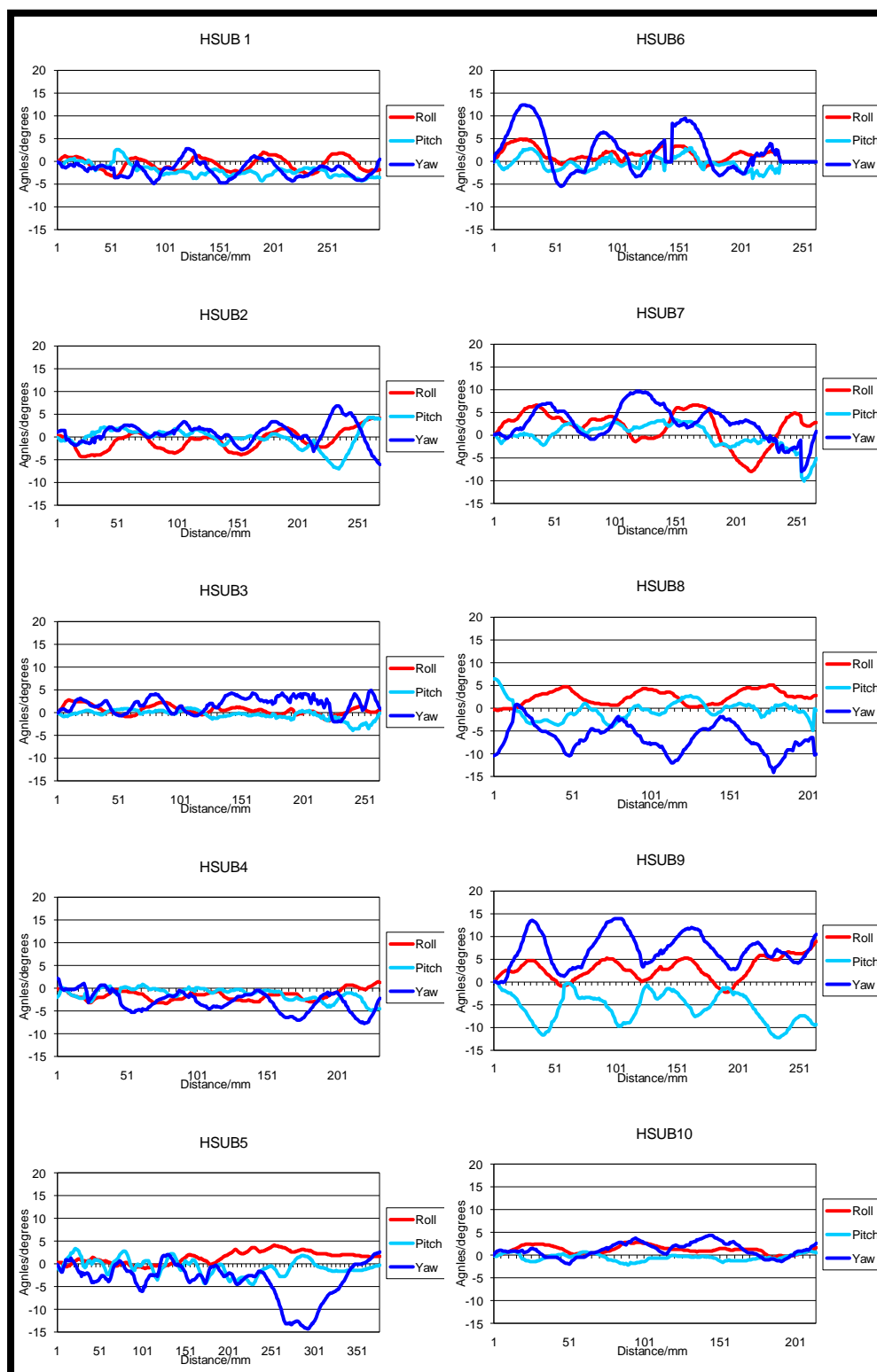


Figure 8-22: Human 6DOF Trunk

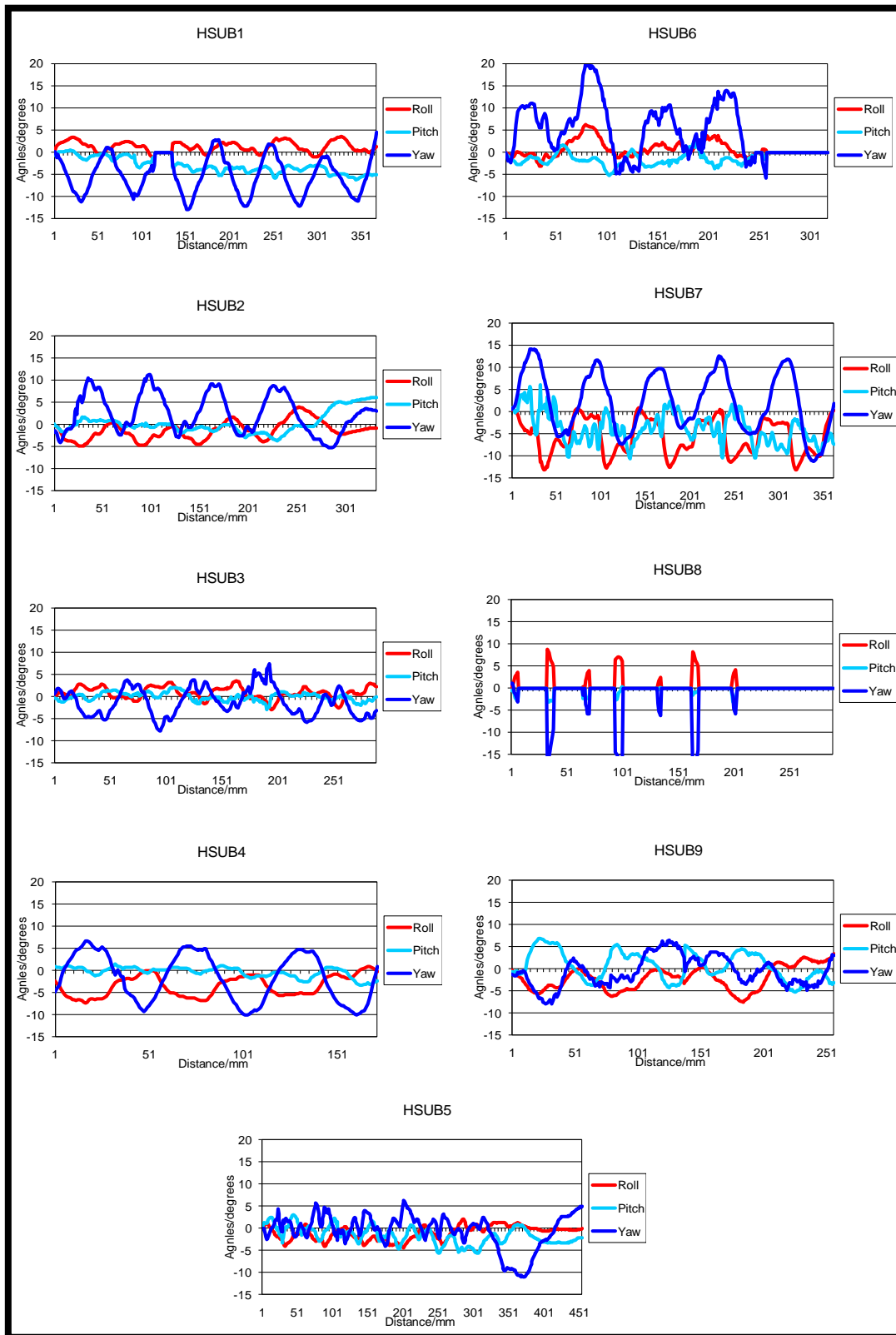


Figure 8-23: Human 6DOF Pelvis

E. Surgeries

Middle cerebral artery occlusion surgery

Rats were anaesthetised and the rat's core body temperature was kept at $36.7 \pm 1^\circ\text{C}$ using automated heat blankets with temperature feedback (Harvard, UK). Laser Doppler probe was used to assess changes in cerebral blood flow (CBF) to the middle cerebral artery (MCA) territory and was monitored using a Laser Doppler Perfusion Monitor (Moor Instruments, UK).

An incision was then made in the neck, the mandibular glands, pretracheal strap, and sternomastoid muscles were retracted to expose the right carotid artery (CA) and the vagus nerve was gently dissected and retracted away. Subsequently, silk sutures were tied on the external carotid artery (ECA) and CA and a microclip was placed on the internal carotid artery (ICA). A second loose suture was placed on the CA above the initial suture, and a small incision was made in the CA for filament insertion. The filament (390 or 410 μm , Docol Company, USA) was inserted and the loose suture was tightened around the filament to allow release of the microclip. The filament was then advanced up the ICA (approximately 20mm) to the MCA branch and decrease in blood flow was monitored by the Laser Doppler Perfusion Monitor (Moor Instruments, UK).

The filament was removed after 30 minutes, the microclip was replaced. The incision in the CA was sealed with electrocoagulation using bipolar diathermy probes (Aesculap, Germany) attached to a cautery unit (Diathermo MB122, Veterinary

Instrumentation, UK), prior to release of all sutures so that complete reperfusion of all vessels was achieved.

The muscles and glands were guided back into place, the incisions sutured. Animals received 2.5mL of physiological saline and 5% glucose (Animal Care Limited, UK) subcutaneously prior to recovery, and those with severe weight loss were re-hydrated daily in a similar fashion until weight stabilized. No animal's weight fell below 80% of their presurgery weight. All cages were provided with moistened rat chow and cereal to facilitate eating during the first postoperative week and 1mg/mL of Paracetamol (Boots, UK) was provided in the drinking water one day prior to surgery and for 3 days after to assist with pain relief.

Grafting

7-12 days following MCAO surgery, 10 of the 23 animals received grafts of E14 whole ganglionic eminence tissue. Pregnant Wistar dams were sacrificed at E14 days of embryonic age. The embryos were removed and the whole ganglionic eminence was carefully dissected out, as done previously (Björklund, 1992 S.B., 1992) The tissue pieces were then dissociated into a cell suspensions as described in (Björklund, 1992 S.B., 1992). 500, 000 cells, in a 2 μ l solution were injected into the lesioned hemisphere, using a 10 μ l Hamilton microsyringe connected to a thin-walled widebore needle (dia = 0.25mm). The rats were anesthetized with isoflurane (Abbott, Queensborough, UK) and were stereotactically injected unilaterally with the cells. The coordinates were set according to bregma and dura: tooth bar -2.3, anterior / posterior +1.4, lateral -3, dorso-ventral -4 and -4.5. Injection volume was 2 μ l and the injection rate was 1 μ l over 90 seconds, with 1 μ l deposited at each depth. The

needle was left in place for 3 min before withdrawal, cleaning and suturing of the wound. Paracetamol (Boots, UK) was provided in the drinking for 3 days after surgery to assist with pain relief.

F. Belief values for simplex plots

Belief values for simplex plots

Table 8-4: BOEc values for the PRE_CN compared to PRE_GRa and PRE_LE dataset

ANIMAL SUBJECT	BOEc		
	m {PRE_GRa and PRE_LE}	m{PRE_CN}	m{ ϕ }
PRE_LE 1	0.4002	0.3040	0.2958
PRE_LE2	0.6981	0.1207	0.1812
PRE_LE3	0.1573	0.4894	0.3534
PRE_LE4	0.2360	0.4630	0.3010
PRE_LE5	0.1568	0.6759	0.1673
PRE_LE6	0.1071	0.7126	0.1803
PRE_LE7	0.1151	0.7793	0.1056
PRE_LE8	0.1572	0.6213	0.2215
PRE_LE 9	0.2621	0.4666	0.2713
PRE_LE 10	0.6055	0.1909	0.2035
PRE_GRa1	0.2117	0.6893	0.0989
PRE_GRa2	0.8713	0.0258	0.1029
PRE_GRa3	0.8739	0.0317	0.0944
PRE_GRa4	0.6079	0.1378	0.2543
PRE_GRa5	0.2569	0.4018	0.3413
PRE_GRa6	0.9074	0.0236	0.0690
PRE_GRa7	0.1545	0.6335	0.2121
PRE_CN1	0.5853	0.3373	0.0774
PRE_CN2	0.0434	0.8450	0.1116
PRE_CN3	0.5693	0.2494	0.1814
PRE_CN4	0.2177	0.4279	0.3544
PRE_CN5	0.2092	0.5456	0.2452
PRE_CN6	0.4460	0.2499	0.3041
PRE_CN7	0.8758	0.0330	0.0913
PRE_CN8	0.1679	0.5327	0.2995
PRE_CN9	0.2571	0.5077	0.2353
PRE_CN10	0.2373	0.4749	0.2878

Table 8-5: BOEc values for the PRE_GRa compared to PRE_CN and PRE_LE dataset

ANIMAL SUBJECT	BOEc		
	m{PRE_CN and PRE_LE}	m{PRE_GRa}	m{ ϕ }
PRE_CN1	0.039873	0.908503	0.051624
PRE_CN2	0.825645	0.06645	0.107906
PRE_CN3	0.085023	0.792453	0.122524
PRE_CN4	0.456333	0.183778	0.359888
PRE_CN5	0.810816	0.07219	0.116994
PRE_CN6	0.745061	0.105978	0.148962
PRE_CN7	0.339007	0.393815	0.267178
PRE_CN8	0.584798	0.130903	0.2843
PRE_CN9	0.10539	0.74259	0.15202
PRE_CN10	0.63831	0.111444	0.250246
PRE_LE 1	0.684096	0.141503	0.174401
PRE_LE2	0.175203	0.508484	0.316313
PRE_LE3	0.357133	0.256672	0.386195
PRE_LE4	0.659981	0.160692	0.179328
PRE_LE5	0.775403	0.098586	0.126011
PRE_LE6	0.798685	0.080887	0.120428
PRE_LE7	0.751107	0.120323	0.128571
PRE_LE8	0.769068	0.097812	0.13312
PRE_LE 9	0.536272	0.158931	0.304797
PRE_LE 10	0.207383	0.468045	0.324572
PRE_GRa1	0.37294	0.501602	0.125459
PRE_GRa2	0.076709	0.802726	0.120565
PRE_GRa3	0.142586	0.720474	0.13694
PRE_GRa4	0.076384	0.799003	0.124613
PRE_GRa5	0.365035	0.24678	0.388185
PRE_GRa6	0.080791	0.797252	0.121957
PRE_GRa7	0.309693	0.510613	0.179694

Table 8-6: BOEc values for the PRE_LE compared to PRE_GRa and PRE_CN dataset

ANIMAL SUBJECT	BOEc		
	m {PRE_CN and PRE_GRa}	m{PRE_LE}	m{ ϕ }
PRE_CN1	0.951851	0.021622	0.026527
PRE_CN2	0.264067	0.617648	0.118285
PRE_CN3	0.876932	0.026243	0.096825
PRE_CN4	0.290043	0.328663	0.381294
PRE_CN5	0.040879	0.854392	0.104729
PRE_CN6	0.023473	0.83499	0.141537
PRE_CN7	0.011925	0.889394	0.098682
PRE_CN8	0.308167	0.381018	0.310815
PRE_CN9	0.846496	0.026685	0.126819
PRE_CN10	0.217211	0.515295	0.267493
PRE_GRa1	0.927717	0.015823	0.05646
PRE_GRa2	0.569935	0.305958	0.124107
PRE_GRa3	0.460992	0.434563	0.104445
PRE_GRa4	0.700076	0.140352	0.159572
PRE_GRa5	0.359944	0.276542	0.363514
PRE_GRa6	0.565302	0.323462	0.111236
PRE_GRa7	0.763138	0.067176	0.169686
PRE_LE 1	0.061473	0.756545	0.181981
PRE_LE2	0.146006	0.610503	0.24349
PRE_LE3	0.43831	0.209262	0.352427
PRE_LE4	0.169589	0.612983	0.217428
PRE_LE5	0.049906	0.837995	0.112099
PRE_LE6	0.085303	0.78734	0.127358
PRE_LE7	0.102425	0.792974	0.1046
PRE_LE8	0.151449	0.701427	0.147125
PRE_LE 9	0.27449	0.445176	0.280334
PRE_LE 10	0.204454	0.563084	0.232463

Table 8-7: BOEc values for the PRE_CN compared to POST_CN dataset

ANIMAL SUBJECT	BOEc		
	m {PRE_CN}	m{POST_CN}	m{ ϕ }
PRE_CN1	0	0.994902	0.005098
PRE_CN2	0.57423	0.295996	0.129774
PRE_CN3	0.226962	0.635265	0.137773
PRE_CN4	0.883719	0.018784	0.097497
PRE_CN5	0.93161	0.005556	0.062834
PRE_CN6	0.947668	0.004285	0.048047
PRE_CN7	0.962922	0.005243	0.031836
PRE_CN8	0.88732	0.025695	0.086985
PRE_CN9	0.42138	0.298055	0.280565
PRE_CN10	0.934888	0.007433	0.057679
POSTCN1	0.237261	0.634506	0.128233
POSTCN2	0.127558	0.74167	0.130772
POSTCN3	0.244024	0.633823	0.122153
POSTCN4	0.452582	0.437703	0.109714
POSTCN5	0.486271	0.410586	0.103143
POSTCN6	0.375715	0.543251	0.081033
POSTCN7	0.435911	0.251222	0.312867
POSTCN8	0.014065	0.958799	0.027136
POSTCN9	0.310857	0.624465	0.064678
POSTCN10	0.415877	0.49917	0.084953

Table 8-8: BOEc values for the PRE_GRa compared to POST_GRa dataset

ANIMAL SUBJECT	BOEc		
	m {PRE_GRa}	m{POST_GRa}	m{ ϕ }
PRE_GRa1	0.01539	0.887862	0.096749
PRE_GRa2	0.986165	0	0.013835
PRE_GRa3	0.994269	0	0.005731
PRE_GRa4	0.955358	0.021014	0.023627
PRE_GRa5	0.98238	0.000709	0.016911
PRE_GRa6	0.923308	0.061327	0.015365
PRE_GRa7	0.749539	0.187993	0.062469
POST_GRa1	0.073376	0.66482	0.261804
POST_GRa2	0.216293	0.608849	0.174858
POST_GRa3	0.625729	0.31111	0.06316
POST_GRa4	0.263662	0.653123	0.083215
POST_GRa5	0.084207	0.855037	0.060756
POST_GRa6	6.88E-05	0.988687	0.011244
POST_GRa7	0.143052	0.698932	0.158016
POST_GRa8	0.087048	0.889956	0.022996
POST_GRa9	0.000119	0.991469	0.008412
POST_GRa10	0.293297	0.6228	0.083903

Table 8-9: BOEc values for the PRE_LE compared to POST_LE dataset

ANIMAL SUBJECT	BOEc		
	m {PRE_LE}	m{POST_LE}	m{ ϕ }
PRE_LE1	0.848984	0.038397	0.112619
PRE_LE2	0.991438	0.001805	0.006757
PRE_LE3	0.174662	0.570487	0.254851
PRE_LE4	0.32063	0.451562	0.227808
PRE_LE5	0.543176	0.241311	0.215513
PRE_LE6	0.518442	0.237276	0.244282
PRE_LE7	0.527718	0.302417	0.169865
PRE_LE8	0.493848	0.333956	0.172196
PRE_LE9	0.660727	0.175954	0.16332
PRE_LE10	0.990048	0.002017	0.007935
POST_LE1	0.129525	0.717395	0.15308
POST_LE2	0.365079	0.604605	0.030316
POST_LE3	0.014313	0.849176	0.136511
POST_LE4	0.008592	0.944213	0.047196
POST_LE5	0.284844	0.563015	0.152141
POST_LE6	0.058448	0.789073	0.152479
POST_LE7	0.48211	0.382521	0.13537
POST_LE8	0.458182	0.404941	0.136877
POST_LE9	0.03334	0.887318	0.079342
POST_LE10	0.499244	0.29415	0.206606

Table 8-10: BOEc values for the POST_CN compared to POST_GRa dataset

ANIMAL SUBJECT	BOEc		
	m {POST_CN}	m{POST_GRa}	m{ ϕ }
POSTCN1	0.845946	0.066156	0.087898
POSTCN2	0.790485	0.039375	0.170139
POSTCN3	0.341046	0.549236	0.109718
POSTCN4	0.464269	0.41594	0.119791
POSTCN5	0.69359	0.190758	0.115651
POSTCN6	0.760667	0.136452	0.102881
POSTCN7	0.831624	0.074432	0.093944
POSTCN8	0.096158	0.85366	0.050182
POSTCN9	0.007325	0.94679	0.045885
POSTCN10	0.335909	0.593345	0.070746
POST_GRa1	0.23642	0.479394	0.284186
POST_GRa2	0.202219	0.609124	0.188657
POST_GRa3	0.548939	0.367321	0.08374
POST_GRa4	0.272549	0.548472	0.178978
POST_GRa5	0.134255	0.7426	0.123144
POST_GRa6	0.024479	0.915944	0.059577
POST_GRa7	0.191955	0.456372	0.351673
POST_GRa8	0.521213	0.369034	0.109753
POST_GRa9	0.010512	0.930441	0.059047
POST_GRa10	0.460015	0.292412	0.247573

Table 8-11: BOEc values for the POST_LE compared to POST_GRa dataset

ANIMAL SUBJECT	BOEc		
	m{POST_GRa}	m{POST_LE}	m{ ϕ }
POST_GRa1	0.788802	0.135421	0.075777
POST_GRa2	0.000484	0.981563	0.017952
POST_GRa3	0.918752	0.012574	0.068674
POST_GRa4	0.650297	0.229714	0.11999
POST_GRa5	0.973213	0.003555	0.023233
POST_GRa6	0.943916	0.007442	0.048641
POST_GRa7	0.955108	0.005235	0.039657
POST_GRa8	0.905574	0.058359	0.036067
POST_GRa9	0.950544	0.00936	0.040096
POST_GRa10	0.944416	0.015629	0.039954
POST_LE1	0.063857	0.821798	0.114345
POST_LE2	0.093213	0.796829	0.109958
POST_LE3	0.554185	0.377874	0.067941
POST_LE4	0.096846	0.848699	0.054455
POST_LE5	0.07736	0.826403	0.096237
POST_LE6	0.011844	0.977813	0.010342
POST_LE7	0.021705	0.900567	0.077728
POST_LE8	0.104759	0.770884	0.124357
POST_LE9	0.003626	0.974386	0.021989
POST_LE10	0.154671	0.779403	0.065926

Table 8-12: BOEc values for the POST_LE compared to POST_CN dataset

ANIMAL SUBJECT	BOEc		
	m{POST_LE}	m{POST_CN}	m{ ϕ }
POSTCN1	0.619182	0.179957	0.20086
POSTCN2	0.787148	0.093191	0.11966
POSTCN3	0.787708	0.096163	0.11613
POSTCN4	0.793458	0.087171	0.119372
POSTCN5	0.724302	0.164025	0.111673
POSTCN6	0.016912	0.941286	0.041802
POSTCN7	0.4581	0.291052	0.250848
POSTCN8	0.745704	0.133977	0.120319
POSTCN9	0.525772	0.388638	0.085589
POSTCN10	0.019553	0.929835	0.050613
POST_LE1	0.21469	0.655805	0.129504
POST_LE2	0.951148	0.007348	0.041504
POST_LE3	0.06583	0.807942	0.126228
POST_LE4	0.430088	0.218782	0.351131
POST_LE5	0.035227	0.866125	0.098648
POST_LE6	0.062948	0.821123	0.115929
POST_LE7	0.051213	0.840564	0.108223
POST_LE8	0.077692	0.816828	0.105481
POST_LE9	0.025226	0.87827	0.096504
POST_LE10	0.084893	0.79442	0.120687